



**University of
Nottingham**

UK | CHINA | MALAYSIA

Curcumin Containing Chitosan- Pectinate Nanoparticulate Drug Delivery System for Colon Cancer Treatment

**Enas Ali Alkhader, BSc Pharmacy, MSc
Pharmaceutical Sciences**

*Thesis submitted to the University of Nottingham in fulfilment of the
requirements for the Degree of Doctor of Philosophy*

April 2018

*To the most precious diamonds in my life, my father and my
daughter Mariah, to you I dedicate this work.*

This thesis is the result of the author's original work except for quotations and citations, which have been duly acknowledged. It has not been previously or concurrently submitted for any degree at the University of Nottingham Malaysia Campus or any other institution.

Enas Ali Alkhader

Date: 18/4/2018

ACKNOWLEDGEMENTS

First and foremost, I dedicate my work to Allah, the Almighty, for he empowered me the strength to persist all the way long, and granted me the blessing to finish this thesis the way it is.

My immense debt of gratitude goes to my supervisor Prof. Nashiru Billa, for his exceptional supervision, knowledge, expertise, patience, and guidance from the day this project idea was born, to the final draft of this thesis.

I would also like to thank my co-supervisor Prof. Clive Roberts (Head, School of Pharmacy, UNUK) for his assistance and advice that have contributed to the completion of this project.

I would like to express my gratitude to Prof. Andrew Morris (Dean, School of Pharmacy, UNMC) for his precious advices and for his role as my internal assessor, your advices during the viva were well taken.

A very special gratitude goes to Prof. Rozita Rosli (University Putra Malaysia, UPM) for allowing me to use MAKNA-UPM cancer research laboratories for all the cell studies conducted in this project. I would like to express my gratitude to Madam Tommini Saleh for her exceptional guidance and teaching through the whole duration of my work in MAKNA labs. Her expertise has immensely helped in the completion of my work.

My sincere gratitude goes to Prof. Kah-Hay Yuen (University of Sains Malaysia, USM) for allowing me to use his laboratories for the animal studies conducted in this project. Heartfelt thanks goes to Mr. Eng Kwong Seow, Ms. Zhuan Lee, and Dr. Sherlyn Chin for their outstanding assistance during my work at USM.

I would like to express my heartfelt gratitude to the Graduate School of UNMC for the training programs organized at all stages of the PhD journey, with a special mention to Dr. Jiin Woei Lee, Dr. Tissa Chandesa, and Dr. Maysoun Mustafa for the valuable information, advice, and the enthusiasm they shared during the training workshops.

I would like to thank all the lab technicians, the academic, and administrative staff of the School of Pharmacy, UNMC for their support in numerous ways, you all have contributed, in a way or another, in the completion of this project.

I would like to express my sincere gratitude to my colleague at the Drug Delivery Lab (UNMC), Rayan Sabra, you have been much more than a lab colleague, you have been a dear friend who immensely eased my PhD journey. Your spiritual, technical, and practical support have immensely helped in the completion of this project. Special thanks goes to my colleagues Nur Aliana Hidayah Binti Mohamed, you have been a genuinely caring friend, Lee Shi Ting, Janet Tan Sui Ling, Rajesh Sreedharan Nair, and Wai Jing Luen, as well as former colleagues Dr. Yamina Boukari, Dr. Hilda Amekyeh, and Nabil Ahmad Siddiqui for all of the support, help, and encouragement they provided in my journey.

To my role model, my dearest father, no words could ever express my gratitude, you have supported this journey from the very first day by all it means. Your encouragement, support, and inspiration throughout my whole life have guided me towards this. I would have never achieved any of this without you. My eternal cheerleader, my beloved mother, your encouragement, support, and full heart prayers have guided me along the way. Your excitement whenever I achieved a significant milestone in my journey was my dose of encouragement to move forward. To my loving journey partner, my husband Emad, thank you for sharing

and easing this journey, thank you for being by my side in my moments of crisis. My wholehearted thanks goes to my siblings for believing in me and for their continuous encouragement and support, who asked for nothing but my happiness and success. Lastly, I would like to thank my dear friends and everyone who contributed in a way or another in my success. I am grateful for having all of these caring people in my life.

TABLE OF CONTENTS

	Page
DEDICATION	i
DECLARATION	ii
ACKNOWLEDGMENTS	iii
TABLE OF CONTENTS	vi
LIST OF FIGURES	xii
LIST OF TABLES	xvi
LIST OF EQUATIONS	xvii
LIST OF ABBREVIATIONS	xviii
ABSTRACT	xxiv
CHAPTER 1: INTRODUCTION	1
1.1 General Overview	2
1.2 Colon and Colorectal Cancer	4
1.2.1 The Human Colon	4
1.2.2 Colorectal cancer	6
1.3 Curcumin	16
1.3.1 Chemical Properties of Curcumin	17
1.3.2 Therapeutic Properties of Curcumin	19
1.3.2.1 Antioxidant activity	20
1.3.2.2 Anti-Malarial activity	22
1.3.2.3 Anti-inflammatory activity	23
1.3.2.4 Anti-bacterial activity	26
1.3.2.5 Neuroprotective activity	27
1.3.2.6 Anti-cancer activity	27
1.3.3 Cocktail of CUR with conventional anticancer drugs	29
1.3.4 Clinical studies on CUR as an anticancer agent	31
1.4 Nanomedicine	32
1.4.1 Challenges in Nanomedicine	35
1.4.2 Types of “nanocarriers”	36
1.4.2.1 Polymeric nanoparticles	36
1.4.2.2 Micelles	38
1.4.2.3 Dendrimers	40
1.4.2.4 Liposomes	43
	vi

1.4.2.5	Solid Lipid Nanoparticles (SLN)	46
1.4.3	Methods of preparation for polymeric nanoparticles	48
1.4.3.1	Preparation methods from dispersion of preformed polymer	50
1.4.3.1.1	Solvent Evaporation	50
1.4.3.1.2	Nanoprecipitation	51
1.4.3.1.3	Emulsification/solvent diffusion	53
1.4.3.1.4	Salting-out technique	55
1.4.3.2	Preparation methods from dispersion of monomers	57
1.4.3.2.1	Emulsion polymerization	57
1.4.3.2.2	Interfacial Polymerization	59
1.4.3.3	Ionic Gelation	60
1.4.4	Nanomedicine in clinical practice	61
1.4.5	Nanoformulations of CUR	64
1.5	Drug Delivery to the colon	67
1.5.1	Strategies for targeted colonic therapy	67
1.5.1.1	Pro-drugs	68
1.5.1.2	pH- dependent systems	68
1.5.1.3	Time- dependent systems	69
1.5.1.4	Microbially- triggered systems	70
1.5.2	Mucoadhesion	71
1.5.2.1	Polymers used in mucoadhesion	71
1.5.2.1.1	Anionic polymers	72
1.5.2.1.2	Cationic polymers	73
1.6	Aims and objectives of the present research	74
1.6.1	Aims	74
1.6.2	Colorectal cancer	74
CHAPTER 2: FORMULATION OF CURCUMIN CHITOSAN PECTINATE NANOPARTICLES		76
2.1	Introduction	77
2.1.1	Polymer of choice 1: Chitosan	77
2.1.2	Polymer of choice 2: Pectin	78
2.1.3	Sodium tripolyphosphate (TPP) as the cross-linking agent	80
2.1.4	Particle size and zeta potential	81
2.1.5	Scanning Electron Microscopy (SEM)	83
2.1.6	Fourier Transform Infrared Spectroscopy	84
2.1.7	X-Ray Diffractometer	85
2.1.8	Differential Scanning Calorimetry	86
2.1.9	Aims and Objectives in this Chapter	88
2.2	Materials and Methods	89
2.2.1	Materials	89
2.2.2	Formulation of chitosan-pectinate composite nanoparticles	89

2.2.2.1	Preliminary formulations of CUR chitosan-pectinate composite nanoparticles based on order of addition	89
2.2.2.2	Sub-formulations and optimization of the preliminary formulation	90
2.2.3	Size and zeta potential measurement	90
2.2.4	SEM imaging	91
2.2.5	FT-IR analysis	91
2.2.6	XRD analysis	91
2.2.7	DSC analysis	91
2.3	Results and discussion	92
2.3.1	Particle size and zeta potential measurement	92
2.3.2	Morphology of CUR-CS-PEC-NPs and CS-PEC-NPs	99
2.3.3	FT-IR spectra	101
2.3.4	XRD data	103
2.3.5	DSC analysis	103
2.4	Conclusion	105
	CHAPTER 3: MUCOADHESION, RELEASE, AND STABILITY STUDIES	106
3.1	Introduction	107
3.1.1	Mucin	107
3.1.2	Mucoadhesion process	108
3.1.3	High Performance Liquid Chromatography	109
3.1.3.1	HPLC analysis of CUR	110
3.1.4	Aims and Objectives	111
3.2	Materials and Methods	111
3.2.1	Materials	111
3.2.2	Mucoadhesion studies	112
3.2.3	HPLC assay for CUR	112
3.2.4	HPLC method validation	113
3.2.5	Determination of encapsulation efficiency and encapsulation capacity	113
3.2.6	CUR release from CUR-CS-PEC-NPs	113
3.2.6.1	CUR release from CUR-CS-PEC-NPs in different simulated fluids	113
3.2.6.2	CUR release from CUR-CS-PEC-NPs in simulated gastrointestinal tract fluids	115
3.2.7	Stability Studies	116
3.2.7.1	Storage	116
3.2.7.2	Photosensitivity	116
3.2.7.3	Thermal	117
3.3	Results and Discussion	117
3.3.1	Mucoadhesion studies	117

3.3.2	HPLC assay for quantification of CUR	124
3.3.3	Encapsulation efficiency (EE%)	127
3.3.4	CUR release from CUR-CS-PEC-NPs	128
3.3.5	Stability Studies	136
3.3.5.1	Storage stability studies	136
3.3.5.2	Protection of CUR from photodegradation	141
3.3.5.3	Protection of CUR from thermal degradation	144
3.4	Conclusion	146
CHAPTER 4: IN VITRO EVALUATION OF FORMULATION		147
4.1	Introduction	148
4.1.1	Cell culture	148
4.1.2	Cell lines	149
4.1.3	Fluorescence microscopy	150
4.1.4	Mycoplasma	152
4.1.5	MTT assay	153
4.1.6	Aims and objectives	154
4.2	Materials and methods	155
4.2.1	Materials	155
4.2.2	Maintenance of cell culture	156
4.2.3	Subculture of cells	156
4.2.4	Cells counting	156
4.2.5	Check for mycoplasma	157
4.2.6	MTT assay	158
4.2.6.1	MTT assay for HT-29 cells	158
4.2.6.2	MTT assay for MRC-5 cells	158
4.2.7	Cellular uptake	159
4.2.7.1	Qualitative cellular uptake	159
4.2.7.2	Quantitative cellular uptake	159
4.2.8	Cellular apoptosis viewed under fluorescent microscope	160
4.2.9	Statistical analyses	160
4.3	Results and discussion	160
4.3.1	Maintenance of HT-29 and MRC-5 cells	161
4.3.2	Mycoplasma detection	162
4.3.3	Cell viability assay	163
4.3.4	Morphological changes of cells by CUR-CS-PEC-NPs	171
4.3.5	Cellular uptake	174
4.4	Conclusion	179

CHAPTER 5: DEVELOPMENT AND VALIDATION OF A HPLC METHOD AND PHARMACOKINETICS STUDIES ON CUR-CS-PEC-NPS	180
5.1 Introduction	181
5.1.1 HPLC method development and validation	181
5.1.2 In vivo pharmacokinetics studies	182
5.1.3 Aims and objectives	183
5.2 Materials and methods	184
5.2.1 Materials	184
5.2.2 HPLC methods development and validation	185
5.2.2.1 HPLC instrumentation and conditions	185
5.2.2.2 Plasma standards	186
5.2.2.3 Plasma sample preparation	186
5.2.2.4 Specificity	186
5.2.2.5 Linearity and range	187
5.2.2.6 Precision	187
5.2.2.7 Accuracy	187
5.2.2.8 Recovery	187
5.2.2.9 Limits of detection and quantification	188
5.2.3 In vivo Study	188
5.2.3.1 Preparation of CUR-CS-PEC-NPs and SP-CS-PEC-NPs	188
5.2.3.2 Animals	188
5.2.3.3 Procedural care of the rats	189
5.2.3.4 Pharmacokinetics studies	189
5.2.3.5 Data and statistical analyses	190
5.3 Results and Discussion	190
5.3.1 Selection of the internal standard	190
5.3.1.1 Internal standard for CUR analysis method	191
5.3.1.2 Internal standard for SP analyses method	191
5.3.2 Mobile phase composition and elution method	194
5.3.2.1 HPLC method for CUR determination	194
5.3.2.2 HPLC method for SP determination	196
5.3.3 Effects of the plasma and the deproteinising agent on peak resolution and symmetry	198
5.3.4 HPLC method validation	201
5.3.4.1 Specificity	202
5.3.4.2 Effect of plasma (matrix effect)	203
5.3.4.3 Linearity and range	207
5.3.4.4 Precision	210
5.3.4.5 Accuracy	210
5.3.4.6 Recovery	211
5.3.4.7 LOD and LOQ	212
5.3.5 In vivo Pharmacokinetics studies	214
5.3.5.1 Selection of animal model	214
5.3.5.2 Pharmacokinetics studies	215
5.4 Conclusion	219

CHAPTER 6: CONCLUSION AND FUTURE WORK	221
6.1 Conclusion	222
6.2 Suggestions for future work	225
LIST OF PUBLICATIONS FROM THE PRESENT WORK	227
References	228

LIST OF FIGURES

Figure 1.1 The structure of the colon	4
Figure 1.2 Colorectal cancer stages	13
Figure 1.3 Turmeric	17
Figure 1.4 Chemical structure of curcumin	18
Figure 1.5 Curcumin mechanisms of action as an anti-inflammatory agent	25
Figure 1.6 Polymeric nanoparticles	37
Figure 1.7 Polymeric Micelles	39
Figure 1.8 Dendrimers	41
Figure 1.9 Liposomes	43
Figure 1.10 Solid Lipid Nanoparticles (SLN)	47
Figure 1.11 Illustration of preparation methods for polymeric nanoparticles	49
Figure 2.1 Schematic diagram of a typical dynamic light scattering technique	82
Figure 2.2 Schematic diagram of SEM components	84
Figure 2.3 Schematic diagram of the FT-IR	85
Figure 2.4 Schematic diagram of XRD components	86
Figure 2.5 Schematic diagram of DSC components	87
Figure 2.6 Sequence leading to formation of CUR-CS-PEC-NPs	95
Figure 2.7 SEM image of the optimized formulation CUR-CS-PEC-NPs at magnification 10000x (A) and 20000x (B)	100
Figure 2.8 FT-IR spectra of CUR (A), CS (B), PEC (C), TPP (D), CS-PEC-NPs (E), and CUR-CS-PEC-NPs (F)	102
Figure 2.9 XRD patterns of CUR and CUR-CS-PEC-NPs	103
Figure 2.10 DSC thermograms of CUR (A), CS (B), PEC (C), TPP (D), physical mixture of CUR, PEC, CS, and TPP (E), CS-PEC-NPs (F), and CUR-CS-PEC-NPs (G).	105
Figure 3.1 CUR release at simulated GIT fluids	116

Figure 3.2 Schematic illustration of the penetration of polymeric NPs into the GIT mucosa	118
Figure 3.3 Changes in zeta potential of CUR-CS-PEC-NPs and CS-PEC-NPs in pH 1.2 (A), pH 6.8 (B), and pH 7.4 (C)	123
Figure 3.4 Schematic diagram of the drop in zeta potential in mucoadhesion	124
Figure 3.5 Representative chromatogram for CUR at 425 nm (5 μ g/ml)	125
Figure 3.6 Standard calibration curve of CUR	126
Figure 3.7 Cumulative release profiles from CUR-CS-PEC-NPs in pH 1.2, 6.8, and 6.4 (with pectinase)	128
Figure 3.8 FESEM images of PEC-free NPs (A,B) & CS-PEC-NPs (C,D) after treatment with 0.1 N HCl (pH 1.2)	131
Figure 3.9 % cumulative CUR release from CUR-CS-PEC-NPs in simulated fluids	134
Figure 3.10 Morphology of fresh CUR-CS-PEC-NPs (A), and after exposure to treatment in SGF (B), SIF (C), and SCF (D)	135
Figure 3.11 Size, zeta potential, and pDI values of CUR-CS-PEC-NPs at days 1, 7, and 14 of shelf storage	138
Figure 3.12 Morphology of freshly CUR-CS-PEC-NPs (A), at day 7 (B) and day 14 (C) during storage at 4°C	139
Figure 3.13 % retention of CUR from CUR-CS-PEC-NPs and CUR ethanolic solution vials upon exposure to sunlight (A) and UV light at 253 nm (B)	143
Figure 3.14 Thermal stability of CUR-CS-PEC-NPs and CUR at 37 °C	145
Figure 4.1 Basic components of inverted fluorescence microscope	151
Figure 4.2 Mycoplasma positive cells after DAPI staining	153
Figure 4.3 Insoluble formazan precipitated inside and near viable cells	154
Figure 4.4 Hemacytometer grid (A) viable cells (not stained by trypan blue) inside the grid and at the interior perimeters are counted (B)	157
Figure 4.5 HT-29 cells (A,B) and MRC-5 cells (C,D) viewed under an inverted microscope under 20x and 40x magnification, respectively.	162
Figure 4.6 HT-29 cells viewed under fluorescence microscope with 430-495nm filter under 20x (A) and 40x (B) magnification	163
Figure 4.7 HT-29 cell viability after treatment with free CUR, void NPs (CS-PEC-NPs), and CUR-CS-PEC-NPs on days 1, 2, and 3, n=3	165

Figure 4.8 MRC-5 cell viability after treatment with free CUR, void NPs (CS-PEC-NPs), and CUR-CS-PEC-NPs on days 1, 2, and 3, n=5	168
Figure 4.9 Fluorescent nuclear images of untreated cells (A), cells treated with CS-PEC-NPs (B), DMSO (C), 75 μ M (D) and 150 μ M (E) of CUR-CS-PEC-NPs, 75 μ M (F) and 150 μ M (G) of free CUR, and (H) 15 μ M of 5-FU. Arrows indicate fragmentation and formation of irregular edges around the nuclei	173
Figure 4.10 Fluorescence microscopy imaging of the cellular uptake of CUR from high and low equivalent doses of CUR-CS-PEC-NPs and free CUR on days 1, 2, and 3. (20x magnification).	175
Figure 4.11 Retrieved CUR after treatment with high and low doses of free CUR and CUR-CS-PEC-NPs on days 1, 2, and 3, n=3	177
Figure 5.1 Chromatogram for EST (10 μ g/ml) and CUR (20 μ g/ml)	191
Figure 5.2 Chemical structures of SP (A) and Theophylline (B)	192
Figure 5.3 Chromatograms for CAF (A), PIR (B), and theopyridine (C) under the same HPLC conditions	193
Figure 5.4 Chromatograms for EST and CUR using Heath <i>et al.</i> (2003b) method	195
Figure 5.5 Chromatogram of CUR at 425 nm	196
Figure 5.6 Chromatogram of SP dissolved in methanol using mobile phase ratio 70:30 (acetate buffer (pH 4) : acetonitrile)	197
Figure 5.7 Chromatograms of TP and SP at mobile phase ratio and detection wavelength of 70:30, 254 nm (A) and 80:20, 260 nm (B), respectively	198
Figure 5.8 Chromatograms of CUR (A) and SP (B) and their respective IS using the mobile phases as deproteinizing agent	200
Figure 5.9 Chromatograms of CUR (A) and SP (B) and their respective IS using methanol as deproteinizing agent	201
Figure 5.10 Chromatograms of pure solutions of CUR and EST (A) and SP and TP (B)	203
Figure 5.11 Chromatograms of the methanolic extract of blank human plasma using CUR (A) and SP (B) analytical methods	204
Figure 5.12 Chromatograms for spiked plasma showing CUR and EST (20 μ g/ml, each) (A) and SP and TP (20 μ g/ml, each)	205
Figure 5.13 Standard calibration curves of the peak response ratios of analyte to IS versus the corresponding concentration of CUR (A) and SP (B) in human plasma	209
Figure 5.14 Plasma concentration profile of CUR in rats after the oral administration of equivalent doses of free CUR (n=3) and CUR-CS-PEC-NPs (n=4)	218

LIST OF TABLES

Table 1.1 Colorectal cancer stages	12
Table 1.2 Liposome-based products approved for human use	45
Table 1.3 Liposome-based products in clinical trials	46
Table 1.4 Selected nanomedicine products available in market	61
Table 1.5 Selected nanomedicine products in clinical development	63
Table 1.6 List of CUR nanoformulations available on market	65
Table 1.7 CUR nanoformulations under clinical development	66
Table 2.1 Composition of CUR-CS-PEC-NPs	90
Table 2.2 Particle size and zeta potential data obtained for formulations A, B, C, and D of CS-PEC-NPs and CUR-CS-PEC-NPs, n=3	93
Table 2.3 Z-average, zeta potential, and pDI of CS-PEC-NPs AND CUR-CS-PEC-NPs as a function of formulation ratios, n=3	97
Table 2.4 Z-average, zeta potential, and pDI of CS-PEC-NPs AND CUR-CS-PEC-NPs as a function of stirring time, n=3	98
Table 2.5 Z-average, zeta potential, and pDI of CS-PEC-NPs AND CUR-CS-PEC-NPs as a function of stirring speed, n=3	99
Table 3.1 Precision and accuracy of the HPLC method.	127
Table 3.2 Zeta potential and percentage Retention of CUR in CUR-CS-PEC-NPs after exposure to pH 1.2 and 6.8, n=3	132
Table 5.1 Summary of HPLC method validation parameters for CUR (MP: 41:36:23:1 acetonitrile: water: methanol: glacial acetic acid, detected at 425 nm and 262 nm for CUR and EST, respectively)	213
Table 5.2 Summary of HPLC method validation parameters for SP (MP: 80:20 acetate buffer (pH 4): Acetonitrile, detected at 260 nm)	214
Table 5.3 Pharmacokinetic studies of CUR-CS-PEC-NPs and free CUR	217

LIST OF EQUATIONS

Eq. 3.1: % EE% = $\frac{\text{Total CUR added} - \text{unbound CUR}}{\text{Total CUR added}} \times 100\%$	113
Eq. 3.2: % released CUR = $\frac{\text{Amount of released CUR}}{\text{Amount of CUR initially added}} \times 100\%$	114
Eq. 3.3: % CUR retained = $\frac{\text{Amount of CUR from determined from analysis}}{\text{Amount of added CUR}} \times 100\%$	117
Eq. 3.4: <i>Limit of Detection</i> = $3.3 \times \frac{\text{Standard deviation of low conc.}}{\text{Slope of curve}}$	126
Eq. 3.5: <i>Limit of Quantification</i> = $10 \times \frac{\text{Standard deviation of low conc.}}{\text{Slope of curve}}$	126
Eq. 5.1: %CV = $\frac{\text{Standard deviation (SD)}}{\text{Mean concentration}} \times 100\%$	187
Eq. 5.2: Relative error = $\frac{\text{mean measured concentration} - \text{true concentration}}{\text{True concentration}} \times 100\%$	187
Eq. 5.3: % Recovery = $\frac{\text{Mean concentration of drug in spiked plasma}}{\text{Mean concentration of pure drug solution}} \times 100\%$	188
Eq. 5.4: LOD = $\frac{3 \times \text{SD of the LC}}{\text{Slope of the calibration curve}}$	188
Eq. 5.5: LOQ = $\frac{10 \times \text{SD of the LC}}{\text{Slope of the calibration curve}}$	188

LIST OF ABBREVIATIONS

5-ASA	5-amino salicylic acid
5-FU	5-Fluorouracil
5-HETE	5-hydroxyeicosatetraenoic acid
AA	Acrylic Acid
ACF	Aberrant Crypt Foci
AFM	Atomic Force Microscopy
ATPase	Adenosine Triphosphatase
AUC	Area Under the Curve
BBB	Blood Brain Barrier
BCL-2	B-cell lymphoma
BDMC	bis-demethoxycurcumin
CAF	Caffeine
CAR	CAL27-cisplatin resistant
CEA	Carcinoembryonic antigen
C _{max}	Peak plasma concentration
C/LRP	Controlled/Living Radical Polymerization
CMC	Critical Micelle Concentration
CBMC	Carboxymethylcellulose
CS	Chitosan

CUR	Curcumin
CV	Coefficient of Variation
DAPI	4',6'-diamidino-2-phenylindole
DLS	Dynamic Light Scattering
DMCO	Demethoxycurcumin
DMEM	Dulbecco's Modified Eagle's Medium
DMSO	Dimethylsulfoxide
DSC	Differential Scanning Calorimetry
EC	Ethyl Cellulose
EE	Encapsulation Efficiency
ESF	European Science Foundation
EST	17- β -Estradiol
FBS	Foetal Bovine Serum
FESEM	Field Emission Scanning Electron Microscopy
FIT	Faecal immunochemical testing
FITC	Fluorescein Isothiocyanate
FOLFOX	5-fluorouracil plus oxaliplatin
FT-IR	Fourier Transform Infrared
FtsZ	Filamenting temperature-sensitive mutant Z
gFOBT	Faecal Occult Blood Testing

GIT	Gastrointestinal Tract
GST	Glutathione S-transferase
HAT	Histone Acetyltransferase
HC	High Concentration
HDACS	Histone deacetylases
HEPES	4-(2-hydroxyethyl)-1-piperazineethanesulfonic acid
HPLC	High Performance Liquid Chromatography
IBD	Inflammatory Bowel Diseases
IFN- α	Interferon- α
IGF	Insulin-like Growth Factor
IR	Infrared
IS	Internal Standard
K _a	Absorption Rate
K _{el}	Elimination rate
LC	Low Concentration
LCST	Lower Critical Solution Temperature
LDA	Laser Doppler Anemometry
LOD	Limit of Detection
LOQ	Limit of Quantification
MALDI-TOF	Matrix-assisted Laser Desorption/ionization- Time of Flight

MC	Mid Concentration
MP	Mobile Phase
mTOR	Mammalian target of rapamycin
MTT	(3-(4,5-dimethylthiazolyl-2)-2,5-diphenyl tetrazolium bromide)
NAG	NSAID-activated gene-I
NF- κ B	Nuclear factor κ B
NIPAAM	N-isopropylacrylamide
NrF2	Transcription Factor
PAA	Poly(acrylic acid)
PAMAM	Polyamidoamines
PBS	Phosphate Buffered Saline
PCL	Poly(epsilon-caprolactone)
PCS	Photon Correlation Spectroscopy
PDLLA	Poly(DL-Lactic acid)
PEC	Pectin
PGE ₂	Prostaglandin E ₂
pI	Isoelectric point
PIR	Piroxicam
PLA	Poly(lactide)

PLGA	Poly (Lactide-c-glycolide)
PLL	Poly(L-lysine)
PMMA-MMA	poly(methyl methacrylate-co-methacrylic acid)
PPI	Polyproplimines
PSMA	Prostate Specific-membrane Antigen
PVA	Polyvinyl Alcohol
PVP	Polyvinylpyrrolidone
RME	Receptor Mediated Endocytosis
RNS	Reactive Nitrogen Species
ROS	Reactive Oxygen Species
RP	Reversed phase
RPMI-1640	Roswell Park Memorial Institute – 1640 Medium
RSD	Relative Standard Deviation
SCF	Simulated Colonic Fluid
SD	Standard Deviation
SDH	Shikimate dehydrogenase
SELDI-TOF	Surface-enhanced Laser Desorption/ ionization- Time of Flight
SEM	Scanning Electron Microscopy
SGF	Simulated Gastric Fluid

SIF	Simulated Intestinal Fluid
SLN	Solid Lipid Nanoparticles
SP	Sulphapyridine
SSZ	Sulphasalazine
$T_{1/2}$	Elimination half-life
TBARS	Thiobarbituric acid relative substances
T_c	Crystalline Transition Temperature
THF	Tetrahydrofuran
T_{max}	Time of occurrence
TP	Theophylline
TPP	Sodium Tripolyphosphate
TSGs	Tumour-suppressor genes Guaiac-based
UV	Ultraviolet
VP	Vinylpyrrolidone
WHO	World Health Organization
XRD	X-Ray Diffractometry

ABSTRACT

Curcumin, the active constituent of the rhizome *Curcuma longa* has been extensively studied as an anticancer agent for various types of tumours. However, its efficacy as an anticancer agent is constrained due to poor absorption, rapid metabolism, degradation in acidic media and consequently, low oral bioavailability. In the present study, we aim to formulate a curcumin-containing mucoadhesive nanoparticulate delivery system that offers protection to curcumin from the degradative effects of the upper digestive tract system but capable of releasing the payload in the colon for the localised treatment of colorectal cancer. Such a system should have a good surface coverage locally at the tumour site and ideally, capable of traversing the tumour. Thus, nanoparticulate delivery is most suited to achieve this objective. The latter was formulated using chitosan and pectin as polymers due to their biodegradability and non-toxicity. The objectives of this study were (i) to fabricate, optimize and characterize the curcumin-containing delivery system; (ii) to evaluate the mucoadhesive propensity, release of curcumin from the carrier, and stability of the formulation in various milieu; (iii) to investigate the *in vitro* antiproliferative efficacy of the formulation as well as the cellular uptake profiles; and (iv) to proof the concept of the formulation using animal modules. The formulated nanoparticulate system had a z-average of 206.0 nm (\pm 6.6 nm), zeta potential of +32.8 mV (\pm 0.5 mV), and encapsulation efficiency of 64%. The nanoparticles were more mucoadhesive at alkaline pH compared to acidic pH. Furthermore, more than 80% release of curcumin was achieved in simulated colonic medium as opposed to negligible release in simulated gastric and intestinal fluids, respectively. The nanoparticles were taken-up by HT-29 colorectal cancer cells which ultimately resulted in a tremendous reduction in cell propagation. This anti-proliferative effect of the encapsulated curcumin was similar to that of free curcumin at equivalent

doses which confirms that the encapsulation process did not affect the anticancer efficacy of curcumin. The bioavailability of curcumin from the nanoparticles was enhanced by 4-folds after oral administration after 6 hr of treatment. Moreover, the half-life, C_{max} , and AUC of curcumin were significantly improved. A lower elimination rate was observed from the formulation compared to equivalent doses of free curcumin. These findings are a strong indication of the potential of the studied formulation for the possible treatment of colon cancer via oral administration.

Chapter 1

Introduction

1 Introduction

1.1 General Overview

According to the World Health Organization (WHO) media centre key facts, 8.2 million deaths occurred worldwide in 2012 because of cancer, making it the leading cause of death among diseases. Unfortunately, the annual cancer cases are expected to jump up to 22 million in two decades from 2012 where it was 14 million case in that year (WHO media Center, 2014).

Despite recent advances in cancer therapy, treatment remains a challenging task. For example, surgery is associated with high risk of damage to nearby organs and tissues, pain, infections and recurrence of the disease (Bornstein *et al.*, 1991; Cohen *et al.*, 2000; Crawford *et al.*, 2005; Gamba *et al.*, 1992). While radiation therapy has common side effects like skin changes, fatigue, diarrhoea, nausea and vomiting and many others, which may affect the patient's quality of life (Bentzen, 2006; Dearnaley *et al.*, 1999; Scholefield & Eng, 2014). Chemotherapy, being one of the most common cancer treatment options as neoadjuvant, adjuvant, or the sole therapy given has manifests serious side effects, including fatigue, pain, sores in the mouth and throat, nausea and vomiting as well as blood disorders (Farrell *et al.*, 2013; Groopman & Itri, 1999; Molassiotis *et al.*, 2014).

Plants have been extensively studied as a natural source for cancer treatment due to their proved efficacy in treating many types of cancer and the advantage that they manifest fewer side effects compared to the chemotherapeutic agents (Bhanot *et al.*, 2011; Nirmala *et al.*, 2011; Pezzuto, 1997).

Curcumin (CUR), commonly known as turmeric, is a natural polyphenol derived from rhizome of the plant *Curcuma longa* is one of the plant agents that has

showed anti-cancer activity through researches in the last 50 years (Adams *et al.*, 2004; Kanai *et al.*, 2012; Tang *et al.*, 2010). Although CUR has an effective and safe colon anticancer activity (Cheng *et al.*, 2013; Howells *et al.*, 2011; Mudduluru *et al.*, 2011), its beneficial effects are limited due to low absorption efficacy, rapid metabolism and elimination (Anand *et al.*, 2012). Hence, there is the need to enhance the oral bioavailability of CUR via appropriate strategies. Using adjuvants like piperine, the oral bioavailability and delivery of CUR was improved by piperine inhibiting CUR's metabolizing enzymes (Bhutani *et al.*, 2009; Yallapu *et al.*, 2012). Micelles, liposomes and phospholipids complexes are other strategies under investigation (Anand *et al.*, 2007). Recently, nanoparticle technology had a special interest as a drug delivery system for therapeutic agents (Yih and Al-Fandi, 2006; Hamidi *et al.*, 2008) and explored for CUR as well. Poly(lactide-co-glycolide) (PLGA) based CUR nanoformulations were successful (Khalil *et al.*, 2013) as well as chitosan (CS) CUR nanoparticles (NPs) (Chuah *et al.*, 2011) and CUR loaded fibrinogen NPs (Sanoj *et al.*, 2011).

We believe that delivering CUR in NPs to the colon is a good strategy for increasing the bioavailability at that region. In this regard, the delivery system should have the ability of protecting CUR from the onslaught acids and enzymes through its journey from the mouth to the colon. Since the cancer is restricted to the colon in colorectal cancer there is the likelihood of enhanced therapy with such a system. In a previous study, CUR-CS NPs were successfully fabricated in which these NPs demonstrated good mucoadhesive and anticancer properties (Chuah *et al.*, 2011). In that study the effect of acid and enzymatic conditions on the mucoadhesive and anticancer properties of the NPs are not ascertained. The aim is to develop a nanoparticulate delivery system with enhanced mucoadhesive properties and able to

withstand the acidic and enzymatic conditions of the upper gastrointestinal tract (GIT).

We also aim to prove the concept of the formulation using animal modules.

1.2 Colon and Colorectal Cancer

1.2.1 The Human Colon

The human colon (large intestine) is a muscular, U-shaped tube approximately 1.5 meters long in an average size adult. The colon is a part of the lower GIT that extends from the ilocaecal valve to the rectum.

The human colon (Figure 1.1) consists of the ascending and transverse segments, in which are the posterior segments, which lack mesentery. This is followed by the descending and sigmoid segments, which are the anterior and have mesentery. The four segments of the colon are sacculated. The caecum is poorly determined and continuous within the human colon (Kararli, 1995; Moran & Jackson, 1992) .

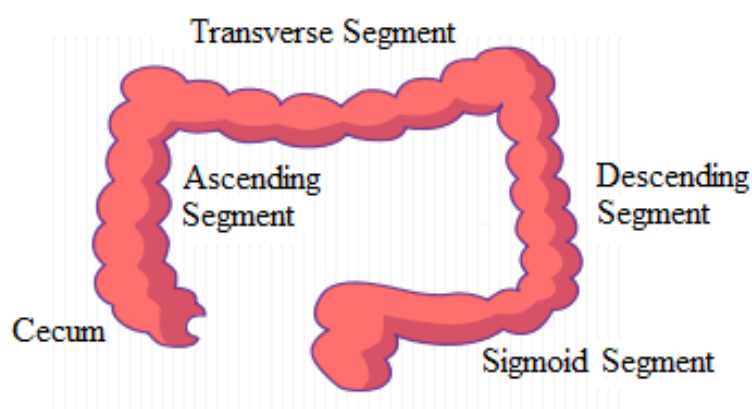


Figure 1.1 The structure of the colon (*Drawn using Chemdraw® Pro 8.0, PerkinElmer*).

The wall of the colon, in cross-section, encompasses of a fine mucosal layer, thicker submucosal layer and the muscularis mucosae. The later comprises of two distinct layers, the circular and outer longitudinal layer, separated by a thin layer of connective tissues. Moreover, the muscularis mucosae is opulent with perirectal fat

(Brown, 2007). Compared to the small intestine, the colon luminal surface lacks well-defined villi, is less closely packed microvilli (if present) and does not differentiate into enterocytes (Kararli, 1995).

The colon develops during the embryological development phase from two parts: the ascending colon to the proximal transverse colon develops from the midgut while the distal transverse colon to sigmoid colon develops from the hind gut (Snell, 2008). The development subsists in three rotational phases. In the first phase, also called the temporary physiological intestinal herniation, the umbilical loop undergoes counter-clockwise 90° rotation. This phase occurs in the 8th week of the embryological development. Followed by the second phase at the 10th week where a new counter-clockwise 90° rotation occurs. Finally, the third stage, fixation stage, starts between the 11th and 12th week and ends with birth (Baud *et al.*, 2008; Engin, 2015).

The pH values of the colonic fluids are 7.0 ± 0.7 , 6.6 ± 0.8 and 6.4 ± 0.6 in the left, mid and right colon, respectively. The colon pH depends highly on the type of the ingested food (Evans *et al.*, 1988; Kararli, 1995). Transit time of food in the colon varies from 8-72 hr (Kararli, 1995).

The colon has various functions including water and electrolyte absorption, storing and evacuating stool, cistern function for bacterial metabolism and fermentation and metabolic functions. Approximately 1.5 L of materials passes through the colon daily, in which 1.3-1.4 L is absorbed and 0.1-0.2 L stool water is evacuated daily. The storage sites of the colon are the ascending and transverse segments while the aqueduct function is mainly executed by the descending and sigmoid segments (Kararli, 1995; Moran & Jackson, 1992). Within the GIT, the colon has the most abundant number and variety of microorganisms, approximating 7-10 log per gram per weight compared to

0-5 and 0-7 log per gram per weight in the stomach and small intestine, respectively. The colonic normal flora comprises of over 400 different species in which the anaerobic predominate, accounting for 99% of the cultivable organisms throughout the GIT. The beneficial bacteria in the colon play a major role in producing a variety of B-vitamins, folate and sulphur-containing amino acids that are absorbed from the colon. These bacteria also produce short chain fatty acids which contribute in the growth of the colonic mucosa and contribute in metabolism such as the hydrolysis of glucuronide conjugates (Canny & McCormick, 2008; Finegold & Angeles, 1969; Kararli, 1995; Moran & Jackson, 1992).

Colonic dysfunction may be manifested as motility or mucosal diseases. The former includes diarrhoea, constipation, irritable bowel syndromes and diverticular disease, while the latter includes polyps, inflammatory bowel disease (IBD), colonic infestation and carcinoma (Moran & Jackson, 1992). In the next section, I shall present salient features related to colorectal cancer and how it relates to the present investigation.

1.2.2 Colorectal cancer

According to the WHO media center (2014), colorectal cancer was the third most common type of cancer amongst men and the second amongst women leading to 694,000 worldwide deaths for the year 2012. In England, colorectal cancer was the fourth most common type of cancer in 2013, accounting for 12.6% and 10.4% of the registered cancer cases in males and females, respectively (Cancer registration statistics, 2015). In Malaysia, colorectal cancer is the most common type of cancer in males whilst it is the second one in females (Veetil *et al.*, 2017).

Most colorectal tumours arise from benign adenomatous polyps from the mucosa followed by subsequent changes within the cells lining the bowels, eventually, leading to a malignant transformation and invasive carcinoma. In rare cases, some types of benign and malignant colorectal tumours may arise from other cell types like lymphocytes and muscles (Brown, 2007; Irving *et al.*, 2010; Scholefield & Eng, 2014).

The etiological factors causing colorectal cancer are various including environmental, genetic susceptibility and somatic changes during the initiation and progression of benign adenomatous polyps from the mucosa. Several studies aimed at identifying specific genes causing colorectal cancer have presented two types of molecular defects: alterations in several oncogenes (K-ras) and alterations on tumour-suppressor genes (TSGs) (Brown, 2007).

Age is a major risk factor in colorectal cancer incidences and death rates. Over 90% of new colorectal cancer cases occur in patients at 50 years and older. However, since the 1990s, new colorectal cancer incidences have occurred in patients younger than 50 as well. Worldwide, men are at a greater risk of developing colorectal cancer than women. Although specific reasons for differences in incidence rates and mortality among gender are not well-understood but could be related to hormonal, genetic and environmental interaction (Gao *et al.*, 2008; Scholefield & Eng, 2014). Colorectal cancer incidence rates and mortality vary geographically, where the highest rates are found in the developed and high-income countries like Australia and Canada, whilst presentation is generally lower in the developing countries (Fatima & Robin, 2009; Scholefield & Eng, 2014). However, this statistic is bound to change due to affluence in some previously categorised 'low-income' countries due to affluence or modifications in lifestyle. Although family history of colorectal cancer does not increase the rate of incidence of colorectal cancer through genetic predisposition, it is

nonetheless a major risk factor since it combines genetic and environmental factors to trigger manifestation. Having a first-degree relative diagnosed with colorectal cancer may double the risk of having the disease (Scholefield & Eng, 2014). Patients with a history of adenoma, prior colorectal cancer, prior large polyps, IBD, especially patients with history of long duration ulcerative colitis are at increased risk of developing colorectal cancer in their lifetime (Eaden *et al.*, 2001; Gupta *et al.*, 2007; Scholefield & Eng, 2014). Recent studies (Larsson *et al.*, 2005; Deng *et al.*, 2012; Shikata *et al.*, 2013) have strongly supported the association between *diabetes mellitus* and the increased risk of developing colorectal cancer in both men and women. Two mechanisms have been proposed: (i) inhibition of insulin-like growth factors (IGF) binding proteins, which increases the free and bioavailable IGF-I, and (ii) increased concentrations of faecal bile acids (Larsson *et al.*, 2005; Shikata *et al.*, 2013). However, long-term insulin therapy has also been associated with increased risk of colorectal cancer as well (Larsson *et al.*, 2005; Deng *et al.*, 2012; Shikata *et al.*, 2013). Several modifiable lifestyle risk factors immensely increase the incidence rates of colorectal cancer including heavy alcohol consumption, smoking, red and processed meat consumption, obesity, and low physical activity (Fedirko *et al.*, 2011; Huxley *et al.*, 2009; Kirkegaard *et al.*, 2010; Ogino & Stampfer, 2010).

A third of colorectal cancer cases, especially at the early stages of the disease, are asymptomatic. Moreover, other bowel diseases such as ulcerative colitis, diverticulosis and irritable bowel syndrome manifest symptoms similar to those with colorectal cancer. Some of the symptoms associated with colorectal cancer are abdominal pain, change in bowel habit, and rectal bleeding. Moreover, most of the patients are diagnosed with anaemia and positive faecal occult blood tests. Other symptoms include fatigue, anorexia, diarrhoea, constipation, nausea, vomiting, rectal

pain, and the presence of mucus in stools. Studies have shown no association between the symptoms of the disease and age or gender of the patient. However, some symptoms can be correlated with the location of the disease (Majumdar *et al.*, 1999). The presence of anaemia besides any other symptom of fatigue, anorexia, abdominal pain, nausea, or vomiting is associated with proximal colorectal cancer. While the presence of altered stool consistency, rectal bleeding besides any other symptom of diarrhoea, rectal pain, tenesmus, or mucus in stools are associated with distal colorectal cancer (Majumdar *et al.*, 1999; Miskovitz & Betancourt, 2005; Adelstein *et al.*, 2011). In some cases, patients may have phlebitis and pulmonary embolism because of the breaking and lodging of blood clots in one of the vessels feeding the lungs during its migration through the veins back to the heart. Disruptions to the immune system before, during, or after colorectal cancer diagnosis cause shingles. In advanced stages, the cancer may metastases to the other organs in which organ-specific symptoms appear. For example, symptoms of cancer spreading to the liver include jaundice, low blood concentration of albumin, coagulation disturbances, bleeding, and pain localized in the upper-right part of the abdomen, which may radiate to the back or the right shoulder. If the colorectal cancer has spread to the lungs, symptoms start as a simple cough that increase in intensity, accompanied with blood, shortness of breath, tightness and chest discomfort at later stages (Adrouny, 2002).

Early detection and accurate diagnosis of colorectal cancer are major prognostic factors for optimal treatment and higher survival rates. Since colorectal cancer symptoms appear at a later stage of the disease, regular population screening is essential for early detection of colorectal cancer. However, physical examination, including abdomen palpitation and digital rectal exam cannot detect the signs of colorectal cancer. Therefore, specific colorectal cancer screening procedures ought to be used (Miskovitz,

2010; Steele & McDonald, 2014). Guaiac-based faecal occult blood testing (gFOBT) technology has been used for several years. Guaiac is capable of detecting peroxidase activity of haem but not the degradation products of haem. Besides, Guaiac does not detect dietary haem. The gFOBT technology is more sensitive in detecting bleeding lesions in the colon compared to the upper GIT. However, gFOBT has low clinical applications due to the low analytical sensitivity and the fact that bleeding is intermittent in colorectal cancer cases in general (Scholefield & Eng, 2014). Faecal immunochemical testing (FIT) assays the antibodies targeting human haemoglobin. Qualitative and quantitative FIT tests are available which are specific for human haemoglobin. However, qualitative FIT analytical sensitivity is low and hence, results in high false positive rates. Furthermore, haemoglobin quantification has low accuracy and varies among different faecal compositions. However, the usage of gFOBT in combination with FIT reduces the false positive rates (Scholefield & Eng, 2014). Flexible sigmoidoscopy has been proposed as the primary screening method for colorectal cancer at the age of 60, along with adenomas removal. A highly specific and sensitive screening modality is the colonoscopy, providing visualization of the large bowel besides the ability to remove the adenomas. In addition, colonoscopy is highly sensitive in polyp detection. However, using colonoscopy in the population screening is still controversial. Besides this, both of the flexible sigmoidoscopy and colonoscopy are, in some cases, associated with morbidity and mortality (Scholefield & Eng, 2014). New promising screening approaches have recently been developed, including, the DNA microarray-based tumour gene expression profiles, DNA methylation measurements of specific protein panels (Ramaswamy *et al.*, 2001). Others include detection of specific RNAs associated with colorectal cancer, using techniques like surface-enhanced laser desorption/ ionization - Time of flight (SELDI-TOF) and

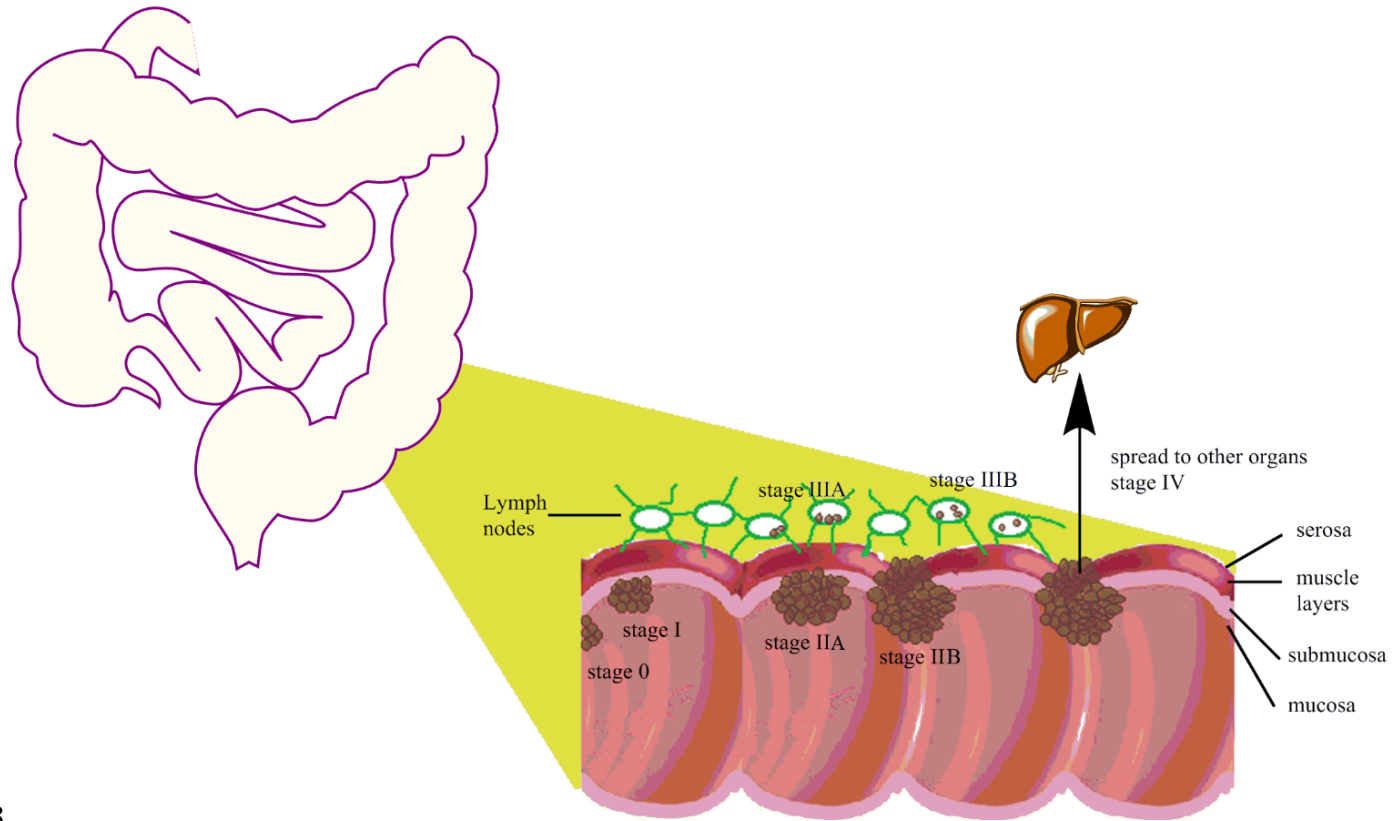
matrix-assisted laser desorption/ionization - Time of flight (MALDI-TOF), mass spectrograph and trained Labrador retriever to detect colorectal cancer by the smell of breadth and watery stool (Ramaswamy *et al.*, 2001; Scholefield & Eng, 2014). Once invasive colorectal cancer has been diagnosed, pathologists will recommend further pathological examinations. Surgical biopsy of the colon and lymph nodes are usually recommended for studying the spread and prognosis of the disease (Miskovitz, 2010).

The stage in the development of colorectal cancer is fundamental in determining the optimum treatment plan and prognosis. Dukes *et al.*,(1932) established the first colorectal cancer staging. Dukes' classification is based on the depth of colorectal cancer in the bowel wall, in addition to the embroilment of nearby lymph nodes. Colorectal cancer that does not exceed the mucosa is classified as stage A. Stage B involves deeper tissues but outside the rectum and without the involvement of the lymph nodes whilst stage C involves the lymph nodes. A later modification of Dukes' classification is called the Astler-Coller modification which includes stage D, where the colorectal cancer spreads to other organs (Adrouny, 2002). Further modification and specifications of Dukes' classification led to the current staging system, the TNM staging system, adopted by the American Joint Committee for Cancer Staging and End Results. This staging system is categorized into three junctures. The T stage (T) reflects the size and extent of spreading of the cancer to the nearby tissues and organs. Second category symbolized (N), reflects the involvement of the nearby lymph nodes. The final stage (M), shows the presence or absence of cancer spreading to distant areas of the body (Miskovitz, 2010). After determining the TNM category, another staging process, called the stage grouping, is further determined. The stage grouping phases are summarized in Table 1.1 and illustrated in Figure 1.2 (American Cancer Society, 2004; Connell *et al.*, 2004). Regardless of the stage in the colorectal cancer, the location of

the tumour is another prognostic determinant. Colon carcinomas might be easier to recover compared to rectal carcinoma at the same stage of development. Moreover, within the colon itself, the ascending and sigmoid colon carcinomas have better recovery outcomes compared to the transverse and descending colon carcinoma at the same stage (Miskovitz, 2010).

Table 1.1 Colorectal cancer stages

Stage	Description	5-year survival rate
Stage 0	Earliest stage of cancer, in which has not exceeded the mucosa of the colon or rectum. Also called <i>carcinoma in situ</i> or intramucosal carcinoma.	>90%
Stage I	The cancer has penetrated the mucosa into the submucosa or into the muscularis propria yet, has not spread to the nearby lymph nodes or distant areas.	93.2%
Stage IIA	The cancer has penetrated the wall of the colon or rectum into the outermost layers yet, has not spread to the nearby lymph nodes or distant areas.	84.7%
Stage IIB	The cancer has penetrated the wall of the colon or rectum into other nearby tissues or organs yet, has not spread to the nearby lymph nodes or distant areas.	72.2%
Stage IIIA	The cancer has penetrated the mucosa into the submucosa or into the muscularis propria and has spread to one to three nearby lymph nodes. Distant areas are not involved.	83.4%
Stage IIIB	The cancer has penetrated the wall of the colon or rectum into other nearby tissues or organs and has spread to one to three nearby lymph nodes. Distant areas are not involved.	64.1%
Stage IIIC	The cancer has spread to four or more nearby lymph nodes regardless of extent of penetration in the colon or rectum. Distant areas are not involved.	44.3%
Stage IV	The cancer has spread to distant areas like lung, liver, ovary or peritoneum regardless the extent of penetration in the colon or rectum and nearby lymph nodes involvement.	8.1%



3

Figure 1.2 Colorectal cancer stages (Drawn by Chemdraw®Pro 8.0, PerkinElmer and Microsoft paint® 1709)

On the basis of the progression of the disease, colorectal cancer treatment and prognosis depend on the depth of the tumour, the extent of lymph node's involvement, and the metastases of the disease to other organs (Miskovitz, 2010). The standard treatment options for colorectal cancer are surgery, radiofrequency ablation, cryosurgery, chemotherapy, radiation therapy and targeted therapy (Solbiati *et al.*, 2001; Miskovitz, 2010; Berman *et al.*, 2016; Martling *et al.*, 2016). Surgery, is the standard treatment option for all stages of colorectal cancer, in addition to liver metastasis and recurrent disease cases (Berman *et al.*, 2016). Surgery can be performed either as a local excision, colon resection or laparoscopic surgery (Miskovitz, 2010; Brown, 2007). Postoperative side effects include pulmonary complications, abnormal wound healing, bowel perforation, abscesses, fistula, haemorrhage, infection, and sexual dysfunction and urinary retention in men (Milsom *et al.*, 1998; Miskovitz, 2010; Scappaticci *et al.*, 2005). Radiation therapy is another local treatment option for stages II and III (Table 1.1), however it is usually used as an adjuvant treatment with chemotherapy, pre- or post-surgery to decrease the local recurrence and increase survival rates (Birgisson *et al.*, 2005; Miskovitz, 2010; Berman *et al.*, 2016). Unfortunately, radiation therapy is associated with long-lasting side effects including impotency in men and vaginal dryness in women (Miskovitz, 2010). Other side effects of radiation therapy include gastrointestinal complications, bowel obstruction, skin irritation, fatigue and the occurrence of a secondary primary cancer (Birgisson *et al.*, 2005; Martling *et al.*, 2016; Miskovitz, 2010). Chemotherapy has been used for colorectal cancer treatment since the 1950s. It is the standard treatment option for stages III and IV (Table 1.1), liver metastases and recurrent colorectal cancer and it is usually administered as an adjuvant with surgery or radiation therapy (Miskovitz, 2010; Berman *et al.*, 2016). Numerous chemotherapeutic agents are used for colorectal cancer

either as a mono or combined therapy including 5-fluorouracil (5-FU), irinotecan, capecitabine, leucovorin, and oxaliplatin (Cutsem *et al.*, 2015; Miskovitz, 2010). Unfortunately, chemotherapy is associated with a long list of debilitating side effects including nausea, vomiting, diarrhoea, sore mouth, myelosuppression, immunosuppression, hair loss (Coates *et al.*, 1983; Wu *et al.*, 2005), mucositis (Buhl *et al.*, 1999), hepatotoxicity (Rubbia-Brandt *et al.*, 2004), and anemia (Groopman & Itri, 1999). The radio-frequency ablation is an image-guided procedure that includes the ablation of the tumour using ion agitation produced by electrodes. Intraperitoneal haemorrhage, hepatic abscesses, GIT perforation, and portal hypertension (Livraghi *et al.*, 2003; Solbiati *et al.*, 2001; Wood *et al.*, 2000). In cryosurgery, tumours are frozen using cryoprobes and left to be reabsorbed. Although this technique sacrifices less normal tissues compared to surgery, it cannot be used in multiple metastases cases (Onik *et al.*, 1991). Cryosurgery is associated with a phenomenon called “cryoshock phenomenon” which includes multi-organ failure, intravascular coagulation and severe coagulopathy, besides liver failure, abscess, bile fistula, and wound infection (Seifert & Morris, 1998; Seifert *et al.*, 1999). Immunotherapy is a new approach in which antibodies are used to help the patient’s immune system fight cancer cells. Side effects include flu-like symptoms, nausea, vomiting, diarrhoea, and rash (Miskovitz, 2010). Due to the aforementioned side effects associated with chemotherapy, there is an interest in discovering alternative agents that are just as effective but manifest fewer side effects. It has been proposed that chemotherapeutic agents from plant origin fit this requirement because they are natural. In the next section, I would describe in detail some of the salient features of one such compound, CUR, that has received significant attention in the past decade.

1.3 Curcumin

Turmeric (Figure 1.3), the powdered rhizome of the plant *Curcuma longa*, has been anciently used in the Indian subcontinent as food preservative, dye due to its distinctive yellow colour, and as a spice (Aggarwal *et al.*, 2007). Starting from the time of Ayurveda (1900 BC), turmeric was therapeutically used as an anti-inflammatory, wound healing, scars lightening, in cosmetics (Aggarwal *et al.*, 2007), cure for jaundice, digestive enhancer, appetite suppressant, treating stomach and liver problems, and in cosmetics (Steinhauser, 2015; Wattenberg *et al.*, 1992). Arab merchants introduced turmeric to Europe in the 13th century and was named “Indian saffron” (Aggarwal *et al.*, 2007).

Researchers have found that CUR (diferuloylmethane) (3%) is the active ingredient of the spice turmeric and is responsible for its therapeutic activities (Steinhauser, 2015). CUR currently a subject of extensive studies due to acclaimed variety of therapeutic potential including anti-inflammatory, antiangiogenic, chemotherapeutic, antioxidant, hepatoprotective, immunomodulation, treatment of arthritis, lung fibrosis, gallstone, cardiovascular disease, among others (Ravindran *et al.*, 2007; Braun & Cohen, 2010; Aggarwal *et al.*, 2007).



Figure 1.3 Turmeric (*adopted from www.authoritynutrition.com*)

1.3.1 Chemical Properties of Curcumin

The chemical profile of turmeric indicates a composition of several phytochemicals including CUR, demethoxycurcumin (DMCO), bis-demethoxycurcumin (BDMC), turmerone, and curnone (Sasikumar, 2012). In addition to other nutrients including protein, carbohydrates, phosphorous, and potassium, among others (Hegde *et al.*, 2013; Nair, 2013). However, it is believed that the curcuminoid, CUR, imparts the distinctive yellow colour to turmeric and is responsible for the wide variety of the therapeutic activities of the spice (Hegde *et al.*, 2013).

CUR has a bright yellow colour even at very low doses (Boga *et al.*, 2013; Nair, 2013). It gives red and yellow coloured solutions in basic and acidic media, respectively (Bernabé-pineda *et al.*, 2004). It is reported to have a UV-absorption maxima at 420-430 nm, attributed to its conjugated diaryl heptanoid chromophore (Bernabé-pineda *et al.*, 2004; Nair, 2013; Sasikumar, 2012). CUR also exhibits fluorescence under UV light, and it has a distinct fluorescent excitation and emission at 435 and 520 nm, respectively (Nair, 2013; Park & Lee, 2015; Priyadarsini, 2009).

CUR was first isolated and obtained from turmeric in the 19th century (Aggarwal *et al.*, 2007) and is estimated to comprise of 2-7% of turmeric constituents (Sasikumar, 2012). The chemical structure of CUR is 1,7-bis (4-hydroxy-3-methoxy-phenyl)-1,6-heptadiene-3,5-dione (Figure 1.4) (Sharma *et al.*, 2005; Chen *et al.*, 2006; Maheshwari *et al.*, 2006; Sasikumar, 2012).

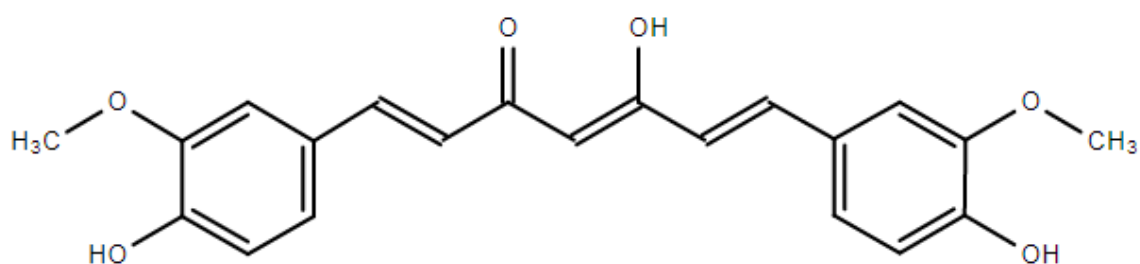


Figure 1.4 Chemical structure of CUR

The molecular formula of CUR is C₂₁H₂₀O₆, its molecular weight is 368.39 Da (Hegde *et al.*, 2013; Lin & Lin, 2008). It has a melting point of 183 °C (Aggarwal *et al.*, 2006) and pKa values of 7.8, which is attributed to the acetylacetone group, 8.5 and 9.0 which are attributed to the hydrogen of the phenol groups (Hjorth *et al.*, 2002; Bernabé-pineda *et al.*, 2004). It acts as a potent H-atom donor at pH 3-7, whereas it mainly acts as an electron donor at pH above 8 (Barzegar, 2012). This therapeutic agent is insoluble in water, however, it is easily soluble in ethanol and acetone (Hjorth *et al.*, 2002; Hegde *et al.*, 2013). Since it is a bis- α,β -unsaturated diketone, it exists in equilibrium with the corresponding tautomer in solution. This bis-keto form predominates in acidic and neutral conditions, while the enol tautomer predominates at pH values above 8 (Aggarwal & Sung, 2008; Anand *et al.*, 2008; Boga *et al.*, 2013). In alkali conditions, CUR dissociates forming feruloyl methane, ferulic acid, and vanillin

(Hjorth *et al.*, 2002; Nair, 2013). CUR has the ability to dimerise into at least two dimeric species (Daniel *et al.*, 2004).

Stability-wise, CUR is considered unstable and especially pH dependant. It is least stable at acidic conditions (Bernabé-pineda *et al.*, 2004; Manju & Sreenivasan, 2011; Shen & Ji, 2012). In addition, CUR has poor photostability (Hjorth *et al.*, 2002). *In-vitro* studies showed that CUR undergoes degradation in cell culture medium containing 10% foetal bovine serum (FBS) (Shen & Ji, 2012). Unfortunately, there are not that many studies aimed at studying the stability of CUR. *In vivo*, however, dihydroferulic acid and ferulic acid have been identified in the bile after oral administration of CUR which reflects its degradation (Shen & Ji, 2012). Surprisingly, some of CUR's degradation products like ferulic acid and vanillin have higher aqueous solubility compared to the parent and hence, similar biological activities (Shen & Ji, 2012).

1.3.2 Therapeutic Properties of Curcumin

Research in recent years has focused on the therapeutic effects of CUR as an alternative to several pharmacological activities (Priyadarsini, 2014). Several studies have confirmed the efficacy of CUR as an anti-inflammatory, antimalarial, antibacterial, antioxidant, and anticancer agent (Biology *et al.*, 2009; Priyadarsini, 2014; Epstein *et al.*, 2017).

Available preparations of CUR for research and clinical trials contain three major curcuminoids, difruloyl methane commonly known as curcumin (CUR), DMCO, and BDMC (Jurenka & Ascp, 2009). Comparative studies have shown different therapeutic potencies for the three analogues. For example, Rubya *et al.*, (1995) found that BMDC is the most potent cytotoxic agent amongst the three analogues. Whereas

Tamvakopoulos *et al.*,(2007) found that DMC was the most stable in cultured cells and most potent as an anticancer agent when compared to the other two analogues. Wei *et al.*,(2006) found that the three analogues have similar antioxidative activities. In contrast, Selvam *et al.*,(2005) found that CUR was more potent as an antioxidant and antiinflammatory agent. Anand *et al.*,(2008) compared various therapeutic activities of the three analogues and found that BDMC is the most potent cytotoxic agent against ovarian cancer cells, DMC is the most potent antiproliferative agent against breast cancer cells, and BDMC and CUR have similar efficacies in preventing colon carcinogenesis. In the next section, I shall give a detailed review of the diverse therapeutic activities of CUR.

1.3.2.1 Antioxidant activity

Oxygen is an obligatory element for living cells and it is contributed in the majority of the crucial biological activities (Sen *et al.*, 2010; Shinde *et al.*, 2012). However, during cellular utilization of oxygen, two major types of by-products called free radicals are produced, reactive oxygen species (ROS) and reactive nitrogen species (RNS) (Sen *et al.*, 2010). ROS includes free radicals and non-radical molecular species (like H₂O₂) (Lushchak, 2014). Free radicals are produced when electrons from the reactive enzymes are transferred to molecular oxygen. Therefore, the oxygen molecule contains one or more unpaired electrons in the outermost orbital (Halliwell, 2012; Kunwar & Priyadarsini, 2011). Besides this, free radicals can be introduced to the body by external factors including UV radiation, cigarettes smoking (Shinde *et al.*, 2012), X-rays, pollutants, interaction with chemicals (Sen *et al.*, 2010), auto-mobile fumes, burning of organic matter during cooking, to mention few (Lobo *et al.*, 2010).

Free radicals are generally involved in chain reactions and are eventually terminated by their destruction (Sen *et al.*, 2010). They are biologically eliminated through a complicated antioxidant system that neutralize the excessive levels of free radicals (Lushchak, 2014). This system includes enzymes such as catalases, superoxide dismutases, and glutathione peroxidases (Sen *et al.*, 2010) in addition to non-enzymatic molecules like albumin, ceruloplasmin, ferritin, and lactoferritin (Bayomi *et al.*, 2013). Normally, a balance between free radical formation and elimination is preserved, however, disturbing this steady state leads to excessive build-up of free radicals leading to a condition called oxidative stress. In this state, serious cellular structural changes and cellular mutations occur (Shinde *et al.*, 2012). The prolonged state of oxidative stress leads to the development of chronic and degenerative diseases such as aging, arthritis, cancer, haemorrhage, hypoxia, cardiovascular and neurodegenerative diseases (Sen *et al.*, 2010; Shinde *et al.*, 2012; Bayomi *et al.*, 2013; Trujillo *et al.*, 2013).

CUR shows a distinctive antioxidant activity similar to those of vitamins C, E and β -carotene (vitamin A) through several pathways (Akram *et al.*, 2010). The phenolic group of CUR scavenge free radicals and hence, prevent lipid peroxidation (Lim *et al.*, 2001; Ataie *et al.*, 2010). In addition, CUR acts indirectly through the interaction with the reactive species to induce the activity of antioxidants and cytoprotective enzymes (Bhullar *et al.*, 2013; Nakmareong *et al.*, 2011; Trujillo *et al.*, 2013). For instance, Nakmareong *et al.*,(2011) found that CUR stimulates vasorelaxation of the isolated porcine coronary artery in addition to its ability to prevent and treat vascular dysfunction in lipopolysaccharide induced endotoxemia.

1.3.2.2 *Anti-Malarial activity*

Malaria, a disease caused by the plasmodium parasite, is an epidemic and deadly disease effecting 300- 500 million individuals every year (Reddy *et al.*, 2005; Mishra *et al.*, 2009; Mimche *et al.*, 2011). Quinine and artemisinin are the drugs of choice for malaria treatment (Mimche *et al.*, 2011). However, malaria remains a frightening worldwide epidemic partially due to the parasite's resistance to available anti-malarial drugs (Cui *et al.*, 2007). Moreover, use of current anti-malarial drugs is restrained due to high cost, short half-life, and limited supply (Reddy *et al.*, 2005; Mishra *et al.*, 2011). Therefore, there is an urgent need to find alternative treatment regimens or develop newer antimalarial drugs and combinational cocktails to overcome drug resistance.

Recent *in vitro* and *in vivo* studies have found that CUR possesses moderate to potent anti-malarial activity through several pathways, including the following (Reddy *et al.*, 2005; Nandakumar *et al.*, 2006; Cui *et al.*, 2007; Mimche *et al.*, 2011):

- i. Down-regulation of histone acetyltransferase (HAT) and histone deacetylases (HDACs), that interferes with histone acetylation and hence, causes DNA damage.
- ii. Generation of ROS in malaria parasite, which induces DNA damage (peroxidant activity).
- iii. Binding to the malarial sarco endoplasmic reticulum calcium adenosine triphosphatase (ATPase) causing metabolic arrest.
- iv. Immunomodulatory activities.
- v. Anti-protozoan activity.

Recently, research has been devoted towards using CUR in combination with anti-malarial agents not only to overcome the latters' limited use, due to drug resistance,

recrudescence, and high cost, but also to enhance the therapeutic efficacy of both drugs and decrease cytotoxicity (Mishra *et al.*, 2009; Reddy *et al.*, 2005). For example, oral administration of CUR followed by artemisinin injection prevented retrogression of the disease (Nandakumar *et al.*, 2006). In another study, Mishra *et al.*,(2011) found that combination of CUR with andrographolide and artesunate enhanced andrographolide anti-malarial effect and decreased the chance of drug resistance without any toxicity.

1.3.2.3 *Anti-inflammatory activity*

Inflammation processes as such are essential for the body. For example, acute inflammation helps in pathogens prevention. However, chronic and untreated inflammations can eventually lead to cancer and other chronic diseases (Basnet & Skalko-basnet, 2011). Normally, pro-inflammatory factors target free radicals, NF- κ B, TNF- α , and NSAID-activated gene-1 (NAG) which, mediate the inflammation. Excessive and uncontrolled exposure to these molecules can lead to chronic diseases (Basnet & Skalko-basnet, 2011). Therefore, the use of anti-inflammatory agents such as NSAIDs, COX-2 inhibitors, and TNF- α inhibitors is necessary to avoid the debilitating effects of uncontrolled inflammation (Basnet & Skalko-basnet, 2011). In the last two decades, CUR has been extensively studied as a natural and potent anti-inflammatory agent for numerous inflammatory conditions, including pancreatitis, postoperative inflammation, rheumatoid arthritis, osteoarthritis (Jurenka & Ascp, 2009), uveitis, *H. Pylori* infections, irritable bowel syndrome, and IBD (Jacob *et al.*, 2007).

The anti-inflammatory effects of CUR is now established and several mechanisms have been proposed as summarized in Figure 1.5 (Chan *et al.*, 1998;

Kawamori *et al.*, 1999; Jacob *et al.*, 2007; Jurenka & Ascp, 2009; Basnet & Skalko-basnet, 2011).

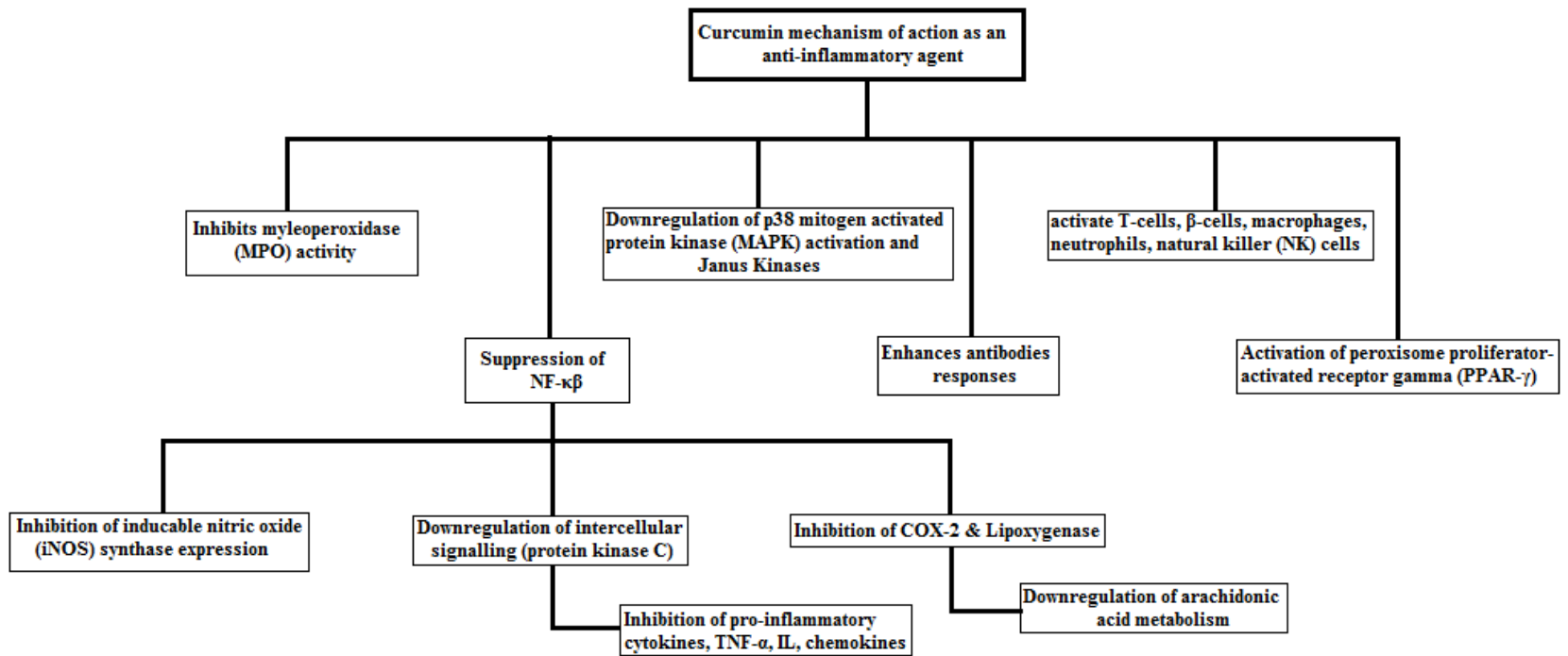


Figure 1.5 CUR mechanisms of action as an anti-inflammatory agent

1.3.2.4 Anti-bacterial activity

The world is facing a major challenge in antibiotic resistance. The continuous evolution of antibiotic resistance is due to therapeutic use, misuse, and abuse of antibiotics (Mun *et al.*, 2013). In addition, ineffectiveness, unfavourable adverse effects, non-compliance, and high cost of conventional therapy have changed the path of antibacterial research towards developing natural alternatives such as CUR (De *et al.*, 2009; Naz *et al.*, 2010).

Researchers have found that CUR acts as a potent antibacterial agent against several gram-positive and gram-negative bacterial strains, such as *E-coli*, *Y. enterocolitica*, *M. tuberculosis*, *S. aureus*, *S. epidermidis*, *Salmonella*, *P. sudomonas*, and *H. pylori* (Bhullar *et al.*, 2013; Chattopadhyay *et al.*, 2004; Mun *et al.*, 2013; Naz *et al.*, 2010; Rai *et al.*, 2008; Vimala *et al.*, 2011). The phenolic groups in CUR form H-bonds with the amino/hydroxyl and hydroxyl groups of the bacterial protein and cellulose polymers, respectively (Ammayappan & Moses, 2009). Moreover, researchers believe that CUR acts as a non-competitive inhibitor of Shikimate dehydrogenase (SDH), thus reduction in the synthesis of the bacterial essential metabolites (De *et al.*, 2009). Furthermore, CUR binds to tubulin and perturbs microtubule polymerization, inhibits the polymerization of the Filamenting temperature-sensitive mutant Z (FtsZ) which perturbs its functions and therefore, leads to inhibition of bacterial proliferation (Ammayappan & Moses, 2009; Kaur *et al.*, 2010; Rai *et al.*, 2008), blocks bacterial respiratory enzymes pathways (Vimala *et al.*, 2011). Finally, CUR has phototoxic effects against *Salmonella* and *E.coli* (Rai *et al.*, 2008).

1.3.2.5 Neuroprotective activity

Neurodegenerative diseases result in an irreversible loss of functional neurons, which results in major mechanical, physiological, and psychological disabilities. Therefore, prophylaxis in highly risked patients is vital (Cole *et al.*, 2007). Researchers found that CUR acts as a potent neuro- and cytoprotective agent and hence, can be used in the prophylaxis and treatment of neurodegenerative diseases such as Alzheimer's, Parkinson's, stroke, head trauma, Huntington's diseases (Thiyagarajan & Sharma, 2004) in addition to its protective effects against cerebral, cardiac, and renal ischemia (Jiang *et al.*, 2007).

CUR is believed to possess neuroprotective effects through its anti-oxidant, anti-inflammatory, and anti-protein aggregation activities (Rajakrishnan *et al.*, 1999; Cole *et al.*, 2007; Yang *et al.*, 2009). It protects the brain from damage through several pathways; it regulates the transcription factor (Nrf2) expression (Yang *et al.*, 2009), inhibits and reverses lipid peroxidation (Complexes *et al.*, 2003; Bala *et al.*, 2006), enhances glutathione content in the brain, and enhances Na⁺, K⁺, -ATPase activity (Rajakrishnan *et al.*, 1999; Bala *et al.*, 2006). Moreover, it prevents peroxynitrite mediated blood-brain barrier disruption (Jiang *et al.*, 2007). Due to its phenolic structure, CUR decreases the levels of thiobarbituric acid relative substances (TBARS) and reduces the levels of cholesterol, phospholipids, and free fatty acids in the brain (Rajakrishnan *et al.*, 1999).

1.3.2.6 Anti-cancer activity

Of particular importance to the present research is the anticancer activity of CUR. Apoptosis is an essential morphological programmed cell death that plays a critical role in the development and tissue homeostasis (Elmore, 2007). It is characterized by

cell shrinkage, membrane blistering and chromatic condensation that eventually, results in cell fragmentation (Hockenbery *et al.*, 1993). Apoptosis is a sophisticated autonomous- genetic program for cell death that requires energy and involves the activation of “caspases”. Caspases are cysteine proteases that are involved in complex events responsible for linking the initiating stimuli to the final vanishing of cells (Hockenbery *et al.*, 1993; Elmore, 2007). Essentially, two major pathways drive apoptosis: the extrinsic and intrinsic (mitochondrial) pathways (Adams & Cory, 2007). The former pathway activates caspase-8 whereas the later activate caspase-9. Subsequently, caspase-8 and -9 activate effector caspases (3,7,6) that mediate cellular destruction. On the other hand, the B-cell lymphoma 2 (Bcl-2) protein controls the intrinsic pathway. Disruption of apoptosis in either pathway results in autoimmune and malignant diseases (Adams & Cory, 2007; Mulik *et al.*, 2010a) .

Research in the last 60 years has found that CUR has potential antitumor effects via suppression of tumour initiation, progression, metastasis of several tumour cells such as colon, epidermis, breast tumours, among others (Johnson *et al.*, 2009). In addition, CUR can sensitize and overcome resistance against several agents that induce apoptosis (Tamvakopoulos *et al.*, 2007). Several researchers reported that CUR significantly inhibits colon tumorigenesis in the initiation and post-initiation stages (Anderson, 2003; Maheshwari *et al.*, 2006). Moreover, Mulik *et al.*,(2010) found that the oral administration of synthetic CUR immensely inhibited the incidence of adenocarcinoma in the progression stage.

The exact mechanism of the anti-tumour effects of CUR is not fully understood, however, various mechanisms have been proposed. CUR suppresses proliferation induced by cancer growth factors and modulate various cell-signalling pathways such as Nrf2, cyclooxygenases, and mitogen-activated protein kinase (Maheshwari *et al.*,

2006; Mulik *et al.*, 2010). Furthermore, CUR induces apoptosis through both the mitochondria dependant and independent mechanisms (Adams & Cory, 2007). CUR inhibits nuclear factor κ B (NF- κ B) which subsequently downregulates gene products such as Bcl-2 (Maheshwari *et al.*, 2006). CUR also induces apoptosis by downregulating AKt/ mammalian target of rapamycin (mTOR) pathway (Johnson *et al.*, 2009). Moreover, CUR inhibits telomerase activity, downregulate Notch-1 signalling, anti-apoptotic proteins, cytochrome C release and caspases-3 and -9 activation (Tamvakopoulos *et al.*, 2007). CUR induces p53 and alternate redox status of the cells in which both induce apoptosis (Aoki *et al.*, 2007; Dandawate *et al.*, 2012).

1.3.3 Cocktail of CUR with conventional anticancer drugs

Several chemotherapeutic agents have been used in cancer treatment however, the use of these agents have been restricted due to high cost, toxicity, drug resistance that leads to the recurrence of diseases (Kunnumakkara *et al.*, 2007; Sreekanth *et al.*, 2011). Therefore, combination therapy was proposed as an alternative for enhancing chemotherapeutic efficacy, particularly in agents with different mechanisms of actions (Kunnumakkara *et al.*, 2007). Furthermore, combination therapy decreases the chances of resistance development or toxicity (Kunnumakkara *et al.*, 2007). Researchers have studied the effectiveness of combining CUR with conventional chemotherapeutic agents in order to sensitize cancer cells towards the chemotherapeutic agents and decrease the chances of toxicity (Hour *et al.*, 2002; Nautiyal *et al.*, 2011; Sreekanth *et al.*, 2011).

5-FU plus oxaliplatin (FOLFOX) is considered the backbone cocktail in colorectal cancer chemotherapy. However, its toxicity and ineffectiveness have urged researchers to investigate combining FOLFOX with a non-toxic but effective agent. Yu

et al.,(2009) investigated using either CUR alone or in combination with FOLFOX, as a treatment and prophylaxis agent against colorectal cancer recurrence. The study has shown that CUR as such or combined with FOLFOX resulted in significant reduction in cancer stem cells. Hence, it can cure and decrease the chances of colorectal cancer recurrence. In another study, Patel *et al.*,(2008) found that combining FOLFOX with CUR resulted in marked apoptosis of colorectal cancer cell lines HCT-116 & HT-29 compared to individual therapies. Nautiyal *et al.*,(2011) studied combining CUR with FOLFOX in treating colorectal cancer and found that this combination is highly effective in inhibiting the tumour growth. In this study, CUR significantly enhanced the sensitivity of colorectal cancer towards FOLFOX. Kamat *et al.*,(2007) studied the apoptic effects of combining CUR with gemcitabine and paclitaxel and found that CUR enhanced the chemotherapeutic anticancer activity in bladder regardless of interferon- α (IFN- α) resistance. In another study, Kunnumakkara *et al.*,(2007) investigated the ability of CUR to sensitize pancreatic cancer to gemcitabine both *in vitro* and *in vivo*. The study concluded that CUR and gemcitabine could be used as a treatment regimen against prostatic cancer. CUR-gemcitabine combination was again studied by Kanai *et al.*,(2011). The findings of this study confirmed the safety and feasibility of using this combination for pancreatic cancer treatment. Sreekanth *et al.*,(2011) found that CUR augmented paclitaxel apoptotic activity against cervical cancer cells. The study showed that this combination significantly reduced the tumour incidence and volume compared to individual therapeutic regimens. Whereas Qian *et al.*,(2011) studied the combination of CUR with adrimycin for hepatocellular carcinoma treatment and concluded that this combination resulted in enhancement of adriamycin apoptotic effect. Apart from the chemotherapeutic agents, researchers have studied combining CUR with other natural products such as green tea, taxol, and Beta-phenylethyl isothiocyanate for oral, cervical,

and prostatic carcinogenesis, respectively. These combinations showed promising, effective, and non-toxic treatment outcomes (Reuter *et al.*, 2008).

1.3.4 Clinical studies on CUR as an anticancer agent

Extensive research has shown the tremendous effectiveness of CUR in preventing and treating several types of cancers such as pancreatic, breast, skin, stomach, duodenum and colorectal cancer. Animal studies emphasized the dose dependant anticancer effects of CUR and recently, the clinical benefits of CUR in patients with several types of cancers have been elucidated (Anderson, 2003; Hatcher *et al.*, 2008; Naksuriya *et al.*, 2014; Sharma *et al.*, 2004).

Several clinical studies investigated the toxicity of CUR, for example, Sharma *et al.*,(2001) study included 15 patients with advanced colorectal cancer who consumed a single oral dose of 36-180 mg CUR for a duration of 4 months where the safety of CUR was confirmed. Cheng *et al.*,(2001) studied a higher dose threshold of 500-8000 mg of daily administration of CUR for three months in 24 patients with resected bladder cancer, stomach metaplasia, oral leukoplakia, Bowen's disease, and cervical intraepithelial neoplasm. This study confirmed the safety of CUR through pharmacokinetic analysis of blood and urine. Moreover, histopathological monthly evaluation was undertaken and in conclusion, they demonstrated the safety, poor absorption, and chemotherapeutic effects of CUR.

Pharmacokinetics studies were performed simultaneously with toxicity studies in a phase I clinical trial for oral CUR aimed at establishing the toxicity and systemic effects of CUR (Sharma *et al.*, 2004). The pilot study included 15 patients with colorectal cancer and analysed three biomarker activity: glutathione S-transferases (GST), levels of deoxyguanosine adduct (M₁G), and inducible prostaglandin E₂ (PGE₂)

as a reflection of CUR effects on carcinogenesis. The study concludes that CUR is effective in preventing and treating colorectal cancer however, low systemic bioavailability restricts its effectiveness. These results are in consistence with another phase I trials that investigated the pharmacokinetics and chemotherapeutic effects of CUR in twelve patients where the findings emphasized the anticancer effects of CUR despite its poor bioavailability (Anderson, 2003). The efficiency of CUR in the prevention of colorectal cancer was studied by Carroll *et al.*,(2011) with 44 participants who met the criteria; smokers, older than 40 years old, and has 8 or more rectal aberrant crypt foci (ACF) were included. Oral CUR was administered for 30 days and researchers assessed the chemoprevention ability of CUR through analyses of prostaglandin PGE2 and 5-hydroxyeicosatetraenoic acid (5-HETE) within the ACF. In consistence with the findings of Dhillon *et al.*,(2008), this study showed that CUR was poorly absorbed yet managed to reduce the ACF number that demonstrates its effectiveness in the prophylaxis against colorectal cancer.

In conclusion, *in vitro*, *in vivo*, and clinical studies suggest that CUR is potent against several types of cancer, including colorectal cancer, which is the subject of the present investigation. However, its effectiveness is restricted due to its poor systemic absorption and low bioavailability. In order to realise the anticancer potential of CUR, some form of formulation intervention is required. In the next chapter, I shall review current trends in formulation technology that address the constraints associated with the effectiveness of CUR and relevant to the present investigation.

1.4 Nanomedicine

Nanotechnology has invaded the contemporary industries and is usually referred to the design, fabrication, and utilization of materials with nanoscale

dimensions (Liu *et al.*, 2007; Park *et al.*, 2008). In the late 1990s, innovative technology has merged medicine in nanotechnology in a new term called nanomedicine (Wagner *et al.*, 2006). Unfortunately, there is no international definition for nanomedicine. The European Science Foundation (ESF) defined nanomedicine as “the science and technology of diagnosing, treating, and preventing disease and traumatic injury, of relieving pain, and of preventing and improving human health, using molecular tools and molecular knowledge of the human body” (Webster, 2006). Whereas the United States’ National Institute of Health Roadmap for Medical Research in Nanomedicine (NIH) defines nanomedicine as “an offshoot of nanotechnology which refers to highly specific medical interventions at the molecular scale for curing disease or repairing damaged tissues, such as bone, muscle, or nerve” (Webster, 2006). Nanomedicine ramifies into several types of nano-devices including nanomachines, nanofibers, nanosensors, and NPs (nanocarriers) (Park *et al.*, 2008).

Research has been extensively studying the application of nanocarriers in various medical applications due to the long list of advantages over conventional medicine. Physical properties of nanocarriers such as particle size, size distribution, surface charge, and surface modification flexibility allows targeted delivery of the cargo (Kumari *et al.*, 2010). Nanocarriers have unique characterization that may be exploited for improved pharmacokinetic properties of drugs compared to traditional medicine (Bhaskar *et al.*, 2010). In addition, nanocarriers have the advantage of releasing drugs in sustained and controlled manners (Malam *et al.*, 2009).

Implicating nanocarriers in drug delivery has several advantages including improved solubility of cargo, inhibition of systemic clearance, enhancing drug stability (Liu *et al.*, 2007), drug delivery across the blood brain barrier (BBB) and blood-cochlear barrier (Bhaskar *et al.*, 2010), reduction in toxicity and hence dosage regiment

whilst at the same time enhancing drug efficacy (Malam *et al.*, 2009). Nanomedicine has been applied in different healthcare sectors such as *in vivo* imaging, *in vitro* diagnostics, biomaterials, active implants, drug nanoformulations, and drug delivery (Wagner *et al.*, 2006). Functional pharmaceutical nanocarriers have been used in dentistry, ophthalmology, pulmonary, cardiology, and neurology, to name a few (Farokhzad & Langer, 2006). Drug release can be tailored in response to various triggers including pH, temperature and environment or changes in concentration of an analyte or enzyme such as glucose, glutathione, matrix metalloproteinases (Farokhzad & Langer, 2006; Mura *et al.*, 2013; Torchilin, 2012).

Conventional chemotherapeutic drugs are associated with debilitating drawbacks such as severe toxicity to normal cells, instability, lack of selectivity, and drug resistance (Liu *et al.*, 2007; Park *et al.*, 2008; Shapira *et al.*, 2011). Therefore, researchers have extensively studied therapeutic alternatives that manifest fewer side effects. Cancer tissues have unique pathophysiology in which tumours have fenestrated vasculature that is dilated and poorly differentiated with high interstitial pressure and poor lymphatic drainage (Liu *et al.*, 2007; Vlerken *et al.*, 2007). Taking advantage of this pathophysiology, nanocarriers can be administered for site-specific delivery into tumour tissue where they may accumulate passively or actively. Furthermore, nanocarriers can be tailored to enhance the cytotoxicity of chemotherapeutic agents, whilst reducing side effects and overcoming drug resistance (Park *et al.*, 2008; Shapira *et al.*, 2011; Vlerken *et al.*, 2007).

Nanocarriers can be administered via various routes such as non-invasive (intranasal, pulmonary, oral and transdermal delivery) (Sosnik & Sarmiento, 2014) as well as invasive routes (Intravascular, subcutaneous, intravenous delivery) (Cheng *et al.*, 2008).

1.4.1 Challenges in Nanomedicine

The application of nanotechnology in medicine is continuously evolving and is seen as a promising approach towards a wide variety of medical applications, such as diagnosis, treatment, and prevention of diseases (Kranz *et al.*, 2011; Linkov *et al.*, 2008). However, there are several challenges associated with nanomedicine.

The most challenging obstacle in nanomedicine is related to the physico-chemical characterization of the nanocarriers so that batch-to-batch variability is not easily achieved. Furthermore, the physico-chemical properties of the nanocarriers can become altered as these delivery systems interact with the biological fluids or environmental conditions during storage (Wicki *et al.*, 2015). In addition, the health risks and environmental side effects associated with nanomedicine development and manufacturing processes have not been assessed (Baun & Hansen, 2008; Linkov *et al.*, 2008; Wicki *et al.*, 2015). There are no regulatory or internationally agreed guidelines governing the production and usage of this class of dosage forms (Wicki *et al.*, 2015).

Despite the potential and appealing features associated with nanomedicine in cancer diagnosis, treatment, and prevention, research is still constrained by complexity and heterogeneity of tumours among patients (Prabhakar *et al.*, 2013; Shi *et al.*, 2016). There is also the difficulty of targeting nanocarriers to solid tumours (Nie, 2010; Shi *et al.*, 2016). Biological factors such as NPs-protein interaction, blood circulation and extravasation into tumours, possess negative influence in the permeability of nanocarriers into the tumour, hence its therapeutic efficacy (Shi *et al.*, 2016). Moreover, the majority of the available data about the therapeutic effects of NPs are based on *in vitro* and *in vivo* studies.

1.4.2 Types of “nanocarriers”

NPs used in drug delivery systems are submicron-sized systems or devices that include polymeric NPs, micelles, dendrimers, liposomes, and solid lipid nanoparticles (SLN) where each system has unique physico-chemical properties.

1.4.2.1 Polymeric nanoparticles

Polymeric NPs (Figure 1.6) are particles with size below 1 μm fabricated usually from biodegradable polymers (Hans & Lowman, 2002). They may consist of two or more polymer chains with different hydrophobicity called copolymers that self-assemble in a core-shell structure in an aqueous environment (Muller *et al.*, 2000). Drugs may be conjugated to the side chain of the linear polymers and through manipulating the ratios of the forming polymers, we can control the degradation rate of the NPs and hence, drug release (Cho *et al.*, 2008). Polymers used can be either natural such as albumin, alginate, CS, and collagen or synthetic such as polyacrylates, polycaprolactones, and polylactide-polyglycolid (Panyam & Labhasetwar, 2003; Soppimath *et al.*, 2001; Cho *et al.*, 2008). Natural polymers are less preferred because of the variety in purity and degree of crosslinking that might affect the functionality of the delivery (Hans & Lowman, 2002).

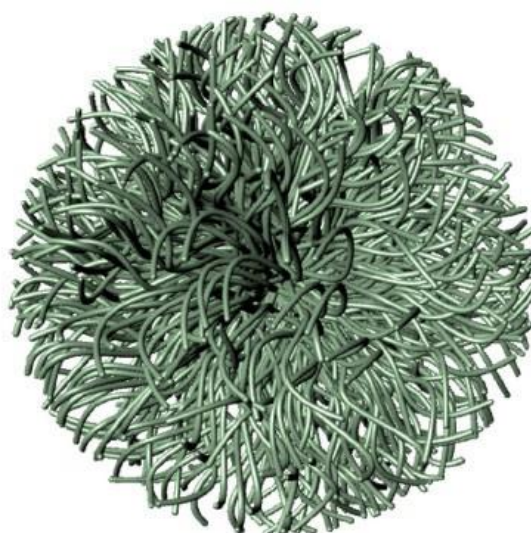


Figure 1.6 Polymeric NPs (*adopted from www.dovepress.com*)

Several methods are used in the production of polymeric NPs such as solvent diffusion, solvent evaporating, solvent displacement, interfacial deposition, nanoprecipitation, multiple emulsion, salting out, polymerization, and ionic gelation (Hans & Lowman, 2002; Soppimath *et al.*, 2001). According to the method of preparation, the embedded drug is either covalently bounded to or physically encapsulated in the polymer matrix (Cho *et al.*, 2008). Polymeric NPs can be structured either in nanocapsule or nanosphere form, where the former consists of a liquid or semi-solid core immersed in a solid shell, the latter is completely solid matrix (Vauthier & Bouchemal, 2009).

Polymeric NPs may be biodegradable, biocompatible (Hans & Lowman, 2002), flexible, and stable delivery systems that are capable of embedding a wide range of therapeutic agents with high loading capacity (Patel *et al.*, 2012). In addition, they protect the embedded agent and release it in controlled and sustained manner (Soppimath *et al.*, 2001). Moreover, many polymers used in the fabrication of

polymeric NPs have been safely used in humans for decades (Cho *et al.*,2008; Sanna *et al.*,2014).

Several polymeric NPs are under preclinical and clinical studies. For example, Paclitaxel-incorporating PEG-modified polyaspartate polymeric micelles (NK105) is in phase I clinical studies, whereas paclitaxel containing Monomethoxy polyethylene glycol-d,l-lactide polymeric micelles (Genexol-PM[®]), Doxorubicin-incorporated PEG-polyaspartic acid polymeric micells (NK911), cyclodextrin-poly(ethylene glycol) copolymer conjugated to camptothecin (CRLX101), and Cisplatin-incorporating polyethylene glycol poly(glutamic acid) polymeric micelles (NC-6004) are in phase II clinical studies (Sanna *et al.*,2014; Chan *et al.*,2010; Cho *et al.*,2008).

Two polymeric NPs are currently available in market, namely, Aboscan[®] a dextran-fabricated NPs using iron oxide for the diagnostic imaging of the spleen and liver, and Abraxane[®] an albumin-fabricated NPs using paclitaxel for breast cancer treatment (Patel *et al.*, 2012).

1.4.2.2 Micelles

Introduced in early 1990s, polymeric micelles are a mesoscopic drug delivery system with a unique core-shell structure (Figure 1.7). The hydrophobic part of the copolymer self-assemble into the inner core which embed the hydrophobic drug, whereas the hydrophilic part forms the water shell protecting the encapsulated hydrophobic drug from the aqueous environment (Kedar *et al.*, 2010). Polymeric micelles can be formed either by a single polymer-drug conjugation or through complexation of two oppositely charged poly-ions (Kataoka *et al.*, 2012). The small particle size (<100 nm) of the polymeric micelles gives the resemblance of natural

carriers such as viruses, hence they cannot be recognized *in vivo* by the reticuloendothelial system (Lavasanifar *et al.*, 2002).

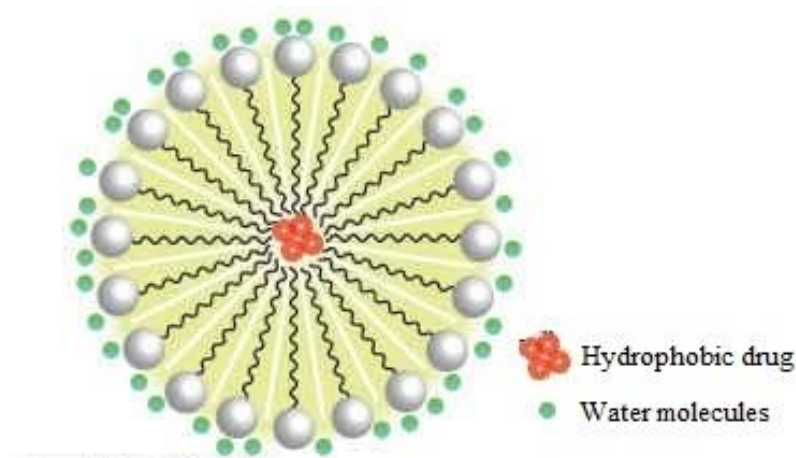


Figure 1.7 Polymeric Micelles (Adopted and modified from www.sigmaldrich.com)

Polymeric micelles can be fabricated by di-block copolymers, tri-block copolymers, or graft copolymers. The selection of the copolymer depends on the intended application of the micelles formation. Some polymers are suited for controlled drug release, prolong systemic circulation time, or introduction of targeting moieties (Kedar *et al.*, 2010). The main driving force for polymeric micelles formation is the core segregation from the aqueous environment and it starts upon reaching the threshold concentration called critical micelle concentration (CMC). Micelles with lower CMC values are more stable and have lower rate of dissociation thus, more drug would be available at the target site (Kataoka *et al.*, 2012; Kedar *et al.*, 2010). Formulation of polymeric micelles is achieved in two steps: synthesis of the block copolymer and then conversion into micelles (Kedar *et al.*, 2010). Micelles can also be formed through electrostatic interactions, metal complexation, hydrophobic interactions, and hydrogen bonding (Kataoka *et al.*, 2012; Kedar *et al.*, 2010). Methods of micellization are

dialysis, self-emulsion evaporation, microsphere separation, oil-in-water emulsion, and rapid heating methods (Kedar *et al.*, 2010).

Compared to amphiphilic micelles, polymeric micelles have lower CMC values (Gaucher *et al.*, 2005). The major obstacle in the manufacture of polymeric micelles is the temporal control. Temporal control means that a slight deviation in the environment temperature from the lower critical solution temperature (LCST) results in micelle degradation, hence immature drug release occurs. Therefore, local modification of patient body temperature is required (Matsumura, 2008).

In vitro studies on polymeric micelles incorporating anticancer agents have shown promising findings. Therefore, several anticancer agents-loaded with micelles are under clinical investigations. Paclitaxel loaded micelles, NK105, is under Phase I/II studies for the determination of the recommended dose, maximum tolerated dose, dose-limiting toxicity, and pharmacokinetics in several cancers (Matsumura, 2008; Matsumura & Kataoka, 2009). Cisplatin-loaded micelles, NC-6004, is under phase II studies designed to determine the toxicity (Matsumura, 2008; Matsumura & Kataoka, 2009). NK102, SN-38 encapsulated micelles is under Phase II studies. The study will be continued until disease progression or inadmissible toxicity occurs (Matsumura, 2008; Matsumura & Kataoka, 2009). NK911, doxorubicin-incorporated micelles is under phase II clinical trials against metastatic pancreatic cancer whereas, Epirubicin-loaded micelles, (NC-6300), is under phase I study to determine the safety and efficacy of dose against advanced solid tumours (Cabrera & Kataoka, 2014).

1.4.2.3 Dendrimers

First proposed in late 1970's as a monodispersed and structure-controlled system, dendrimers (Figure 1.8), have a unique well-defined, highly branched and

globular polymer architecture formulated in three-dimensional molecular arrangement (Emanuele & Attwood, 2005; Esfand & Tomalia, 2001; Gillies & Fréchet, 2005; Kurtoglu *et al.*, 2009; Liu & Fréchet, 1999; Zhang *et al.*, 2008). Compared to conventional polymers, dendrimers are globular in shape, have more controlled structure and molecular weight, and a wider functional surfaces (Emanuele & Attwood, 2005; Liu & Fréchet, 1999). The unique globular structure comprises of a core (zero generation) and multiple layers of repeated units called generations; where low generations represent an open structures, and higher generations are more globular and dense, therefore, a plethora of dendrimers architectures have been fabricated (Emanuele & Attwood, 2005; Liu & Fréchet, 1999; Zhang *et al.*, 2008).

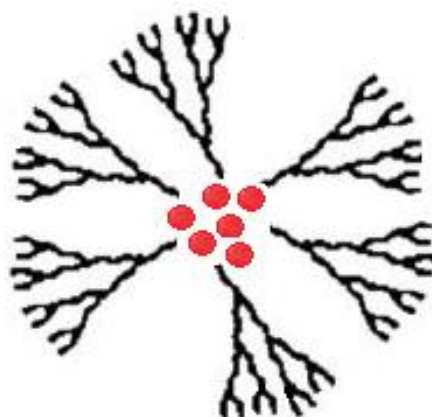


Figure 1.8 Dendrimers (*Drawn using Microsoft paint®*, 1709)

Two distinct strategies are used for dendrimers synthesis: The divergent and the convergent synthesis. In the former, the dendrimer growth starts from the core followed by a stepwise addition of the outer layers. Whereas in the latter, the growth starts at the chain ends followed by the addition of molecules towards the core (Esfand & Tomalia, 2001; Liu & Fréchet, 1999). Both of the strategies involve two-steps reactions sequence: growth step and activation step. In addition, clean and side reactions-free processes are required in both strategies. Besides the difference in the structural

formation order, convergent strategy incurs better control of the structure, while the divergent strategy is better for large-scale production (Liu & Fréchet, 1999). However, both strategies are tedious and time-consuming. Therefore, new strategies are being proposed such as double stage convergent growth and orthogonal coupling strategies (Liu & Fréchet, 1999). In nanomedicine, several types of dendrimers have been used including polyamidoamines (PAMAM), polyesters (PGLSA-OH), and polyproplimines (PPI), among others (Mignani *et al.*, 2013).

Drugs can be encapsulated in dendrimers via numerous interactions such as electrostatic, hydrophobic, hydrogen bond, and covalent interactions (Emanuele & Attwood, 2005). Dendrimers can be designed to have therapeutic targeted propensities, where disease specific-signals such as oxidative, chemical and environmental changes serve as a trigger for the cleavage between dendrimers linkers and thus, drug release (Mignani *et al.*, 2013). Dendrimers have been used in various applications including enzyme mimicking, gene and drug delivery, diagnostic agents, immunodiagnostics, vaccines, antivirals, antibacterial, and anticancer therapeutics (Emanuele & Attwood, 2005; Esfand & Tomalia, 2001; Gillies & Fréchet, 2005; Liu & Fréchet, 1999).

Dendrimers have several advantages related to their unique structure such as uniformity, controlled size, low polydispersity, flexible surface group (Patri *et al.*, 2005). Furthermore, they may overcome biological constraints that hinder targeting to tumour site (Mignani *et al.*, 2013). Moreover, these delivery systems expedite passive targeting of drugs to the solid tumours (Gillies & Fréchet, 2005). The manufacture of dendrimers is expensive and raises toxicity and biocompatibility concerns. Furthermore, dendrimers have poor biodistribution, which shortens their blood circulation time and hence, less therapeutic efficacy is achieved (Liu & Fréchet, 1999).

Notwithstanding, there are a number of dendrimers currently in preclinical development such as folic acid-PAMAM dendrimers, poly propyleneimine dendrimers, ligand- conjugated PEG-poly-L-lysine dendrimers, and poly (glycerol-succinic acid) dendrimers for epithelia cancer, HIV, malaria, and various cancer treatments, respectively. Poly-L-Lysine dendrimer (VivaGel®) is under phase I clinical studies for antimicrobial protection from HIV and genital herpes infections (Zhang *et al.*, 2008).

1.4.2.4 Liposomes

Liposomes (Figure 1.9) are mesoscopic colloidal particles that can be prepared from synthetic or natural phospholipid layers embracing aqueous compartments (Lian & Ho, 2001; Mezei & Gulasekharam, 1980; Sharma & Sharma, 1997). Liposomes were first introduced in 1970 as drug delivery systems for targeted drug delivery and enhancing the therapeutic indices of drugs (Gregoriadis & Florence, 1993; Lian & Ho, 2001). The structure versatility of liposomes allows the encapsulation of a wide range of drugs with variable lipophilicities (Gregoriadis & Florence, 1993; Sharma & Sharma, 1997). The gel-liquid crystalline transition temperature (T_c) of phospholipids determines the degree of fluidity of the liposomal membrane at ambient temperature (Gregoriadis & Florence, 1993).

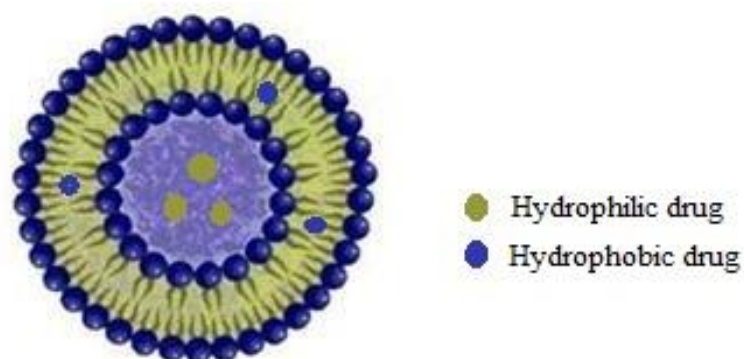


Figure 1.9 Liposomes (*adopted and modified from www.intechopen.com*)

Liposomes are mainly composed of neutral charge phosphatidylcholine with fatty acid chains of various lengths and degree of saturation. To a lesser extent, cholesterol is included in the lipid formulation (Gregoriadis & Florence, 1993; Malam *et al.*, 2009). The simplest method of liposomes formulation is the thin-film hydration method. However, it produces liposomes with low encapsulation efficiency (EE%). Therefore, the freeze-drying preformed liposome dispersion method was developed (Sharma & Sharma, 1997). Based on the liposomes composition and intracellular delivery mechanisms, liposomes are classified into five types: i) conventional liposomes, ii) cationic liposomes, iii) long circulating liposomes, iv) pH-sensitive liposomes, and v) immunoliposomes (Sharma & Sharma, 1997).

Another classification of liposomes is based on the liposomes-biological interactions into: non-interactive sterically stabilized liposomes (LCL) and highly interactive cationic liposomes. While the former has longer circulation half-life, the later has higher affinity to cell membranes, thus, suitable for intracellular genetic material delivery (Sharma & Sharma, 1997).

Liposomal physical properties such as lipid composition, size, charge, membrane fluidity, steric hindrance, charge density, and permeability defines liposomal-biological interactions, which in turn determine the drug intracellular activity (Lian & Ho, 2001; Sharma & Sharma, 1997). Liposomes can be administered orally or parenterally (subcutaneously, intramuscularly, intravenously) (Lian & Ho, 2001; Mezei & Gulasekharam, 1980) and they can be used in a wide range of applications such as diagnostic imaging, oral drug therapy (Sharma & Sharma, 1997), gene therapy (Lian & Ho, 2001), vaccination, and antimicrobial and antineoplastic therapy (Gregoriadis & Florence, 1993). They are biodegradable and have physical and structural similarities to biological membranes. They may be used to enhance the pharmacologic properties

of drugs (Gregoriadis & Florence, 1993). Compared to the crude drug in aqueous solution, liposomal encapsulation enhances drug absorption and biodistribution (Lian & Ho, 2001). However, the therapeutic applications of liposomes are limited due to their batch to batch variability, constraints in sterilization, low EE% and rapid clearance from systemic circulation (Allen & Cullis, 2013; Lian & Ho, 2001; Sharma & Sharma, 1997).

Table 1.2 shows liposome-based products approved for human use, whereas Table 1.3 lists liposome-based products in clinical trials (Allen & Cullis, 2013; Evaluate, 2017; FDA, 2018; Lian & Ho, 2001; Saif, 2014; Sharma & Sharma, 1997; Tak *et al.*, 2018).

Table 1.2 Liposome-based products approved for human use

Product	Drug	Indication
Abelect TM	Amphotericin B	Serious fungal infections
Ambisome TM	Amphotericin B	Serious fungal infections
Amphocil TM	Amphotericin B	Serious fungal infections
Amphotec TM	Amphotericin B	Serious fungal infections
CPX-351	Cytarabine; Daunorubicin	Acute myeloid leukemia
DaunoXome TM	Daunorubicin citrate	Kaposi sarcoma in AIDS
DepoDur TM	Morphine sulphate	Pain after surgery
DepoCyt TM	Cytosine	Lymphomatous
Diprivan TM	Propofol	Anesthesia
Doxil TM	Doxorubicin	- Kaposi sarcoma in AIDS
Caelyx TM		- Refractory ovarian cancer
Estrasorb TM	Estrogen	Menopausal therapy
Exparel TM	Bupivacaine	Local anaesthetic
Myocet TM	Doxorubicin	Breast cancer
Visudyne TM	Verteporphin	Wet macular degeneration

Table 1.3 Liposome-based products in clinical trials

Product	Drug	Status	Indication
Allovectin-7	HLA-B7 Plasmid	Phase II	Gene therapy for metastatic cancers
Alocrest	Vinorelbine	Phase I	Newly diagnosed or relapsed solid tumours
Antragen TM	Tretinoin	Phase II/III	Kaposi sarcoma in AIDS
Brakiva	Topotecan	Phase I	Relapsed solid tumour
CPX-1	Irinotecan HCl: Floxuridine	Phase II	Colorectal cancer
Endo-Tag-1	Paclitaxil	Phase II	Pancreatic cancer
Nyotran TM	Nystatin	Phase II/III	Candidemia
Ventus TM	Prostaglandin E1	Phase III	Acute respiratory distress syndrome
MBP-436	Oxaliplatin	Phase II	Gastric cancer and gastro-esophageal junction
MM-302	Doxorubicin	Phase I	Breast cancer
MM-398	CPT-11	Phase III	Gastric and pancreatic cancer
ThermoDox	Doxorubicin	Phase III	Refractory chest wall breast cancer

1.4.2.5 Solid Lipid Nanoparticles (SLN)

SLN (Figure 1.10) were first proposed in 1991 as alternative drug delivery systems to conventional carriers such as liquid oils, liposomes, and emulsions (Mehnert & Mader, 2001; Muller *et al.*, 2000; Müller *et al.*, 2002). SLN are particles in the nano-size range with a solid-lipid matrix and are made from solid lipids and stabilized by surfactants (Wissing *et al.*, 2004). The solid state of the lipids reduces the mobility of

the embedded drugs which hinders the drug release (Mehnert & Mader, 2001; Muhlen *et al.*, 1998).

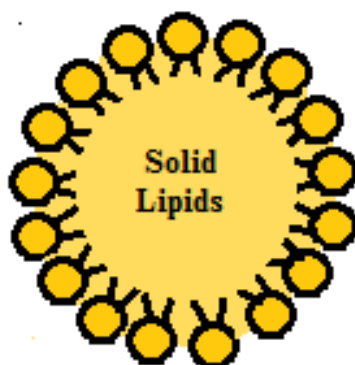


Figure 1.10 SLN (Drawn using Microsoft Paint® 1709)

SLN are prepared using any of the following techniques: i) high shear homogenization which is sub-divided into hot and cold homogenization methods for heat sensitive and highly heat sensitive drugs, respectively ii) microemulsion iii) solvent emulsification-diffusion or –evaporation iv) double emulsion, and v) high speed sonication/ stirring (Blasi *et al.*, 2007; Mukherjee *et al.*, 2009; Muller *et al.*, 2000).

Drugs can be embedded between lipid layers, the fatty acid chains, or in imperfections within the lipid matrix (Wissing *et al.*, 2004). Based on the drug incorporation location, 3 models can be recognised: solid solution model, core-shell model which could be either drug-enriched shell or drug-enriched core model (Muller *et al.*, 2000). The stability and release of incorporated drugs depend mainly on the physical characteristics of the SLN (particle size, zeta potential, crystallinity), (Muller *et al.*, 2000) . SLN can be administered via various routes including oral, transdermal, ocular, rectal, pulmonary and parenteral routes (Mukherjee *et al.*, 2009; Muller *et al.*, 2000; Wissing *et al.*, 2004). However, toxicity profiles following parenteral route are not available yet (Muller *et al.*, 2000).

Various drugs have been incorporated in SLN such as cortisone, diazepam, menadione, methasone, valeraten, prednisolone, retinol, timolol, to mention few (Mehnert & Mader, 2001). They are physically stable, may manifest controlled release kinetics, and have superior tolerability (Wissing *et al.*, 2004). Compared to conventional drug delivery systems, SLN may be non-toxic and can be formulated without the need for organic solvents. In addition, they can be easily sterilized (Mehnert & Mader, 2001; Schwarz *et al.*, 1994).

1.4.3 Methods of preparation for polymeric nanoparticles

Polymeric NPs have been extensively studied as a drug delivery system for small and large molecules. Therefore, several preparation methods have been proposed (Nagavarma *et al.*, 2012; Rao & Geckeler, 2011). Essentially, the preparation techniques include two main steps. The first step comprises the preparation of the emulsified system, whereas the NPs are fabricated in the second step. Classification of the preparation method depends on the first step, which could be either polymerization of monomers or dispersion of a preformed polymer (Nagavarma *et al.*, 2012; Vauthier & Bouchemal, 2009; Pinto Reis *et al.*, 2006; Rao & Geckeler, 2011). Method selection depends on several factors including physico-chemical characteristics of the target drug, required physico-chemical parameters of the NPs, target site, application, among others (Pinto Reis *et al.*, 2006; Rao & Geckeler, 2011). Figure 1.11 illustrates the different types of preparation methods.

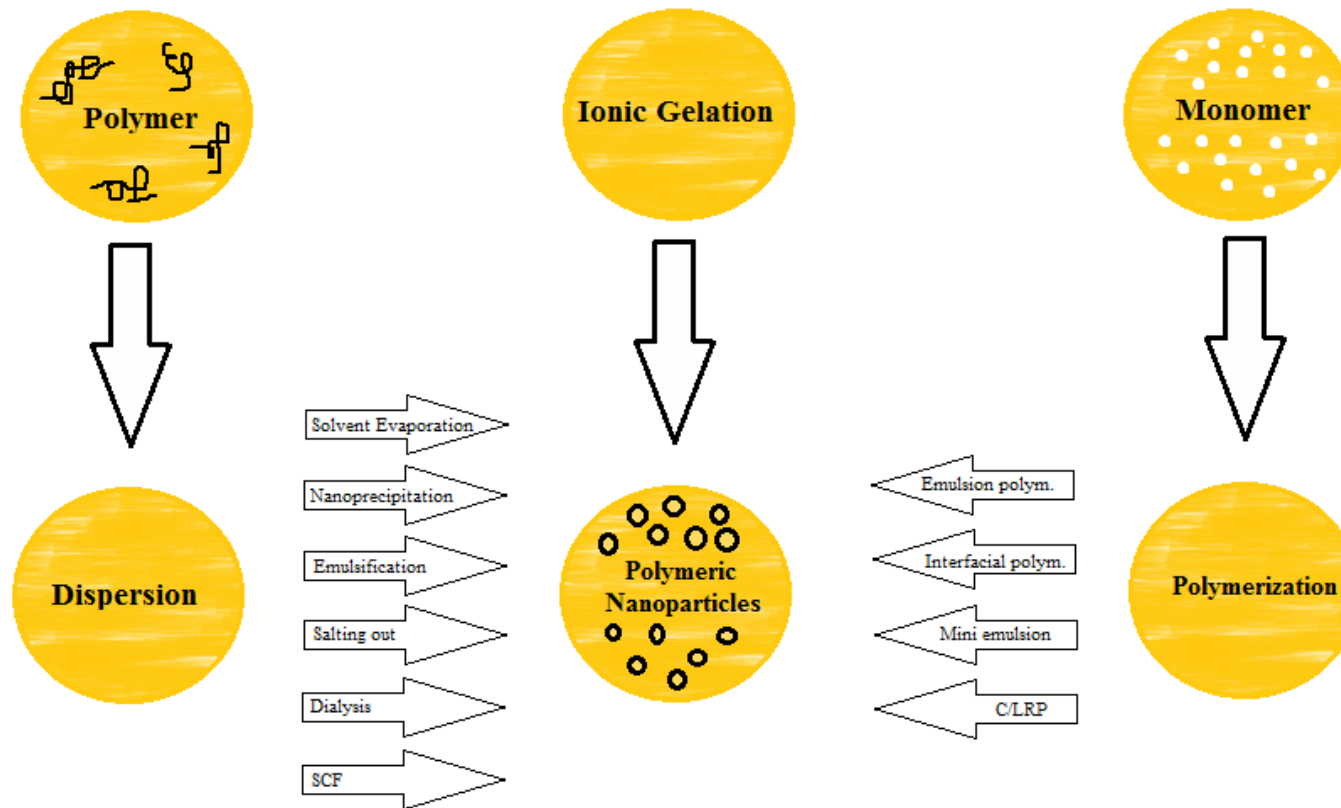


Figure 1.11 Illustration of preparation methods for polymeric nanoparticles

* SCF: Supercritical fluid technology

* C/LRP: Controlled/Living Radical Polymerization

1.4.3.1 Preparation methods from dispersion of preformed polymer

Different methods may be used to successfully formulate NPs by dispersion of preformed polymers. These methods are reviewed in the following sections.

1.4.3.1.1 Solvent Evaporation

Solvent evaporation was the first developed method for polymeric NPs preparation from preformed polymers (Nagavarma *et al.*,2012; Vauthier & Bouchemal, 2009). In the first step, the emulsion is prepared by dissolving the polymer in a volatile solvent such as chloroform, dichloromethane, ethyl acetate or acetone via high-speed homogenization or ultra-sonication (Nagavarma *et al.*,2012; Vauthier & Bouchemal, 2009). The formulated emulsions could be either single-emulsions (w/o) or double-emulsions ((w/o)/w). The NPs are then fabricated by evaporating the solvent of the polymer by diffusion through the continuous phase of the emulsion. This step is achieved by either continuous magnetic stirring at room temperature or increasing the temperature under pressure (Pinto Reis *et al.*,2006; Rao & Geckeler, 2011). Finally, formulated NPs are collected by ultracentrifugation, washing with purified water, and finally, lyophilization (Kumari *et al.*,2010; Mohanraj *et al.*,2006).

The particle size range can be controlled by managing the polymer concentrations, type and concentration of the stabilizer, viscosity of aqueous and organic phases, stirring speed, and temperature (Mohanraj *et al.*,2006; Pinto Reis *et al.*,2006). Examples of frequently used polymers are poly(lactide) (PLA), PLGA, poly(epsilon-caprolactone) (PCL), ethylcellulose (EC), cellulose acetate phthalate, among others (Pinto Reis *et al.*,2006; Vauthier & Bouchemal, 2009).

Lee *et al.*,(2006) used solvent evaporation method to prepare polymeric NPs from CS derivatives fluorescein isothiocyanate (FITC)- conjugated glycol CSs (FGCs)

using diluted chloroform as the solvent. Fabricated NPs size ranges were 150-500 nm, and were stable in phosphate buffered saline (PBS) for 20 days at 37°C. Gómez-Gaete *et al.*,(2007) encapsulated dexamethasone in PLGA NPs using the solvent evaporation technique for ocular delivery. Particle size and zeta potential produced were 230 nm, -4 mV, respectively. Dexamethasone was completely released after 4 hr at 37°C medium. However, loading capacity was relatively low (2.3%). Although the solvent evaporation method is simple (Rao & Geckeler, 2011), it is time consuming, there is the possibility of stabilizer binding on the surface of the NPs, the likelihood of nanodroplet cohesion during the evaporation step, and the difficulty of scaling-up (Pinto Reis *et al.*,2006; Rao & Geckeler, 2011; Lee *et al.*,1999).

1.4.3.1.2 Nanoprecipitation

Nanoprecipitation, also called solvent displacement, was first developed by Fessi *et al.*,(1992). Nanoprecipitation technique has three basic components: i) polymer (synthetic, semi-synthetic, or natural), ii) polymer solvent iii) non-solvent of the polymer (Rao & Geckeler, 2011; Vauthier & Bouchemal, 2009). After dissolving the polymer in water-miscible solvent, this organic solution is slowly added to the aqueous phase under slight and continuous stirring, vice versa addition successfully formulate the NPs as well (Thioune *et al.*, 1997; Yordanov & Dushkin, 2010). Subsequently, rapid diffusion of the polymer solution in the non-solvent phase results in the aggregation of the polymer chains and thus, instant formation of the NPs (Rao & Geckeler, 2011; Galindo-rodriguez *et al.*,2004). Finally, The polymer solvent is removed by evaporation (Vauthier & Bouchemal, 2009; Legrand *et al.*,2007).

Polymers commonly used are PLA, PLGA, Eudragit, cellulose derivatives, among others (Rao & Geckeler, 2011; Vauthier & Bouchemal, 2009; Bilati *et al.*,2005).

Organic solvents used should be miscible in water and easily evaporated such as acetone, tetrahydrofuran (THF), ethanol, mixtures of two or three solvents (Thioune *et al.*, 1997; Yordanov & Dushkin, 2010; Rao & Geckeler, 2011; Vauthier & Bouchemal, 2009).

The principle of this method is based on the Marangoni effect, which is related to the interfacial turbulence of the polymer after displacement of the solvent with water (Bilati *et al.*, 2005). This effect results in decreasing the interfacial tension between the two phases, hence, increasing the surface area and finally, NPs formation (Rao & Geckeler, 2011; Govender *et al.*, 2016; Galindo-rodriguez *et al.*, 2004).

The physico-chemical characteristics of the NPs are affected by the diffusion conditions, miscibility of the organic phase, organic phase and aqueous phase ratio, polymer type and concentration, in addition to the surfactant type and concentration, if added (Bilati *et al.*, 2005; Govender *et al.*, 2016; Legrand *et al.*, 2007; Yordanov & Dushkin, 2010).

Nanoprecipitation method is a simple, one-step, easy, fast, reproducible, economic, and well characterized polymers are used (Bilati *et al.*, 2005; Govender *et al.*, 2016; Legrand *et al.*, 2007; Yordanov & Dushkin, 2010). However, water soluble drugs are poorly incorporated (Bilati *et al.*, 2005).

Shen *et al.*, (2011) developed PEG-b-PCL and PEG-b- Poly(acrylic acid) (PAA) NPs incorporated with β -carotene as a model drug. The NPs were successfully developed for biomedical applications, such as imaging and drug delivery. The size range was 50-500 nm with a maximum drug loading capacity of 50%. In another study, Dhar *et al.*, (2008) employed the nanoprecipitation technique to fabricate Pt(IV) prodrug-PLGA-PEG NPs encapsulating cisplatin targeting prostate cancer. The NPs

were formulated to target Prostate Specific-membrane Antigen (PSMA), which is overexpressed in prostate cancer. The particle size and loading efficiency were 140 nm and 6%, respectively. The release kinetics showed sustained release of drug over 80 hr.

1.4.3.1.3 Emulsification/solvent diffusion

Emulsification/solvent diffusion, also called spontaneous emulsification, is a modified technique of the emulsification/solvent evaporation technique (Nagavarma *et al.*, 2012; Miller, 1988). It was first proposed based on using organic solvents, however, it was adapted in the salt-out technique (Pinto Reis *et al.*, 2006). The simplest model of this technique comprises of water, hydrocarbon, and fatty acid or a short-chain alcohol (Miller, 1988). In more advanced versions, 1-3% of mixed emulsifiers can be added (El-Aasser *et al.*, 1988). First, the drug-containing polymer is dissolved in a partially water-miscible solvent. Secondly, the solution is saturated with water to reach initial thermodynamic equilibrium of both phases (Nagavarma *et al.*, 2012). Thirdly, solvent diffusion is promoted by dilution with an excess of water (Bouchemal *et al.*, 2006). Fourthly, the super-saturated solution of oil in water is emulsified in an aqueous solution containing stabilizer which leads to solvent diffusion to the external phase and hence, formation of NPs as an oil droplets in an aqueous continuous phase. Finally, the solvent is expelled by filtration or evaporation (Kwon *et al.*, 2001).

Emulsification occurs in the aqueous phase (Miller, 1988). For successful emulsification, fatty alcohol and ionic surfactant should be thoroughly mixed in the water phase before the addition to the oil phase (El-Aasser *et al.*, 1988). Examples of solvents used are propylene carbonate and benzyl alcohol whereas polyvinyl alcohol (PVA) and gelatine can be used as stabilizers (Kwon *et al.*, 2001). The fatty alcohol chain length should be at least 12 carbons (El-Aasser *et al.*, 1988). Based on the system

composition and their physico-chemical characterization, two mechanisms are proposed for the spontaneous emulsification: nucleation and growth, and diffusion and stranding (Bouchemal *et al.*, 2008).

Unlike the emulsification/solvent evaporation technique, spontaneous emulsification is not caused by interfacial turbulence but by the diffusional process itself (Miller, 1988). The spontaneity of the emulsification process is affected by several factors such as the interfacial and bulk viscosity, interfacial tension, surfactant concentration and structure, and phase transition region. The spontaneity of emulsification in turn, affects the nanoparticle size and size distribution (Bouchemal *et al.*, 2008). Usually, size range produced using this technique is 100-450 nm (El-Aasser *et al.*, 1988; Kwon *et al.*, 2001).

Nanoformulations produced by spontaneous emulsification are known to be stable. Several hypotheses have been proposed to explain their stability. One hypothesis is the formation of a molecular complex at the oil-water interface which decreases the interfacial tension (El-Aasser *et al.*, 1988). Another hypothesis is the formation of a viscous film at the oil-water interface which acts as a steric stress to aggregation (El-Aasser *et al.*, 1988). In addition, it is believed that the formation of aqueous crystals decreases the *van der Waals* attractive forces hence, support the stability of the nanoformulations. Finally, deterred diffusion of the oil phase to the aqueous phase maintains its stability (El-Aasser *et al.*, 1988).

Examples of drugs encapsulated using this technique are doxorubicin, coumarin, indocyanine, and cyclosporine (Nagavarma *et al.*, 2012). Advantages of spontaneous emulsification are simplicity, reproducibility, ability of scaling-up, high EE%, and narrow size distribution (Nagavarma *et al.*, 2012; Bouchemal *et al.*, 2008).

However, a major drawback is the need to expel high volumes of water in which water-soluble drugs might leak out and hence, decreases the EE% (Nagavarma *et al.*,2012).

Quintanar-Guerrero *et al.*,(1998) studied the possibility of using spontaneous emulsification technique in fabrication of biodegradable nanocapsules. They used different polymers such as PLA, Eudragit E, and poly (ϵ -caprolactone). The nanocapsules formulation was confirmed by density gradient centrifugation, the presence of a unique density band, scanning electron microscopy (SEM) and atomic force microscope (AFM) images. Particle size range was 174-346 nm and were stable at least for a month. In a different study, PLGA nanospheres were produced using spontaneous emulsification technique encapsulating water soluble and insoluble agents, 5-fluoruracil (5-FU) and indomethacin, respectively. Both nanospheres were successfully formulated using acetone as solvent, in contrast, dichloromethane and chloroform failed to produce particles in the submicron size. Particle size ranges were 200-300 nm and 600-800 nm for 5-FU and indomethacin, respectively. The drugs were homogeneously dispersed in the PLGA. 5-FU was poorly encapsulated compared to indomethacin and release kinetics showed burst initial release for both drugs. However, the initial burst release was avoided in the case of indomethacin by increasing the molecular weight of PLGA. Indomethacin release was more sustained for up to 120 hr compared to 50 hr for 5-FU nanospheres (Niwa *et al.*, 1993).

1.4.3.1.4 Salting-out technique

Salting-out technique, also called reverse-emulsification, is essentially a modification in the composition of the emulsion/solvent diffusion technique (Nagavarma *et al.*,2012; Vauthier & Bouchemal, 2009; Pinto Reis *et al.*,2006). It is

based on the separation of the water miscible solvent from the aqueous phase through the salting-out effect (Nagavarma *et al.*,2012).

Basically, a salting-out agent is used in high concentrations to efficiently achieve their effect in the aqueous phase. The selection of the salting-out agent is critical as it plays a major role in the EE% (Nagavarma *et al.*,2012). Examples of salting-out agents are electrolytes such as aluminium chloride, calcium chloride, magnesium acetate, magnesium chloride, or non-electrolytes such as sucrose (Nagavarma *et al.*,2012; Pinto Reis *et al.*,2006; Vauthier & Bouchemal, 2009; Ibrahim *et al.*,1992; Allémann *et al.*,1992; Astete & Sabliov, 2006). Colloid stabilizers, such as polyvinylpyrrolidone (PVP) or hydroxyethylcellulose, are used to improve the stability of the formulated NPs (Nagavarma *et al.*,2012; Vauthier & Bouchemal, 2009; Pinto Reis *et al.*,2006). Examples of polymers used in this technique are PLA, PLGA, poly(methacrylic) acid, Eudragit E, and ethyl cellulose (EC) (Nagavarma *et al.*,2012; Pinto Reis *et al.*,2006; Astete & Sabliov, 2006; Allémann *et al.*,1992). The organic phase solvent should be miscible in water, such as acetone and THF (Vauthier & Bouchemal, 2009; Astete & Sabliov, 2006). This technique is used to encapsulate lipophilic drugs and they are usually dissolved in the organic phase (Vauthier & Bouchemal, 2009).

After dissolving the drug in the organic phase, it is emulsified in an aqueous phase containing high concentrations of the salting-out agent and the colloidal stabilizer (Nagavarma *et al.*,2012). Subsequently, the oil in water emulsion is diluted with fast addition of excess amount of water until the diffusion of the solvent into the aqueous phase is fulfilled (Vauthier & Bouchemal, 2009). The diffusion will induce polymer precipitation in the form of NPs. Finally, the solvent and salting-out agent are expelled either by filtration or centrifugation (Astete & Sabliov, 2006; Ibrahim *et al.*, 1992).

Salting-out technique is low time- and energy-consuming. The major drawback is the need for a purification step during the solvent and salting-out agent elimination process (Astete & Sabliov, 2006).

Kumar *et al.*,(2004) fabricated PLGA NPs using the salting-out technique for DNA delivery. The NPs had particle size and zeta potential of 200 nm and 10 mV, respectively. The NPs successfully encapsulated DNA to be used in the DNA delivery. In another study, Zweers *et al.*,(2004) studied the degradation of polymeric NPs prepared using the salting-out technique. Three types of NPs were formulated, poly(DL-lactic acid) (PDLLA), PLGA, and poly(ethylene oxide)-PLGA diblock copolymer (PEO-PLGA). PEO-PLGA and PLGA NPs degraded within 8 and 10 weeks respectively, whereas PDLLA NPs retained their physico-chemical properties for two years.

1.4.3.2 Preparation methods from dispersion of monomers

1.4.3.2.1 Emulsion polymerization

Emulsion polymerization is one of the fastest NPs preparation techniques (Nagavarma *et al.*,2012). In the industry, this method is of high interest as it forms NPs with high concentration of the polymer and low viscosity (Manguian *et al.*, 2006). This technique is subdivided into two categories according to the employment of surfactants: i) conventional and ii) surfactant-free emulsion polymerization (Rao & Geckeler, 2011). While the former technique utilizes surfactants for NPs stabilization, the latter uses amphiphilic di-block copolymers. The latter is favoured as it is less toxic, time and cost saving, and manifests better electrosteric stabilization (Nagavarma *et al.*,2012; Manguian *et al.*,2006; Rao & Geckeler, 2011).

Essentially, the system comprises of monomers of low water solubility and water. The system might also include water soluble initiator and surfactant as well (Thickett & Gilbert, 2007; Rao & Geckeler, 2011). Colloidal stabilizers can be electrostatic, steric, or polymers (Thickett & Gilbert, 2007).

Generally, this technique has to be processed in acidic conditions to linger the anionic polymerization rate and hence, formulate polymeric NPs instead of polymeric aggregations (Vauthier & Bouchemal, 2009). In the conventional technique, monomer is dispersed into an emulsion, whereas in the surfactant-free technique, the monomer is dissolved in an aqueous phase. Afterward, the polymerization is initiated either with an initiator molecule (ion or free radical) or by high-energy radiation (gamma radiator or UV light). Subsequently, chain growth occurs as the monomers collide with each other according to the anionic polymeric mechanism (Nagavarma *et al.*,2012; Thickett & Gilbert, 2007). Eventually, 100 nm particles containing many polymers are collected by centrifugation (Mohanraj *et al.*,2006; Rao & Geckeler, 2011). Drug is either dissolved in the polymeric medium or adsorbed onto formed NPs after polymerization (Mohanraj *et al.*,2006).

Examples of monomers used are styrene, butyl acrylate/ styrene, and methyl methacrylate (Rao & Geckeler, 2011).

This technique has been used for the production of a variety of special polymers such as adhesives, binders, construction materials, diagnostic tests, and drug delivery systems (Asua, 2004).

The advantages of this technique include the possibility of producing polymers with special properties and environmentally friendly since water is used as the dispersion medium (Asua, 2004; Thickett & Gilbert, 2007). However, efficient

production requires accurate online control and delicate understanding of the polymerization process, difficulty in preparing monodispersed and controlled particle size batches. Furthermore, efficient methods are required for residual monomers and surfactants discarding (Thickett & Gilbert, 2007; Asua, 2004; Rao & Geckeler, 2011).

1.4.3.2.2 Interfacial Polymerization

Interfacial polymerization is one of the well-established methods for polymeric NPs preparations (Nagavarma *et al.*, 2012; Rao & Geckeler, 2011). It is considered a low-energy emulsification method (Vauthier & Bouchemal, 2009).

Both positively and negatively charged surfactants can be used either in the aqueous or organic phase (Dallas *et al.*, 2007). Lipophilic drugs are encapsulated with high EE% using interfacial polymerization such as calcitonin, darodipine, octreotide, and insulin (Vauthier & Bouchemal, 2009; Pinto Reis *et al.*, 2006). Physico-chemical characterization of the formulated polymers depends on the reaction conditions (Dallas *et al.*, 2007). Fabricated NPs using this technique have hollow polymer morphology (Rao & Geckeler, 2011).

Advantages of this technique are reproducibility, high loading efficiencies, the ability to increase NPs concentration at final stages of the process, *in situ* formation of the polymers, narrow size distribution, and homogeneous dispersions (Dallas *et al.*, 2007; Fessi *et al.*, 1989). However, drawbacks of this technique include the need to use organic solvents and tedious (Reis *et al.*, 2006).

Kuo & Wen, (2008) used interfacial polymerization technique for polyaniline o/w NPs formation from aniline monomers. Monodispersed spherical particles with a size range of 5-15 nm were produced.

1.4.3.3 Ionic Gelation

Ionic gelation technique, also called ionotropic gelation or coacervation, is one of the few organic solvent-free techniques used in polymeric nanoparticle fabrication as its processed in entirely aqueous media (Nagavarma *et al.*, 2012). In this technique, polymeric NPs are fabricated using biodegradable hydrophilic polymers based on electrostatic interactions between oppositely charged polymer moieties with the cross-linking agent to form hydrogels (Mohanraj *et al.*, 2006; Patil *et al.*, 2010).

Ionic gelation technique includes the drop-wise addition of two dilute aqueous phases, the polymer and the cross-linking agent (Nagavarma *et al.*, 2012; de Pinho Neves *et al.*, 2014). Inter- and intra- electrostatic linkages created between the oppositely charged groups form spherical coacervates in the submicron size range (Patil *et al.*, 2010). Eventually, the liquid transforms into hydrogel beads comprising of NPs (Fan *et al.*, 2012).

Physico-chemical characteristics of the NPs varies according to the polymer and cross-linking agent concentrations, as well as the ionic gelation conditions (Vauthier & Bouchemal, 2009). Alginate, carboxymethylcellulose (CBMC), CS, and gellan gum are examples of polymers used in this technique (Patil *et al.*, 2010).

Ionic gelation technique possesses a long list of advantages such as the spontaneity in formation of NPs under mild conditions, non-toxicity, low-cost, non-requirement of organic solvents, simplicity, convenience, speed, and amenability (de Pinho Neves *et al.*, 2014; Fan *et al.*, 2012). On the other hand, NPs formed are of poor mechanical strength, which limits their applications in drug delivery (Agnihotri *et al.*, 2004).

Ionic gelation technique has been widely applied in the formulation of NPs for the delivery of insulin (Avadi *et al.*, 2010; Sadeghi *et al.*, 2008), proteins (Calvo & Remunan-Lopez, 1997), DNA and RNA (Katas & Alpar, 2006), cyclodextrin (Sajeesh & Sharma, 2006), and CUR (Chuah *et al.*, 2011).

1.4.4 Nanomedicine in clinical practice

Worldwide, over 207 companies have devoted their business share towards nanomedicine activities. In fact, amongst the variety of drug delivery systems, nanomedicine accounts for more than 70% of the market share (Wang *et al.*, 2012). Despite the various challenges in nanomedicine, few first generation formulations have shed lights to the market. The most widely used nanotechnology products is colloidal gold *in vitro* diagnosis, which is used as a rapid test kit for HIV, ovulation, and pregnancy test (Wagner *et al.*, 2006). Nanomedicine for cancer diagnosis, imaging, and treatment has gained intense interest. Some products are already in use while others are showing promising outcomes in clinical studies (Shi *et al.*, 2016).

Tables 1.4 and 1.5 represent examples of nanomedicine products on the market and in clinical development, respectively (Kalepu & Nekkanti, 2015; Kudo *et al.*, 2016; Shi *et al.*, 2016; Von Hoff *et al.*, 2016; Wagner *et al.*, 2016; Wang *et al.*, 2012; Zhao *et al.*, 2017)

Table 1.4 Selected nanomedicine products available in market

Drug Name	Composition	Indication	Type of nanomedicine	Manufacturer's name, county
Abelcet	Amphotericin B	Fungal infections	Liposomes	Enzon, USA
Abraxane	Paclitaxel	Cancer	Polymeric NPs	Celgene, USA

Ambisome	Amphotericin B	Fungal infections	Liposomes	Gilead, USA. Fujisawa, Japan
Amphotec	Amphotericin B	Fungal infections	Liposomes	InterMune, USA
DaunoXome	Daunorubicin	Kaposi sarcoma	Liposomes	Gilead, Japan
Doxil	Doxorubicin	Kaposi sarcoma	Liposomes	Ortho Biotech, USA.
Depocyt	Cytarabine	Cancer	Liposomes	SkyePharma, London
Epaxal Berna	Hepatitis vaccine	Hepatitis A	Polymeric NPs	Berna Biotech, Switzerland
Feridex	Iron oxide NPs coated with dextran	Liver/ spleen lesion imaging	Polymeric NPs	Berlex, USA
Genexol-PM	Paclitaxil	Breast cancer	Micelles	Samyang, Korea
Inflexal Berna	Virosomal influenza vaccine	Influenza	Liposomes	Berna Biotech, Switzerland
Marqibo	Vincristine sulphate	Post-gemcitabine metastatic pancreatic cancer	Liposomes	Talon therapeutics, USA
Myocet	Doxorubicin	Breast cancer	Liposomes	Zeneus pharma, UK
Oncaspar	PEGylated asparaginase	Acute lymphoblastic leukemia	Polymeric NPs	Enzon, USA
Onivyde	Irinotecan	Pancreatic cancer	Liposomes	Baxalta innovations, Austria

Resovist	Iron oxide NPs coated with dextran	Liver/ spleen lesion imaging	Polymeric NPs	Bayer Schering Pharma, Germany
SMANCS	Neocarzinostatin	Liver and renal cancer	Nanoconjugates	Pola pharma, Korea
Panzem NCD	2-methoxyestradiol	Gliblastoma	Nanocrystals	CASI pharmaceuticals, USA

Table 1.5 Selected nanomedicine products in clinical development

Drug Name	Composition	Indication	Type of nanomedicine	Status
AI-850	Paclitaxel	Solid tumours	Polymeric NPs	Phase I
ALN-VSP	siRNA	Liver cancer	Liposomes	Phase I
ABI-009	Rapamycin	malignant PEComa	Albumin NPs	Phase II
AuroLase	Gold coated silica NPs	Head and neck cancer	Liposomes	Phase I
BIND-014	Docetaxel	Prostate cancer	Polymeric NPs	Phase II
BioVant	Calcium phosphate	Vaccine adjuvant	Calcium phosphate NPs	Phase I
CALAA-01	siRNA	Cancer	Polymeric NPs	Phase I
NC-6004	Cisplatin	Cancer		Phase III
MBP-426	Oxalipatin	Solid tomours	Liposomes	Phase I
MM-302	Doxorubicin	Breast cancer	Liposomes	Phase II/III
NK-012	SN-38	Cancer		Phase II
NK-105	Paclitaxel	Cancer	Polymeric micelle	Phase III
NPI 32101	Silver NPs	Atopic dermatitis	NPs	Phase II

Paliperidone palmitate	Paliperidone palmitate	Schizophrenia	Nanocrystals	Phase IV
ThermoDox	Doxorubicin	Hepatocellular carcinoma	Liposomes	Phase III

1.4.5 Nanoformulations of CUR

CUR has been shown to possess promising therapeutic activities against a plethora of health conditions. Moreover, CUR has gained special interest due its low toxicity even at high therapeutic concentrations. Particularly, CUR is the subject of extensive interest as a chemopreventive and chemotherapeutic agent (Yallapu *et al.*, 2010). However, its therapeutic effectiveness is restrained due to its low oral bioavailability, poor pharmacokinetics, poor aqueous solubility, extensive intestinal and hepatic metabolism, and rapid elimination (Cheng *et al.*, 2013; Shaikh *et al.*, 2009; Yallapu *et al.*, 2010; Yen *et al.*, 2010).

To overcome these limitations and to enhance its therapeutic effects, research has been devoted toward encapsulating CUR in various delivery systems such as liposomes, SLN, micelles, and polymeric NPs (Gupta *et al.*, 2009; Yallapu *et al.*, 2010; Yen *et al.*, 2010). Moreover, CUR nanoformulations are known to prolong the circulation time in the body, manifest sustained release, allow targeted delivery, and help to linger its half-life (Cheng *et al.*, 2013).

Yallapu *et al.*,(2010) fabricated CUR-PLGA NPs conjugated with monoclonal antibodies specific for cisplatin-resistant ovarian cancer treatment. Steady and prolonged release of CUR was achieved. Pre-treatment with CUR enhanced the *in vitro* sensitivity on ovarian cancer cells toward cisplatin. Therefore, decreased dose of cisplatin and radiation was required for ovarian cancer treatment. In another study, Gupta *et al.*,(2009) encapsulated CUR in silk fibroin and CS NPs for cancer treatment.

In vitro studies demonstrated enhanced cellular uptake and efficiency of CUR against MCF-7 and MDA-MB-453 breast cancer cells for eight days. However, a slight loss of CUR occurred during the NPs preparation process. Kim *et al.*,(2011) aimed to enhance the water solubility and bioavailability of CUR by encapsulating it in albumin NPs. It was believed that this would improve its anticancer activity. Fabricated NPs were in the size range of 130-150 nm. Water solubility was enhanced by 300-folds compared to pure CUR. Moreover, on-shelf stability was enhanced and hence, its biological effectiveness was not affected. The biological distribution was enhanced and elimination rates were reduced in mice administered with CUR NPs compared to pure CUR. In terms of its anticancer activity, *in vivo* studies demonstrated that tumour growth was significantly suppressed in CUR NPs administered mice compared to those received pure CUR.

Table 1.6 and Table 1.7 summarize available CUR nanoformulations on market (Yallapu *et al.*, 2012) and CUR nanoformulations under clinical development (Conlan *et al.*, 2017; Kocher *et al.*, 2015; Schiborr *et al.*, 2014; Storka *et al.*, 2015; Yallapu *et al.*, 2015), respectively.

Table 1.6 List of CUR nanoformulations available on market

Trade name	Ingredients, formulation	Manufacturer's name and country
Curcumin C3 complex [®] vegetarian capsules	Curcumin C3 complex, curcuminoids and <i>piper nigrum</i> fruit extract.	BesVite Inc, USA.
CurcuPlus D Ultra [™]	CUR, ascorbyl palmitate, microcrystalline cellulose, maltodextrin, silicon dioxide, soy lecithin, and stearic acid	Advanced Orthomolecular research Inc., Canada
Enhansa	A special CUR compound	Lee sislby compounding pharmacy, USA.

Liposomal CUR	CUR, lecithin, and potassium sorbate. Liposomes	NanoLiposomal Nutritionals, USA.
NanoBioSphere™	CUR, vitamin E, sunflower oil, and additives. SLN	Life enhancement products, USA.
<i>N</i> -curcusb	CUR NPs	Konark herbals and health care, India.
Nanocurcuma	CUR in nanocolloids	Nano Tech Miso-N, Korea
Nutrivene Longvida™	CUR and soy lecithin, NPs	International nutrition, USA.

Table 1.7 CUR nanoformulations under clinical development

Study title	Therapeutic indication	Status	NCT or Ref.
Phase I Clinical trial investigating the ability of plant exosome to deliver curcumin to normal and malignant colon tissues	Colon cancer	Phase I	NCT 01294072
The oral bioavailability of curcuminoids in healthy humans is markedly enhanced by micellar solubilisation but not further improved by simultaneous ingestion of sesamin, ferolic acid, naringenin and xanthohumol.	Prevention and treatment of inflammatory diseases	Phase 0	NCT 01982734
The oral bioavailability of curcumin from micronized powder and liquid micelles is significantly increased in healthy humans and differs between sexes.	Bioavailability and toxicity studies	Phase 0	NCT 01925287
Safety, tolerability and pharmacokinetics of liposomal curcumin (Lipocurc™) in healthy humans	Bioavailability and toxicity studies	Phase I	NCT 01403545

1.5 Drug Delivery to the colon

Targeted drug delivery to the colon is gaining increased interest not only for local disease treatment such as irritable bowel syndrome, IBD, ulcerative colitis, and colon cancer (Jain *et al.*, 2007; Yang *et al.*, 2002) but for systemic absorption for drugs which are unabsorbed or unstable in the upper GIT as well (Abraham Rubenstein, 1990; Sinha & Kumria, 2003). Advantages of using the colon as target site for drug absorption in spite of the fact that it is not suited for absorption is that dosage forms have longer transit times, there is reduced digestive enzymatic activity, and higher response to absorption enhancers in formulation compared to the upper GIT (Jain *et al.*, 2007; Sinha & Kumria, 2003). Moreover, targeting drugs to the colon for localised treatment reduces the required dose for systemic absorption for the same treatment and thus, side effects is reduced (Abraham Rubenstein, 1990; Sinha & Kumria, 2003). Unfortunately, successful delivery of drugs to the colon without premature drug release or degradation in the upper GIT is challenging (Sinha & Kumria, 2003).

1.5.1 Strategies for targeted colonic therapy

The colon is located at the distal part of the GIT and therefore, drug delivery systems targeting the colon should protect the cargo from being released in the stomach or small intestine. Yet, the delivery system should have the functionality of sensing arrival to the colon based on the different anatomical and physiological characteristics peculiar to the colon. The sensing should be the basis of trigger of cargo release. In the next sections, I shall discuss some of the pharmaceutical strategies designed for the development of colon-targeted therapy.

1.5.1.1 Pro-drugs

The term “pro-drug” refers to a pharmaceutical inactive derivative of a drug linked to a carrier where cleavage of the prodrug brought about either spontaneously or enzymatically leads to drug release (Chourasia & Jain, 2003; Sinha & Kumria, 2003). The triggering mechanism for the drug release depends on the type of the linkage (Chourasia & Jain, 2003).

Typical examples of pro-drugs relevant to colonic delivery are the azo-linkages in balsalazine, ipsalazine, sulfasalazine, and olsalazine that bears 5-amino salicylic acid (5-ASA) for the treatment of IBD (Abraham Rubenstein, 1990; Chourasia & Jain, 2003; Rubinstein, 2005). Amino acids with $-\text{COOH}$ and $-\text{NH}_2$ functionality may be conjugated with drugs where the linkage is hydrolysed by colonic microflora (Sinha & Kumria, 2003). Sugar conjugates such as cellobiose, galactose, and glucose are further examples of prodrugs that may be hydrolysed enzymatically by the colonic microflora such as glycosidase and glucuronidase (Sinha & Kumria, 2003; Yang *et al.*, 2002). The major drawback in this approach is the need to re-evaluate the pro-drug formulation since it is regulatory considered a new chemical substance (Sinha & Kumria, 2003; Yang *et al.*, 2002).

1.5.1.2 pH-dependent systems

The pH-dependent systems are based on the peculiar pH values of the colon (pH 6-8) compared to the stomach and small intestine (pH 1-2 and pH 6-7, respectively). In such systems, the formulation is coated with polymers that withstand the acidity and neutral pH conditions of the upper GIT. However, the polymers may ionize, swell or disintegrate in the colon due to the pH and thus release the drug (Chourasia & Jain, 2003; Rubinstein, 2005). Examples of such polymers are the Eudragit® products.

Particularly, Eudragit® L and Eudragit®S (Chourasia & Jain, 2003). In addition to cellulose acetaphthalate (Rubinstein, 2005). The disadvantages of this approach are the close pH values of the small and large intestine, variance of pH values in some health conditions, and inter-/ intra subjects variations (Yang *et al.*, 2002).

1.5.1.3 Time- dependent systems

The concept of time-dependent systems in colon drug delivery is delaying drug release until the formulation arrives the colon. The formulation should withstand the acidic conditions of the stomach and undergoes lag time, which is the time required to transit from the mouth to the colon (Yang *et al.*, 2002; Chourasia & Jain, 2003). In these systems, the drug is coated with a swellable hydrophilic polymer, which resists the acidic conditions in the stomach, swells in the pH medium of the colon and thus, releases the drug. The delayed time of release depends on the physico-chemical properties and concentration of the polymer (Sangalli *et al.*, 2001).

The first formulation fabricated based on this system was Pulsincap®. The main body is made of hydrogel plug coated with hydrophobic materials that is covered with hydrophilic cap. To protect the whole body from the acidic conditions, it is covered with an enteric polymer which dissolves in the small intestine, the concentration of the hydrogel plug determines the time required for the contents to be released (Chourasia & Jain, 2003).

Hydroxyl propyl methyl cellulose has been used to deliver pseudo ephedrine HCl and diltiazem HCl using this strategy (Roy & Shahiwala, 2009).

The disadvantages of this principle are the variable gastric time emptying, unpredictable gastrointestinal motility and its effect on GI transit of the drug, and

variability in gastric transit properties in certain health conditions such as IBD, diarrhoea, and ulcerative colitis (Philip & Philip, 2010).

1.5.1.4 Microbially- triggered systems

The disadvantages of the previously mentioned systems such as pH inter- and intra- variability, gastrointestinal transit time variability, and pre-mature drug release make these systems unideal for colon drug delivery (Sinha & Kumria, 2003). Therefore, researchers have proposed newer approaches to specifically deliver drugs to the colon based on microbial trigger (Sinha & Kumria, 2003). The concept utilizes the fact that the normal flora of the colon release enzymes specifically there that are capable of hydrolysing certain linkages such as the azo and saccharides linkages (Chourasia & Jain, 2003; Philip & Philip, 2010; Rubinstein, 2005). The polymers are capable of protecting the drug from the pH conditions of the upper GIT. Moreover, specifically deliver drugs to the colon (Philip & Philip, 2010). The vast majority of research on these systems have been devoted towards using natural polysaccharides. The advantages of using them are their availability, reasonable prices, flexibility, and safety in use. They can be obtained from natural sources, examples including, pectin (PEC), inulin, and guar gum, animals like chondroitin sulphate and CS, or microbial origin such as dextran (Philip & Philip, 2010). For example, CS has been used as enteric-coated capsule to deliver 5-(6)-carboxy fluorescein, CS succinate and PEC for diclofenac sodium and Idomethacin delivery, respectively (Philip & Philip, 2010).

Limitations of this system are the premature drug release in the upper GIT due to the swelling of the carrier and the microbial variety among populations (Rubinstein, 2005).

1.5.2 Mucoadhesion

Mucoadhesion has been employed in delivery systems as an attractive incorporation in pharmaceutical formulations where the GI residence time of dosage forms can be prolonged significantly (Boddupalli *et al.*, 2010; Carvalho *et al.*, 2010; Khutoryanskiy, 2011; Shaikh *et al.*, 2011). The first therapeutic application of this concept was Orabase[®] in which gum tragacanth was mixed with dental adhesive to deliver penicillin to the oral mucosa (Khutoryanskiy, 2011). Recent statistics show an expanding interest in employing mucoadhesion of drug delivery sector (Andrews *et al.*, 2009; Khutoryanskiy, 2011).

Mucoadhesive formulations should be adhesive, small, flexible, have high drug loading efficiency, and have controlled drug release properties (Boddupalli *et al.*, 2010). Mucoadhesive drug delivery systems can be formulated as lozenges, tablets, films, gels, and solid micro- and nano- particulate systems (Carvalho *et al.*, 2010; Khutoryanskiy, 2011) and they may be administered by ocular, nasal, buccal, gingival, gastrointestinal, vaginal, and rectal (Boddupalli *et al.*, 2010; Khutoryanskiy, 2011).

The advantages of mucoadhesive drug delivery over conventional methods are their prolonged residence time that may be used to achieve superior bioavailability of cargoes (Andrews *et al.*, 2009; Boddupalli *et al.*, 2010; Khutoryanskiy, 2011; Shaikh *et al.*, 2011).

1.5.2.1 Polymers used in mucoadhesion

Several factors dictate choice of polymer to achieve mucoadhesive properties, including type of functional groups, molecular weight, chain length, conformation, degree of hydration, pH, charge, concentration, cross-linking density, and flexibility (Andrews *et al.*, 2009; Salamat-Miller *et al.*, 2005). For good mucoadhesive properties,

polymers should have certain structural characteristics including strong hydrogen-bonding groups, strong cationic or anionic charges, high molecular weight, adequate chain flexibility, surface energy properties favouring dissemination onto mucous (Khutoryanskiy, 2011; Lehr *et al.*, 1992).

Generally, adhesive polymers are mainly classified into three major categories: Synthetic and natural, water soluble and water insoluble, and charged and uncharged polymers (Roy *et al.*, 2009).

1.5.2.1.1 Anionic polymers

Anionic polymers are the most commonly used mucoadhesive polymers in pharmaceutical formulations because of their high mucoadhesive properties and low toxicity (Andrews *et al.*, 2009). Typical examples are carboxymethylcellulose (CBMC), PAA, poly carbophil, poly(methacrylic acid), PEC, sodium alginate, and Xanthan gum (Grabovac *et al.*, 2005; Khutoryanskiy, 2011; Park & Robinson, 1984). The strongest mucoadhesive functionality of anionic polymers is observed under acidic conditions (Khutoryanskiy, 2011). Amongst the anionic polymers, carbopol, has the highest molecular weight and degree of cross-linking, and showed the longest period of mucoadhesion (Grabovac *et al.*, 2005).

Mucin and anionic polymers have several structural similarities including negative charge and the presence of network of macromolecules, highly hydrated, form expanded networks, and have several carboxyl groups (Andrews *et al.*, 2009). These similarities are believed to be the source of the mucoadhesive interactions with anionic polymers which leads to four possible mechanisms: i) strong hydrogen-bonding between the carboxylic groups and oligosaccharide chains of the anionic polymers and mucin, respectively ii) electrostatic interactions iii) hydrophobic interaction, and iv)

inter-diffusion of the expanded networks (Andrews *et al.*, 2009; Bernkop-Schnürch, 2005; Khutoryanskiy, 2011; Leung & Robinson, 1988). In the present work, PEC was used as the anionic component of the composite and a detailed discussion of its physico-chemical properties that are of relevance to the work is discussed in chapter 2.

1.5.2.1.2 Cationic polymers

Although anionic polymers show good mucoadhesive properties, they are unable of forming mucoadhesive hydrogels. In contrast, cationic polymers have good mucoadhesive properties and are capable of forming them (Lehr *et al.*, 1992). Mucoadhesive properties of cationic polymers have been extensively studied and used in pharmaceutical formulation for mucoadhesive drug delivery (Khutoryanskiy, 2011). Examples of such polymers are CS, dimethylaminoethyl-dextran, aminodextran, polylysine, and polybrene (Khutoryanskiy, 2011; Lehr *et al.*, 1992; Park & Robinson, 1984). Amongst them, CS has been extensively used due to its good biocompatibility, biodegradability, and low toxicity (Roy *et al.*, 2009).

The main mechanism of mucoadhesion is by electrostatic interaction between the positive functional groups, and the sialic acid and sulphonic acid substructures of the cationic polymer and mucin, respectively (Farokhzad & Langer, 2006). However, it is believed that other interactions such as hydrogen-bonding and hydrophobic effects also play role in the mucoadhesion functionality of the cationic polymers (Andrews *et al.*, 2009; Roy *et al.*, 2009). The degree of contribution of each interaction vary according to the solution pH and the presence of other chemicals (Khutoryanskiy, 2011; Roy *et al.*, 2009; Smart, 2005). In the present work, CS was used as the cationic component of the composite and a detailed discussion of its physico-chemical properties that are of relevance to the work is discussed in chapter 2.

1.6 Aims and objectives of the present research

1.6.1 Aims

The therapeutic efficacy of CUR as an anticancer agent has been widely acclaimed. The major drawback for use of CUR in colorectal cancer treatment is its low oral bioavailability. In this work, we believe that by encapsulating CUR in nanoparticulate delivery system that possess mucoadhesive propensity and capable of resisting the degradative effects of the upper GIT, we might be able to deliver therapeutic levels of CUR to the colon. We recognize the significance of protecting CUR from the onslaught of enzymatic or milieu effects of the upper GIT to act locally on tumours. We also recognise that the delivery system should ideally have a wide surface coverage to be effective against possible recurrence, especially if malignant. Therefore, the overarching objective of the present work was to develop a nanoparticulate delivery system with CUR as cargo since these have the largest surface area to volume ratio of all dosage forms. The NPs must meet desired physico-chemical characteristics and so a significant amount of work was dedicated to *in vitro* studies. Further studies were carried *in vivo* using animal models in order to test the proof of concept.

1.6.2 Objectives

- In chapter 2, we shall discuss the effects of formulation and processing variables on the physico-chemical properties of the NPs with a view to producing particles that demonstrate the lowest z-average, pDI, and highest surface charge.

- In chapter 3, we shall examine the mucoadhesive properties of the CUR-CS-PEC-NPs and the release profiles of CUR as a function of several physiological constraints.
- Chapter 4 entails studies on the anti-proliferative effects of the NPs CUR-CS-PEC-NPs and investigation of cellular uptake of the NPs by the cells.
- The final chapter (chapter 5) shall examine the proof of the above concepts in *in vivo* settings through bioavailability assessment and other physiological studies.

Chapter 2

Formulation of Curcumin Chitosan Pectinate Nanoparticles

2 Formulation of curcumin chitosan pectinate nanoparticles

2.1 Introduction

2.1.1 Polymer of choice 1: Chitosan

With regard to oral drug delivery, NPs present several advantages including protecting drug from degradation, enhanced cellular uptake by endocytosis (Bowman & Leong, 2006; Mohanraj *et al.*, 2006) controlled and sustained drug release, site-specific targeting and amenability to various other applications (Gelperina *et al.*, 2005). NPs can be fabricated to adsorb on tissues and organs (Gelperina *et al.*, 2005; Kayser *et al.*, 2005; des Rieux *et al.*, 2006). Moreover, the tiny size dimension means that they possess the highest surface to volume ratio of any other type of delivery system. CS is biodegradable and biocompatible so it is safe to use on biological systems. Its physical properties may be modulated at relevant pH for various applications (George & Abraham, 2006; Vaghani *et al.*, 2012). Thus, it has been widely used in the food industry as an additive (Lorenzo-Lamosa *et al.*, 1998), in medicine for wound healing (Skaugrud *et al.*, 1999), in the pharma industry as a pharmaceutical excipient (Dodane & Vilivalam, 1998; Singla & Chawla, 2001), and as a permeation enhancer (Bowman & Leong 2006; des Rieux *et al.* 2006). Moreover, CS has mucoadhesive properties and recent research have been devoted towards studying its potential as DNA, gene, vaccines, protein, peptides carrier, and drug targeted delivery systems (Agnihotri *et al.* 2004; Bowman & Leong, 2006; Bayat *et al.* 2008; Dodane & Vilivalam, 1998; Singla & Chawla, 2001). With regard to the present work, we recognise that the major limitation in using CS for colon drug delivery is its rapid dissolution in gastric pH (George & Abraham, 2006; Lorenzo-Lamosa *et al.*, 1998). Therefore, some forms of formulation intervention must be taken into account if a viable colon-targeted CS nanoparticulate system is to be realised.

There are a number of CS-nanoparticle dosage forms currently under study. Qi *et al.* (2004) prepared CS NPs encapsulating copper for antibacterial activity. The antibacterial activity was studied against several microorganisms where antibacterial activity was correlated with adherence of the bacteria to the surface of the NPs. Mitra *et al.* (2001) fabricated dextran-doxorubicin conjugate CS NPs in order to decrease the toxicity of doxorubicin. The NPs were prepared using the microemulsion method, which produced monodispersed NPs of 100 ± 10 nm diameters. The drug-conjugate encapsulated in CS NPs was successfully delivered to the tumour site with extended circulation and accumulation time. The mean tumour volume was the lowest in drug-conjugate CS NPs compared to pure drug-conjugate and crude CS NPs after 90 days of treatment. He *et al.* (2017) formulated CS-Sodium tripolyphosphate (TPP) NPs using the ionic gelation method as a carrier for insulin. The NPs had high EE% and released insulin in a pH-dependent manner. In another study, Gan *et al.* (2005) used the ionic gelation method to produce CS-TPP NPs intended for gene and protein delivery with a size range of 100-250 nm. Moreover, they found that low molecular weight CS produced smaller sized NPs compared to the medium and high molecular weight CS.

2.1.2 Polymer of choice 2: Pectin

PEC is a heterogeneous polysaccharide and is the major component of the cell wall of most plants (Ashford *et al.*, 1993; Munjeri *et al.*, 1997). It is made up of polygalacturonic acid esterified with methoxy groups via $\alpha(1-4)$ glycosidic linkages (Malviya & Kulkarni, 2012; Liu *et al.* 2006). It may be classified broadly into two major groups based on the degree of esterification (Liu *et al.* 2006). Commercially, PEC is extracted from apple pomace and citrus peels (Sriamornsak, 2003; Willats *et al.*, 2006), and is produced as a white to light brown powder (Sriamornsak, 2003). It is non-toxic and therefore has been safely used in food industries for many years as a gelling and

thickening agent in dairy products (Liu *et al.*, 2006) as a thickener (Malviya & Kulkarni, 2012) and a colloidal stabilizer (Sriamornsak, 2003). In pharmaceutical industry, PEC has been used to lower blood cholesterol and glucose concentration, anti-diarrhoeal agent, and in weight control management (Sriamornsak, 2003; Willats *et al.*, 2006).

At low pH, PEC is insoluble and its molecules tend to shrink due to the decrease in the carboxylic groups repulsion forces (Awasthi, 2011; Liua *et al.*, 2003; Sriamornsak, 2003). Moreover, PEC resists degradation by gastric and intestinal enzymes whilst completely degrades by enzymes from colonic flora (Awasthi, 2011; Sriamornsak, 2003). Therefore, PEC possesses requisite properties relevant to the present investigation. In fact, this polymer has been extensively studied as a potential carrier for targeted colon delivery (Munjeri *et al.*, 1997; Liua *et al.*, 2003; Cui *et al.*, 2009). However, PEC is soluble in the pH range of the small intestine (pH 6-7), resulting in the swelling of delivery systems and premature release of cargo. To overcome this obstacle, it is recommended that PEC be used in combination with other polymers such as CS, alginate, and Eudragit to form more stable matrices (Liu *et al.*, 2006; Awasthi, 2011; Semdé *et al.*, 2000).

Jung *et al.* (2013) successfully formulated PEC hydrogel beads for colon drug delivery with relatively high encapsulation efficiencies and restrained drug release at acidic pH, yet significant release at colonic conditions. Therefore, it is sensible to consider a composite formulation of PEC and CS to address the requirement of a restrained release of cargo in the upper GIT but yield significant release at colonic conditions.

Composite microparticles based on CS, alginate, and PEC have been produced for oral delivery of proteins with a pH-dependent drug release functionality. Drug release was significantly higher at higher pH compared to lower pH medium. Additionally, drug release was highest in media of high pH with colonic enzymes (Yu *et al.*, 2009).

In the present investigation, we wished to fabricate orally administered CUR-containing NPs that may retain the drug load in the stomach and small intestine and only release in the colonic conditions with attendant mucoadhesive functionality. In this regard, PEC protects the composite formulation from the pH within the upper GIT. Furthermore, degradation of both PEC and CS materialises at the colon, which favours release of CUR (Liu *et al.*, 2006; Semdé *et al.*, 2000).

2.1.3 Sodium tripolyphosphate (TPP) as the cross-linking agent

Ionic gelation technique was chosen in this study because it is a nontoxic procedure and that the use of organic solvents was kept to a minimum. There are a variety of other crosslinking agents including gum arabic, glutaraldehyde, and genipin (Shu & Zhu, 2002). However, chemically-induced cross-linking agents such those imposed by glutaraldehyde and genipin may alter the physico-chemical properties of CS in resultant formulations, in addition to toxicity and other undesirable concerns (Mi *et al.*, 2003; Shu & Zhu, 2002). Furthermore, gum arabic interaction with polycationic polymers such as CS results in formulations with low encapsulation efficiencies (Avadi *et al.*, 2010). On the other hand, TPP is non-toxic, simple to use (Rodrigues *et al.* 2012; Fan *et al.* 2012) and relatively inexpensive (Shu & Zhu, 2002). Technically, it has quick gelling property and crucially, has been extensively and successfully used as the cross-linking agent in CS-based NPs (de Pinho Neves *et al.*, 2014; Mi *et al.*, 2003). de Pinho

Neves *et al.* (2014) formulated CS-TPP (CS-TPP) NPs and in such instances, the formation of the NPs is through ionic interaction between the positively charged amino groups of CS ($-\text{NH}_3^+$) and the negatively charged tripolyphosphate groups of TPP (P_3O_5^-) which forms inter- and intramolecular cross linkages with CS (Fan *et al.* 2012).

2.1.4 Particle size and zeta potential

Particle size and zeta potential are two essential physical parameters used in predicting the stability and functionality of NPs (Shekunov *et al.*, 2007). The most commonly used method for particle size measurement is the Dynamic Light Scattering (DLS), also called photon correlation spectroscopy (PCS) and quasi-elastic light scattering (Shekunov *et al.*, 2007). As illustrated in Figure 2.1, a laser beam (A) is fluctuated according to the NPs Brownian motion (B). Afterward, the detected fluctuations (C) are converted to a size dispersion using Stokes-Einstein equation. In this technique, cost and time are an added advantage and values recorded indicate absolute measurement without the need for further information (Bootz *et al.*, 2004; Hoo *et al.*, 2008; Shekunov *et al.*, 2007).

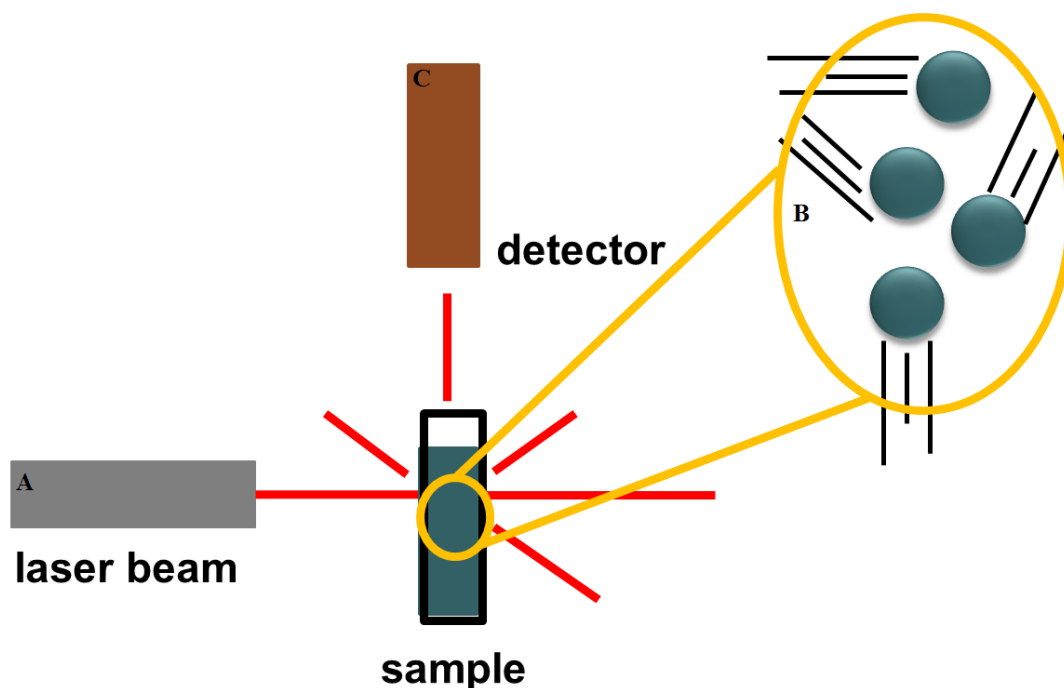


Figure 2.1 Schematic diagram of a typical DLS technique (*Adopted and modified from www.sustainable-nano.com*)

The zeta potential gives an indication of the surface charge on the NPs and can be correlated to the stability of the dispersion (Xu, 2008). It can be measured using a laser Doppler micro-electrophoresis method in which an electric field is applied to a nanoparticle dispersion moving with a velocity related to their zeta potential (Clogston & Patri, 2011). The velocity is measured based on the light scattering effects and converted to zeta potential using the Henry equation. Advantages of this method are accuracy, sensitivity, versatility, and values are not affected by the liquid motion (Clogston & Patri, 2011; Xu, 2008).

In this study, we aim to study the particle size and zeta potential of particles produced as these play essential roles in the effective delivery of the NPs to the colorectal tumour cells. For instance, smaller particle size, particularly <500 nm, are required for enhanced adhesion and cellular uptake into the colorectal tumour cells (Jung *et al.*, 2000; Yin *et al.*, 2005).

2.1.5 Scanning Electron Microscopy

Scanning electron microscopy (Figure 2.2) was introduced by M. Von Adrenne in 1938. However, it was subsequently developed until first commercialized in 1965 (McMullan, 1995; Reichelt, 2007). Compared to light microscopes, SEM provides much higher magnification and resolution, up to 150,000x and 10 nm, respectively therefore, allowing to distinctly visualise nano-sized objects (Instruments, 2017).

In SEM, a fine probe of electrons with energies up to 40 kV is focused and scanned at the surface of the specimen, which results in the formation of secondary electrons, backscattered electrons, auger electrons, photons of various energies, and characteristic X-rays. The interpretation of these secondary electrons provides an image of the specimen (Bogner *et al.*, 2007; Rochow, 1978). The SEM technique provides two and three dimensional image of the specimen shows fine morphological details of the particles. The image provides direct information on size and size distribution, which are vital parameters in our study (Bogner *et al.*, 2007; Bootz *et al.*, 2004; Reichelt, 2007).

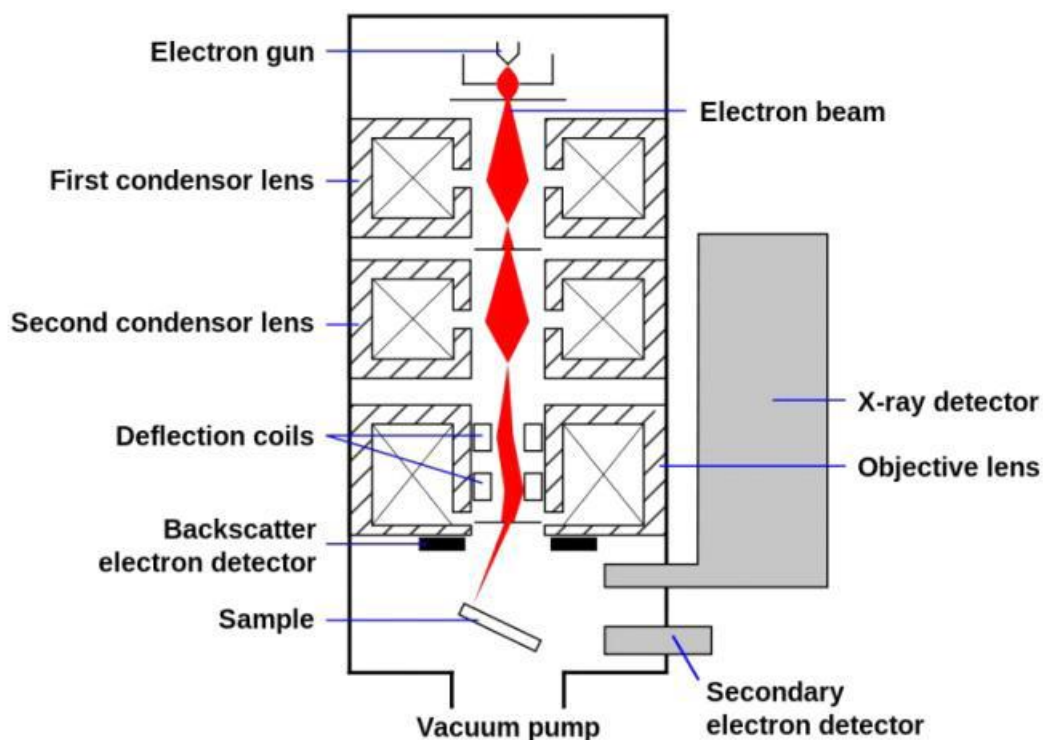


Figure 2.2 Schematic diagram of SEM components (*Choudhary & Priyan, 2017*)

2.1.6 Fourier Transform Infrared Spectroscopy

The invention of the Fourier Transform Infrared Spectroscopy (FT-IR) can be traced back to late 1880s when Alber A. Michelson invented Michelson interferometer (Jaggi, 2006). FT-IR spectroscopy comprises of the emission, absorption, and reflection of spectrums attained by fourier transform of an optical interferogram. FT-IR spectroscopy is not restricted to the infrared (IR) frequency but can be used in the visible and far UV range as well (Jaggi, 2006). The instrument includes a black box of three optical inputs; IR source, He-Ne laser and a white light (Jaggi, 2006). The optical sources share the same beam splitter and mirrors, which are connected to an interferometer (Figure 2.3). The later generates a record of intensities as a signal called interferogram. The software then converts the interferogram to spectrum which represents a measurement of IR light intensity versus a property of light (Jaggi, 2006; Smith, 2011). FT-IR is used for the qualitative and quantitative analysis of samples and

for the determination of aromaticity, aliphaticity, and oxygenation rate of samples (Lamontagne *et al.*, 2001; Smith, 2011; Vlachos *et al.*, 2006).

In our study, it is essential to investigate whether the formulation process leads to the formation of new chemical interactions, which may result in an altered performance of the polymers and/or CUR. Therefore, FT-IR analysis was performed as an accurate and sensitive method for studying the interactions among the NPs.

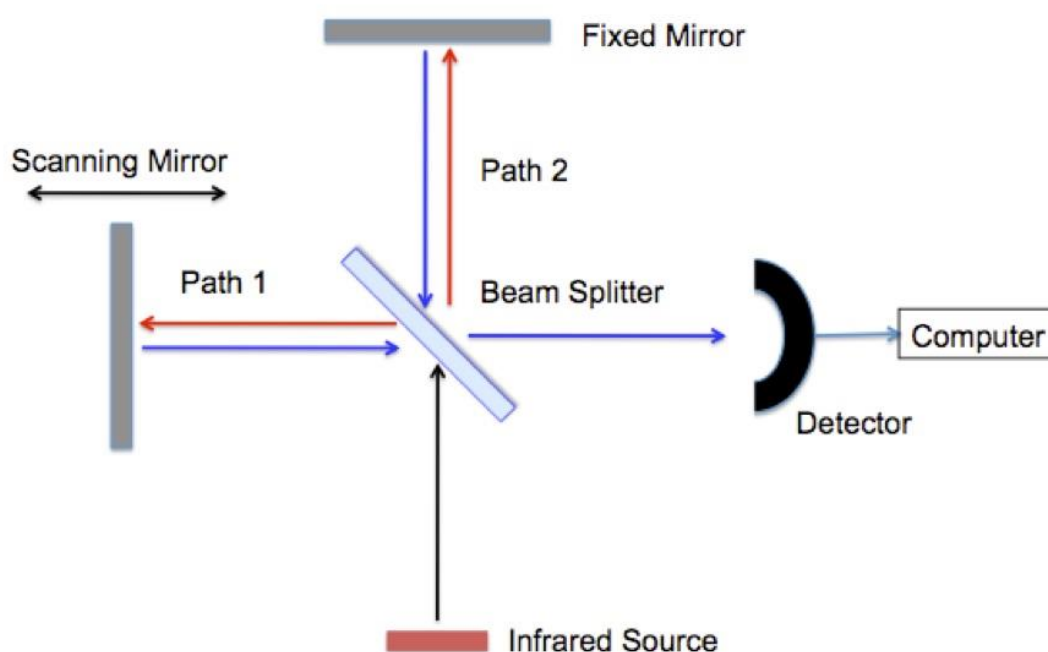


Figure 2.3 Schematic diagram of the FT-IR (Adapted from chem.libretexts.org)

2.1.7 X-Ray Diffractometer

X-ray diffractometry (XRD) is based on the fact that atoms in crystals are periodically arranged and so diffract light (Chauhan & Chauhan, 2014). As illustrated in Figure 2.4, the XRD comprises of an X-ray source (A), which directs the rays towards the sample (B) (US 6,665,372 B2, 2003). A detector (C) that detects the scattered, diffracted, or reflected X-rays in a pattern peculiar to the sample's structure

(US 6,665,372 B2, 2003). A goniometer controls the sequential relative angular positions between the X-ray source, the sample and the X-ray detector (Goebel, 1994). Finally, the intensity of the pattern is plotted versus the angle of the detector in an output called diffractogram (Chauhan & Chauhan, 2014).

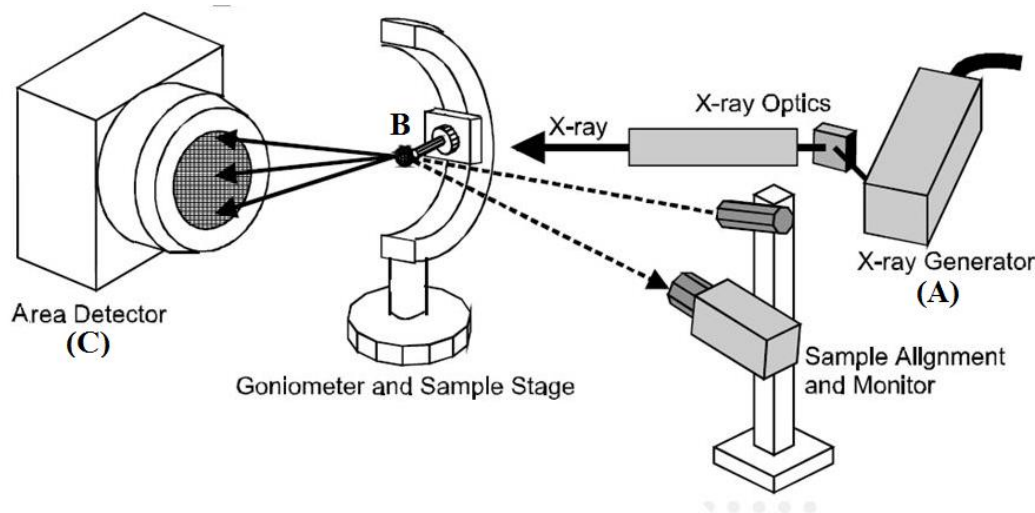


Figure 2.4 Schematic diagram of XRD components (*Adopted and modified from www.slideplayer.com, Brighton, 2015*)

Samples analysed using XRD should be in the form of fine powder. A wide variety of samples can be studied including organic and inorganic compounds, polymers, metals, fibres, pharmaceutical, and nanomaterials (Chauhan & Chauhan, 2014).

XRD can be employed to study the crystalline content and phase of a material which might give indication on the release profiles of the material (Chauhan & Chauhan, 2014). XRD provides simple, easy, reliable, and sensitive analysis of samples (Chauhan & Chauhan, 2014), thus it was used in this study.

2.1.8 Differential Scanning Calorimetry

Differential scanning calorimetry (DSC) (Figure 2.5) is the most commonly used thermal analytical technique where the difference in energy inputs of a sample

and a reference is measured as a function of temperature over a duration of time (Barton, 1985; Gill *et al.*, 1993; Gill *et al.*, 2010; TAINstruments, 2017).

A furnace generates the main heat flow symmetrically and simultaneously through the sample and reference cells located in a disk containing temperature sensors. The temperature is then raised over time and endothermic or exothermic energy changes required to keep the temperature of both cells identical is plotted as a function of time and temperature (Höhne *et al.*, 2003; Gill *et al.*, 2010).

In nanomedicine, DSC is used for characterization of materials, comparison studies, safety and stability investigations, quality control, glass transition and crystallization behaviours. In our study, it was used to ascertain the crystalline state of the encapsulated CUR (Höhne *et al.*, 2003; Gill *et al.*, 2010; TAINstruments, 2017).

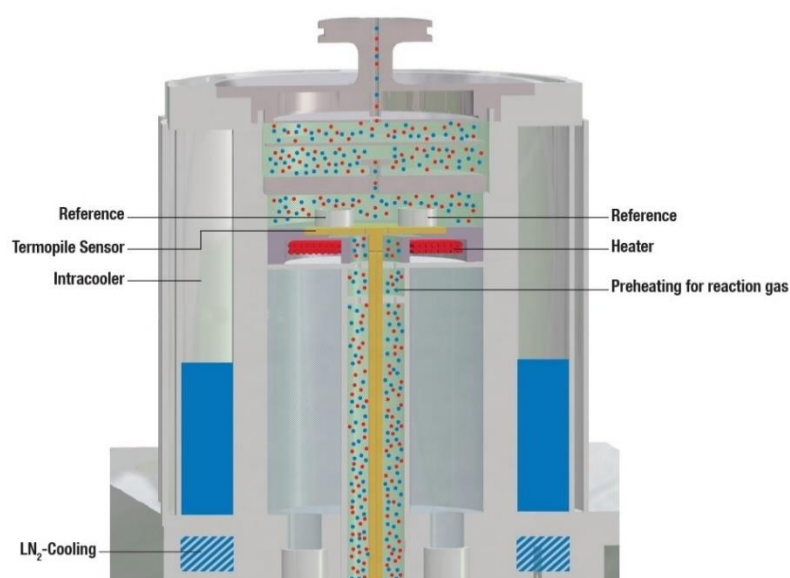


Figure 2.5 Schematic diagram of DSC components (*Adpoted from www.linseis.com*)

2.1.9 Aims and Objectives in this Chapter

The aim of this chapter was to formulate a CUR-containing CS-pectinate composite nanoparticulate using sodium TPP as the cross linker. The effects of processing and formulation parameters on the physical properties of the particles were also evaluated.

2.2 Materials and Methods

2.2.1 Materials

Material	Supplier
Curcumin analytical standard	Fluka, USA
Low molecular weight chitosan	Sigma Aldrich, USA
Low methoxy pectin	CP Kelco, USA
Methanol (analytical grade)	R&M chemicals, UK
Absolute ethanol	R&M chemicals, UK
Glacial acetic acid	R&M chemicals, UK
Sodium hydroxide	Merck, Germany

2.2.2 Formulation of chitosan-pectinate composite nanoparticles

2.2.2.1 Preliminary formulations of CUR chitosan-pectinate composite nanoparticles based on order of addition

The stock solution of CUR was prepared by dissolving CUR in methanol at 1 mg/ml. CS was dissolved in 2% v/v acetic acid at 0.15% w/v and pH adjusted to 5 using 2M sodium hydroxide (NaOH). TPP, PEC and CaCl₂ were dissolved in purified water at 0.05% w/v, 0.05%, and 0.943% respectively. Four primary formulations of CUR-containing CS-pectinate NPs (CUR-CS-PEC-NPs) were prepared as shown in Table 2.1. The formulations differ in the order of adding the solutions, all of which were performed under magnetic stirring at 500 rpm. The formed NPs were centrifuged at 4000 rpm (18°C) for 20 min and the supernatant discarded. The collected NPs were re-dispersed in purified water for further analysis. Controls NPs (CS-PEC-NPs) of the four formulations were prepared in the same manner without the addition of CUR.

Table 2.1 Composition of CUR-CS-PEC-NPs

Order of addition	Formulation A	Formulation B	Formulation C	Formulation D
1	300 µg of CUR drop wise into 25 ml of PEC solution with stirring	300 µg of CUR drop wise into 25 ml of CS solution with stirring	300 µg of CUR drop wise into 25 ml of PEC solution with stirring	
2	25 ml of TPP solution added at 12.5 ml/ min with stirring		25 ml of CS solution added at 12.5 ml/ min with stirring	25 ml of CaCl ₂ added at 12.5 ml/ min with stirring
3	Additional stirring for 1hr			Additional stirring for 10 min
4	25 ml of CS solution added at 12.5 ml/ min with stirring	25 ml of PEC solution added at 12.5 ml/ min with stirring	25 ml of TPP solution added at 12.5 ml/min with stirring	25 ml of CS solution was injected with stirring
5	Further stirring for 1hr			

2.2.2.2 Sub-formulations and optimization of the preliminary formulation

Further optimization was carried out by varying the quantities of CS, TPP, and PEC (3:1:1, 3:2:1, 4:1:1, 4:2:1, 5:1:1, and 5:2:1, respectively). Subsequent optimization of stirring times at order 3 and 5 respectively (2 min and 20 min; 2 min and 40 min, and 2 min and 60 min) at variable stirring speeds (500, 800, and 1000 rpm).

2.2.3 Size and zeta potential measurement

The size of the NPs was assessed as z-average diameter and the surface charge as zeta potential using Zeta Sizer Nano Series[®] (Malvern Instruments, UK) equipped with a 4 mW He-Ne laser at wavelength of 633 nm. Hydrodynamic diameter (d nm) was measured by Dynamic Laser Scattering (DLS) at a scattering angle of 173°. The

zeta potential (mV) was determined by Laser Doppler Anemometry (LDA). The NPs were diluted before reading. CS-PEC-NPs and CUR-CS-PEC-NPs were diluted up to 1 and 10 folds, respectively. Samples were run in triplicate and mean reading was taken.

2.2.4 FESEM imaging

Field Emission Scanning Electron Microscopy (FESEM) (Model Quanta 400F, FEI Company, US) at 10 kV was used to observe the morphology and surface topography of the NPs. Samples were prepared by placing one drop of NPs suspension on the stub and left to dry at ambient temperature 24 hr before viewing.

2.2.5 FT-IR analysis

FT-IR spectra of CS, PEC, TPP, CUR, CS-PEC-NPs and CUR-CS-PEC-NPs were obtained using a Spectrum RX1 FT-IR spectrometer (Perkin Elmer, USA). Potassium bromide (KBr) disks containing the material of interest were prepared at a ratio of 98:2 KBr to material respectively. Data were acquired between 4000 cm^{-1} and 400 cm^{-1} with 64 runs and 4 cm^{-1} resolution at interval of 1 cm^{-1} . Data captured were presented as the FT-IR spectra.

2.2.6 XRD analysis

Evidence of chemical association within the NPs was ascertained using XRD 7000 diffractometer (Shimadzu, Japan). Freeze-dried samples were finely grounded and prepared as a film followed by irradiation with $\text{CuK}\alpha$ generated at 40 kV an 80 mA. Data were recorded at 2θ ranged between 0 and 40° at a scanning speed of 0.5°/min.

2.2.7 DSC analysis

Thermal analysis of CUR-CS-PEC-NPs and CS-PEC-NPs were used to provide additional information on the polymer-drug interactions, if any and the nature of formed

NPs using DSC under nitrogen gas at a flow rate of 20 mL/min. Sample weight ranged from 8 to 12 mg except for CUR which was 1.8 mg. Samples were prepared in aluminium pans using a standard pneumatic press and then heated from 0°C to 350°C at a heating rate of 5°C/min. The reference was sealed aluminium pan.

2.3 Results and discussion

2.3.1 Particle size and zeta potential measurement

The four formulations (A, B, C and D) were formed based on the order of adding the components (CS, PEC, TPP) except for formulation D where CaCl₂ was used as the cross linker instead of TPP. Collected NPs as described in section 2.2.2 were re-dispersed in purified water for further analysis using Zetasizer[®] to determine particle size and zeta potentials of CS-PEC-NPs and CUR-CS-PEC-NPs. Data collected is summarized in Table 2.2 below.

Table 2.2 Particle size and zeta potential data obtained for formulations A, B, C, and D of CS-PEC-NPs and CUR-CS-PEC-NPs, n=3

Formulation		Particle size (nm)	Zeta Potential (mV)
A	CS-PEC-NPs	1115.0 ± 2.0 *	+17.7 ± 0.5 *
	CUR-CS-PEC-NPs	1296.6 ± 5.5 *	+13.7 ± 0.3 *
B	CS-PEC-NPs	Visible particles/ Phase separation	
	CUR-CS-PEC-NPs		
C	CS-PEC-NPs	206.0 ± 0.6 *	+24.0 ± 0.3
	CUR-CS-PEC-NPs	211.3 ± 2.0 *	+23.5 ± 0.4
D	CS-PEC-NPs	Visible particles/ Phase separation	
	CUR-CS-PEC-NPs		

* Significantly different between groups (P< 0.001) for each formulation

One of the key goals in nanomedicine is to ensure that the particles are of a low size dimension. Therapeutically, this is crucial in instances where uptake of the particles by relevant tissue is the goal. Smaller sized NPs are more effectively taken up in the epithelia of the colonic mucosa (des Rieux *et al.*, 2006). Phase separation due to extremely large particles (macroparticles) was observed in formulations B and D. In formulation B, TPP was added to CS, which resulted in the formation of NP whereupon the addition of PEC did not result in the incorporation of the latter in the NPs. Instead, the negative carboxylic groups of PEC ($-\text{COO}^-$) electrostatically interacted with the free amino groups of CS (NH_3^+) available on the surface of the NPs. This resulted in an increase in size and hence the formation of macroparticles. Similarly, in formulation D macroparticles were formed because of the use of CaCl_2 as the cross linker. PEC-based nanoformulations have been fabricated using CaCl_2 as cross-linker (Mishra *et al.*, 2012) where ionotropic gelation occurs between Ca^{+2} the $-\text{COO}^-$ groups of PEC. In

formulation D, however, the addition of CS would have been after the NPs were formed (due to ionic gelation between CaCl_2 and PEC) thus, resulting in another ionotropic interaction between free $-\text{COO}^-$ groups of PEC and the $-\text{NH}_3^+$ groups of CS. Simultaneously, repulsive forces would exist between $-\text{NH}_3^+$ groups in CS and Ca^{+2} in CaCl_2 , all of which contribute to the formation of macroparticles. In formulation A, both PEC and TPP have negative functionalities and thus compete in interacting with the positive binding sites of CS and this impedes cross-linking propensity of TPP with CS leading to the formation of microparticles as well. NPs were successfully formed in formulation C, where the initial ionotropic interaction was formed between CS and PEC thus suppressing the negative functionality of PEC. Therefore, on addition of TPP it was possible for the negative groups of TPP to electrostatically interact with any free positive binding sites in CS which resulted in the formation of viable NPs. Figure 2.6 summarizes what we believe are the sequences of events leading to the formation of CUR-CS-PEC composite NPs. Formulation C was selected for further optimization based on the physical parameters measured. In Formulation C, there was a slight increase in CUR-CS-PEC-NPs size ($p=0.0143$) compared to the blank NPs due to the encapsulation of CUR.

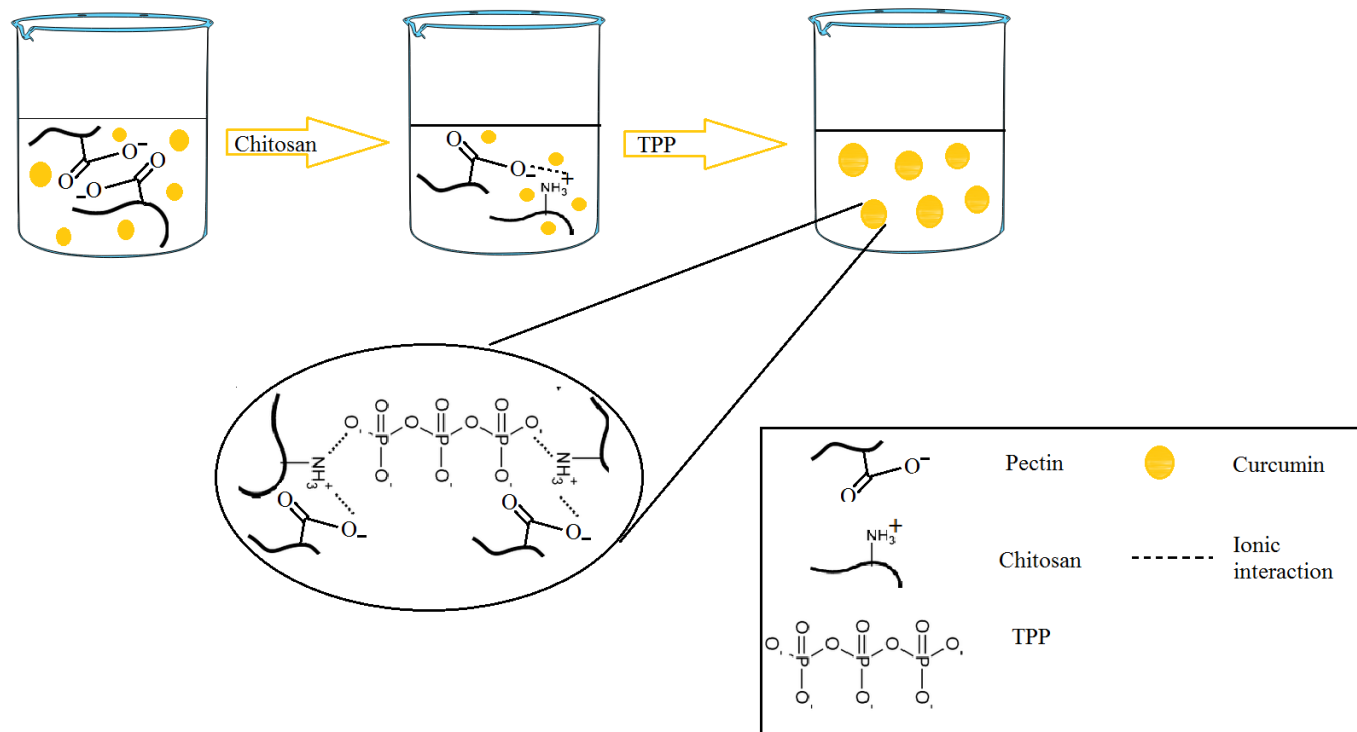


Figure 2.6 Sequence leading to formation of CUR-CS-PEC-NPs

The effects of formulation variables on the physical properties of the NPs are summarized in Tables 2.3, 2.4, and 2.5. Table 2.3 shows the effects of varying CS, TPP, and PEC concentrations and ratios. Increasing TPP ratio in formulations 3:2:1, 4:2:1, and 5:2:1 resulted in a dramatic increase in the size of the particles, causing the formation of macroparticles and phase separation. This could be due to increased inter- and intramolecular interactions between TPP and CS and PEC (Fan *et al.* 2012). Increasing CS concentration caused a decrease in size of NPs due to the availability of free binding sites explained below (de Pinho Neves *et al.*, 2014). CS molecules have two forces in equilibrium namely electrostatic repulsion due to protonated amino groups of CS and inter-chain hydrogen bonding interaction between CS molecules. At high concentrations of CS (>0.20% w/v) hydrogen interaction between CS molecules becomes stronger causing the involvement of more CS molecules in the cross-linking during the formation of a single particle thus resulting in an increase in particle size (Fan *et al.* 2012). Therefore, the highest CS concentration used in the present study was 0.25% w/v. Based on the DLVO theory, higher potential energy is required to achieve better stability, thus higher zeta potential values are required. The zeta potential values were all in positive; however, we observed higher potentials in the smaller NPs which reflects better stability. Hunter (1981) reported that NPs with zeta potential higher than ± 30 mV are more stable. This threshold was achieved in formulations 4:1:1 and 5:1:1. CUR is known to exist in tautomeric forms such as the 1,3, -diketo and two equivalent enols forms (Manolova *et al.*, 2014). The enol form ($-\text{RCO}_4^-$) predominates in organic solvents as in the present study and competes with the TPP ($-\text{P}_3\text{O}_{10}^-$) for $-\text{NH}_3^+$ groups of CS. Additionally, due to the bulkier size of CUR relative to TPP, some free $-\text{NH}_3^+$ cannot be approached by TPP due to the steric hindrance and this explains the insignificant lower z-potential of CUR-CS-PEC-NPs relative to CS-PEC-NPs. One of

the goals in the present formulation work is to produce NPs with practically as low as possible z-average due to the intended application. Such NPs with low z-average are desirable due to high surface-to-volume ratio. Moreover, narrow size distribution of the NPs (pDI < 0.500) enhance their cellular uptake as well as their stability (Nam et al., 2009), This threshold was achieved in ratio 5:1:1. Thus, ratio 5:1:1 was subsequently selected for studying the effect of stirring time and stirring speed on the physical properties of the NPs.

Table 2.3 Z-average, zeta potential, and pDI of CS-PEC-NPs AND CUR-CS-PEC-NPs as a function of formulation ratios, n=3

Formulation (CS:TPP:PEC)		Particle size (nm)	pDI	Zeta potential (mV)
3:1:1	CS-PEC-NPs	206.0 ± 0.6 *	0.475	+ 24.0 ± 0.3
	CUR-CS-PEC-NPs	211.3 ± 2.0 *	0.574	+ 23.5 ± 0.4
3:2:1	CS-PEC-NPs	Visible particles and phase separation		
	CUR-CS-PEC-NPs			
4:1:1	CS-PEC-NPs	200.9 ± 6.9 *	0.331	+ 30.7 ± 1.8
	CUR-CS-PEC-NPs	298.8 ± 9.5 *	0.526	+ 30.0 ± 0.4
4:2:1	CS-PEC-NPs	Visible particles and phase separation		
	CUR-CS-PEC-NPs			
5:1:1	CS-PEC-NPs	201.9 ± 8.5	0.359	+ 35.0 ± 1.5
	CUR-CS-PEC-NPs	203.2 ± 3.2	0.381	+ 34.5 ± 1.2
5:2:1	CS-PEC-NPs	Visible particles and phase separation		
	CUR-CS-PEC-NPs			

* Significantly different between groups (P < 0.001) for each ratio

From Table 2.4, we observed a direct relation between the stirring time and the z-average for both CUR-CS-PEC-NPs and CS-PEC-NPs. Ionic gelation is a spontaneous process and so the initially formed NPs become disrupted on prolonged stirring and grow in size. This disruption of the nanoparticle fabric also causes a decrease in zeta potential with longer stirring times. From a formulation and stability standpoint, a stirring speed of 500 rpm for 2 min. after the addition of CS to PEC followed by an additional 20 min. of stirring after the addition of TPP was deemed to be optimum and selected and so this formulation was further optimized using stirring speeds of 500, 800 and 1000 rpm. The data on the effect of stirring speed on the physical properties of both the CUR-CS-PEC-NPs and CS-PEC-NPs are shown in Table 2.5. Optimal physical properties in terms of z-average and pDI were obtained when stirring speed was 500 rpm, however, NPs formed at stirring speed of 800 and 1000 had higher zeta potential values which could be attributed to the compromised cross-linking properties of the NPs, thus, higher available (NH_3^+) groups of CS is available. This effect of stirring speed on size of the NPs has also been reported previously and is attributed to sheer mixing which interrupts the cross linkages of the fabric imposed by TPP much like the effects of extended stirring times (Zhu *et al.*, 2014).

Table 2.4 Z-average, zeta potential, and pDI of CS-PEC-NPs AND CUR-CS-PEC-NPs as a function of stirring time, n=3

Stirring time (min.)		Particle size (nm)	pDI	Zeta potential (mV)
2/20	CS-PEC-NPs	194.9 ± 1.1	0.341	+ 33.8 ± 1.3
	CUR-CS-PEC-NPs	200.6 ± 6.6	0.377	+ 32.8 ± 0.5
2/40	CS-PEC-NPs	195.9 ± 0.4 *	0.312	+ 22.4 ± 0.5
	CUR-CS-PEC-NPs	285.9 ± 4.1 *	0.510	+ 22.0 ± 0.5
2/60	CS-PEC-NPs	198.9 ± 2.5 *	0.253	+ 23.7 ± 0.4

	CUR-CS-PEC-NPs	210.0 ± 3.5 *	0.264	+ 23.2 ± 0.7
--	----------------	---------------	-------	--------------

* Significantly different between groups (P< 0.001) for each stirring time

Table 2.5 Z-average, zeta potential, and pDI of CS-PEC-NPs AND CUR-CS-PEC-NPs as a function of stirring speed, n=3

Stirring speed (rpm)		Particle size (nm)	pDI	Zeta potential (mV)
500	CS-PEC-NPs	194.9 ± 1.1	0.341	+ 33.8 ± 1.3
	CUR-CS-PEC-NPs	200.6 ± 6.6	0.377	+ 32.8 ± 0.5
800	CS-PEC-NPs	215.2 ± 4.4	0.547	+ 43.4 ± 0.6
	CUR-CS-PEC-NPs	231.7 ± 9.8	0.662	+ 40.6 ± 1.8
1000	CS-PEC-NPs	287.0 ± 20.5	0.443	+ 37.8 ± 0.9
	CUR-CS-PEC-NPs	289.0 ± 9.6	0.721	+ 36.5 ± 1.0

* The data obtained between groups for each stirring speed were statistically insignificant (P>0.001)

2.3.2 Morphology of CUR-CS-PEC-NPs and CS-PEC-NPs

FESEM was used to study the morphologies and surface topographies of the NPs. Representative images of the CUR-CS-PEC-NPs at two magnifications, 10 000x (A) and 20 000x (B) of the optimized formulation are shown in Figure 2.7. Generally, The NPs were spherical in shape and the sizes were in agreement with those obtained from the photon correlation analysis described in section 2.3.1. The NPs in both cases appear to be well-separated from each other suggesting that sufficient electrical charge is retained by the individual particle. The surface of the NPs is free of fissures or cracks which indicate effective cross-linking. Similar findings were observed in the literature (Ha *et al.*, 2012; Mathew *et al.*, 2012).

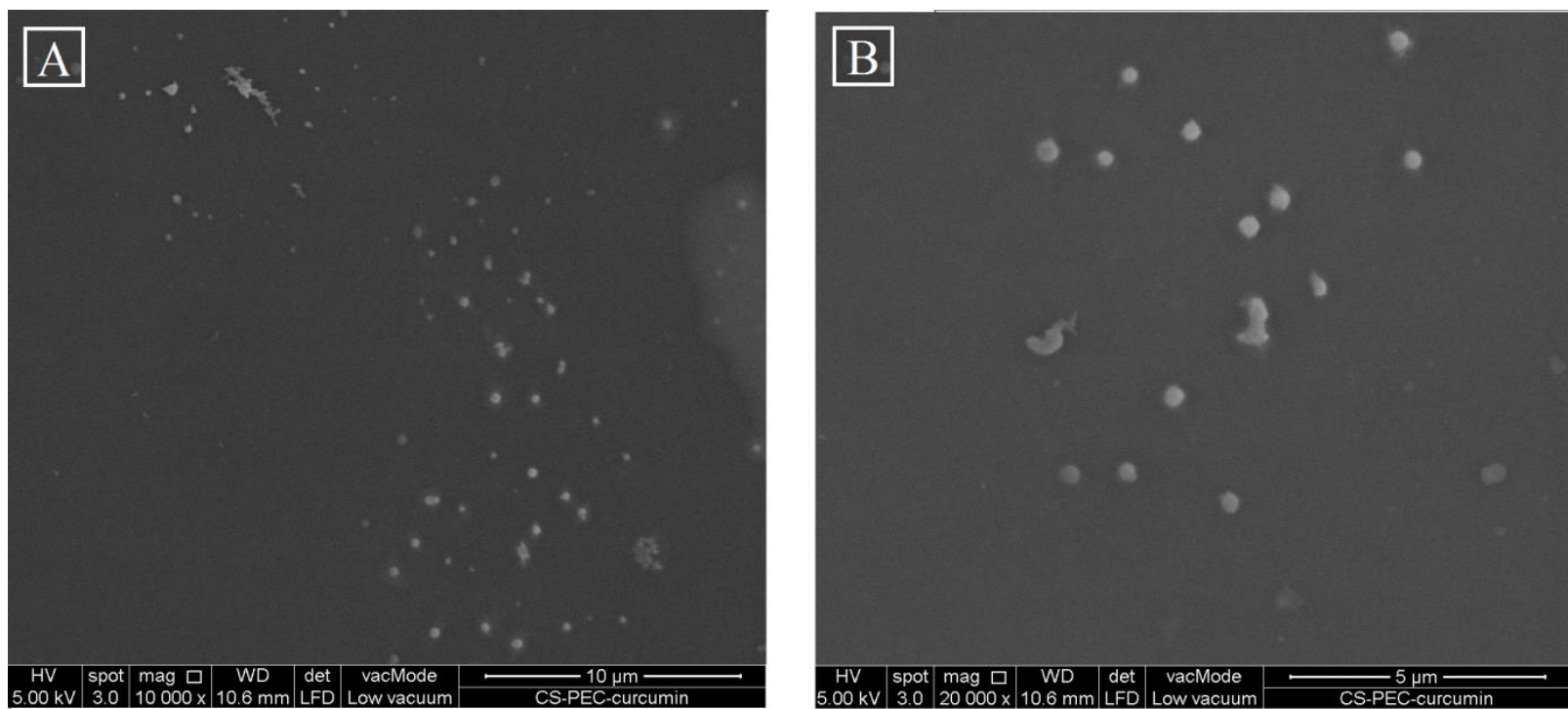


Figure 2.7 SEM image of the optimized formulation CUR-CS-PEC-NPs at magnification 10 000x (A) and 20 000x (B)

2.3.3 FT-IR spectra

The FT-IR spectra of the raw materials and formulated NPs are presented in Figure 2.8. In the raw materials, stretching vibrations of C=O group of CUR (A) appears at 1604 cm^{-1} . No peaks can be observed within the range of $1800\text{-}1650\text{ cm}^{-1}$ which suggests that CUR is present in the keto-enol tautomeric form (Kolev *et al.*, 2005). The CS spectrum (B) shows a broad peak at 3434 cm^{-1} which is attributed to the stretching vibration of the hydroxyl groups whilst the amide I (NH₂) bending vibration presents at 1653 cm^{-1} . Furthermore, a peak appears at 1389 cm^{-1} corresponds to the N-H stretching of amide and ether bonds and the peak at 1081 cm^{-1} assigns to a secondary hydroxyl group (Paulino *et al.*, 2006; Das *et al.*, 2010). The broad peak of PEC (C) at 3400 cm^{-1} is assigned to the stretching frequency of -OH group. The peak at 1051 cm^{-1} is related to C=C or C=O double bonds within PEC while the peak at 1639 cm^{-1} is assigned to asymmetric stretching bands of COO⁻ groups (Gopi *et al.*, 2014; Shi & Gunasekaran, 2008). The characteristic peak at 1129 cm^{-1} is assigned to P=O groups of TPP (D) while the one at 899 cm^{-1} is related to the P-O-P asymmetric stretching (Martins *et al.*, 2012; Mi *et al.*, 2003).

The aforementioned bands were all present in both the formulations CUR-CS-PEC-NPs and CS-PEC-NPs, spectra (E and F, respectively). We may conclude that these groups are not typically involved in covalent chemical bonding with the other components during the formulation process. The FT-IR spectra of CUR-CS-PEC-NPs are similar to those from CS-PEC-NPs except for a slight shifting of the amine peak at 1562 cm^{-1} which is attributed to CUR loading in CUR-CS-PEC-NPs. Furthermore, the peak attributed to CUR is absent in the CUR-CS-PEC-NPs spectrum which assures CUR loading in the latter.

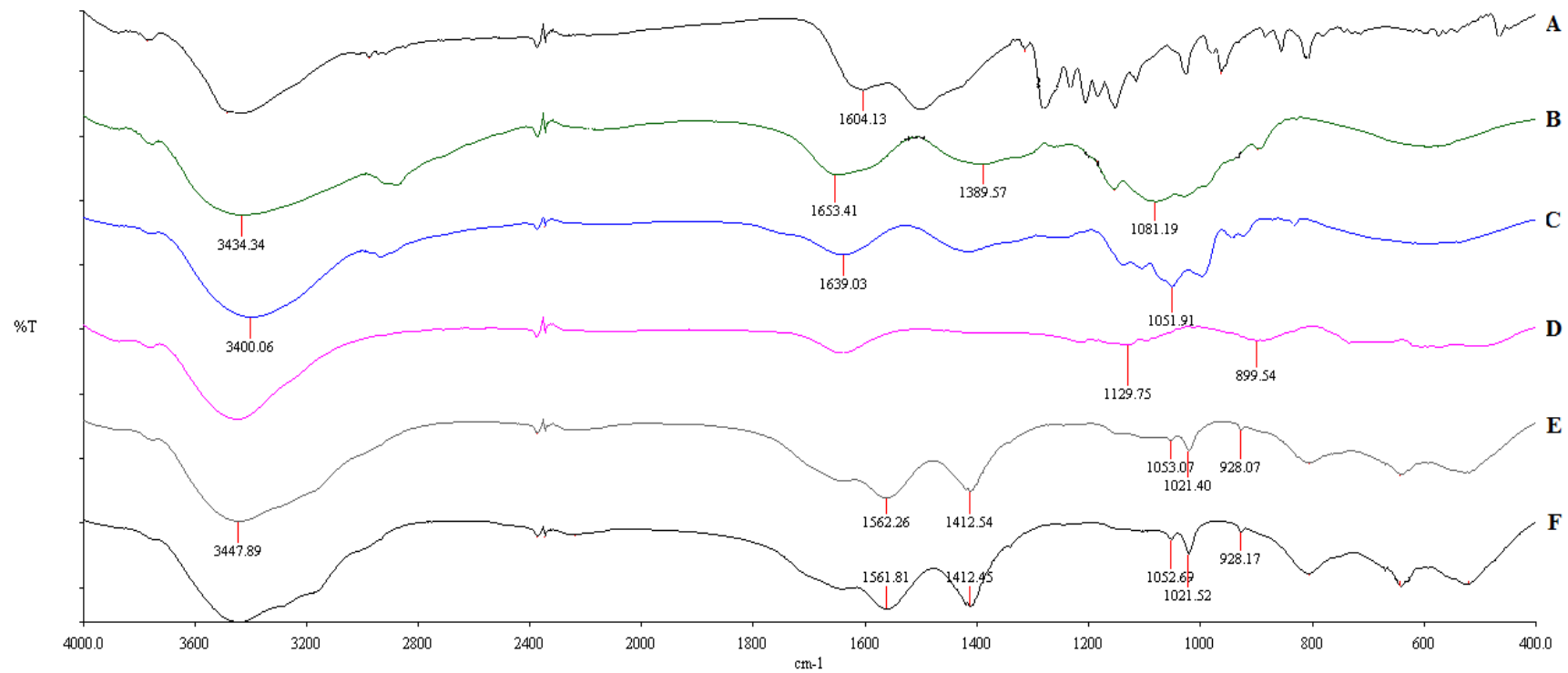


Figure 2.8 FT-IR spectra of CUR (A), CS (B), PEC (C), TPP (D), CS-PEC-NPs (E), and CUR-CS-PEC-NPs (F)

2.3.4 XRD data

To investigate the state of CUR after encapsulation into the CUR-CS-PEC-NPs an XRD analysis was performed. The XRD data of CUR (Figure 2.9) shows its diffraction pattern peaks 7.93° , 12.48° , 17.72° , 18.18° , 23.53° , and 24.60° implying a characteristic crystalline structure 2θ range of $7\text{--}30^\circ$. In contrast, these peaks are absent in CUR-CS-PEC-NPs suggesting its conversion to the amorphous state because of the intermolecular interaction between CS, PEC, and TPP. A similar change in structure of entrapped CUR was also reported by several researchers (Anitha *et al.*, 2011; Gou *et al.*, 2011a; Rejinold *et al.*, 2011; Yallapu *et al.*, 2010a; Yen *et al.*, 2010). This is crucially significant as the crystalline encapsulation of a drug hinders its release profile.

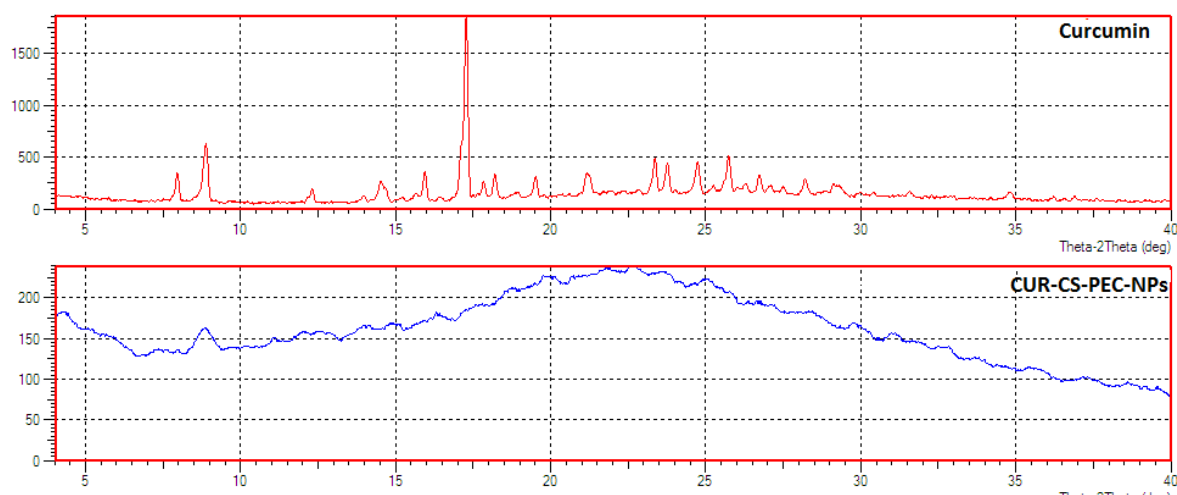


Figure 2.9 XRD patterns of CUR and CUR-CS-PEC-NPs

2.3.5 DSC analysis

To further ascertain the physical nature of the NPs, thermal analyses were carried out on both the optimized CUR-CS-PEC-NPs and CS-PEC-NPs in comparison with the raw materials. Figure 2.10 shows the DSC data where CUR (A), shows a sharp melting peak at 178.7°C , whilst CS (B) shows endothermic peak at 113.9°C and an exothermic peak at 307.4°C . PEC (C) has a transition peak at 190°C . Endothermic peaks

are correlated with loss of water associated with the hydrophilic groups in CS while the exothermic peaks result from the degradation of polyelectrolytes followed by the hydration and depolymerization reactions which happen due to the partial decarboxylation of the protonated carboxylic groups and oxidation reactions of the polyelectrolytes (Sarmiento *et al.*, 2006). TPP (D) shows a typical melting point of the salt at 116.6 °C. The thermograms of the physical mixture of CS, PEC, TPP, and CUR (E) showed similar peaks observed in the pure samples.

Thermograms of the formulations (CS-PEC-NPs and CUR-CS-PEC-NPs, F and G, respectively) show a broad endothermic peak at about 89.5°C this is due to complexation of TPP because the sharpness of this peak in the physical mixture is lost but prominent in TPP. There is a broad exothermic peak at 269.3°C in both formulations and this is due to CS but is slightly shifted at 307.4°C in pure CS because of weak interaction. Furthermore, the melting point of CUR cannot be seen in the thermograms of CUR-CS-PEC-NPs because CUR is molecularly dispersed in the NPs in the amorphous state. This finding agrees with those of (Dandekar *et al.*, 2010; Mohanty & Sahoo, 2010; Xie *et al.*, 2011). Data obtained from the DSC analysis complements those of the FT-IR and X-ray diffractometry.

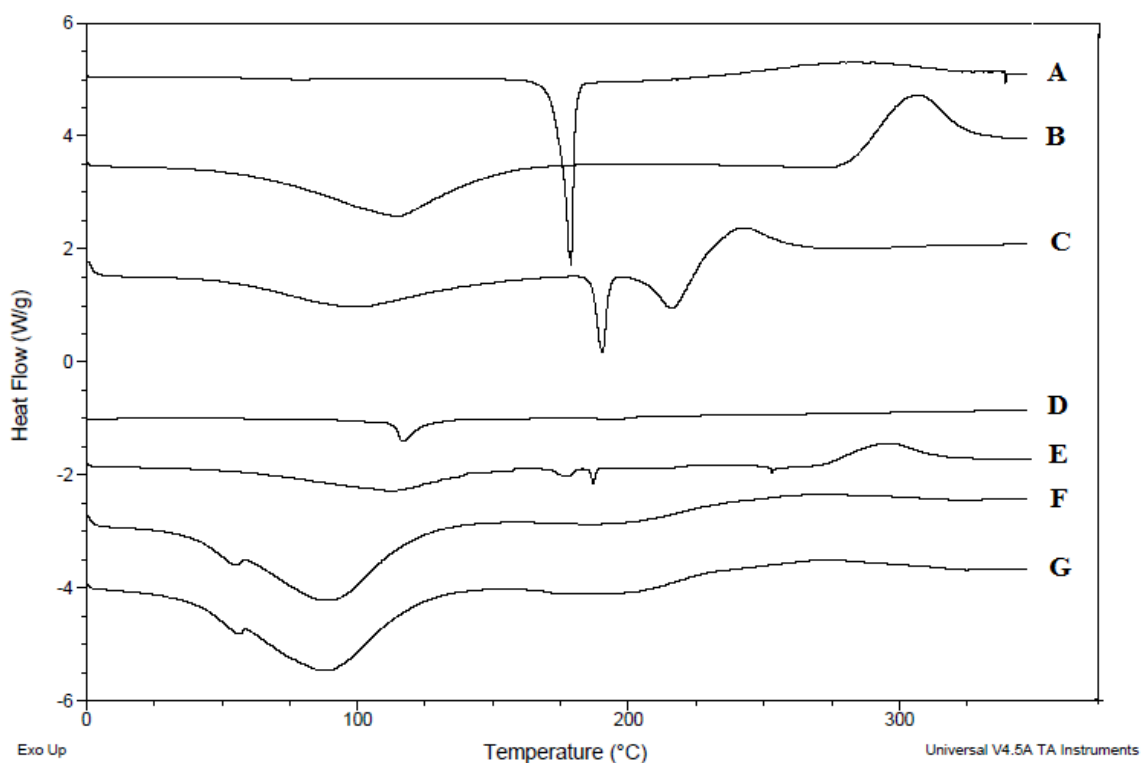


Figure 2.10 DSC thermograms of CUR (A), CS (B), PEC (C), TPP (D), physical mixture of CUR, PEC, CS, and TPP (E), CS-PEC-NPs (F), and CUR-CS-PEC-NPs (G).

2.4 Conclusion

In summary, CUR-CS-PEC-NPs have been successfully formulated and optimized in terms of desirable physical properties. The most enticing properties were found with CS:TPP:PEC ratio of 5:1:1, most optimum stirring speed and stirring time were found to be 500 rpm and 2 min./20 min., respectively. The NPs were characterised in terms of size, pDI, zeta potential, morphology, chemical functional groups, and the physical state of CUR. These data present us with the incentive for further optimisation in terms of EE% of the NPs for CUR, release profile of CUR as a function of various physiological challenges, stability, and mucoadhesion at relevant physiological conditions. These would be discussed in detail in Chapter 3.

Chapter 3

Mucoadhesion, release, and stability studies

3 Mucoadhesion, release, and stability studies

3.1 Introduction

3.1.1 Mucin

The intestinal mucus is synthesized by specialized goblet cells and secreted by the epithelial GIT surface and is a water insoluble viscoelastic gel that adheres to the epithelia of the GIT (Atuma *et al.*, 2001; Strugala *et al.*, 2003; Andrews *et al.*, 2009). The thickness of the GIT mucus varies between 50-500 μm in the stomach and decrease distally to a range of 15-150 μm in the colon (Pullan *et al.*, 1994; J *et al.*, 1991; Bickel & Kauffman, 1981; Bravo-Osuna *et al.*, 2007). A balance between synthesis and secretion rates and abrasion through enzymatic digestion and/or mechanical shear maintains the thickness. Any imbalance may led to pathological conditions such as ulcerative colitis (Atuma *et al.*, 2001). Despite the low pH of the luminal cavity of the stomach, the pH of the mucosal surfaces ranges from 5.23-8.1 throughout the entire GIT (Atuma *et al.*, 2001; Bahari *et al.*, 1982; Flemstrom & Kivilaakso, 1983).

About 95% of the mucus gel comprises of water along with sulphated glycoproteins (up to 5%), and to a lesser extent free proteins, mineral salts, and lipids (Allen & Snary, 1972; Allen & Garner, 1980). The gel-forming properties of the mucus are manifested due to the high molecular weight of mucin. The glycoproteins are rich in amino acid residues such as serine, proline, and threonine. Moreover, glycoproteins contain fructose, glucosamine, galactose, galactosamine and sialic acid. Glycoprotein units are joined by disulphide bridges covalently attached to protein cores. In addition to glycoproteins, 5-10% of mucin consists of non-covalently bonded proteins. The sialic acid units of the glycoproteins ($\text{pK}_a = 2.6$) and the sulphate groups are responsible for the negative surface charge of mucin at neutral pH (Andrews *et al.*, 2009).

Functionally, the mucus layer protects epithelia from the degradation and erosive effect of gastric acid, digestive enzymes, free radicals, and bacterial and ingested toxins and abrasion. Furthermore, it acts as lubricant, facilitating the passage of food through the GIT and protects it from mechanical injury. In the colon, the mucosal layer serves as a favourable environment for the colonic microflora, whilst at the same time, prevents bacteria from adhering onto it. This way, bacterial infections are prevented (Atuma *et al.*, 2001; Bickel & Kauffman, 1981; Carbajal *et al.*, 2000; Strugala *et al.*, 2003).

3.1.2 Mucoadhesion process

The term “adhesion” refers to the molecular interaction at the interface between materials (Marshall *et al.*, 2010). When, at least, one of these materials is a biological surface, it is called “bioadhesion”. When the biological material is particularly restricted to the mucus layer, the term “mucoadhesion” is used (Smart, 2005; Bravo-Osuna *et al.*, 2007; Chickering & Mathiowitz, 1999). Recently, researchers have shown interest in taking advantage of mucoadhesion in localized and systemic drug delivery due to the extended contact time (Smart, 2005) of formulation with mucosa.

Researchers have proposed several theories explaining the mucoadhesion mechanism including adsorption, diffusion, electronic, fracture, mechanical, and wetting theories (Dodou *et al.*, 2005; Smart, 2005; Peppas & Sahlin, 1996; Chickering & Mathiowitz, 1999). Therefore, we may conclude that mucoadhesion is a complex process that cannot be explained based on a single theory. The phenomenon of mucoadhesion is best explained by a combination of theories. Firstly, the contact stage, where the mucoadhesive compound binds to the mucus (mechanical theory), gets wetted and swells (wetting theory). Through this wetting stage, the mucus-material

interfaces are physically bonded (electronic and adsorption theories) so that the material and mucin chains interpenetrate and entangle (diffusion theory) forming additional covalent and non-covalent bonds (diffusion, electronic, and adsorption theories) (Dodou *et al.*, 2005; Smart, 2005; Bravo-Osuna *et al.*, 2007; Chickering & Mathiowitz, 1999). Mucoadhesive materials bind to mucus through a variety of forces including van der Waal's, hydrophobic, hydrogen, ionic, or covalent bonds (Dodou *et al.*, 2005; Bravo-Osuna *et al.*, 2007; Peppas & Sahlin, 1996; Marshall *et al.*, 2010; Chickering & Mathiowitz, 1999).

Factors affecting the mucoadhesive propensity of a material include intrinsic (structural) factors such as optimum molecular weight, degree of cross-linking, high chain flexibility, optimum surface tension, or external (environmental) factors such as the environment pH and temperature, length of contact time, presence of metal ions, and the shear rate of the environment (Dodou *et al.*, 2005; Bravo-Osuna *et al.*, 2007; Smart, 2005; Chickering & Mathiowitz, 1999).

3.1.3 High Performance Liquid Chromatography

The High Performance Liquid Chromatography (HPLC) technique was proposed in the late 1960s and has undergone several modifications since (Ornaf & Dong, 2005). It is a physical separation and quantification technique operated by carrying the analyte in a liquid phase. The separation is achieved by the distribution of the constituents between the mobile phase (MP) (liquid phase) and immobilized stationary phase (column) (Ornaf & Dong, 2005). There are several other chromatographic techniques however HPLC is the most versatile (Sandie Lindsay, 1997; Ornaf & Dong, 2005; Zhang *et al.*, 2008; White, 1981) because of its superior sensitivity, precision, resolution, reliability, reproducibility, shorter analysis time, and

lower cost (White, 1981; Zhang *et al.*, 2008). HPLC technique is widely used in food, forensic, environmental, clinical, and pharmaceutical industries (Zhang *et al.*, 2008).

Physical separation is achieved in the stationary phase (column), which consists of uniform silica particles with spherical or irregular shape with sizes that range between 3-50 μm . They may be coated with various chemical groups in order to impart the desired level of polarity. This in turn is the basis of separation between analytes and the bonded phase of the column (Engelhardt, 1979; Lindsay, 1997; White, 1981). Based on the stationary phase polarity, two separation modes are available, namely, normal phase and reversed phase (RP) chromatography. The former comprises of a polar (silica) stationary phase, whereas the latter consists of non-polar (C18) stationary phase (Lindsay, 1997). The MP is carefully chosen in order to match the right balance between retention of analyte of interest against a matrix background.

Separated constituents are detected by a wide variety of detectors such as IR, refractive index, fluorescence, and ultraviolet light (UV/visible) detectors. The latter is the most frequently used detector due to its reasonable prices and sensitivity (Zhang *et al.*, 2008; Lacourse, 2002; Christie, 1992). The choice of the detector is aligned to the maximum sensitivity obtained for the analyte. In the present pursuit, a UV detector was used for CUR because of the sensitivity of this technique to maximum absorption at specified wavelength.

3.1.3.1 HPLC analysis of CUR

Several HPLC methods have been proposed for the quantification of CUR, mostly employing UV-vis for detection (Wichitnithad *et al.*, 2009; Wang *et al.*, 1997; Syed *et al.*, 2015; Pak *et al.*, 2003; Hsu *et al.*, 2001; Ireson *et al.*, 2002; Ma *et al.*, 2007;

Garcea *et al.*, 2004). In this chapter, we used the method proposed by Wichitnithad *et al.*, (2009) due to simplicity and sensitivity, albeit after minor modification.

3.1.4 Aims and Objectives

CUR-CS-PEC-NPs were successfully formulated and characterized as described in chapter 2. This chapter was dedicated to studying the mucoadhesion properties of the NPs, CUR release in various media as well as the stability of CUR-CS-PEC-NPs.

3.2 Materials and Methods

3.2.1 Materials

Material	Supplier
CS-PEC-NPs	Prepared as described in Chapter 2
CUR-CS-PEC-NPs	Prepared as described in Chapter 2
Curcumin analytical standard	Fluka, USA
Low molecular weight chitosan	Sigma Aldrich, USA
Low methoxy pectin	CP Kelco, USA
Methanol (analytical grade)	R&M chemicals, UK
Absolute ethanol	R&M chemicals, UK
Glacial acetic acid	R&M chemicals, UK
Sodium hydroxide	Merck, Germany
Acetonitrile (HPLC grade)	RCI Labscan, Thailand
Phosphate-Buffered Saline (PBS) pH 7.4	Sigma Aldrich, USA
Mucin type III from porcine stomach	Sigma Aldrich, USA
Pectinase (<i>Aspergillus niger</i>)	Abnova, Taiwan
Pepsin (from porcine stomach)	Nacalai Tesque, Japan
Pancreatin	Nacalai Tesque, Japan
4-(2-hydroxyethyl)-1-piperazineethanesulfonic acid (HEPES)	Nacalai Tesque, Japan
Hydrochloric Acid (37%)	R&M chemicals, UK
Sodium Deoxycholate $\geq 97\%$	Sigma Aldrich, Germany

3.2.2 Mucoadhesion studies

The mucoadhesive propensity of the CUR-CS-PEC-NPs was determined by dispersing them in type III mucin solution obtained from porcine stomach at 0.1, 0.2, 0.4 and 0.6 mg/ml. The degree of mucoadhesion was obtained by measuring the changes in the zeta potential of the particles after interaction with mucin (Bhatta *et al.*, 2012; Takeuchi *et al.*, 2005). The CS-PEC-NPs and CUR-CS-PEC-NPs mucin suspension were vortex-mixed for one minute followed by incubation in an incubating shaker operated at 180 rpm for 1 hr at 37°C. The zeta potential of the NPs was then measured using the Zetasizer and the drop in zeta potential was recorded as a measure of degree of interaction of CS-PEC-NPs or CUR-CS-PEC-NPs with mucin.

3.2.3 HPLC assay for CUR

An HPLC method adapted from Wichitnithad *et al.*, (2009) was used for the detection of encapsulated CUR within CUR-CS-PEC-NPs and for the CUR release after minor modification. The HPLC system comprised of a Series 200 pump, Perkin Elmer, USA equipped with UV/Vis detector (Series 200 UV/Vis detector, Perkin Elmer, USA) operated at a detection wavelength of 425 nm. A reverse phase column (ZORBAX Eclipse Plus C18, 250 mm x 4.6 mm, 5 µm, Agilent, USA) was used as the stationary phase and the MP consisted of 40:60 acetonitrile: 2% acetic acid filtered through 0.45 µm regenerated cellulose membrane filter (Agilent Technologies, Germany) prior to analysis which was run at a flow rate 2.0 ml/min.

CUR standard solutions were prepared in methanol (0.15625-10 µg/ml). The responses from the calibration curve were then quantified based on the area under the curve (AUC). The coefficient of determination (R^2) and line equation were determined

from the calibration curve. Sample concentrations were determined by comparing resulting area with those obtained from the standard calibration curve.

3.2.4 HPLC method validation

Because of the slight modification in the HPLC method used, validation in terms of method repeatability and accuracy was done. CUR solutions comprised 0.3125, 50 and 100 µg/mL representing low, medium and high concentration, respectively. The three concentrations of CUR solution were analysed in triplicate on the same day to determine intra-day precision and accuracy, whereas triplicate analysis on three consecutive days were performed for inter-day precision and accuracy determination.

3.2.5 Determination of encapsulation efficiency

The unbound CUR from CUR-CS-PEC-NPs pellet collected by centrifugation as described in section 2.2.2.2 was washed off twice in methanol. The amount of CUR in the methanol rinse and the supernatant were both analysed to determine the total unbound CUR using the HPLC method described in section 3.2.3. For the supernatant and rinse, 20 µl was injected directly onto the HPLC. The reported values are the means of three independent runs. The percentage of EE% was calculated as follows:

$$\% \text{ EE\%} = \frac{\text{Total CUR added} - \text{unbound CUR}}{\text{Total CUR added}} \times 100\% \quad \text{Eq. 3.1}$$

3.2.6 CUR release from CUR-CS-PEC-NPs

3.2.6.1 CUR release from CUR-CS-PEC-NPs in different simulated fluids

The variation in pH within the GIT and the effects of colonic enzymatic activity on the integrity of CUR-CS-PEC-NPs were studied. For this purpose, CUR-CS-PEC-NPs were collected by centrifugation as described in section 2.2.2.2 and washed. A 20 mg/ml suspension of CUR-CS-PEC-NPs were suspended in phosphate buffer saline

(pH 6.4) containing 1% (w/v) tween 80 and 2.5% (w/v) pectinase enzyme as simulated colonic content. Similarly, CUR-CS-PEC-NPs were suspended in 0.1 N HCl (pH 1.2) and HEPES buffer (pH 6.8) mimicking the stomach and small intestine mediums, respectively (Dutta & Sahu, 2012; Saboktakin *et al.*, 2011; Beaulieu *et al.*, 2002; Luo *et al.*, 2012; Chen & Subirade, 2005; Jain *et al.*, 2006). Each of the three types of the fluids containing CUR-CS-PEC-NPs were seeded into eight sampling vials and subjected to rotary shaking (WiseCube®, Witeg Inc., Germany) at 180 rpm incubated at 37°C. CUR release was studied over 6 hr at 20 min., 40 min., 1 hr, 2 hr, 3 hr, 4 hr, 5 hr, and 6 hr by withdrawing one vial from each of the media and its content centrifuged at 4000 rpm for 10 min to pellet the particles. The amount of CUR released was determined in the supernatant using the HPLC analytical procedure described in section 3.2.3 in three independent runs. The percentage of CUR released was calculated from the calibration curve described in section 3.2.4 and calculated as follows:

$$\% \text{ released CUR} = \frac{\text{Amount of released CUR}}{\text{Amount of CUR initially added}} \times 100\% \quad \text{Eq. 3.2}$$

To study the protective effects of PEC on the CUR-CS-PEC-NPs, PEC-free NPs were prepared as described in section 2.2.2.2 (i.e. without the addition of PEC). CUR-CS-PEC-NPs and PEC-free NPs were suspended in 0.1 N HCl (pH 1.2) for 1 hr, removed and air-dried followed by viewing under FESEM as described in section 2.2.4.

Since the CUR-CS-PEC-NPs are designed to transit the upper GIT followed by exposure in the alkaline conditions of the distal GIT, the effect that this variable pH might have on the physical integrity of the CUR-CS-PEC-NPs was studied by suspending the NPs in pH 1.2 for one hr, retrieving by centrifugation and then re-exposure in pH 6.8 for 2 hr. The zeta potential values and percentage retention of CUR were determined as described in sections 2.2.3 and 3.2.5, respectively.

3.2.6.2 *CUR release from CUR-CS-PEC-NPs in simulated gastrointestinal tract fluids*

CUR-CS-PEC-NPs are designed to transit the upper GIT followed by the alkaline conditions of the distal GIT. Thus, the effects of such pH variation and enzymatic activity on CUR release from the CUR-CS-PEC-NPs were studied. Firstly, the collected CUR-CS-PEC-NPs were suspended in simulated gastric fluid (SGF) (0.1 N HCl, pH 1.2, containing pepsin at concentration of 0.1% (w/v)) for 1 hr. Then, CUR-CS-PEC-NPs were retrieved and suspended in simulated intestinal fluid (SIF) (HEPES buffer (pH 6.8) containing pancreatine and sodium deoxycholate at concentrations of 1% and 0.8% (w/v), respectively), for two hr. Finally, CUR-CS-PEC-NPs were retrieved and suspended in simulated colonic fluid (SCF) (PBS (pH 6.4) containing 1% (w/v) tween 80 and 2.5% (w/v) pectinase enzyme) (Dutta & Sahu, 2012; Saboktakin *et al.*, 2011; Beaulieu *et al.*, 2002; Luo *et al.*, 2012; Chen & Subirade, 2005; Jain *et al.*, 2006). Figure 3.1 illustrates the aforementioned process. At designated time intervals (20 min., 40 min., 1 hr, 2 hr, 4 hr, and 6 hr) the amount of CUR released was determined in the supernatant using the HPLC method described in section 3.2.3 in three independent runs and reported as the mean of these runs. The physical integrity of CUR-CS-PEC-NPs were investigated by studying the morphological changes on them at 30 min, 2.5 hr, and 6 hr using the SEM imaging as described in section 2.2.4.

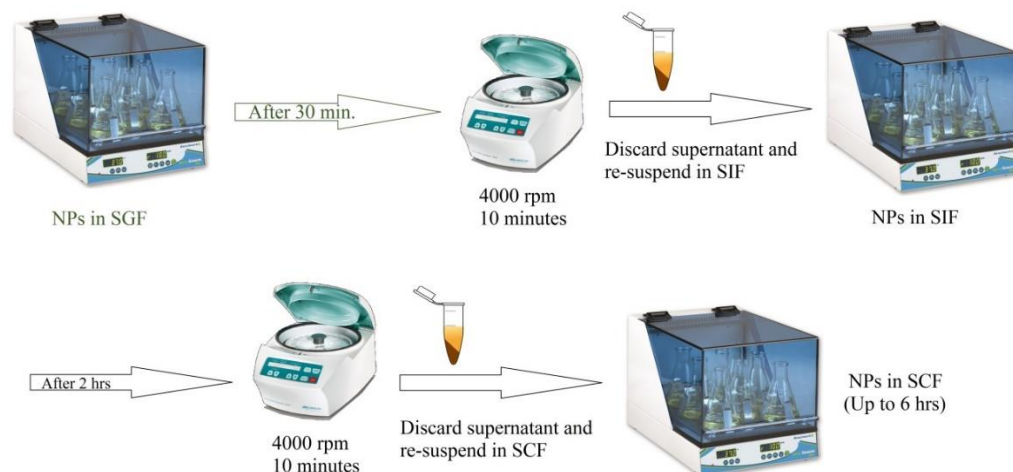


Figure 3.1 CUR release at simulated GIT fluids (*adopted with modification from www.jocuri-fotbal.info*)

3.2.7 Stability Studies

3.2.7.1 Storage

The effects of storage on the physical integrity of CUR-CS-PEC-NPs was conducted at 4°C for 14 days. Physical characterization of CUR-CS-PEC-NPs including particle size, zeta potential, and SEM imaging were conducted as described in sections 2.2.3 and 2.2.4, respectively. Studies were conducted on day 0, 7, and 14.

3.2.7.2 Photosensitivity

CUR is photosensitive, therefore, CS-PEC matrix must offer necessary protection to encapsulated CUR from the degradative effects of light. This was studied after exposing equivalent concentrations of CUR encapsulated in CUR-CS-PEC-NPs and free CUR within transparent vials to sunlight and UV light (263 nm) for 6 hr. At predetermined time intervals (2, 4, and 6 hr) CUR-CS-PEC-NPs were collected by centrifugation. CUR was retrieved by hydrolysing the CUR-CS-PEC-NPs in methanol with vortex mixing for 1 minute followed by filtration through 0.22 µm syringe filter.

The filtered solution was then run using the HPLC method described in section 3.2.3. The reported values are the means of three independent runs. The percentage of retained CUR was calculated as follows:

$$\% \text{ CUR retained} = \frac{\text{Amount of CUR determined from analysis}}{\text{Amount of added CUR}} \times 100\% \quad \text{Eq. 3.3}$$

3.2.7.3 Thermal

To investigate the extent of protection offered by the CS-PEC matrix to CUR against hydrolysis induced by thermal exposure as is likely under physiological conditions, (37°C), equivalent concentrations of CUR encapsulated in CUR-CS-PEC-NPs and free CUR were exposed to 37°C for three days. At day 1, 2, and 3, samples were sacrificed and CUR-CS-PEC-NPs were collected by centrifugation at 4000 rpm for 10 min. and then hydrolysed by vortex shaking the samples in methanol. This was further centrifuged at 4000 rpm for 10 min and the supernatant filtered using a 0.22 µm syringe. CUR was quantified using the HPLC method described in section 3.2.4 and the % of retrieved CUR was calculated using Eq. 3.3.

3.3 Results and Discussion

3.3.1 Mucoadhesion studies

The term “adhesion” refers to the attractive interaction between two different surfaces (Salamat-Miller *et al.*, 2005). Mucoadhesion, in particular, is the process where materials attach to the mucosal membranes of the body (Salamat-Miller *et al.*, 2005).

As explained in section 3.1.2, there are six theories explaining the mucoadhesion process. Namely, the electronic, the adsorption, the wetting, the diffusion (Dodou *et al.*, 2005), the mechanical, and the fracture theories (Smart, 2005).

In practice, however, the mucoadhesion process is complex and it includes a combination of all of the mucoadhesion theories (Dodou *et al.*, 2005). Figure 3.2 illustrates the behaviour of mucoadhesive NPs at the mucosal layers (Bravo-Osuna *et al.*, 2007).

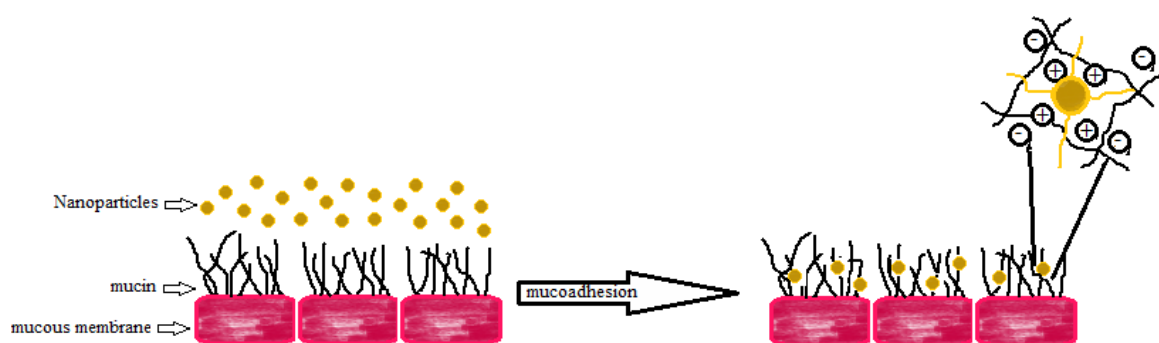


Figure 3.2 Schematic illustration of the penetration of polymeric NPs into the GIT mucosa

Hydrophilic polymers interact with the mucosal layer through interpenetration followed by secondary non-covalent bonding (hydrogen bonding). The degree of polymer/mucous interaction depends mainly on the polymeric structure, type of functional groups, degree of hydration, and polymer concentration (Andrews *et al.*, 2009).

Several experimental setups are available for evaluating the mucoadhesion of formulations including tensile tests, rheology (Tamburic & Craig, 1997), atomic force microscopy (AFM) (Sudhakar *et al.*, 2006), and mucin- interaction assessments (Woertz *et al.*, 2013). Generally, *in vitro* evaluation is preferred over *in vivo* studies mainly due to cost and ethical constraints related to sacrificing animals for such studies (Woertz *et al.*, 2013). Using freshly excised animal mucosa provides characteristics close to those of humans, however, its use is restricted due to intra-subject heterogeneity, partial loss during purification and ethical issues (Woertz *et al.*, 2013).

Therefore, researchers have developed synthetic materials from animal and plant sources as a substitutes for mucous membrane (Woertz *et al.*, 2013). Mucin type III from porcine stomach is one such example. After the rehydration of the lyophilised mucin, it possesses similar physiological, histological, and structural properties to those of the human mucosal membrane with minimal variability between batches (Sudhakar *et al.*, 2006; Liu *et al.*, 2005).

In the present study, the mucoadhesive propensities of the CS-PEC-NPs and CUR-CS-PEC-NPs were determined using mucin type III in four different concentrations (0.1, 0.2, 0.4, and 0.6 mg) maintained in three different pH media (pH 1.2, 6.8, and 7.4) representing different mucosal thickness and GIT segments, respectively. The magnitude of mucoadhesion was obtained by directly measuring the changes in the zeta potential of the NPs after interaction with mucin (Bhatta *et al.*, 2012; Takeuchi *et al.*, 2005).

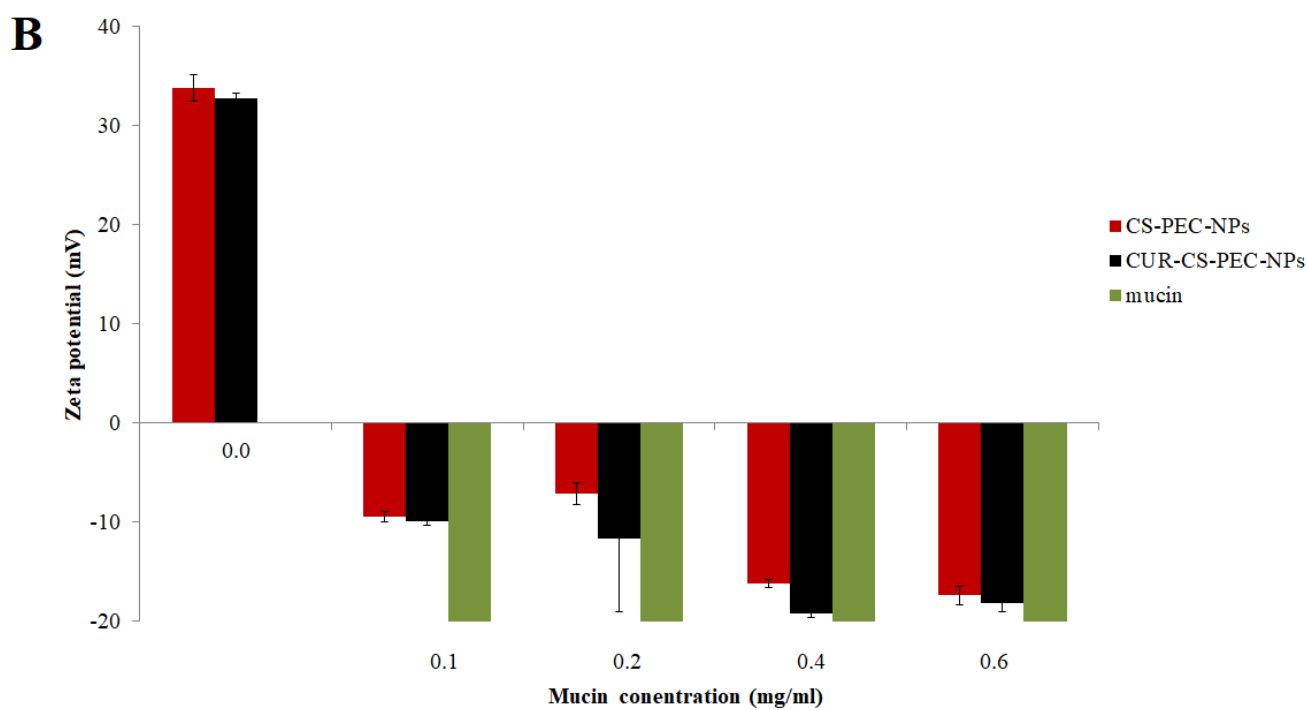
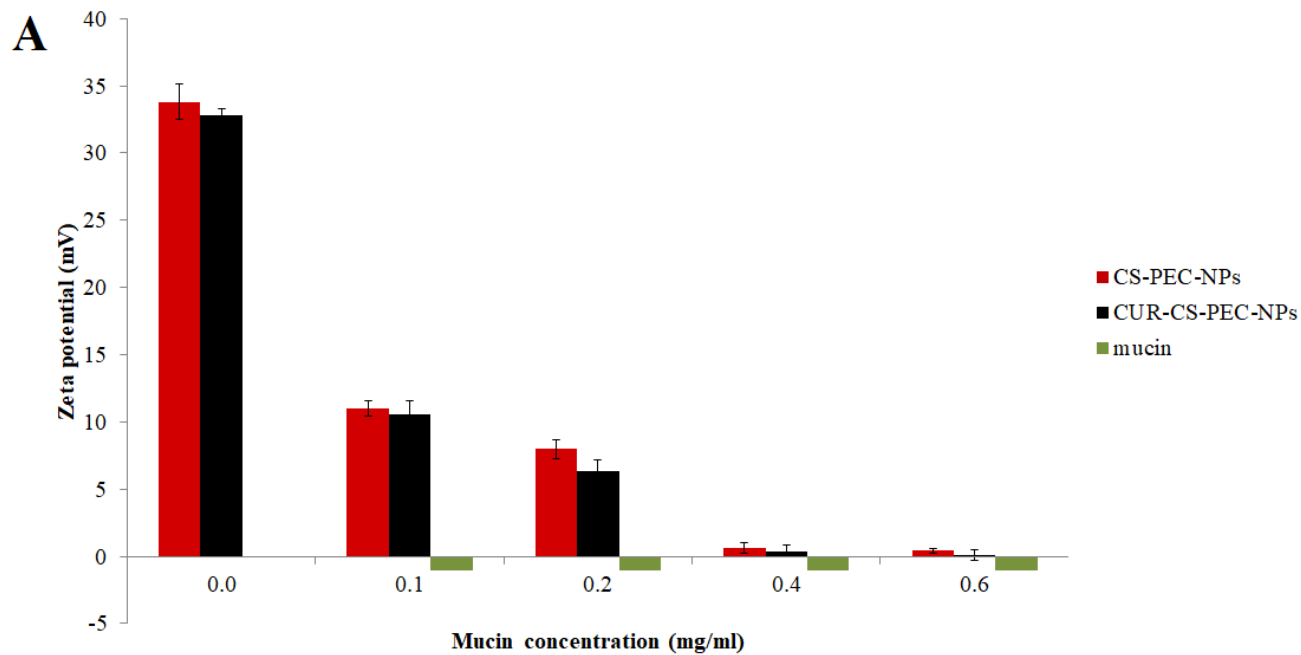
Figure 3.3 represents the drop in zeta potential at pH 1.2 (A), 6.8 (B), and 7.4 (C) where a direct relationship between the drop in zeta potential and mucin concentration is observed. The drop in zeta potential is a measure of the extent of mucoadhesion to CS-PEC-NPs and CUR-CS-PEC-NPs by mucin (Figure 3.4) (Bhatta *et al.*, 2012). The drop in zeta potential of the CUR-CS-PEC-NPs and CS-PEC-NPs at pH 6.8 (B) was more drastic compared to in pH 1.2 (A), suggesting that the NPs are more mucoadhesive at pH 6.8. At pH 7.4 (C), both CS-PEC-NPs and CUR-CS-PEC-NPs registered higher mucoadhesion than in both pH 1.2 and 6.8. Variation in pH affects the surface charge on mucin, CS-PEC-NPs and CUR-CS-PEC-NPs. Mucin has sialic acid residues which have a pKa of 2.6, resulting in a negative charge at physiological pH (pH 7.4).

There was a positive correlation between the drop in zeta potential and pH and this can be explained partly due to the low solubility of CS in acidic media (Lehr *et al.*, 1992) and to the fact that at higher pH the ionised carboxyl functional groups of mucin (COO^-) repel each other and change the spatial conformation from a coiled state into a “rod-like” structure, which results in higher accessibility for inter-diffusion and interpenetration (Bansil & Turner, 2006). The COO^- in mucin allows the positively charged $-\text{NH}_4^+$ groups of CS to form polyelectrolyte complexes which results in mucoadhesion. At higher pH, the amine groups in CS become more positive and therefore forms stronger polyelectrolyte bonds with mucin. Moreover, at higher pH, PEC tends to ionize and swells, resulting in inter-diffusion and formation of inter-chain bridges with the mucin (Lehr *et al.*, 1992). Therefore, the particles are completely covered by mucin at higher pH and thus register identical zeta potential as mucin. In addition, secondary hydrogen bonding between the functional groups of mucin and the OH and NH_2 groups and COOH groups of CS and PEC, respectively, may contribute in the mucoadhesive propensities of the NPs (Lehr *et al.*, 1992; Sriamornsak *et al.*, 2010).

Both CS and PEC possess polymeric characteristics crucial for mucoadhesion including strong hydrogen-bonding functional groups, high molecular weight, strong anionic charges, chain flexibility, and enough surface energy to spread onto mucous (Lehr *et al.*, 1992).

Chuah *et al.*, (2011) reported higher mucoadhesion in CUR-containing NPs compared to control NPs and attributed this to hydrogen bonding and hydrophobic interactions from the phenolic groups and aromatic rings of CUR, respectively. However, this phenomenon was not observed in the present study. In fact, both CUR-

CS-PEC-NPs and CS-PEC-NPs showed identical mucoadhesive propensities in all media studied.



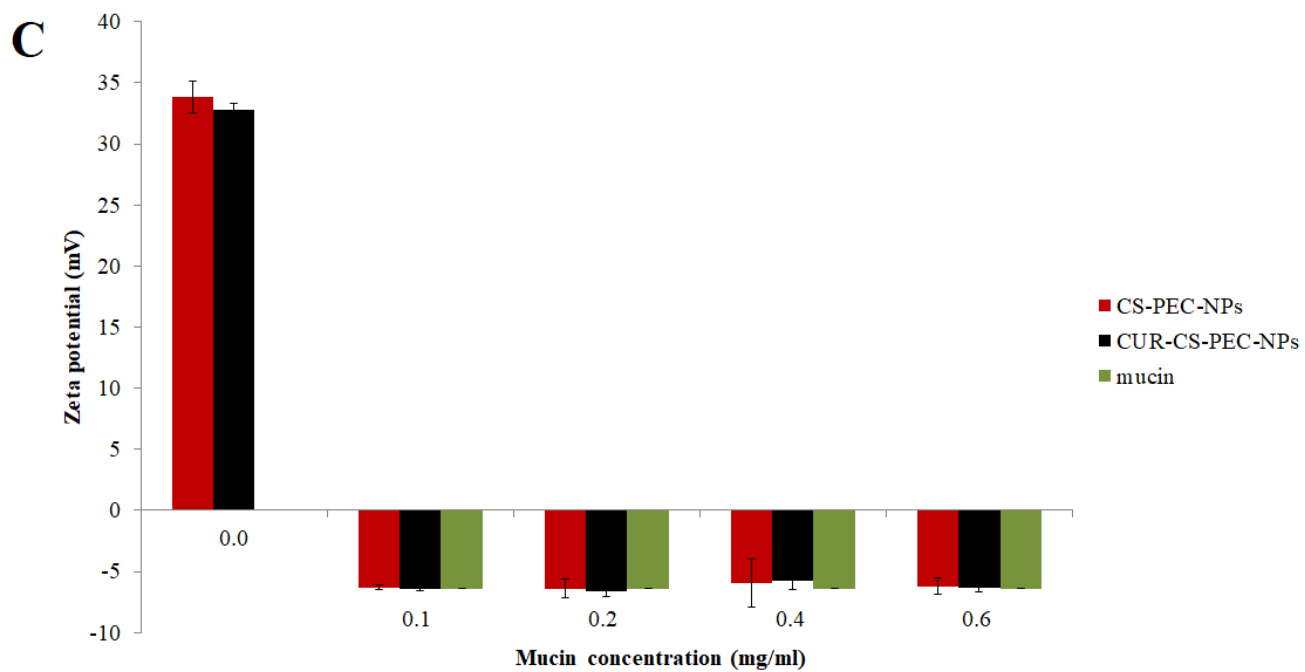


Figure 3.3 Changes in zeta potential of CUR-CS-PEC-NPs and CS-PEC-NPs in pH 1.2 (A), pH 6.8 (B), and pH 7.4 (C)

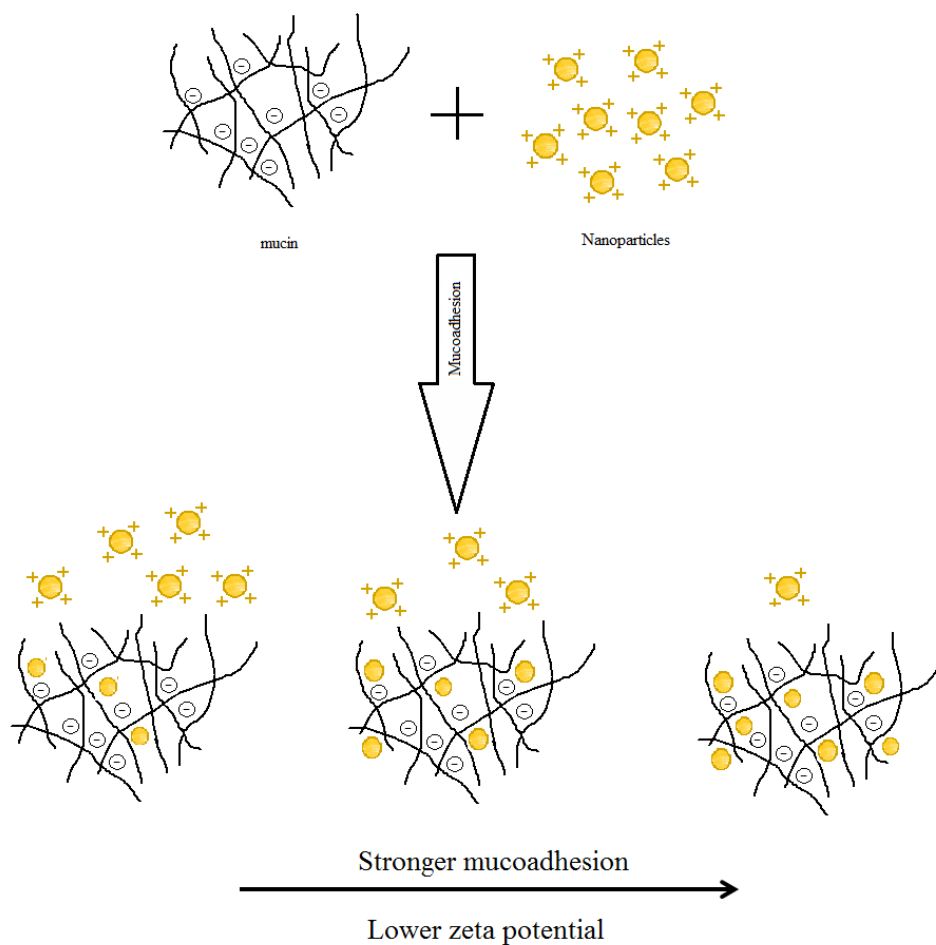


Figure 3.4 Schematic diagram of the drop in zeta potential in mucoadhesion

3.3.2 HPLC assay for quantification of CUR

The amount of CUR encapsulated or released from the CUR-CS-PEC-NPs was quantified using an HPLC system described in section 3.1.3.1. Samples containing CUR were calculated by comparing responses with a standard curve prepared in the same manner. Ideally, the ratio of the peak area to its height is constant, therefore, both peak area and peak height can be used to determine analytes concentration (Lough & Wainer, 1995). However, variations in peak heights may be observed in the presence of peak asymmetry, therefore, most HPLC analysis employ peak area for quantitative calculations as a more reliable alternative (Lough &

Wainer, 1995). Most CUR HPLC analyses are performed using reverse phase HPLC system (Ireson *et al.*, 2002; Wichitnithad *et al.*, 2009; Ma *et al.*, 2007; Garcea *et al.*, 2004) with UV detection as in the present study..

Figure 3.5 shows representative chromatogram obtained by adapting the method described by Wichitnithad *et al.*, (2009) with slight modification. From the chromatogram, it can be seen that peak is fairly symmetric, sharp, well resolved and free from interfering peaks with a retention time of 10.5 min. Figure 3.6 shows linear calibration curve in the range 0.15625-10 $\mu\text{g/ml}$ and R^2 value of 0.9997.

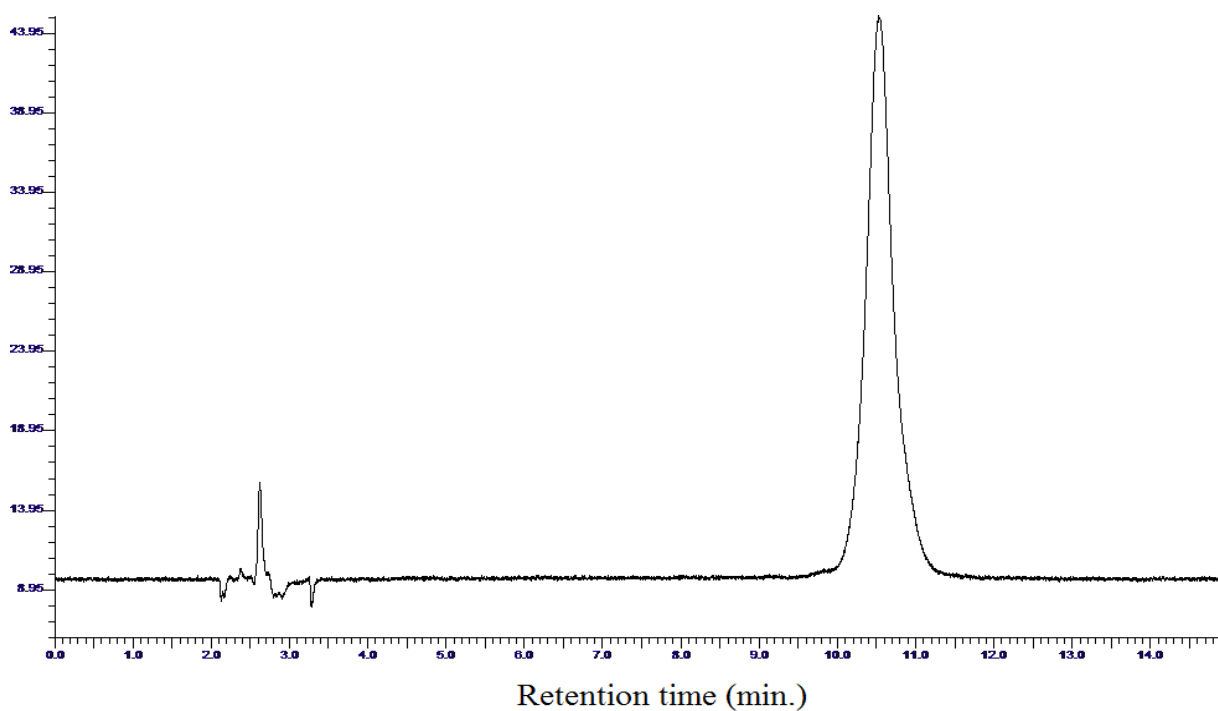


Figure 3.5 Representative chromatogram for CUR at 425 nm (5 $\mu\text{g/ml}$)

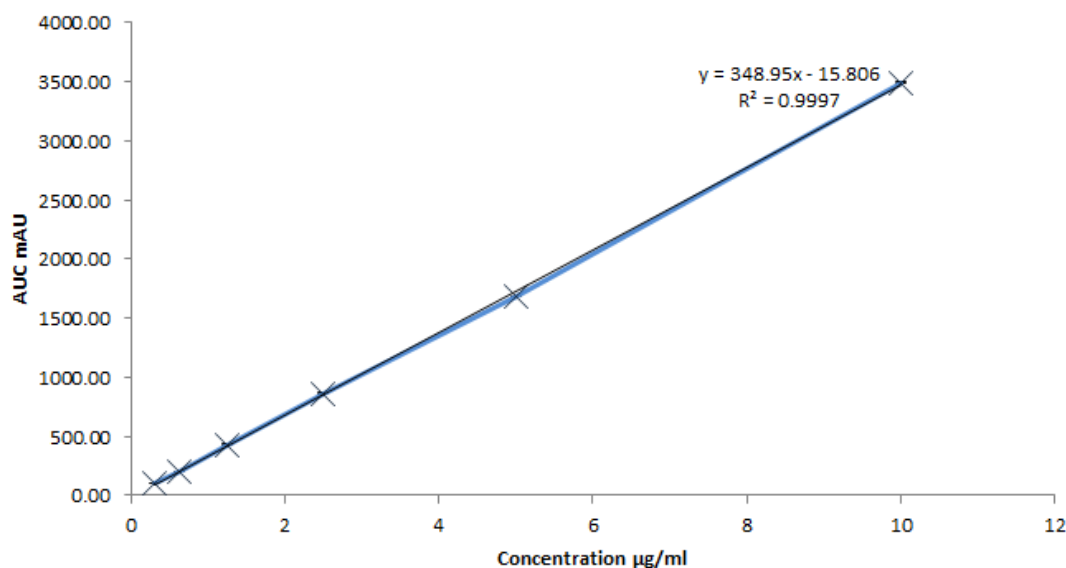


Figure 3.6 Standard calibration curve of CUR

The repeatability or precision of the HPLC analysis was determined as inter- and intra-day precision of the measurements (Table 3.1) for the concentrations 100, 50, 0.3125 µg/ml representing the high (HC), medium (MC), and low (LC) concentrations, respectively. The % relative standard deviation (%RSD) were all below 5.5%. The accuracy of the method was assessed and were in the range of 99.26-109.45% for the HQ and MQ, whereas the LQ accuracy was in the range of 109.86-118.61%. The limit of detection (LOD) and limit of quantification (LOQ) were calculated from equations 3.4 and 3.5, respectively and found to be 0.006 µg/ml and 0.019 µg/ml, respectively.

$$\text{Limit of Detection} = 3.3 \times \frac{\text{Standard deviation of low conc.}}{\text{Slope of curve}} \quad \text{Eq. 3.4}$$

$$\text{Limit of Quantification} = 10 \times \frac{\text{Standard deviation of low conc.}}{\text{Slope of curve}} \quad \text{Eq. 3.5}$$

Table 3.1 Precision and accuracy of the HPLC method.

	Concentration (µg/ml)	Accuracy (%error)	Precision (%RSD)
Intra-day (n=3)			
HQ	100	109.45	0.56
MQ	50	104.60	0.14
LQ	0.3125	109.87	0.01
Inter-day (n=3)			
HQ	100	106.05	5.55
MQ	50	105.81	1.41
LQ	0.3125	113.39	0.01

3.3.3 Encapsulation efficiency (EE%)

CUR is poorly adsorbed from the GIT and possesses very low bioavailability following oral administration hence, various formulations have been proposed to address the poor uptake from the GIT. Das *et al.*, (2010) managed to encapsulate CUR in alginate-CS-pluronic NPs and the EE% was as low as 13%. In contrast, higher CUR EE% was achieved in other formulations. For example, Anitha *et al.*, (2011) encapsulated CUR in dextran sulphate-CS-NPs at 74% EE%, Maya, *et al.*, (2011) had EE% of 87% of CUR in O-carboxymethyl CS NPs, and Liu *et al.*, (2012) formulated CUR-CS-NPs and achieved EE% of 70.9%. CUR is usually dissolved in ethanol prior to the encapsulation process therefore, the water miscibility of ethanolic solutions of CUR behaviour in the aqueous media is crucial to achieving successful encapsulation. This is because CUR is hydrophobic and requires to be in the dissolved state prior to formulation (Das *et al.*, 2010). Higher concentration of CS may enhance the %EE however, this may also increase the particle size (Maya, *et al.*, 2011). In this study, the EE% of the freshly prepared CUR-CS-PEC-NPs was found to be 64%±1.40. The incorporation of ethanolic solution of CUR

into PEC aqueous solution resulted in nanocrystals of CUR. As described in section 2.2.2.2, CS was added to PEC-CUR solution followed by TPP, thus, CUR nanocrystals were incorporated within the CUR-CS-PEC-NPs. EE% can be enhanced by increasing the concentration of CS, however, this will cause increase in the particle size of CUR-CS-PEC-NPs (Murkerjee *et al.*, 2009; Das *et al.*, 2010).

3.3.4 CUR release from CUR-CS-PEC-NPs

Cumulative CUR release in pH 1.2, pH 6.8 and 6.4 (with pectinase) are presented in Figure 3.7. A burst release of 15% of CUR obtained in the first 20 min. was followed by a gradual release over 5 hr. Eventually, a plateau was manifested in 5 hr with cumulative CUR release of $70.0\% \pm 0.2$ at the end of study.

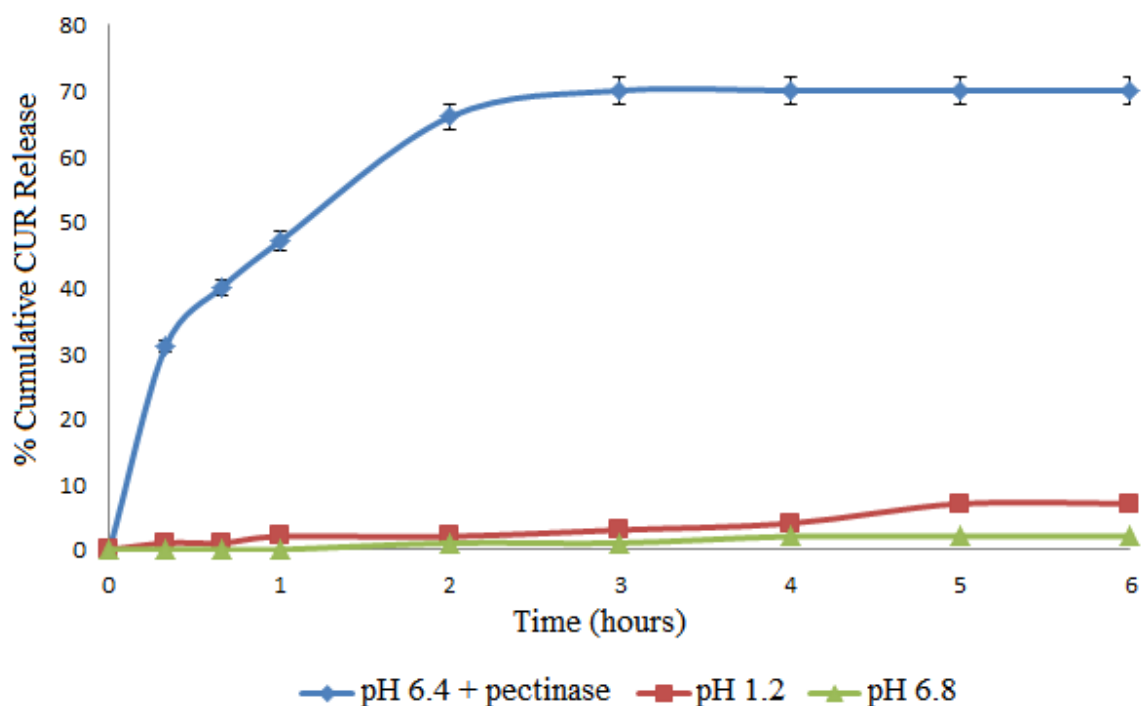


Figure 3.7 Cumulative release profiles from CUR-CS-PEC-NPs in pH 1.2, 6.8, and 6.4 (with pectinase), n=3

Since CS and PEC have different pKa values (6.1-6.5, 2.9-4.1 respectively), based on the Henderson-Hasselbalch equation, they act differently in terms of protonation/deprotonation as a function of pH. In acidic conditions (pH 1.2), the amine groups of CS become protonated, whereas the carboxylic groups of PEC become neutralized. Since the ionization of carboxylic groups of PEC is limited and it has the dominant effect, the coulombic repulsion of the carboxylic groups is reduced which protects CUR-CS-PEC-NPs (Bigucci *et al.*, 2008), however, negligible leaching of CUR was observed at this pH. At pH 7.4, the number of negatively charged carboxylic groups of PEC increases and hence electrostatic repulsion between ionized groups lead to chain repulsion (Munjeri *et al.*, 1997). However, CS is insoluble at this pH so that CUR release was impeded (Yu *et al.*, 2009). Despite this interaction and subsequent cross-linking, the catalytic effect of pectinase on the α -1,4-glycosidic linkages of PEC lead to breakage of existing bonds formed between PEC and CS which causes an initial burst release (Kashyap, 2001). In addition, some of the CUR adsorbed on the surface of CUR-CS-PEC-NPs and those encapsulated near the surfaces might have partially contributed to the initial burst release (Anitha *et al.*, 2011). A maximum release of 70% of CUR over the duration of the study reflects that a significant amount of CUR is retained within CUR-CS-PEC-NPs as similarly observed by other researchers (Das *et al.*, 2010; Yallapu *et al.*, 2010; Murkerjee *et al.*, 2009; Anitha *et al.*, 2011).

At acidic pH, the amino groups of CS undergo protonation hence, becomes soluble in aqueous media (Anitha *et al.*, 2011; Agnihotri *et al.*, 2004). This enhanced solubility of CS allows the penetration of water through CUR-CS-PEC-NPs, which results in swelling that facilitates diffusion of CUR from matrix (Agnihotri *et al.*, 2004). Makhlof *et al.*, (2011) evaluated the release of insulin from CS-TPP NPs in acidic conditions and they found that the NPs were only stable at pH > 3.0. In contrast, in the

typical pH range of the stomach (pH 1-2), the NPs rapidly released insulin due to disintegration and subsequent dissolution. In another study, Boonsongrit *et al.*, (2006) studied the release of insulin and salicylic acid from CS-microspheres at pH 3 showed a burst release of 100% and 80% of insulin and salicylic acid respectively. On the other hand, PEC resists the degradative effects of acidic media and it is readily digested by the colonic microflora (Subudhi *et al.*, 2015). However, PEC is highly hydrophilic and thus, formulations swell easily at the pH range of the small intestine (4.5-7.4) resulting in premature drug release (Mishra *et al.*, 2012). Subudhi *et al.*, (2015) studied the release of 5-FU from PEC-NPs in different pH solutions where a negligible amount of 5-FU was released at pH 1.2 (<12%), whereas rapid release was observed at the pH range (4.5-7.4) despite the absence of enzymatic activity. Similar results were obtained in another study, where Vaidya *et al.*, (2009) evaluated the release of metronidazole from PEC-microspheres at pH 1.2, 4.5, 6.8, and 7.4. Metronidazole release profiles were directly proportional to the pH of the media, with the least drug release of 23%, which increased to 100% after change in the pH from 1.2 to 7.4, respectively. These findings strongly suggest that PEC formulations might have the ability of maintaining their integrity in the gastric media, but may swell and degrade in pH (5.0-7.4), thus resulting in premature drug release in formulations targeting the colon. In this context, these constraints were overcome by fabricating a composite nanoparticulate system comprising of CS and PEC. In such a formulation, PEC contributes to maintaining the integrity of CUR-CS-PEC-NPs in the upper GIT, whereas CS protects CUR-CS-PEC-NPs from swelling in the pH of the small intestine (pH 7.4). With this plan, CUR-CS-PEC-NPs may successfully unload the cargo after colonic arrival prompted by degradation by the colonic microflora.

To study the level of protection offered by PEC against degradation in the acidic medium of the upper GIT, CS-PEC-NPs and PEC-free NPs were suspended in a 0.1 N HCl solution (pH 1.2) for 1 hr and the morphology of both NPs were studied under FESEM (Figure 3.8). PEC-free NPs (A+B) appear swollen and deformed with some degree of distortion after this treatment, which suggests degradation. Despite some negligible swelling, CS-PEC-NPs (C+D) maintained their morphology and integrity.

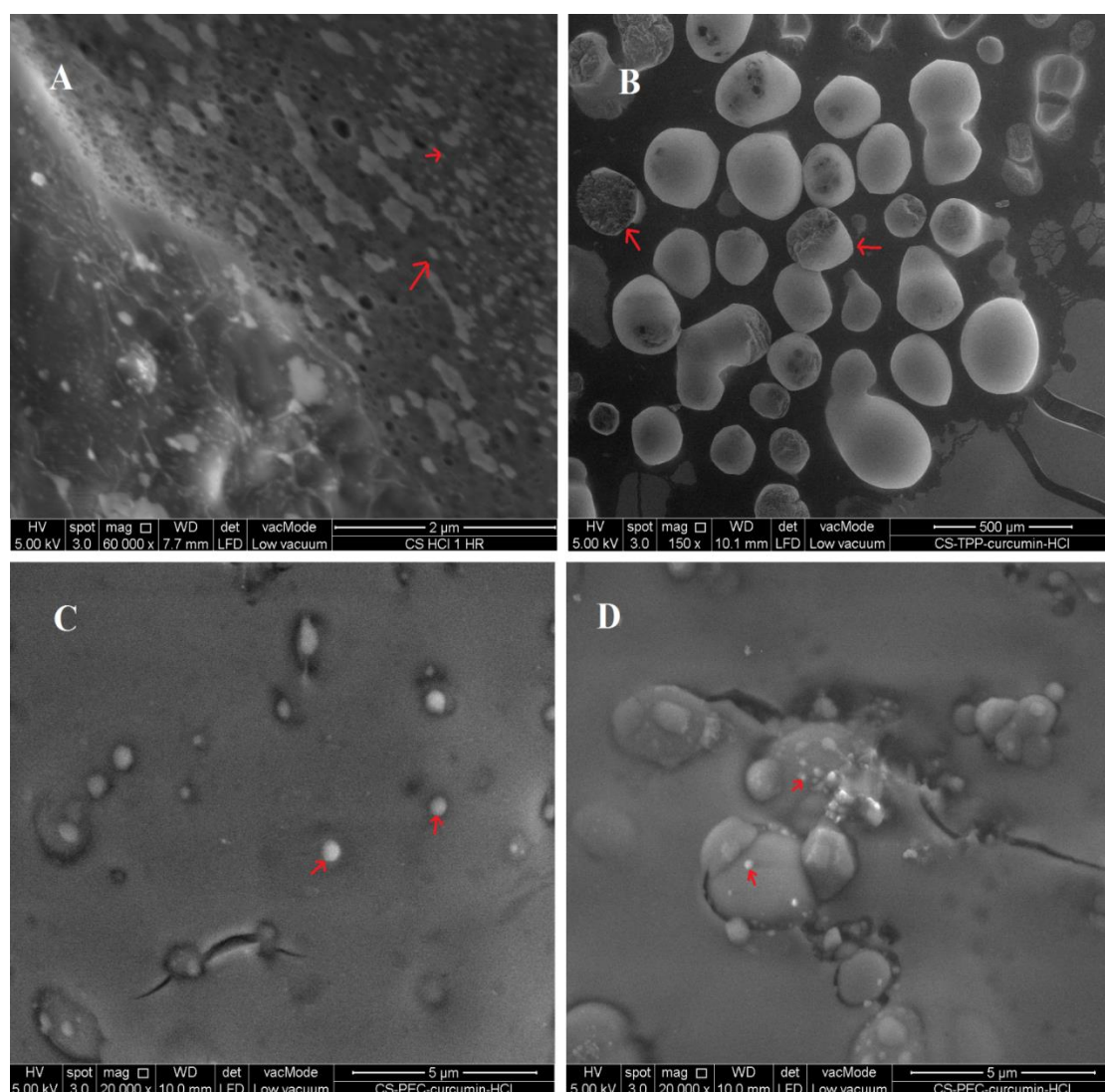


Figure 3.8 FESEM images of PEC-free NPs (A,B) & CS-PEC-NPs (C,D) after treatment with 0.1 N HCl (pH 1.2)

From Table 3.2 we note that there was an increase in the zeta potential of the NPs after exposure to pH 1.2 ($P=0.0383$), representing the stomach. This increase in

zeta potential is due to protonation of the amine groups of CS. At this pH, there is also a reduction in the magnitude of the negative charge on the carboxylic moiety of PEC. This combined effect on the amine groups and carboxylic acid in acidic media contributes to rise in surface charge. On the other hand, exposure of the CUR-CS-PEC-NPs to pH 6.8 after treatment in pH 1.2, caused a fall in the zeta potential to the initial value (P=0.0395). This change in zeta potential can be attributed to the deprotonation of the carboxylic group of PEC to the charged species ($-\text{COO}^-$), allowing electrostatic interaction between $-\text{NH}_3^+$ of CS. In parallel, the percentage retention of CUR within the CUR-CS-PEC-NPs was ascertained after exposure to the different media. The percentage retention of CUR decreased slightly (P=0.2735) after exposure to pH 1.2, with further decrease (P=0.1963) in pH 6.8, however, this decrease is minimal and suggests that the CUR-CS-PEC-NPs have the potential to retain a significant amount of the payload against a variable pH profile within the GIT.

Table 3.2 Zeta potential and percentage retention of CUR in CUR-CS-PEC-NPs after exposure to pH 1.2 and 6.8, n=3

	CUR-CS-PEC-NPs prior to exposure to media	CUR-CS-PEC-NPs after exposure to pH 1.2	CUR-CS-PEC-NPs after exposure to pH 6.8
Zeta potential (mV)	+33.1 ± 1.1	+37.9 ± 2.5	+33.0 ± 1.3
Retention (%)	64% ± 2%	62% ± 2%	60% ± 1%

Following oral delivery, the CUR-CS-PEC-NPs will transit through the stomach and the small intestine before arriving the colon. Therefore, the release of CUR in these sequential sections of the GIT was studied *in vitro* as follows. Initially, CUR-CS-PEC-NPs were exposed to SGF for 1 hr, retrieved, and then re-suspended in SIF for 2 hr. Finally, CUR-CS-PEC-NPs were suspended in SCF for 4 hr and then retrieved by

centrifugation. The CUR release data (Figure 3.9) indicates up to 14% release in the SGF which is attributable to slight swelling (see Figure 3.10B) in this medium. As discussed earlier in this section, this swelling is attributable to CS. In SIF, further swelling can be observed (see Figure 3.10C), however the release was negligible. In contrast to both of these media, release of CUR was fast in colonic medium. Maximum cumulative release of 86% was observed after 7 hr of the study. Similar drug release profiles were reported in the literature for PEC-formulation for colon delivery of 5-FU and metronidazole (Subudhi *et al.*, 2015; Vaidya *et al.*, 2009), respectively. Figure 3.10D shows the morphology of CUR-CS-PEC-NPs after the 7 hr study period where, CUR-CS-PEC-NPs appear to have lost their integrity. Furthermore, very tiny debris can also be seen which might constitute degraded fragments of the NPs.

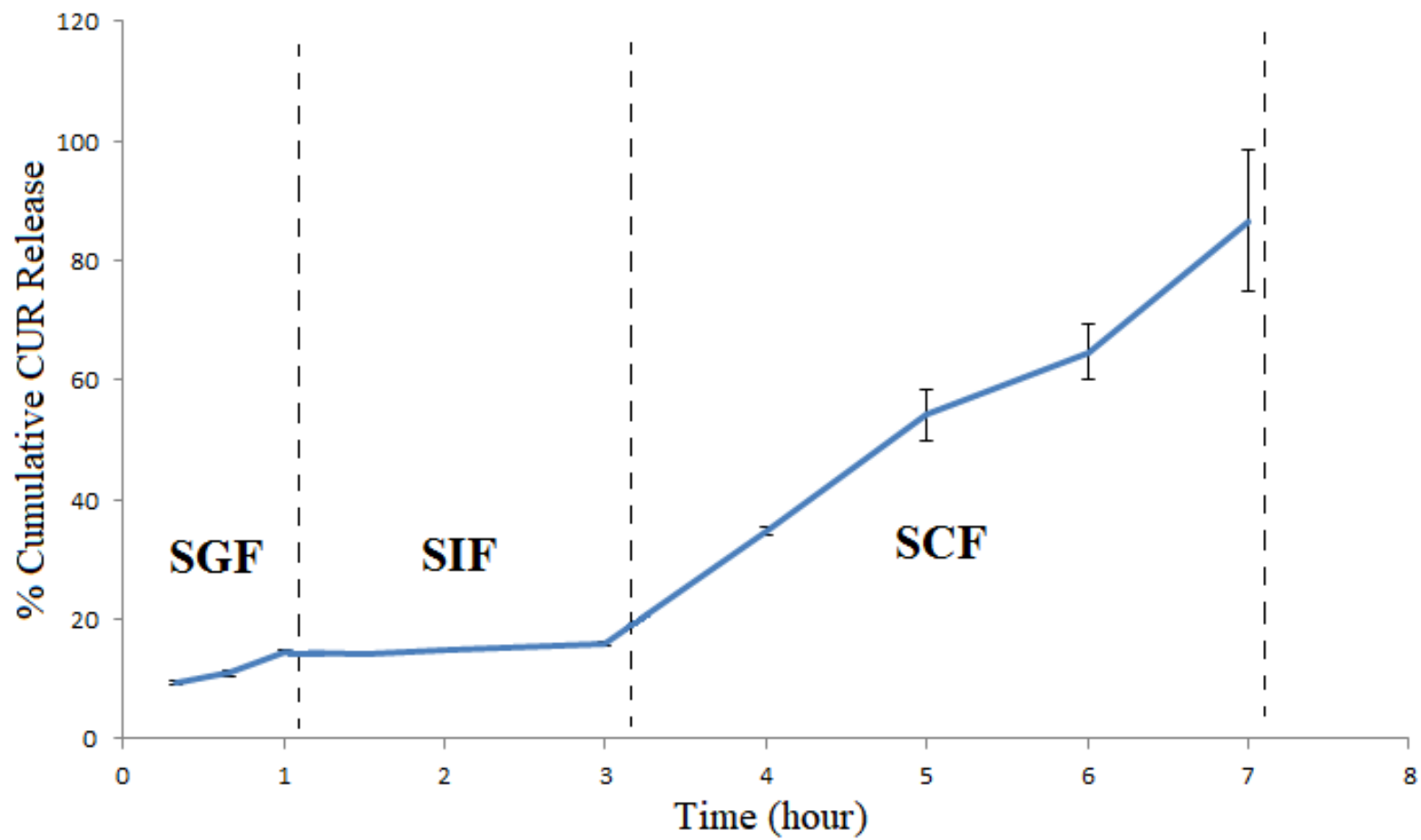


Figure 3.9 % cumulative CUR release from CUR-CS-PEC-NPs in simulated fluids, n=3

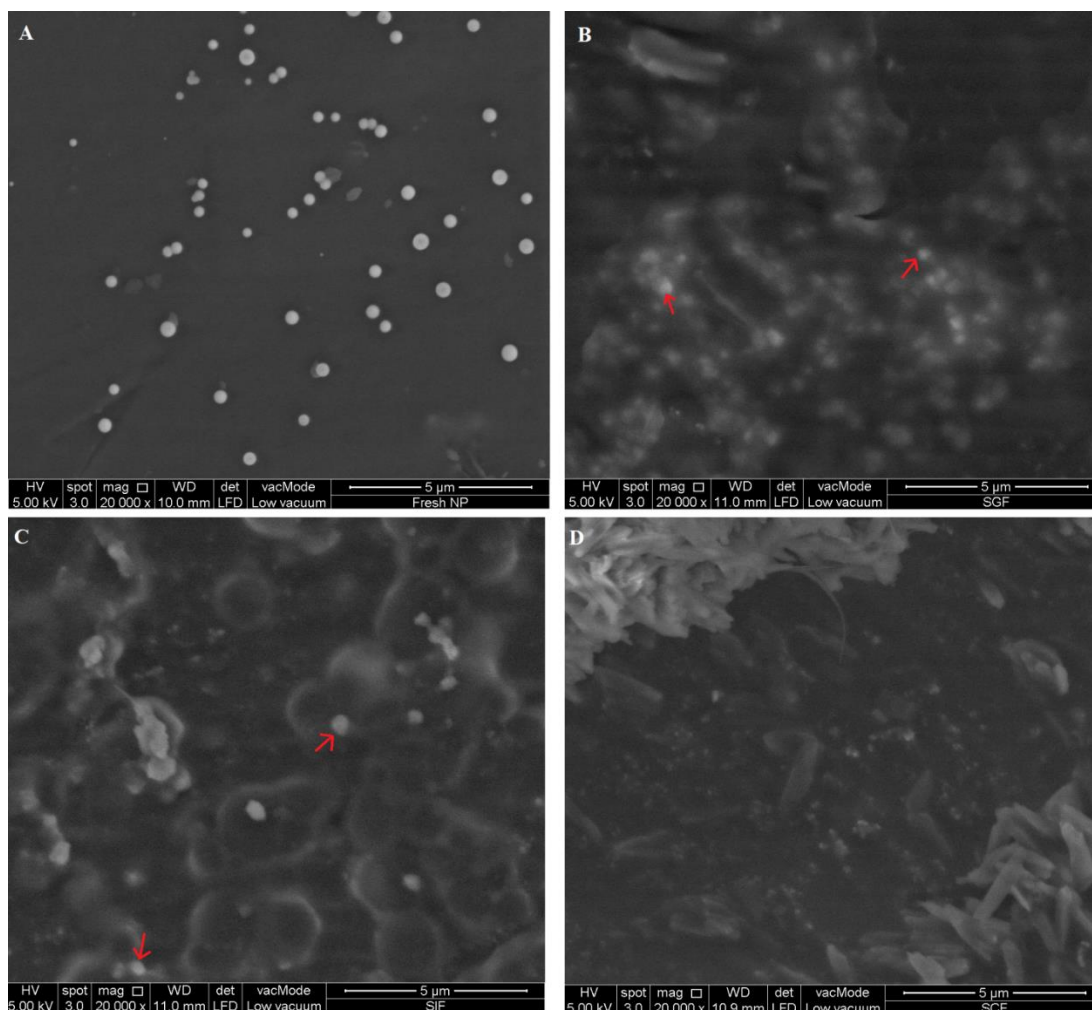


Figure 3.10 Morphology of fresh CUR-CS-PEC-NPs (A), and after exposure to treatment in SGF (B), SIF (C), and SCF (D)

CUR release from polymeric NPs depends on degree of cross-linking, size, density, and morphology (Agnihotri *et al.*, 2004). In addition, environmental factors such as pH of medium and the presence of enzymes play a vital role in the drug release (Agnihotri *et al.*, 2004). In the present study, we believe that CUR release is a combination of three release phases: firstly, the slight release of CUR in the upper GIT in simulated GIT and SIF fluids is attributable to CUR that was absorbed at the surface and near surface area of within the matrix of the NPs. Further release in these two media may involve leached CUR from the swelled matrix. After its exposure to the colonic simulated fluids, PEC became degraded, hence the degraded fragments of the NPs

provided a larger mass transfer of the cargo to the medium and hence a faster rate of release was observed.

3.3.5 Stability Studies

3.3.5.1 Storage stability studies

The stability of the CUR-CS-PEC-NPs with regard to storage like any other dosage form is crucial as it determines the possible shelf life of the particular formulation (Wilson *et al.*, 2010). Such studies might include physical appearance, texture, odour, colour, particle size, morphology, and chemical changes (Wilson *et al.*, 2010). In the present study, the tendency of the CUR-CS-PEC-NPs to maintain their physico-chemical characteristics (size, zeta potential, and morphology) as a function of time was studied by storing the NPs in a refrigerator (4°C) for 14 days. Collated data on particle size and zeta potential as well as morphology are presented in Figures 3.11 and 3.12 respectively. In Figure 3.11, we observed a significant decrease in the particle size of CUR-CS-PEC-NPs at day 7. However, Figure 3.12B (Day 7) shows a collection of large and small particles, which can be explained by the fact that the DLS analysis is based on an average determination. The increase in pDI value ($p=0.0113$) reflects the high variability in the particle size distribution. Therefore, stability analysis based on DLS analysis alone may lead to misleading conclusions.

It is likely that the smaller sized fraction in the range are contribution from fragments of the particles produced during storage whilst the larger sized particles are produced due to swelling or Ostwald's ripening. Swelling is likely to be the cause for the increase in size of CUR-CS-PEC-NPs because the particles retained their spherical morphology (Figure 3.12B). In contrast, Figure 3.12C (Day 14) shows an irregularly shaped particles (pointed with red arrows) which might be attributed to the

degradation/fragmentation and shrinkage of the NPs followed by a minor degree of swelling. This phenomenon was confirmed by the observation in further decrease in particle size observed from the DLS measurements. On the other hand, there was an insignificant decrease in zeta potential between day 7 and day 14 ($p=0.5525$ and 0.2659 for days 7 and 14, respectively). This attest to the fact that the zeta potential is mainly contributed by the surface moieties. Due to the changes in size and morphology with storage, the shelf-life stability studies were discontinued at day 14. These findings reflects the low storage stability of CUR-CS-PEC-NPs, thus, the particles need to be freeze-dried and reconstituted prior to administration.

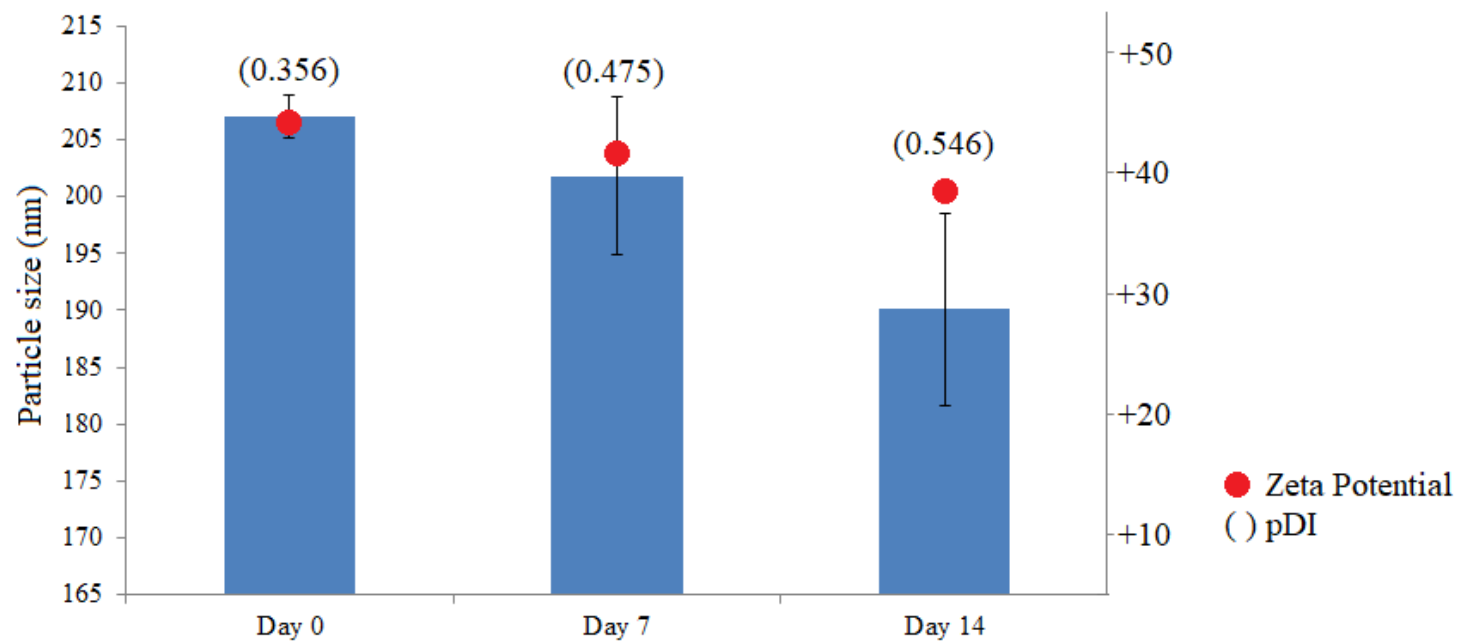


Figure 3.11 Size, zeta potential, and pDI values of CUR-CS-PEC-NPs at days 0, 7, and 14 of shelf storage (n=3)

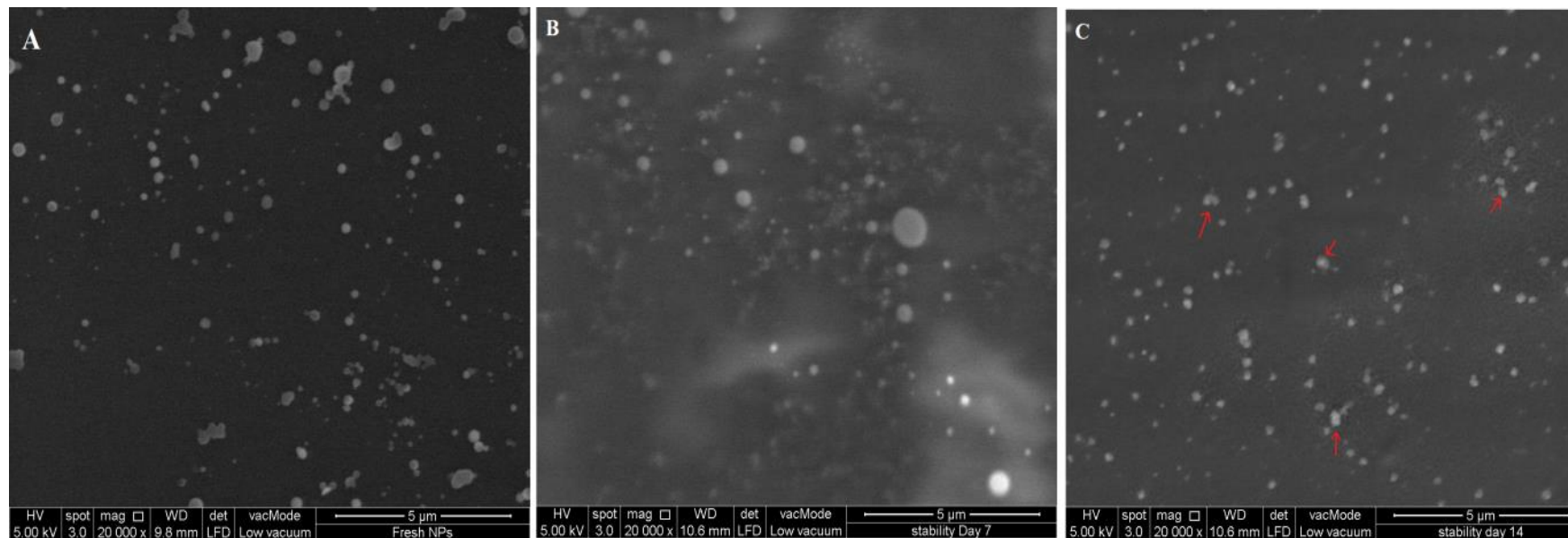


Figure 3.12 Morphology of freshly CUR-CS-PEC-NPs (Day 0) (A), at day 7 (B) and day 14 (C) during storage at 4°C

Polymeric NPs such as those containing PEC and CS lose their integrity in the presence of enzymes such as pectinase. However, it was reported that such NPs prepared by ionic gelation might degrade in aqueous media in the absence of enzymes (López-León *et al.*, 2005). NPs storage stability also depends on the ionic strength of the medium, pH conditions, cross-linking density, particle size, and particle size distribution (Fan *et al.*, 2012). CUR-CS-PEC-NPs were metastable and failed to maintain their integrity upon storage. This could be attributed to the erosion of the NPs in aqueous environments. Subsequently, increment in particle size was observed in Figure 3.12B and eventually, spontaneous disintegration (López-León *et al.*, 2005). In addition, the free polymeric chains might have interacted with the NPs network leading to further intermolecular entanglements and swelling (Rampino *et al.*, 2013). The small size of CUR-CS-PEC-NPs is partially responsible for its poor stability. In fact, larger polymeric NPs have more inter- and intra-hydrogen bonding, thus, produce more stable nanogels (Rampino *et al.*, 2013).

Spontaneous disintegration and aggregation of polymeric NPs under mild storage conditions in short duration of time is common amongst the polymeric NPs (Rampino *et al.*, 2013; López-León *et al.*, 2005; Borchard, 2001; Luo *et al.*, 2004). In contrary, some research reported the stability of polymeric NPs for durations exceeded 3 months (Wilson *et al.*, 2010; Fan *et al.*, 2012). NPs stability might be enhanced by increasing the cross-linking density via increasing suitable cross linker such as TPP. However, this significantly increases the NPs diameter as reported in section 2.3.1 (Fan *et al.*, 2012). Stabilizers such as polyethylene glycol (PEG) and PVA might be used to enhance the NPs stability (Wu *et al.*, 2011).

3.3.5.2 Protection of CUR from photodegradation

CUR undergoes photodegradation both in solid and solution forms. Research found that photoanalysis of CUR upon exposure to sunlight is higher compared to UV light. In fact, CUR has been used as a photosensitizer in micellar formulations (Priyadarsini, 2009). The mechanism of photo-degradation in CUR is not well understood, however, it is believed to occur by the cleavage of the β -diketone link resulting in the formation of smaller phenolic compounds such as vanillin and ferulic acid. The presence of iron and aluminium salts influence CUR photo-degradation (Priyadarsini, 2009). Coradini *et al.*, (2014) studied the photoprotection of CUR encapsulated in lipid-core nanocapsules. The study included the exposure of CUR nanocapsules to UV light and found that the lipid nanocapsules significantly protected CUR from UV-decomposition. Half-lives of CUR solution and CUR-loaded lipid nanocapsules were 4.29 ± 0.62 and 7.25 ± 0.54 min., respectively. Xiao *et al.*, (2015) found that encapsulated CUR in polymeric matrix immensely protected it against UV degradation. After 270 min. of UV treatment, only 25% of CUR was retrieved from ethanolic CUR solution. On the other hand, >50% of CUR was retrieved from carboxymethyl CS NPs.

Since CUR is encapsulated in its inactive form in CUR-CS-PEC-NPs, it is hypothesized that CUR wont undergo degradation when exposed to light. To ascertain this hypothesis, equivalent amounts of pure CUR and CUR-CS-PEC-NPs were exposed to sunlight and UV light (253 nm) in transparent vials for 6 hr. % retrieved CUR as shown in Figure 3.13. From the data obtained in Figure 3.13A, pure CUR undergoes extensive photodegradation and was almost completely degraded at the end of the study, in contrast, CUR-CS-PEC-NPs significantly protect CUR from degradation, and however, 23% of CUR had undergone photo-degradation at the end of the study. UV

light had a milder photo-degradative effect on both CUR and CUR-CS-PEC-NPs (Figure 3.13B). 94% of encapsulated CUR was protected in CUR-CS-PEC-NPs, whereas more than 50% of pure CUR was degraded at the duration of the study.

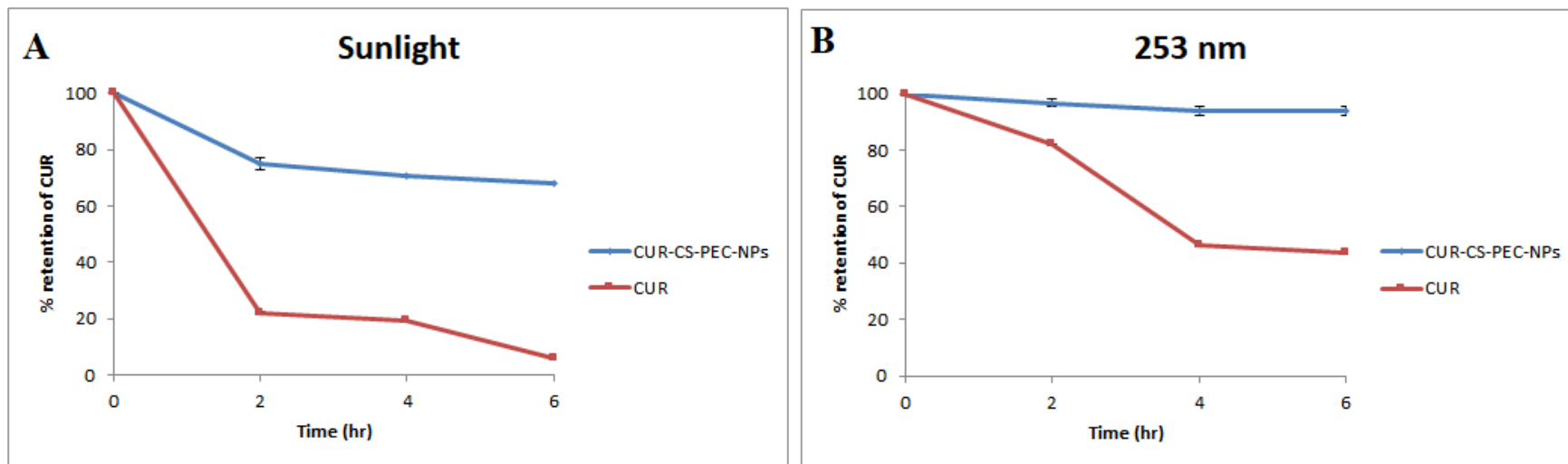


Figure 3.13 % retention of CUR from CUR-CS-PEC-NPs and CUR ethanolic solution vials upon exposure to sunlight (A) and UV light at 253 nm (B), n=3

The enhanced photostability of CUR in the NPs could be attributed to its encapsulation in the inactive form (Jiayin Zhao & Wu, 2006). In addition, the accumulation of CUR within CUR-CS-PEC-NPs protected by the polymeric matrix away from light and the oxidizing environment such as ROS and water could be a contributing factor (Suwannateep *et al.*, 2012). Thus, CUR photostability was assured via encapsulation in the CS-PEC-NPs.

3.3.5.3 *Protection of CUR from thermal degradation*

CUR might undergo decomposition at physiological temperature (37°C) during its transit to the colon. To ascertain the stability of the CUR-CS-PEC-NPs in protection of the CUR by thermal degradation, CUR-CS-PEC-NPs and pure CUR were placed in water bath at 37°C for three days. Sampling was performed at the end of each day where retrieved CUR was assayed using HPLC. The CS-PEC-NPs matrix protected CUR from thermal degradation for the whole duration of the study, whereas gradual decomposition of pure CUR was observed where less than 60% of CUR was retained at the end of the study (Figure 3.14). It is believed that due to the presence of CUR in amorphous state in the CUR-CS-PEC-NPs in addition to the protection offered by the CS-PEC-NPs matrix, CUR was less prone to becoming degraded due the thermal changes. These findings were in agreement with Kumara & Madhysyghan (2015) and Rahman *et al.* (2014).

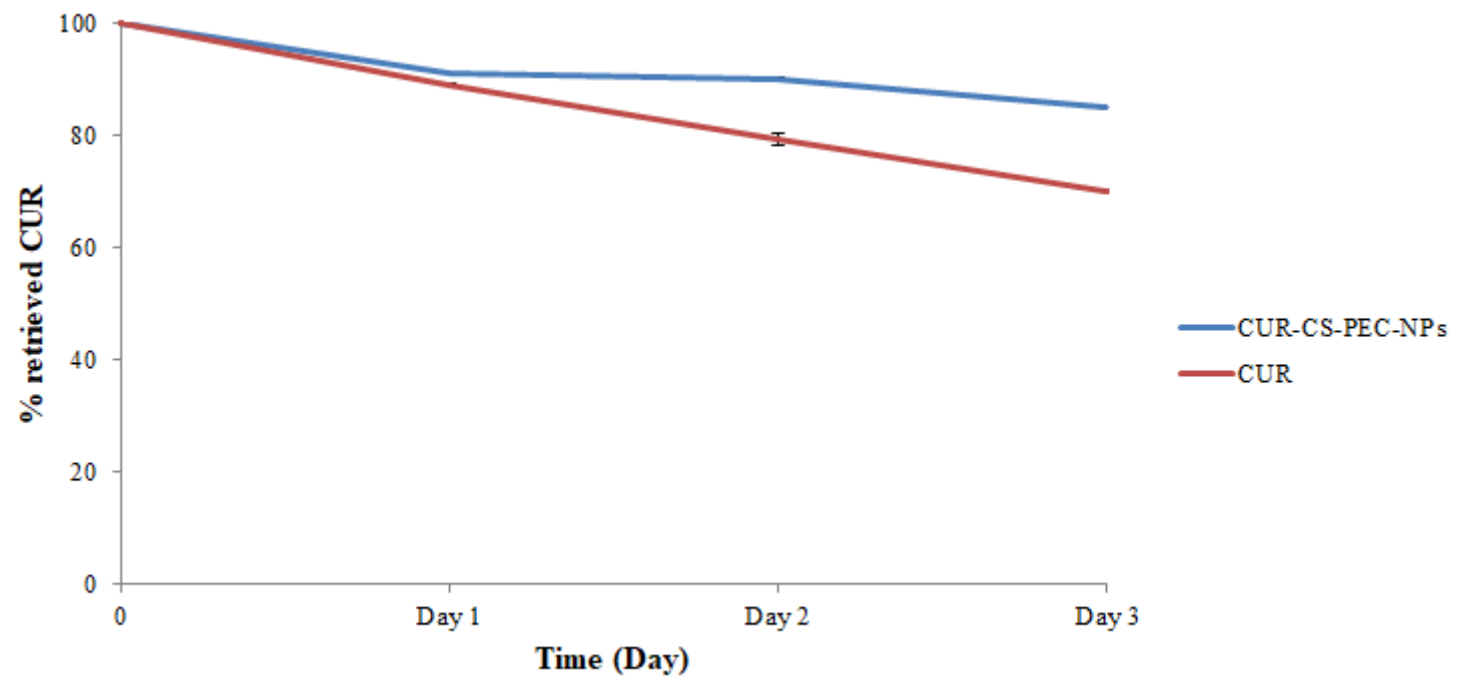


Figure 3.14 Thermal stability of CUR-CS-PEC-NPs and CUR at 37 °C, n=3

3.4 Conclusion

In this chapter, the ability of CS-PEC-NPs to encapsulate CUR, maintain their integrity in the upper GIT and unload CUR in the colonic conditions were confirmed *in vitro*. The *in vitro* mucoadhesion between CUR-CS-PEC-NPs and mucin was also confirmed. These findings could provide indication on how CUR-CS-PEC-NPs might interact with the various GIT conditions *in vivo*. It is anticipated that CUR-CS-PEC-NPs would behave in a similar manner *in vivo*, where prolonged contact with the colonic epithelium might occur, in addition, CUR-CS-PEC-NPs might remain intact through their transit in the upper GIT and eventually, deliver CUR in the colon. The CUR-CS-PEC-NPs appeared to be unstable for storage up to 14 days when in solution, however, freshly prepared CUR-CS-PEC-NPs significantly protect their CUR cargo from light and thermal effects of the physiological temperature. The CUR-CS-PEC-NPs are thus well primed for further investigation where the anti-cancer and apoptotic efficacy and as well cellular uptake will be discussed in chapter 4.

Chapter 4

In Vitro Cell Evaluation of Formulation

4. *In Vitro* Evaluation of Formulation

4.1 Introduction

4.1.1 Cell culture

Cell culture, first introduced in 1907, is the process by which cells are removed from an animal or plant and subsequently grown in controlled artificial environment (Invitrogen 2010; ATCC, 2003). The primary culture is the first batch of cells after isolation from the tissues and the subculture (passage) represent subsequent cultures from the primary stock. Subcultures require a new vessel and fresh growth medium for growth to manifest (Invitrogen, 2010).

Primary cultures generate heterogeneous population of cells, whereas subcultures cells generate a homogeneous cell line (subclone) (ATCC, 2003). The primary cells can undergo limited number of passages due to Hayflick Limit effect, culture conditions, and depletion of nutrients (ATCC, 2003). Essential nutrients for cells growth include amino acids, carbohydrates, salts and vitamins which are supplied by the growth medium. Growth factors, hormones, lipids, and binding proteins can be obtained from the serum (Allaire *et al.*, 2010; Invitrogen, 2010). Foetal and new-born calf sera are favoured for cell culture work as they provide higher concentrations of components (Langdon, 2003). Environmental conditions include controlled temperature ($36.5^{\circ}\text{C} \pm 1^{\circ}\text{C}$), pH (7.2-7.4), gases (O_2 and 5% CO_2), and osmotic pressure (Invitrogen, 2010).

Cell culture is one of the essential tools used in cellular and molecular biology, it is used as a model system for studying the normal physiology of cells, cytotoxicity testing, nutritional studies, carcinogenesis (ATCC, 2003; Invitrogen, 2010). It is extensively used in drugs development and genetic engineering (Allaire *et al.*, 2010).

The main advantages of employing cell culture for these applications are the consistency and reproducibility of the obtained results (Invitrogen, 2010).

One of the major challenges in cell culture is contamination which could be bacterial, viral, yeast, or fungal (Perlman, 1962). Biological effects resulting from contamination include competition for nutrients with host cells, secreted by-products which stops the growth of the host cells (Allaire *et al.*, 2010). There are several antibiotics that can be used in cell culture like penicillin, streptomycin, amoxicillin, gentamycin, or combination of two antibiotics. However, long term use of antibiotics is not favourable as it results in antibiotics resistance and hides the presence of contamination such as mycoplasma contamination (Perlman, 1962).

4.1.2 Cell lines

Human colorectal adenocarcinoma cell line HT-29 was used to study the anti-proliferative effects of CUR and CUR-CS-PEC-NPs. The cells produce the secretory component of IgA, carcinoembryonic antigen (CEA), transforming growth factor binding protein, and most crucially, mucin (ATCC, 2017a). HT-29 is one of the most commonly used cell lines for studying the antiproliferative effects of new drug entities or for formulations against colorectal cancer. It was used to study the antiproliferative effects of CUR (Goel *et al.*, 2001; Aggarwal *et al.*, 2003; Song *et al.*, 2005; Johnson & Mukhtar, 2007; Lee *et al.*, 2009) and CUR-nanoformulations (Ha *et al.*, 2012; Deepa, *et al.*, 2014; Anitha, *et al.*, 2014) against colorectal cancer.

MRC-5 are normal lung fibroblast, originally isolated from human lung tissues of 14-weeks old Caucasian male foetus (ATCC, 2017b). It is the most commonly used fibroblast human cells in the production of viral vaccines (Zhang *et al.*, 2014). The major advantage of MRC-5 is its capability to grow for more than 40 passages while

maintaining normal diploid karyotype. Its use as control (normal) cell line against colorectal cancer cell lines have been extensively reported in the literature (Herlyn *et al.*, 1979; Frixen *et al.*, 1991; Bhattacharyya *et al.*, 1994; Tokunaga *et al.*, 2000; Tan *et al.*, 2011; Gandin *et al.*, 2012). Therefore, it was used as the control cell line in this study.

4.1.3 Fluorescence microscopy

Several subjects can be viewed by the light microscope via light reflection, scattering, and absorption. However, the light microscope is not capable of providing optical contrast necessary for detailed visualisation of structural components in materials such as colloids, polymers, crystals, and biological cells (Lavrentovich, 2012). Therefore, fluorescence microscopy was developed in which the contrast between the material (signal) and the surrounding (background) is enhanced (Lichtman & Conchello, 2005). Fluorescence microscopy provides intrinsic selectivity, therefore this technique has become the most commonly used microscopy in biology (Lichtman & Conchello, 2005).

In fluorescence microscopy (Figure 4.1), a laser beam is directed to the specimen. This causes excitation of fluorophores and a shorter wavelength is emitted nanoseconds later. The difference between the excited and emitted wavelength is called Stokes shift. The exciting light is then filtered out while the emitted fluorescence is then reflected as a fluorescent image (Lichtman & Conchello, 2005; Mueller, 2005).

Subjects can be detected by fluorescence microscopy only if they have fluorophores. The efficiency of a subject fluorescing depends on the wavelengths of absorption and emission as well as the outermost electron orbitals of the fluorophores (Lichtman & Conchello, 2005). Organic objects may be intrinsically fluoresce if they

have fluorophores (auto-fluorescence) or they can be labelled with fluorescent compounds (Lichtman & Conchello, 2005). The fluorescent specimen can be viewed directly by the eye or via a rapid camera attached to arc lamps. Light sources of fluorescence microscope are mercury and xenon arc lamps. The former provides several extremely intense light, whereas the latter is relatively even in covering the wavelengths of UV, visible, and near IR. However, both of them are expensive, dangerous, and require special lamp houses (Lichtman & Conchello, 2005).

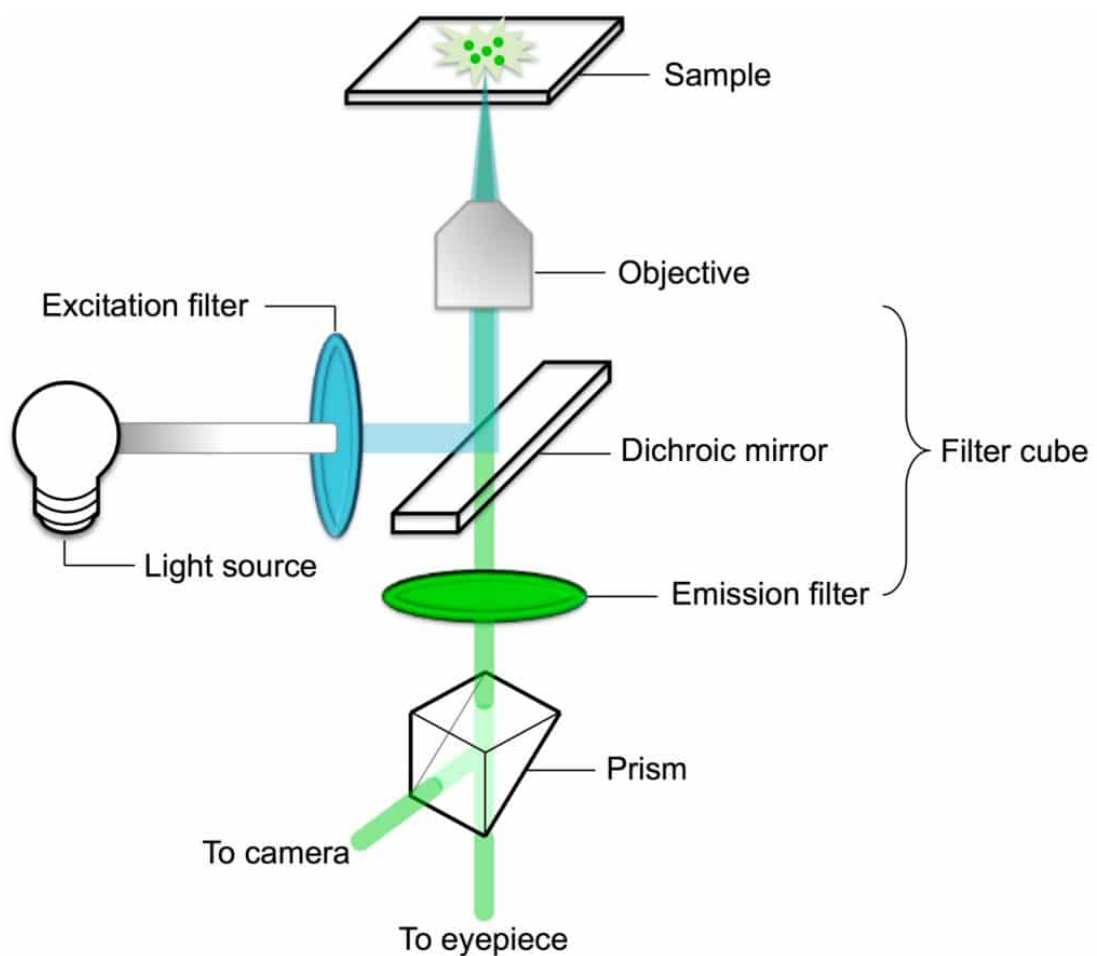


Figure 4.1 Basic components of inverted fluorescence microscope (*Adopted from www.jic.ac.uk*)

4.1.4 Mycoplasma

Amongst the various contaminants prone to cell culture, the most common concern contamination is mycoplasmic infections (Drexler & Uphoff, 2002). Mycoplasmas are tiny self-replicating organisms (Timenestsky, 1997). Contrary to regular bacteria, mycoplasma lack rigid cell walls (Timenestsky, 1997) and grow very slowly (Drexler & Uphoff, 2002). Mycoplasmas were first isolated in 1957 (Timenestsky, 1997). Mammalian and avian cell lines are more vulnerable to mycoplasmic infections (Timenestsky, 1997). Continuous cell lines are more frequently infected compared to primary cell culture (Rottem *et al.*, 2012).

The extent of mycoplasma infection on inhabitant cells depends on the type of the cell lines, the culture conditions, mycoplasma species, and the intensity and duration of mycoplasma infection (Drexler & Uphoff, 2002). The effects might be minimal and the cells might appear healthy, mycoplasmas might interfere in the cell culture structure, growth, and metabolism (Timenestsky, 1997). Nonetheless, mycoplasma infection can cause severe cytopathic effects characterized by feeble, abnormal growth and degeneration of cells, and eventually death of cells (Rottem *et al.*, 2012). A vast array of detection methods have been developed to detect mycoplasma infection in cell cultures such as SEM, colony formation on agar, universal PCR primers, and RNA hybridization (Drexler & Uphoff, 2002). However, these techniques vary in their overall efficiency, require very close quality control and specialized techniques (McGarrity *et al.*, 1983). DNA fuorochrome staining such as 4',6'-diamidino-2-phenylindole (DAPI) and Hoechst 33258 staining provides sensitive, specific, simple, efficient, and cost effective detection method (Drexler & Uphoff, 2002). In such procedure, mycoplasmas characteristic particulate around the host cells can be viewed under fluorescence (Figure 4.2) (Rottem *et al.*, 2012).

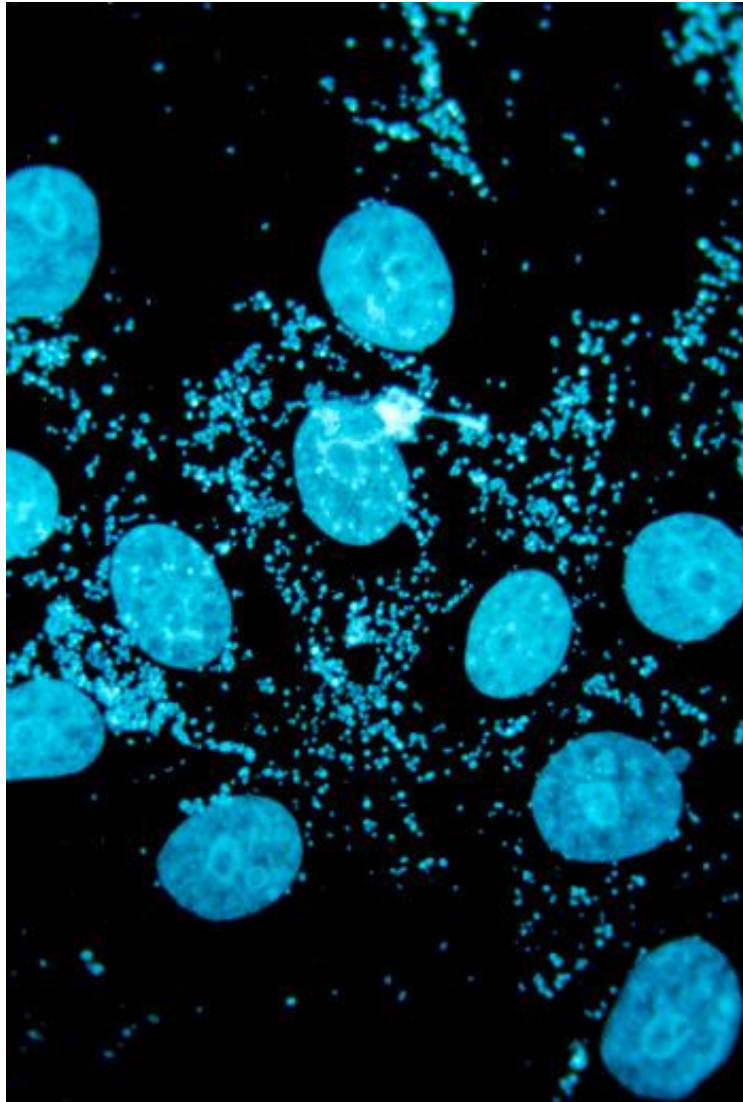


Figure 4.2 Mycoplasma positive cells after DAPI staining (Adopted from www.bionique.com)

4.1.5 MTT assay

The cell viability and proliferation studies are amongst the most crucial *in vitro* assays in new drugs or formulations development process. The yellow tetrazolium MTT (3-(4,5-dimethylthiazolyl-2)-2,5-diphenyl tetrazolium bromide) assay has been widely employed for cell proliferation measurements (Riss *et al.*, 2013; ATCC, 2017). MTT assay has been widely reported in studying cross-resistance amongst drugs, drug sensitivity, drug screening on cell lines, and testing drugs combinations (Langdon, 2003).

MTT gives a yellow aqueous solution and easily penetrates viable cells. It is positively charged and become reduced via the hydrogenases produced by the metabolically viable cells to the water insoluble violet-blue formazan (Figure 4.3) (Stockert *et al.*, 2012; Riss *et al.*, 2013). The generated formazan precipitate inside the cells and near cell surface.

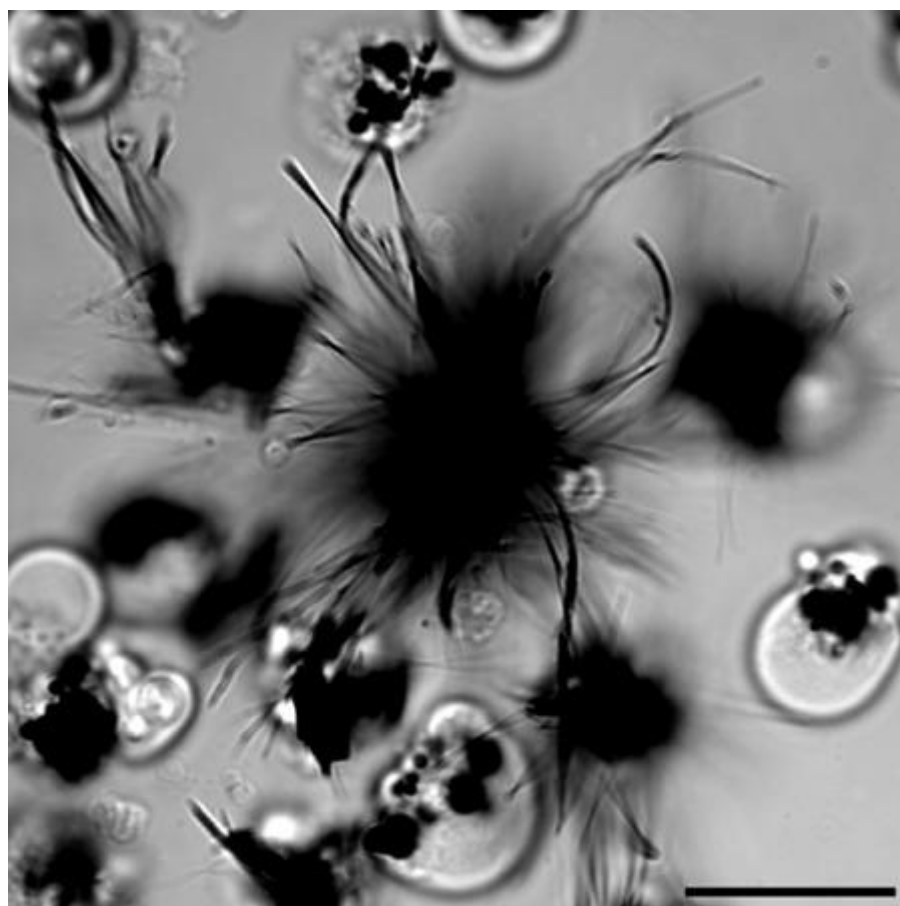


Figure 4.3 Insoluble formazan precipitated inside and near viable cells(Riss *et al.*, 2013)

4.1.6 Aims and objectives

The CUR-CS-PEC-NPs were successfully optimized and characterised as described in chapter 2. The mucoadhesive propensity, drug release profiles, and stability studies were studied in chapter 3. In this chapter, the antiproliferative efficacy and cellular uptake of CUR-CS-PEC-NPs against colorectal cancer cell lines (HT-29)

were evaluated. The selectivity of the CUR-CS-PEC-NPs was also studied. The therapeutic efficacy of CUR-CS-PEC-NPs was studied in comparison with the free CUR to ascertain whether that the anticancer effects of CUR are maintained after encapsulation in CS-PEC-NPs.

4.2 Materials and methods

4.2.1 Materials

Material	Supplier
CS-PEC-NPs	Prepared as described in Chapter 2
CUR-CS-PEC-NPs	Prepared as described in Chapter 2
Dulbecco's Modified Eagle's Medium (DMEM), 4.5 g/l glucose with L-glutamine. Sodium pyruvate-free.	NacalaiTesque, Japan
Roswell Park Memorial Institute (RPMI) – 1640 Medium	Sigma Aldrich, USA
Foetal Bovine Serum (FBS)	NacalaiTesque, Japan
Trypsin EDTA	NacalaiTesque, Japan
(3-(4,5-dimethylthiazolyl-2)-2,5-diphenyl tetrazolium bromide) (MTT)	NacalaiTesque, Japan
Dimethylsulfoxide (DMSO)	NacalaiTesque, Japan
Calcium and Magnesium free Phosphate Buffered Saline (PBS) pH 7.4	NacalaiTesque, Japan
Trypan Blue	Sigma Aldrich, USA
4',6'-diamidino-2-phenylindole (DAPI)	NacalaiTesque, Japan
Penicillin-Streptomycin mixed solution (stabilized)	NacalaiTesque, Japan

4.2.2 Maintenance of cell culture

The human colorectal adenocarcinoma cell line HT-29 and normal lung fibroblast MRC-5 were both donated by the National Cancer Council, Malaysia (MAKNA) laboratory, University Putra Malaysia, Malaysia. The HT-29 and MRC-5 cells were grown as a monolayer culture in Dulbecco's Modified Eagle's Medium (DMEM) and Roswell Park Memorial Institute (RPMI) – 1640, respectively. Media were supplemented with 10% FBS under standard cell culture conditions of 37°C and 5% CO₂.

4.2.3 Subculture of cells

For both cell cultures, cells were harvested by aspirating the medium and gently rinsing the cells with Ca⁺² and Mg⁺² free PBS, twice. Trypsin-EDTA was added to the flasks to detach the cells. After incubation at 37°C for 5-7 min, flasks were gently tapped to detach all cells from the culture surface. The cells were then viewed under inverted microscope (Nikon Eclispe TS1100-F, Japan) to ascertain that all cells were detached. The cells were then re-suspended in fresh media and centrifuged at 1000 rpm at 25°C (Eppendorf 5424, Germany) for 8 min. The supernatant was discarded and the harvested cells were re-suspended in fresh growth media. The cells suspension was then diluted and distributed into several flasks. Penicillin-Streptomycin mixed solution was occasionally used at 1% concentration, however, at least three passages of antibiotics-free media were cultured before any evaluation to minimize any possible interferences in the data duo to antibiotics use.

4.2.4 Cells counting

The cells were harvested from the flask of confluent cells as described in section 4.2.3 and properly diluted with media. A 10 µl aliquot of cells were thoroughly mixed

with 10 μ l of trypan blue. A cover slip was placed on the counting chamber and then 10 μ l of the cells suspension was applied to the surface of the hemacytometer using the two opposing edges of the cover slip and allowed to spread into the chamber by capillary force. The chamber was then viewed under the inverted microscope with a 10X objective. Cells in the four outside gridded squares excluding dead cells stained by trypan blue and the two outer perimeters (Figure 4.4) were counted. The number of cells per 1mm² was calculated as the average of the four counted chamber sides. The total number of cells was calculated as follows:

$$\text{Number of cells per 1 ml} = \text{average cells per 1mm}^2 \times 10^4$$

$$\text{Total number of cells} = \text{number of cells per 1 ml} \times \text{dilution factor of trypan blue} \times \text{dilution factor of media}$$

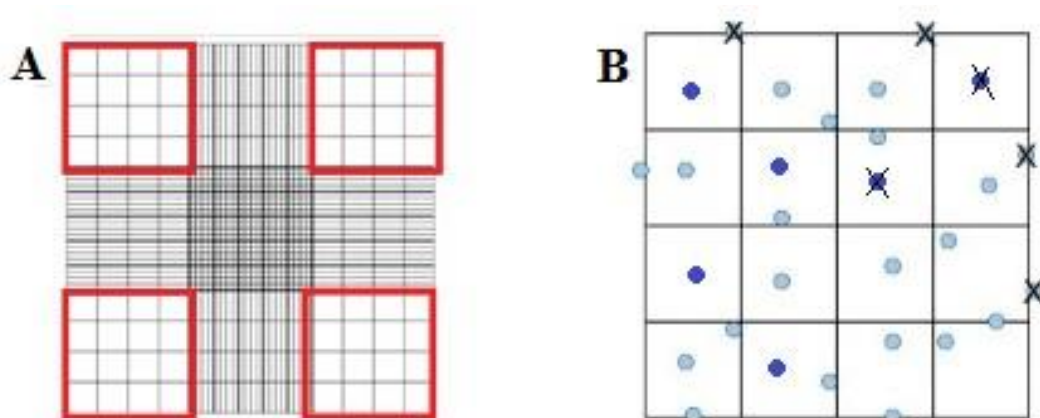


Figure 4.4 Hemacytometer grid (A) viable cells (not stained by trypan blue) inside the grid and at the interior perimeters are counted (B) (*Adopted and modified from www.humanimmunologyportal.com*)

4.2.5 Check for mycoplasma

The HT-29 cells were tested for possible mycoplasma contamination by seeding 1 x 10⁵ cells on a sterile cover slip in a 6 well plate and allowed to attach for 24 hr with appropriate medium. The medium was aspirated and the cells were gently washed with

PBS, twice. The cells were then fixed with 3.7% formaldehyde for 10 min. followed by aspiration and washing of with PBS, once. The cover slips were left to dry for 10 min. A 2 ml aliquot of DAPI working solution (1 μ g/ ml) was added to the cover slips and incubated for 15 min. in dark. Finally, the cover slips were washed with PBS and viewed under inverted fluorescence microscope (AX10, Carl Zeiss, Germany) with 430-495 filter.

4.2.6 MTT assay

4.2.6.1 MTT assay for HT-29 cells

The cell viability (MTT) assay was carried out to determine the effects of CUR-CS-PEC-NPs on HT-29 cell growth. The cells were seeded in a 96 well plates at 2 x 10³ cells/well and allowed to attach for 24 hr. The culture medium was then replaced with medium containing free CUR and CUR-CS-PEC-NPs at the following concentrations: 75, 90, 110, 130, and 150 μ M. The cells treated with CS-PEC-NPs and Dimethylsulfoxide (DMSO) were used as negative controls whereas 15 μ M of 5-FU was used as positive control. At time intervals of 24, 48, and 72 hr, treatment media were aspirated and 10 μ l of MTT solution (5mg/ ml) added. After 4 hr of dark incubation at 37°C, 100 μ l aliquot of DMSO was added and mixed at 40 rpm using a laboratory shaker (S1000 Gyrotwister, Labnet, USA). The plate absorbance was then measured at 570 nm using microplate reader (Epoch, Biotek, USA). The relative growth inhibition compared to untreated cells was measured and the mean values were presented (n=5).

4.2.6.2 MTT assay for MRC-5 cells

The MTT assay was carried out on MRC-5 cells to study the selectivity of CUR-CS-PEC-NPs against tumour cells rather than normal cells. Cells were seeded in 96

well plates at 1×10^5 cells/well and allowed to attach for 24 hr. The culture medium was then replaced with media containing free CUR and CUR-CS-PEC-NPs at 75 or 150 μM , representing low and high treatment concentration, respectively. The cells treated with CS-PEC-NPs and DMSO were used as negative controls whereas 15 μM 5-FU was used as positive control. At time points of 24, 48, and 72 hr, MTT assay was carried out as described in section 4.2.6.1. The relative growth inhibition compared to untreated cells was measured and the mean values were presented ($n=5$).

4.2.7 Cellular uptake

4.2.7.1 Qualitative cellular uptake

Naturally, CUR emits green fluorescence when viewed under a 535-600 nm filter (blue filter, FITC channel). Thus, HT-29 cells were harvested from a confluent culture flask and the cells were seeded in 6 well plates at 1×10^5 cells/well and left to attach for 24 hr. The culture media were then replaced with treatment media containing free CUR and CUR-CS-PEC-NPs at 75 and 150 μM , representing low and high treatment concentration, respectively. Controls used were untreated cells and cells treated with DMSO and CS-PEC-NPs. At time points of 24, 48, and 72 hr, cells were gently washed with PBS, thrice. Fresh PBS was added and cells were viewed under fluorescent microscope with 535-600 nm (blue) filter.

4.2.7.2 Quantitative cellular uptake

The HT-29 cells were harvested from a confluent culture flask and the cells were seeded and treated as described in section 4.2.7.1. At time points of 24, 48, and 72 hr, treatment media were aspirated and cells were gently washed with PBS. Trypsin EDTA was then added and dark incubated at 37°C for 15 min. PBS was then added and cells centrifuged at 1000 rpm for 8 min. The supernatant was then removed and cells

were lysed using methanol with vortex mixing for 1 minute. The suspension was then filtered with 0.22 μm syringe filter and the amount of CUR taken-up by the cells was quantified using the HPLC method described in chapter 3, section 3.2.3.

4.2.8 Cellular apoptosis viewed under fluorescent microscope

The HT-29 cells were harvested from T-25 tissue culture flask and seeded on cover slips fitted in 6 well plates at 1×10^5 cells/well and allowed to attach for 24 hr. Then the medium was aspirated and replaced with medium containing CUR-CS-PEC-NPs representing the lowest and highest effective concentration (75 μM and 150 μM , respectively) and equivalent concentrations of free CUR. Untreated cells, CS-PEC-NPs, and DMSO were used as negative control whilst 5-FU (15 μM) was used as positive control. After 24 hr of treatment, cells were fixed and stained with DAPI solution as described in section 4.2.5 and viewed under fluorescent microscope using 430-495nm (red) filter.

4.2.9 Statistical analyses

All values were expressed as mean \pm SD. Statistical significance was determined by paired *t*-test using GraphPad[®] Prism 5 software, GraphPad Software Inc. Statistical significance was indicated when *P*-values < 0.05.

4.3 Results and discussion

In this chapter, several cellular studies were conducted in an attempt to determine the efficacy as well as the selectivity of CUR-CS-PEC-NPs as anticancer agent. Free CUR was studied as well in order to compare its anticancer activity as crude drug and after encapsulation into CUR-CS-PEC-NPs. The anticancer activity of CUR-CS-PEC-NPs was investigated using the MTT cell viability assay whereas its apoptotic effects were evaluated using fluorescent microscopy. Cellular uptake of CUR-CS-PEC-

NPs by cells was evaluated both qualitatively and quantitatively using fluorescent microscopy and spectrophotometric analysis, respectively.

4.3.1 Maintenance of HT-29 and MRC-5 cells

HT-29 and MRC-5 cells were maintained at standard cell culture conditions. Cells were passaged when confluency is reached every 3-4 days and 5-7 days for HT-29 and MRC-5 cells, respectively. Antibiotics were seldom used, however as precaution, at least three passages of antibiotics-free cultures were carried out before any study to avoid any interference in the obtained results. Figure 4.5 shows HT-29 (A+B) and MRC-5 (C+D) cells viewed under inverted microscope. Both cell lines images show 70% confluency, the beaming circular objects (pointed by red arrows) are floating growing cells which represents the healthiness of the passaged cells.

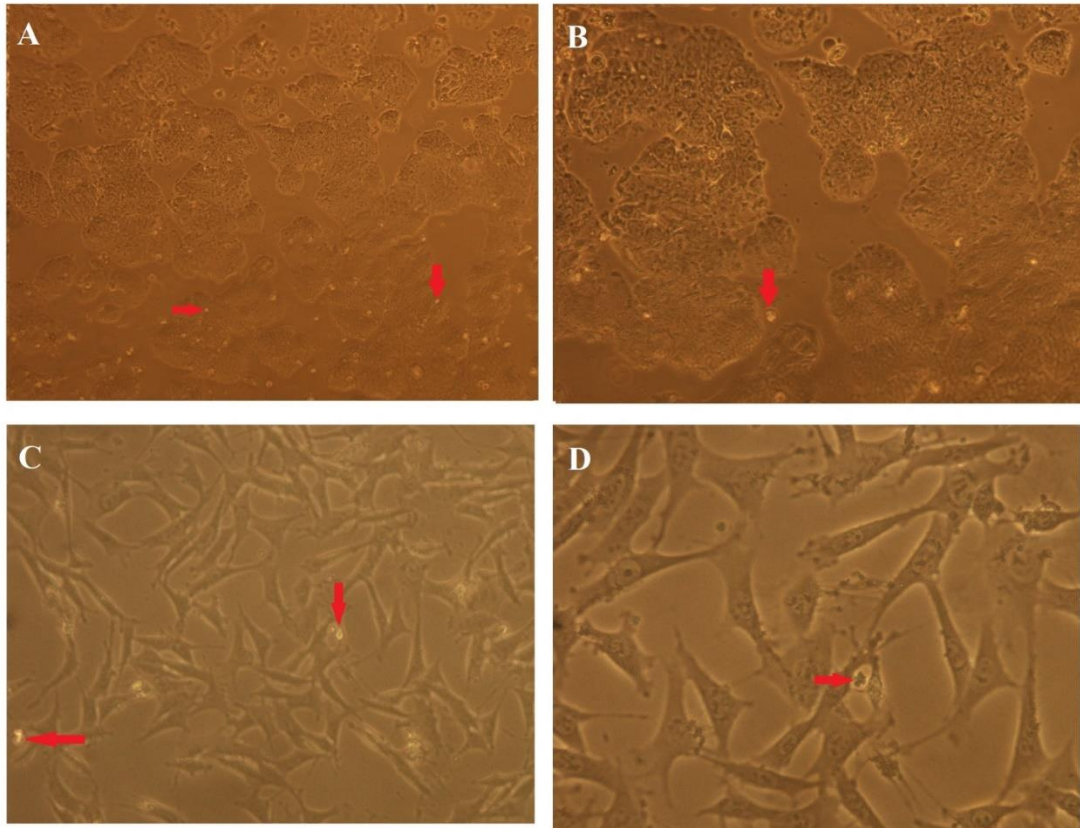


Figure 4.5 HT-29 cells (A,B) and MRC-5 cells (C,D) viewed under an inverted microscope under 20x and 40x magnification, respectively.

4.3.2 Mycoplasma detection

The HT-29 cells were checked for the presence of mycoplasma infection before performing the studies to exclude the possibility of data interferences. Figure 4.6 depicts cells stained with DAPI viewed under fluorescence microscope. The DAPI staining caused the cells to appear in blue and the image shows no mycoplasma.

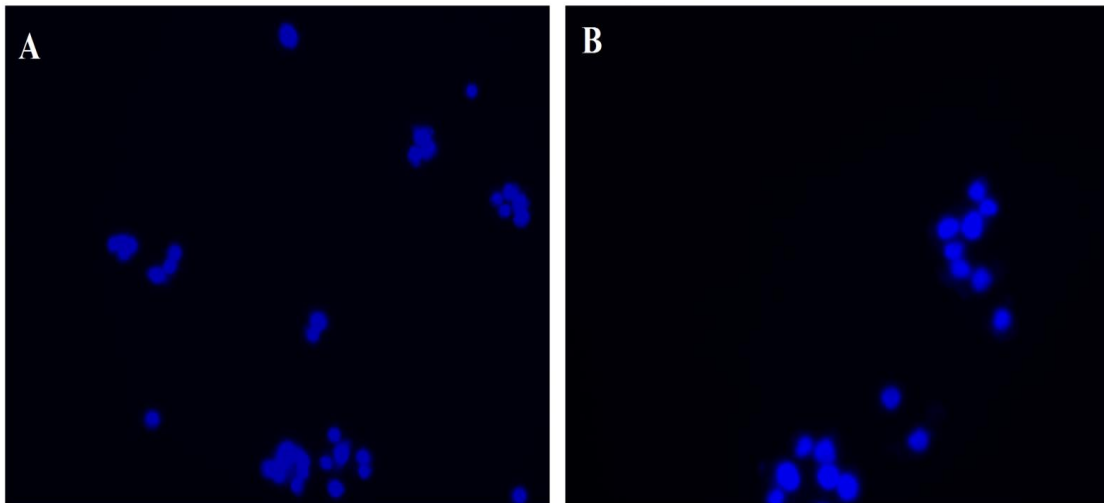


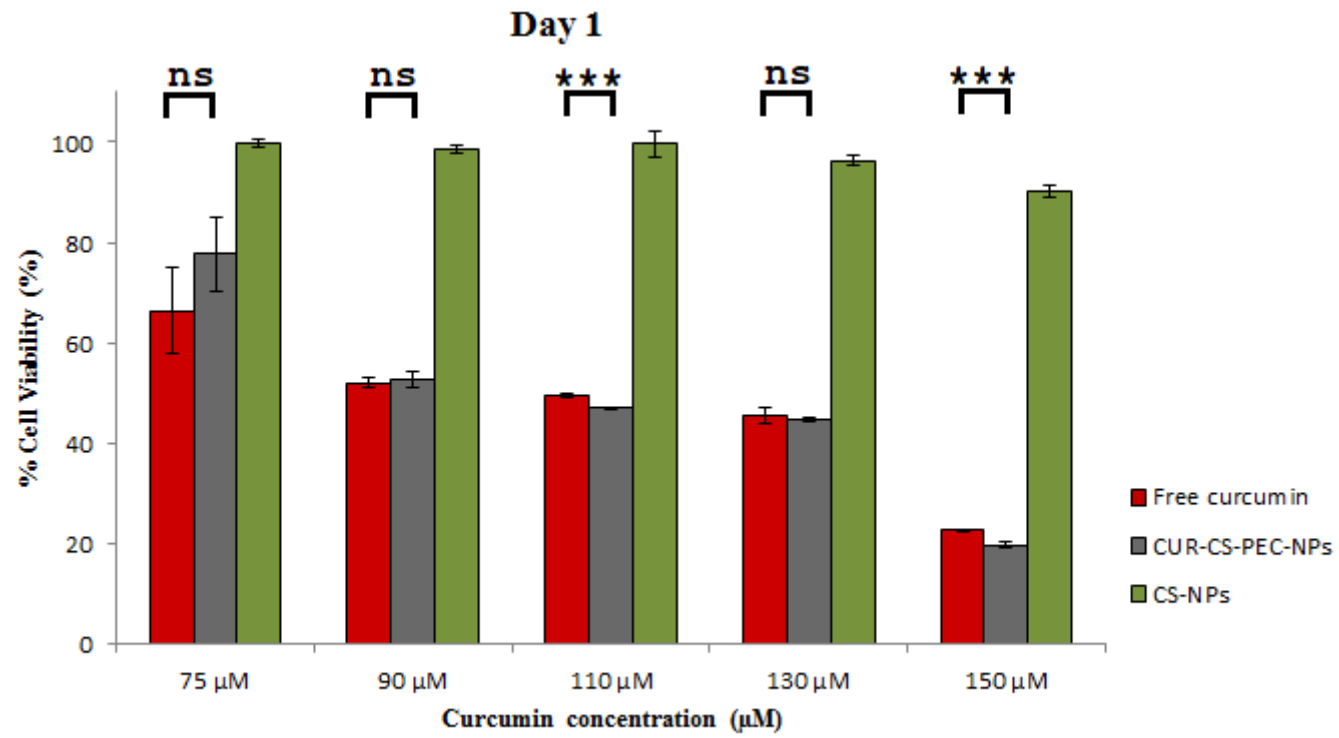
Figure 4.6 HT-29 cells viewed under fluorescence microscope with 430-495 nm filter under 20x (A) and 40x (B) magnification

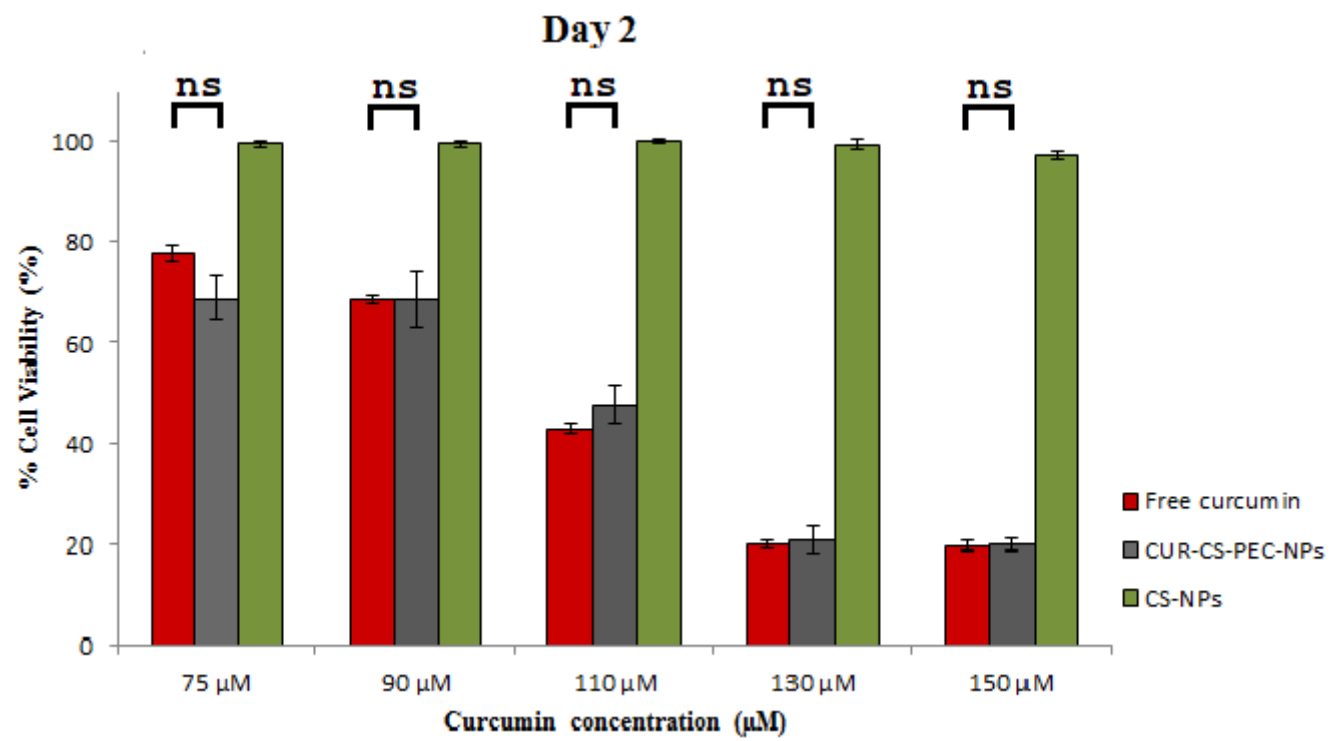
4.3.3 Cell viability assay

We performed the MTT assay to characterize the anticancer properties of CUR-CS-PEC-NPs using human colorectal carcinoma cells HT-29. To study the selectivity of the anti-cancer activity of CUR-CS-PEC-NPs we used normal human lung fibroblasts MRC-5. HT-29 cell lines were exposed to five different concentrations of CUR-CS-PEC-NPs (75-150 μM), besides equivalent concentrations of free CUR and CS-PEC-NPs. Whereas MRC-5 cells were exposed to the lowest and highest treatment concentration of CUR-CS-PEC-NPs (75 and 150 μM of CUR load respectively), in addition to equivalent concentrations of free CUR and weight of void NPs (CS-PEC-NPs). The anticancer activity was inversely related to % cell viability which was measured in comparison to untreated cells. In both cell lines, 15 μM 5-FU and DMSO respectively were used as positive and negative controls. Figure 4.7 shows that CUR-CS-PEC-NPs suppressed cell proliferation in a dose- and time- dependant manner at concentrations similar to that of free CUR. However, both CUR-CS-PEC-NPs and free CUR had negligible toxicity on MRC-5 (Figure 4.8) which confirms the selectivity of CUR-CS-PEC-NPs to HT-29 cells and this can be inferred to as selectively cancer cells.

In the HT-29 cells, increasing CUR-CS-PEC-NPs concentrations caused a significant decrease in % cell viability. Cells treated with 150 μ M showed less than 20% viability on days 1 and 2 and less than 12% on day 3, respectively. In contrast, 75 μ M treatments showed % cell viability of 68-77% on days 1 and 2, and 64% on day 3, respectively. On day 3 a significant decrease in cell viability was observed at all concentrations. The IC_{50} was 110 μ M on days 1 and 2, while it was 90 μ M on day 3.

As illustrated in Figure 4.7, there was an insignificant difference in % cell viability between and CUR-CS-PEC-NPs and CUR at all concentrations for the three days of study, except for concentrations 110 and 150 μ M on day 1 and 110 μ M on day 3. The CS-PEC-NPs aptly showed negligible toxicity against both HT-29 and MRC-5 cells, which confirms that the carrier matrix is non-toxic. In contrast, 5-FU showed % cell viability of 43.07% \pm 13.79, 52.45% \pm 1.64, and 15.31% \pm 3.59 against HT-29 cells on days 1, 2, and 3, respectively. Similar behaviour of 5-FU was observed against MRC-5 cells where % viability observed were 50.51% \pm 4.04, 38.06% \pm 6.35, and 30.51% \pm 2.11 on days 1, 2, and 3, respectively.





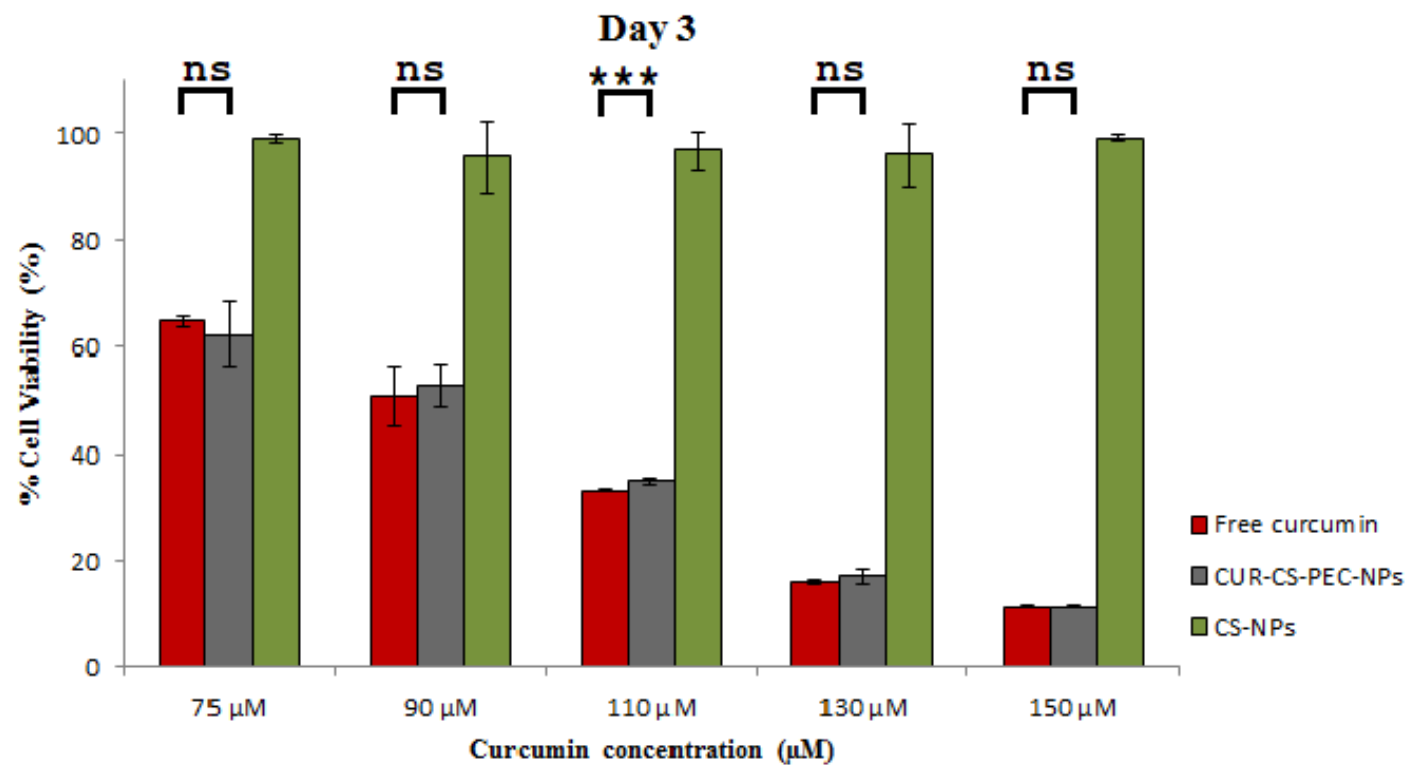
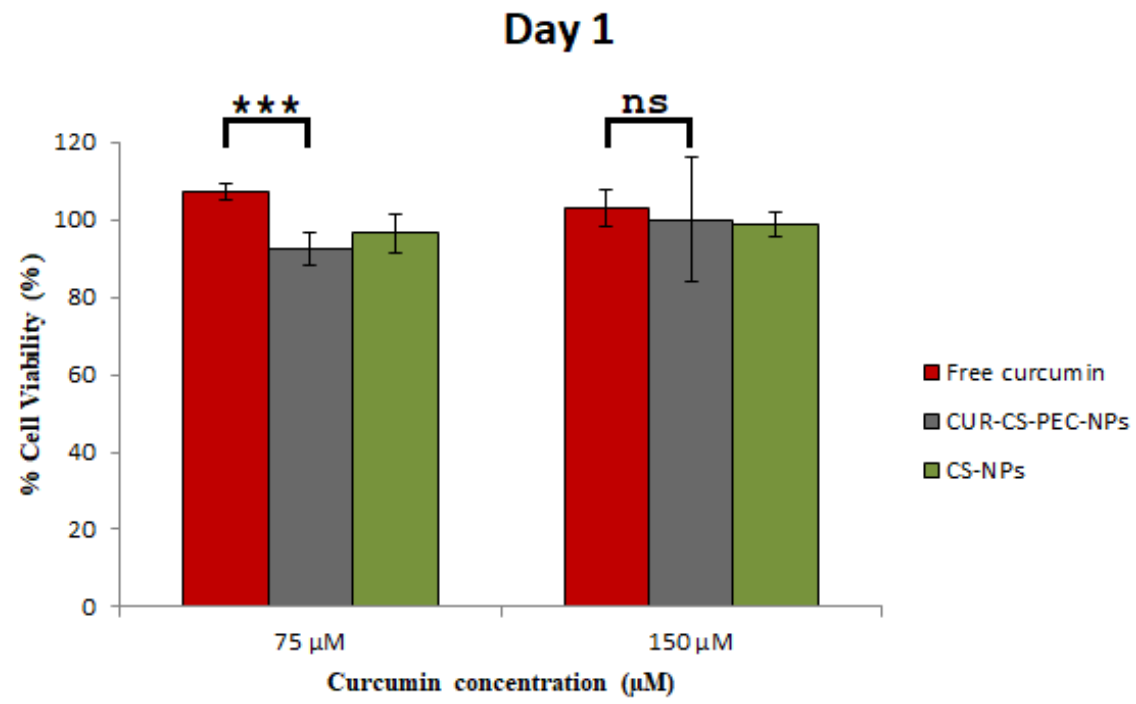
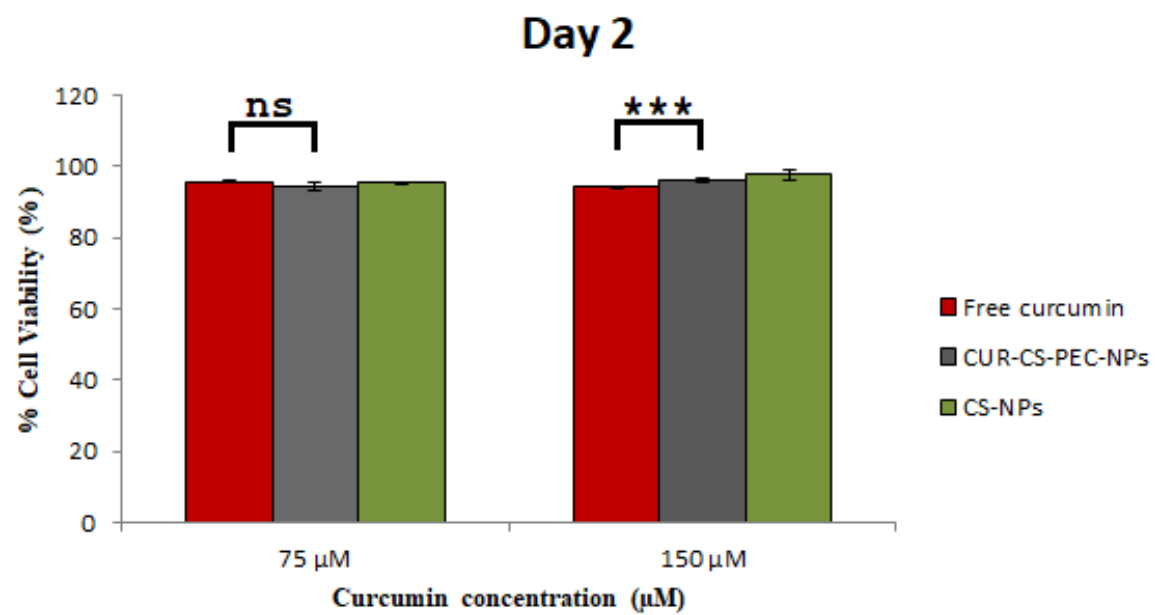


Figure 4.7 HT-29 cell viability after treatment with free CUR, void NPs (CS-PEC-NPs), and CUR-CS-PEC-NPs on days 1, 2, and 3 (ns: not significant; ***p<0.001), n=5





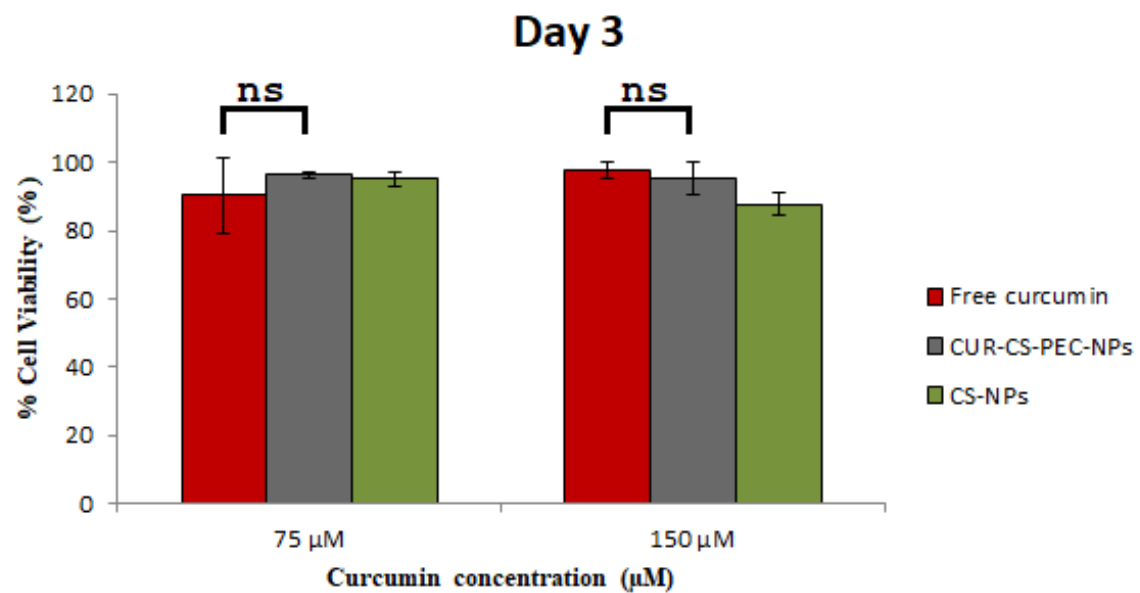


Figure 4.8 MRC-5 cell viability after treatment with free CUR, void NPs (CS-PEC-NPs), and CUR-CS-PEC-NPs on days 1, 2, and 3, n=5

CUR is highly sensitive and vulnerable to degradation. Hence, it is crucial to ascertain whether the anticancer properties were retained after fabrication as CUR-CS-PEC-NPs. Reports on encapsulated CUR in CS/poly(butyl cyanoacrylate) NPs (Duan *et al.*, 2010), PLGA NPs (Nair *et al.*, 2012), CS-g-poly(N-vinylcaprolactam) NPs (Rejinold *et al.*, 2011), β -cyclodextrin NPs (Kazemi-Lomedasht *et al.*, 2013), and sulphate-CS NPs (Anitha *et al.*, 2011) have shown at least similar anticancer activity of encapsulated CUR compared to free CUR. Similarly, the CUR-CS-PEC-NPs showed proportionate cytotoxic activity against HT-29 compared to free CUR, suggesting that the anticancer activity of CUR was not compromised during the nanoparticle fabrication process. On the contrary, both CUR and CUR-CS-PEC-NPs showed no signs of toxicity against MRC-5 cells, which confirms their selectivity towards tumour cells. The CUR uptake by tumour cells was favoured over normal cells not only due to the former being leakier and larger in size, but also due to differences in membrane structure and protein composition (Anitha *et al.*, 2011; Rejinold *et al.*, 2011; Kunwar *et al.*, 2008). The CS-PEC-NPs showed no toxicity against both HT-29 and MRC-5 cells, therefore, CS-PEC-NPs did not contribute to the cytotoxicity observed against HT-29 cells. We may also conclude that the carrier is safe and nontoxic to normal cells. The lack of cytotoxic behaviour of CS-NPs (Das *et al.*, 2010; Anitha *et al.*, 2011; Archana *et al.*, 2013), PEC-NPs (Zhang *et al.*, 2015), and CS-PEC-NPs (Luo & Wang, 2014; Maciel *et al.*, 2017) have also been previously reported.

4.3.4 Morphological changes of cells by CUR-CS-PEC-NPs

To study the induction of cellular apoptosis after the various treatments, cells were examined microscopically after DAPI staining. The morphology of cells treated with CS-PEC-NPs and DMSO (Figure 4.9, B-C), respectively, depicts no signs of hindrance to cell proliferation and similar cell colonies to those observed by control

cells (Figure 4.9A). In addition, no morphological changes to the nuclei was observed, remaining spherical and shiny. This indicates that DMSO and CS-PEC-NPs do not induce apoptosis to HT-29 cells. In contrast, cells treated with equivalent high and low concentrations of CUR-CS-PEC-NPs and free CUR, as well as 15 μ M 5-FU showed significant changes in nuclear morphology (Figure 4.9, D-H), respectively. Apparently, there were internal deflection, fragmentation, formation of irregular edges around the nuclei. Furthermore, the cell membrane looked serrated in this treatment group, suggesting that the apoptotic effects of CUR-CS-PEC-NPs, free CUR and 15 μ M 5-FU were manifested in a similar manner.

Bisht *et al.*, (2011) encapsulated CUR in polymeric NPs using N-isopropylacrylamide (NIPAAAM), vinylpyrrolidone (VP), and acrylic acid (AA). The capability of free CUR and CUR-polymeric NPs to induce stellate cell apoptosis after morphological examination of the nucleus showed that the fragmentation of the nucleus was dose-dependent. Tang *et al.*, (2010) developed CUR-polymeric conjugates as anticancer agent. The cellular apoptotic effects were studied against SKOV-3 and OVCAR-3 ovarian cancer cells and MCF-7 breast cancer cells. The nucleolus fluorescence images obtained by DAPI staining showed significant apoptosis and only few cells survived at the end of the study. Chang *et al.*, (2013) fabricated a water soluble CUR-PLGA NPs for cancer treatment. They studied the anticancer effects of CUR-PLGA-NPs against human oral cancer, CAL27-cisplatin resistant (CAR) cells. Compared to untreated (control) cells, cells treated with CUR-PLGA-NPs showed apoptotic morphological features such as internucleosomal fragmentation under fluorescence microscopy. We may conclude that data from the above studies strongly confirms the apoptotic effects CUR is not markedly changed when fabricated in a suitable nanoformulation.

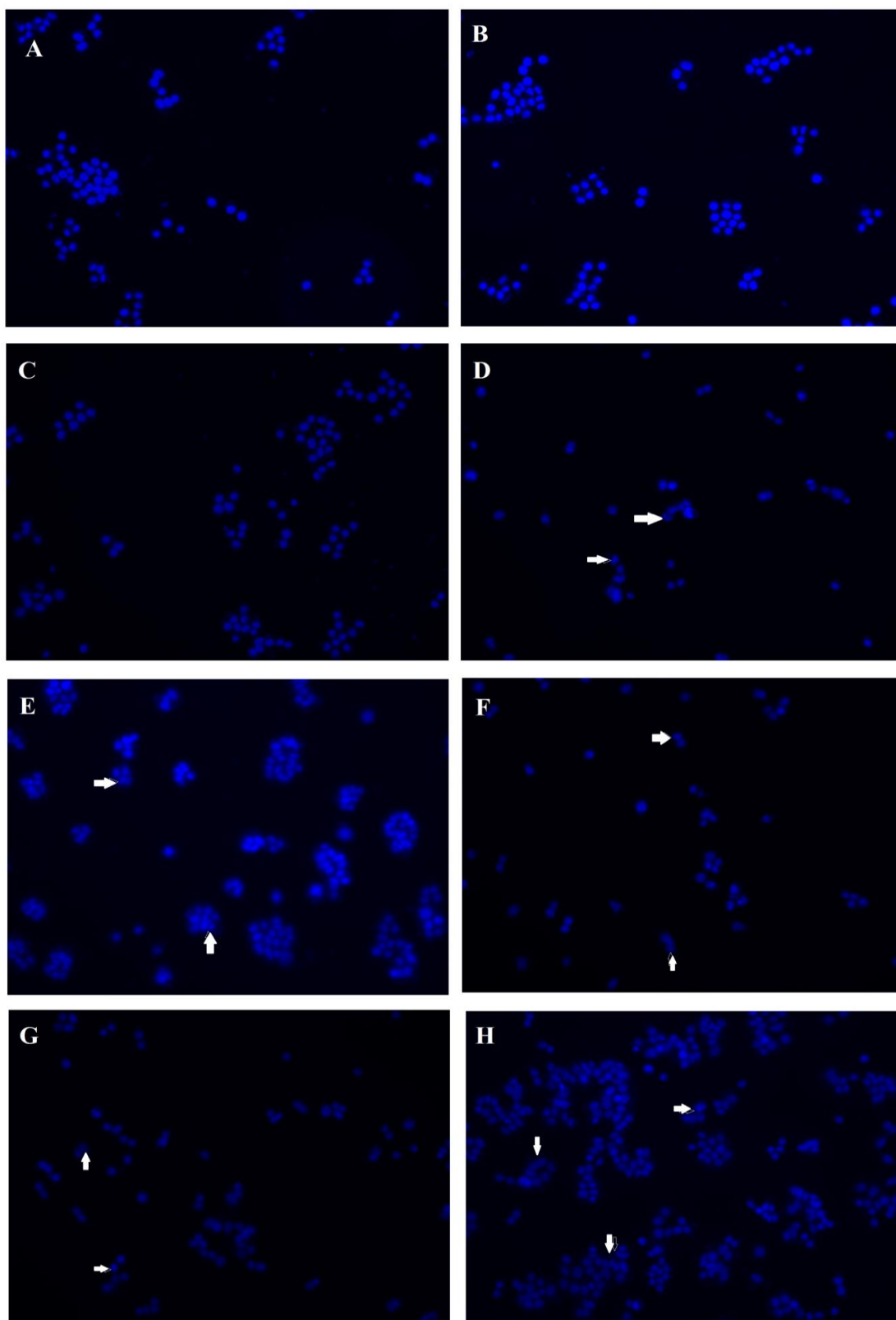


Figure 4.9 Fluorescent nuclear images of untreated cells (A), cells treated with CS-PEC-NPs (B), DMSO (C), 75 μM (D) and 150 μM (E) of CUR-CS-PEC-NPs, 75 μM (F) and 150 μM (G) of free CUR, and (H) 15 μM of 5-FU. Arrows indicate fragmentation and formation of irregular edges around the nuclei

4.3.5 Cellular uptake

Cellular uptake studies are vital in ascertaining the ability of the anticancer formulation to target cells. Capitalizing the photochemical properties of CUR, fluorescence spectroscopy was used to qualitatively evaluate the HT-29 cellular uptake of free CUR and CUR-CS-PEC-NPs. As illustrated in Figure 4.10, untreated cells and CS-PEC-NPs fluorescence images were captured as controls. Images of the cells were taken at 24-hr intervals for 72 hr. Control fluorescent microscopy images seemed dark due to the absence of fluorescence. At low CUR concentration (75 μM) both free CUR and CUR-CS-PEC-NPs, showed moderate fluorescence intensity on day 1. However, the fluorescence intensity of free CUR rapidly decreased with time that it almost diminished on day 3. However, fluorescence intensity of CUR-CS-PEC-NPs, although faint, yet was more visible on days 2 and 3. This could mean that CUR-CS-PEC-NPs are more efficiently assimilated by the cells than free CUR at this concentration. This outcome explains the higher cytotoxicity of CUR-CS-PEC-NPs compared to free CUR at low concentrations on days 2 and 3 (as discussed in section 4.3.3). At both concentrations, CUR gives a green fluorescence from the entire cells which indicates cellular internalization rather than adhesion to the surface of the cells (Ha *et al.*, 2012). Previous studies reported that CS formulated NPs distribute in the whole cells via several discrete pathways (Yun *et al.*, 2009). The results summed up above are in concert with previous reports that indicate that encapsulating CUR in nanocarriers enhances its cellular uptake and subsequent properties (Aseh & Ríos, 2009; Liu *et al.*, 2012). In contrast, on day 1 of high CUR concentration (150 μM) treatment, both free CUR and CUR-CS-PEC-NPs showed highly intensive fluorescence at similar extent. However, the fluorescence intensity decreased gradually on the subsequent days, even though still visible.

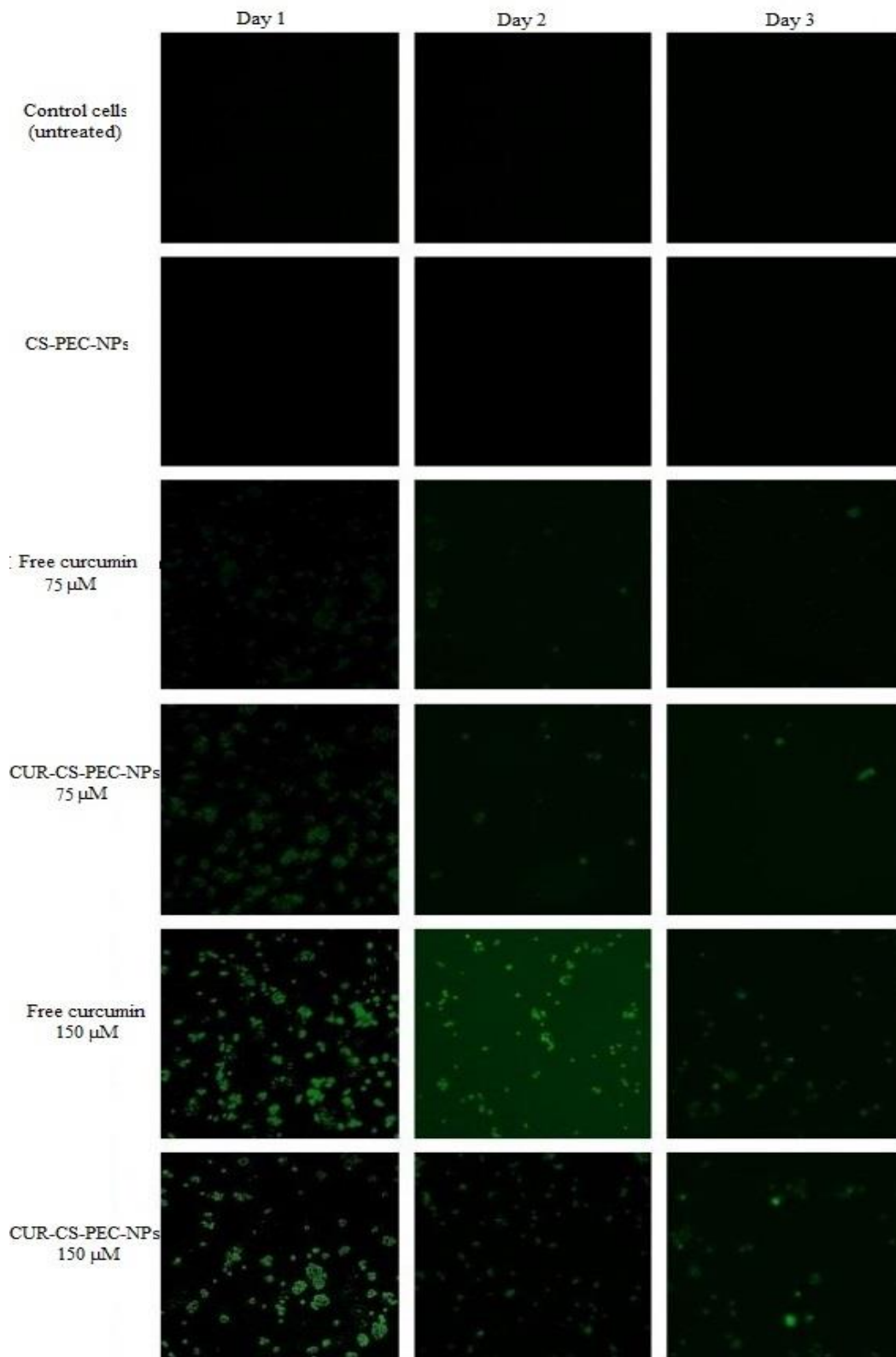


Figure 4.10 Fluorescence microscopy imaging of the cellular uptake of CUR from high and low equivalent doses of CUR-CS-PEC-NPs and free CUR on days 1, 2, and 3. (20x magnification).

Quantitative analyses of CUR after cellular uptake were performed spectroscopically by determining the CUR concentration from the lysed cells. Figure 4.11 shows that CUR cellular uptake was highest on day 1 followed by gradual decrease in the subsequent days. The findings of the cytotoxicity and qualitative cellular uptake studies indicated that CUR uptake by the HT-29 cells was higher from CUR-CS-PEC-NPs compared to free CUR at low concentration (75 μ M) on days 2 and 3. This could be attributed to the mucoadhesive properties of CUR-CS-PEC-NPs which promoted extended contact time with the cells with subsequent release and uptake of CUR at this low concentration. There is also the possibility that intact CUR-CS-PEC-NPs were taken up as well. However, this mucoadhesive advantage was insignificant at high CUR-CS-PEC-NPs concentration which could be diminished due to the high available concentration of CUR. The quantitative cellular uptake showed similar data compared to the qualitative cellular uptake findings.

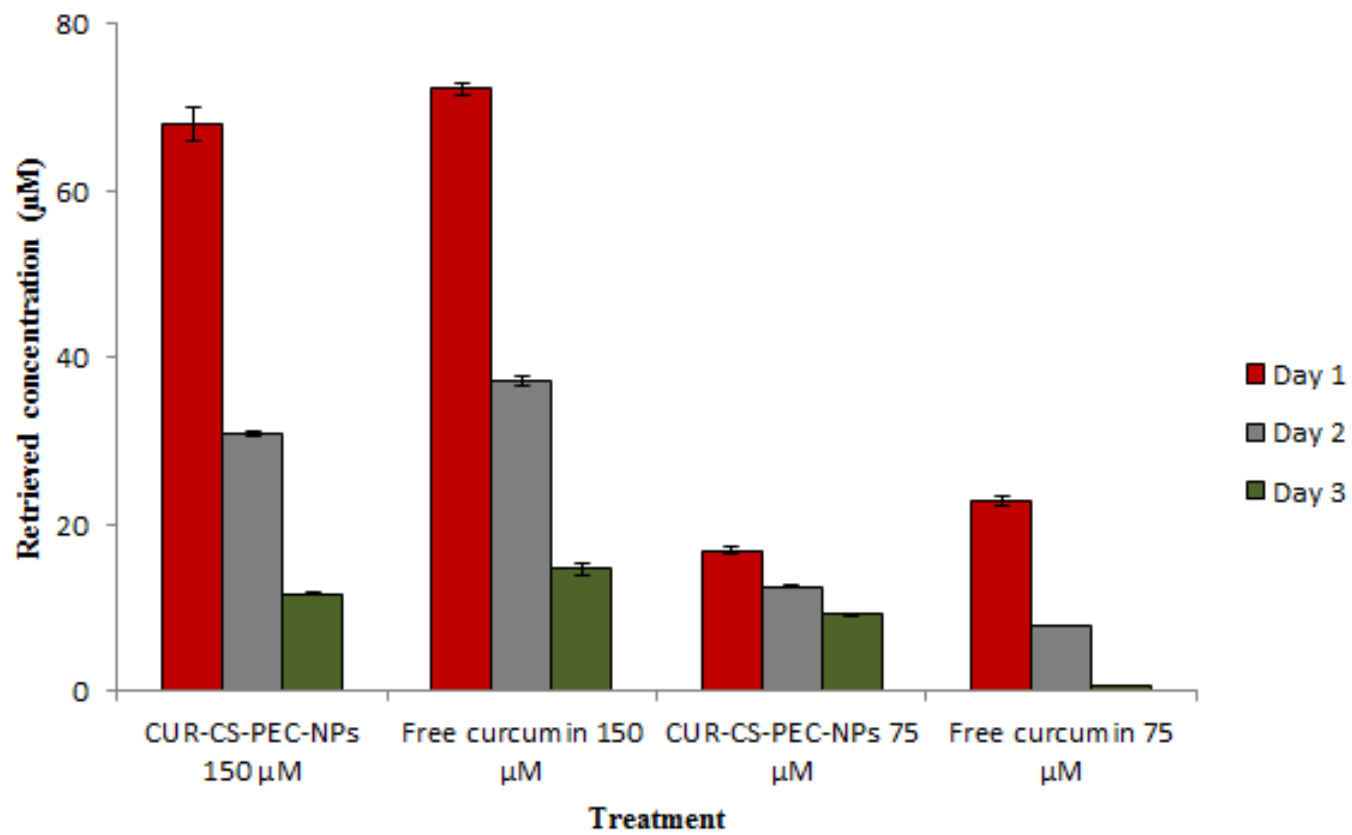


Figure 4.11 Retrieved CUR after treatment with high and low doses of free CUR and CUR-CS-PEC-NPs on days 1, 2, and 3, n=3

NPs can be internalized within the cells via several pathways including direct penetration (Gref *et al.*, 2000), endocytosis, enterocytosis (Jiang *et al.*, 2008), micropinocytosis, and receptor mediated endocytosis (RME) (Alkilany & Murphy, 2010). NPs within the size range of 20-50nm are mostly taken up by nanophagocytosis, whereas nanoparticle in the range of 100-200nm are preferentially taken up by enterocytes (Froehlich, 2016).

Several physico-chemical properties such as particle size, molecular weight, particles shape (Nam *et al.*, 2009), solubility, and surface functionality (He *et al.*, 2010) affect the cellular uptake and intracellular trafficking of the NPs. In addition, the structural influence of the cell type also plays a role in cellular uptake (Nam *et al.*, 2009). For example, small and uniformly sized NPs have better cellular uptake compared to larger particles (Nam *et al.*, 2009). The surface properties of the NPs play major role in their uptake as hydrophobic and positively charged NPs show better cellular uptake (Sanjeeb *et al.*, 2002).

In the present formulation, the small size of the CUR-CS-PEC-NPs, its spherical shape and positive surface charge contributed to the high cellular uptake observed since these factors are crucial to and promote uptake into cells. Consequently, high concentrations of CUR-CS-PEC-NPs led to better cellular uptake of CUR by the HT-29 cells. However, the mucoadhesive properties of CUR-CS-PEC-NPs influenced the cellular uptake of the low initial CUR concentration, whereas at high initial CUR concentrations, the high availability of CUR had the dominant effect in the cellular uptake rather than the mucoadhesion effects. The time-dependant decrease in cellular uptake could be attributed to the degradation of CUR into smaller molecules such as trans-6-(4-hydroxy-3-methoxyphenyl)-2,4-dioxo-5-hexenal, ferulic acid, feruloy methane, and vanillin which lack the auto-fluorescence properties of CUR (Ha *et al.*,

2012) or to the efflux of CUR from the cells with time (Mulik *et al.*, 2010). At low CUR concentration treatment at days 2 and 3, higher cellular uptake of CUR-CS-PEC-NPs was obtained compared to free CUR. This could be attributed to the mucoadhesion of the NPs and to the slow release of CUR from CUR-CS-PEC-NPs, similar results were obtained by Mohanty & Sahoo, (2010) where they have reported higher cellular uptake of CUR-nanoformulation compared to free CUR at low concentrations by different tumour cells. On the other hand, both CUR and CUR-CS-PEC-NPs presented similar cellular uptake behaviour at high CUR concentration, particularly, 67.97 ± 2.09 , 30.81 ± 0.30 , and 11.64 ± 0.05 for CUR-CS-PEC-NPs, and 72.21 ± 0.79 , 37.11 ± 0.66 , and 14.64 ± 0.69 for free CUR, on days 1, 2, and 3, respectively. However, CUR-CS-PEC-NPs have the added advantage of better assimilation in the cell, hence likely to result in better bioavailability at the target site than free CUR.

4.4 Conclusion

In summary, the antiproliferative effects and cellular uptake of CUR was demonstrated upon encapsulation in CUR-CS-PEC-NPs. In fact, the uptake was enhanced after encapsulation, especially at lower concentrations. Morphological examination of nuclei confirmed the apoptotic properties of CUR-CS-PEC-NPs. Thus far, the preceding chapters have indicated that the CUR-CS-PEC-NPs have the property of retaining their integrity when exposed to acid and alkaline milieu and release only a minimal percentage of CUR. They have also demonstrable mucoadhesive properties and release CUR more favourably in the colonic media. More importantly, the CUR-CS-PEC-NPs have demonstrable apoptotic properties comparable to that of pure CUR. On the basis of these findings, we are primed to perform an *in vivo* study using animal models in order to assess the bioavailability and prove the concept, to be discussed in chapter 5.

Chapter 5

Development and Validation of a HPLC Method and Pharmacokinetic Studies on CUR-CS-PEC-NPs

5 Development and Validation of a HPLC method and pharmacokinetic studies on CUR-CS-PEC-NPs

5.1 Introduction

5.1.1 HPLC method development and validation

HPLC is an advanced form of liquid chromatography and it is one of the most commonly used analytical techniques in new drugs and formulations development. HPLC developed analytical method should be simple, utilizes the most common stationary phases and MP, and preferably uses binary MP rather than tertiary or quaternary MP (Shabir, 2004).

The development of an HPLC analytical method comprises of the following steps: Step 1, selection of the preliminary HPLC method and the initial system based on the data available in the literature for the particular analyte (Shabir, 2004). In this step, the basic parameters are chosen, such as sample preparation, mode of chromatographic separation, type of elution (gradient/ isotonic) and type of the detector (Guidlines, 2017). Step 2 entails the selection of chromatographic conditions to retain all analytes, such as the MP strength and the flow rate (Shabir, 2004). Step 3 aims to achieve the best resolution and minimum run time, hence parameters such as column dimensions, packing particle size, run time, and flow rate are optimized in this step (Guidlines, 2017). The final step, step 4, is the method validation which is performed to ascertain the reliability and reproducibility of the analytical method (Shabir, 2004; WHO, 2017).

The extent of the method validation depends on both the purpose of the analysis and to whether the HPLC method was completely developed or slightly modified from a previously validated method (WHO, 2017). Quantitative analytical methods are

validated against several parameters such as specificity, precision, linearity, accuracy, and the limit of detection (UNODC, 2009). The internal standard (IS) is commonly used in analytical methods where it is added in constant volume to both the calibration standards and samples (SW846, 2003). The calibration curve employs the ratio response of the analyte to the IS plotted against their concentrations (Dolan, 2012).

The IS is usually used in methods where multiple sample preparation steps is required and volume recovery at each step may vary (Dolan, 2012). The purposes behind using IS are to minimize the volume variations introduced into the chromatography system and minimize the response variations of the chromatography system, thus, enhancing the accuracy of the analytical method (Dolan, 2012; SW846, 2003). IS used in an analytical method should never be expected to be found in analytical samples, must be available in pure form, responsive to analytical method, have structural resemblance to the analytes, and, ideally, eluted after the analyte (Dolan, 2012; SW846, 2003).

5.1.2 *In vivo* pharmacokinetics studies

As discussed in chapter 1, CUR possesses a variety of therapeutic activities, including anticancer activities. However, its therapeutic usefulness is restricted due to low water solubility (Yallapu *et al.*, 2010), extensive intestinal and hepatic metabolism, and rapid clearance, all of which results in poor bioavailability following oral administration (Cheng *et al.*, 2013). Therefore, research has been focused on encapsulating CUR in delivery systems such as polymeric NPs (Gupta *et al.*, 2009) with a view to addressing some of the above constraints. In general, drug delivery systems developed for enhancing the oral bioavailability of drugs, particularly hydrophobic

drugs, are evaluated through studying the pharmacokinetics behaviour of the respective drugs using animal models (Sjödin *et al.*, 2011; Wan *et al.*, 2012).

Sulphasalazine (SSZ), an anti-inflammatory agent, is composed of sulphapyridine (SP) and 5-aminosalicylic acid (5-ASA) with diazo bond linkage. Following oral administration of SSZ, a small amount of the drug is absorbed in the small intestine, whereas the majority of the dose is hydrolysed by the colonic microflora into SP and 5-ASA, where the former is completely absorbed in the colon (Gu *et al.*, 2011). Thus, SSZ has been used as a marker drug for studying the oro-caecal transit times of dosage forms (Wong & Yuen, 2001; Björnsson & Olsson, 2005; Sunesen *et al.*, 2005).

In pharmacokinetics and *in vivo* investigations, it is usually imperative to perform a pilot study on a limited number of animal models before transposing and/or fine-tuning to the study proper. It allows us to test the feasibility of methods and procedures to be used on a larger scale (Thabane *et al.*, 2010). Pilot studies can be used to assess study procedures, estimate sampling rates, and determine study parameters, among others. In pharmacological studies, it is referred to “proof of concept” studies. Essentially, pilot studies are followed by a full and larger study to obtain clinically relevant data (Arain *et al.*, 2010).

5.1.3 Aims and objectives

The CUR-CS-PEC-NPs were successfully formulated, characterized and studied with regard to *in vitro* release and mucoadhesion in Chapters 2 and 3. The anti-proliferative activities and cellular uptake of the CUR-CS-PEC-NPs were further discussed in chapter 4. The data obtained so far indicates that the CUR-CS-PEC-NPs are mucoadhesive, especially in the colonic milieu whilst the physical integrity of the

particles are retained in the upper GIT. Furthermore, there is evidence that the CUR is released in colonic conditions. To investigate this hypothesis, a pilot study using rats as animal model was performed and the data obtained is discussed in detail henceforth.

Pharmacokinetic investigations rely on a credible analytical procedure able to detect plasma concentrations of drugs being analysed. Consequently, the work in this chapter was divided into two parts; i) development and validation of HPLC analytical methods for the quantitative determination of CUR and SP in plasma and ii) pharmacokinetic studies of CUR-CS-PEC-NPs and SSZ-CS-PEC-NPs on animal models.

5.2 Materials and methods

5.2.1 Materials

Material	Supplier
CUR-CS-PEC-NPs	Prepared as described in chapter 2
Curcumin analytical standard	Fluka, USA
Acetonitrile (HPLC grade)	RCI Labscan, Thailand
Methanol (HPLC grade)	RCI Labscan, Thailand
Glacial acetic acid	R&M chemicals, UK
Sodium acetate trihydrate	NacalaiTesque, Japan
Sulphapyridine	Tokyo Chemical Industry, Japan
Piroxicam	NacalaiTesque, Japan
17- β estradiol	NacalaiTesque, Japan
Absolute ethanol	R&M chemicals, UK
Theophylline	R&M chemicals, UK
Sulphasalazine	Tokyo Chemical Industry, Japan

5.2.2 HPLC methods development and validation

5.2.2.1 HPLC instrumentation and conditions

The HPLC system comprised of a Series 200 pump, Perkin Elmer, USA equipped with UV/Vis detector (Series 200 UV/Vis detector, Perkin Elmer, USA). The stationary phase used was a RP-column ZORBAX Eclipse Plus[®] (C18, 250mm x 4.6 mm, 5 µm), (Agilent, USA) for both the analysis of CUR and SP.

For the CUR analyses, the method described by Heath *et al.* (2003) was adopted with slight modifications as follows: a 1 L MP was prepared by adding 410 ml of acetonitrile, 360 ml of water, 230 ml of methanol, and 10 ml of glacial acetic acid. The resulting mixture was vacuum filtered through 0.2 µm filter paper, thrice and run at rate of 1 ml/min on the HPLC system. The sample volume was 50 µl and the detector set at 425 nm. A 20.0 µg/ml 17-β-estradiol (EST) solution in methanol was used as the IS and deproteinising agent for the plasma samples and simultaneously detected at 262 nm.

For SP analyses, the MP comprised of 80% of acetate buffer (pH 4) and 20% Acetonitrile. Acetate buffer was prepared by mixing 847 ml of 0.1 M acetic acid and 153 ml of 0.1 M sodium acetate trihydrate (Amekyeh, 2016), the resulting mixture was then vacuum filtered with 0.2 µm filter paper, thrice. The MP was run at 1.2 ml/min and 30 µl of the sample was injected with the detector set at 260 nm. A 5 µg/ml theophylline (TP) solution in methanol was used as IS and detected at the same wavelength. The IS solution was also used as the deproteinising agent for these plasma samples.

5.2.2.2 *Plasma standards*

Stock plasma solutions containing CUR and SP at 50 µg/ml and 40 µg/ml, respectively, were prepared by spiking the appropriate amounts of the drugs solutions into appropriate volumes of the human plasma. The stock solutions were subsequently diluted with blank human plasma to prepare the calibration standards for each drug. For methods validation, three concentrations of each drug representing low (LC), mid (MC), and high (HC) concentrations. The LC, MC, HC for CUR were 0.03, 0.3, and 10 µg/ml, and for SP 0.1, 0.5, and 20 µg/ml, respectively.

5.2.2.3 *Plasma sample preparation*

The plasma samples for validation analyses were prepared by transferring 100 µl of drug-spiked plasma and 150 µl of the IS solution into microcentrifuge tubes. The tubes were vortex mixed for 2 min. and then centrifuged at 14000 rpm for 10 min. The clear supernatants were aspirated and filtered using 0.20 µm syringe filter and directly injected onto the HPLC system.

5.2.2.4 *Specificity*

The specificities of the analytical methods were based on individual observation of the chromatograms obtained for the analytes and IS prepared in appropriate solvents. A further test of specificity was based on a run of drug-free plasma and observation of the resulting chromatograms for any interferences at the retention time of the analytes or their respective IS. Finally, analytes and IS were spiked separately in plasma and their chromatographs were visually observed as before. The specificity studies are crucial in excluding peak interferences from the plasma, ascertaining that the analytes elute similarly as pure drug solutions or spiked in plasma, and that the elution of the analyte is not affected by the IS or *vice versa*.

5.2.2.5 *Linearity and range*

The calibration curves for CUR and SP in drug-spiked plasma were obtained over the following concentration ranges: 0.05-10 µg/ml and 0.1-20 µg/ml, respectively. The calibration curves comprised of the ratio of the peak signal of each analyte to that of the respective IS, plotted against the respective concentration. Each analysis response represents the mean of five separate runs.

5.2.2.6 *Precision*

The intra-day and inter-day precision of the analyses at the three validation concentrations for each drug was determined as the reproducibility and repeatability of the developed methods. The percentage coefficient of variation (%CV) was used as the mean value of five independent runs at each concentration and calculated as follows:

$$\%CV = \frac{\text{Standard deviation (SD)}}{\text{Mean concentration}} \times 100\% \quad \text{Eq. 5.1}$$

5.2.2.7 *Accuracy*

The intra-day and inter-day accuracy of the analysis at the three validation concentrations for each drug was determined to study the reliability of the results obtained from the developed method. The relative error was used as the mean value of five independent runs at each concentration and calculated as follows:

$$\text{Relative error} = \frac{\text{mean measured concentration} - \text{true concentration}}{\text{True concentration}} \times 100\% \quad \text{Eq. 5.2}$$

5.2.2.8 *Recovery*

Retrieving CUR and SP from plasma samples after the extraction procedure was investigated by comparing the peak signal of each drug at the three validation concentrations from the spiked plasma samples with those obtained from pure drug

solutions in respective solvent. The data was presented as % recovery and calculated as follows (n=5):

$$\% \text{ Recovery} = \frac{\text{Mean concentration of drug in spiked plasma}}{\text{Mean concentration of pure drug solution}} \times 100\% \quad \text{Eq. 5.3}$$

5.2.2.9 Limits of detection and quantification

The sensitivity of the developed methods were assessed in terms of LOD and LOQ and were determined by employing the lowest concentration of each analyte (LC) and calculated as follows:

$$\text{LOD} = \frac{3 \times \text{SD of the LC}}{\text{Slope of the calibration curve}} \quad \text{Eq. 5.4}$$

$$\text{LOQ} = \frac{10 \times \text{SD of the LC}}{\text{Slope of the calibration curve}} \quad \text{Eq. 5.5}$$

5.2.3 In vivo Study

5.2.3.1 Preparation of CUR-CS-PEC-NPs and SSZ-CS-PEC-NPs

CUR-CS-PEC-NPs were prepared as discussed in section 2.2.2.2. SSZ-CS-PEC-NPs were formulated using the same procedure, however, by using the same amount of SSZ instead of CUR.

5.2.3.2 Animals

Pharmacokinetic studies on CUR and SSZ after oral administration of CUR-CS-PEC-NPs and SSZ-CS-PEC-NPs were conducted on male Sprague-dawley rats (250 g) with prior approval by AWERB, University of Nottingham, UK, approval reference number UNMC7. The animal studies were conducted according to the requirements of the UK Animals (Scientific Procedures) Act 1986 (ASPA) draft Code of Practice for the care and accommodation of animals (February 2013) and carried out

by competent technicians. The rats were obtained from the animal holding unit of University of Science, Malaysia, Penang. The animals were acclimatized 7 days prior to the experiment under standard conditions of temperature, humidity, and light with free access to food and water. The animals were fasted overnight (12 hr). After PO treatment, water and food were allowed at 2 and 4 hr, respectively.

5.2.3.3 Procedural care of the rats

The rats were allowed to move freely in their respective cages throughout the study period. However, they were restricted in metabolic cages during the blood sampling periods. The amount and rate of samplings were limited to decrease the discomfort. The tail end of each rat was clipped only once during the initial blood sampling time. After each sampling time, the wounded tails were swabbed with cotton wool rinsed with 70% alcohol to reduce infections. Wounds were monitored for bleeding after each sampling. Water and food supply were resumed after 2 and 4 hr post-administration, respectively. At the end of the study, the rats were humanely sacrificed.

5.2.3.4 Pharmacokinetics studies

Pharmacokinetic studies were carried out to proof the concept of the colon-specific delivery of CUR in CUR-CS-PEC-NPs. Sprague-dawley rats were randomly divided into three groups (n=4) receiving CUR-CS-PEC-NPs, SSZ-CS-PEC-NPs, and free CUR containing equivalent amount of drug (10 mg/kg body weight). Treatments were administered orally in 2 ml suspensions. Under topical anaesthesia, about 500 μ l of blood sample were collected at predetermined time intervals (0, 1, 2, 4, 6, 8, 12, and 24 hr) from the tail into heparinized microcentrifuge tubes. The blood samples were centrifuged upon collection at 14000 rpm for 10 min. and the supernatant was aspirated

and stored at -80°C until use. CUR and SP concentration in the supernatant were determined by HPLC methods developed in sections 5.3.2.1 and 5.3.2.2, respectively.

5.2.3.5 Data and statistical analyses

Pharmacokinetic parameters were calculated using standard model-independent pharmacokinetic formulas. The obtained plasma concentrations (ng/ml) were plotted against their respective times and the resulting curves were used to obtain the peak plasma concentration (C_{max}), time of occurrence (T_{max}), and elimination half-life ($t_{1/2}$) which was calculated as $0.693/K_{el}$. The extent of drug absorption was measured by calculating the area under the plasma drug concentration time curve (AUC) which was calculated using log trapezoidal rule using GraphPad® Prism 5 software. Absorption rate (K_a), elimination rate (K_{el}) as well as the statistical analysis were calculated using GraphPad® Prism 5 software. Statistical analyses were performed using the student's t-test where p values less than 0.01 and 0.001 are deemed as statistically significant and very statistically significant, respectively.

5.3 Results and Discussion

5.3.1 Selection of the internal standard

As discussed in section 5.1, the IS should ideally have similar solubility and chromatographic behaviour as the analyte (Dolan, 2012). In this regard, the IS should have close structural properties as the analyte. The used HPLC system (Series 200, Perkin Elmer, USA) provides simultaneous multi-wavelength detection, thus, detection of the IS at the same wavelength as the analyte was not necessary in this study.

5.3.1.1 Internal standard for CUR analysis method

IS that have been used in HPLC analyses for CUR include emodin (Han *et al.*, 2011; Sun *et al.*, 2013), 4-hydroxybenzophenone (Ma *et al.*, 2007), tetra-(m-

hydrophonyl)-chlorine (Ireson *et al.*, 2001), and EST (Heath *et al.*, 2003a; Pak *et al.*, 2003; Yu & Huang, 2012). Since EST was the most commonly used IS and readily available, it was chosen as the IS for this procedure.

Figure 5.1 shows a representative chromatogram of a solution containing 20 $\mu\text{g/ml}$ of CUR and 10 $\mu\text{g/ml}$ of EST as IS, detected at 262 nm. The retention times obtained were 6.4 and 9.4 for EST and CUR, respectively. Independent runs of EST and CUR were performed to assign the respective peaks. The chromatogram clearly shows a fairly symmetric and sharp peak of EST using the preliminary HPLC analytical method of CUR, however, optimization of the analytical method was necessary and will be discussed in section 5.3.2.

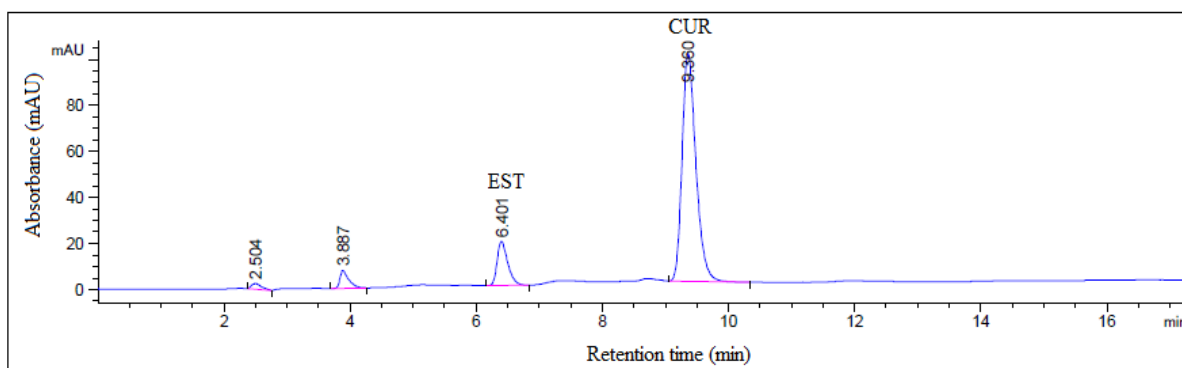


Figure 5.1 Chromatogram for EST (10 $\mu\text{g/ml}$) and CUR (20 $\mu\text{g/ml}$)

5.3.1.2 Internal standard for SP analyses method

IS that have been used in HPLC analysis of SP include benzamide (Chungi *et al.*, 1989), caffeine (CAF) (Kasprzyk-Hordern *et al.*, 2007; Tolika *et al.*, 2011), sulfamethizole (Maudens *et al.*, 2004), piroxicam (PIR) (Amekyeh *et al.*, 2015), and dimenhydrinate (Gu *et al.*, 2011). Amongst all, CAF and PIR were readily available and known for their simple detection with intense peak response (Tolika *et al.*, 2011; Amekyeh, 2016). TP, up to our knowledge, has never been used as IS for SP analysis.

However, it is commonly used as IS in analytical methods, easily dissolved and detected, inexpensive, readily available (Fitzpatrick & McClelland, 1983; Marten *et al.*, 2017), can be detected in short time using readily available MP (Charehsaz *et al.*, 2014), and, most importantly, its chemical structure resembles that of SP (Figure 5.2). Therefore, CAF, PIR, and TP were initially selected as IS for this analytical method.

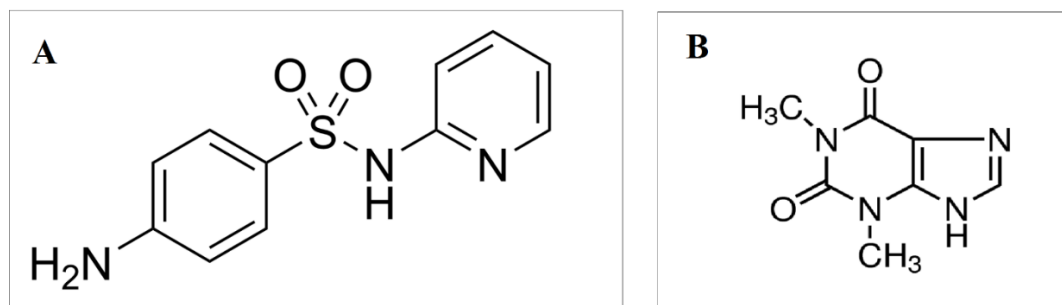


Figure 5.2 Chemical structures of SP (A) and TP (B) (*obtained from www.sigma-aldrich.com*)

Figure 5.3 shows representative chromatograms for CAF (A), PIR (B), and TP (C) at 80 $\mu\text{g/ml}$, 60 $\mu\text{g/ml}$, and 40 $\mu\text{g/ml}$ respectively, under the same chromatographic conditions. The peak responses were detected at 1.86, 13.82, and 3.29 min. for CAF, PIR, and TP respectively. CAF eluted too early and likely to overlap with the plasma peaks and the response peak was relatively broad. PIR run time was too long with improper base peak. In contrary, TP response peak was sharp with suitable retention time. Hence, it was selected as the IS for SP analytical method.

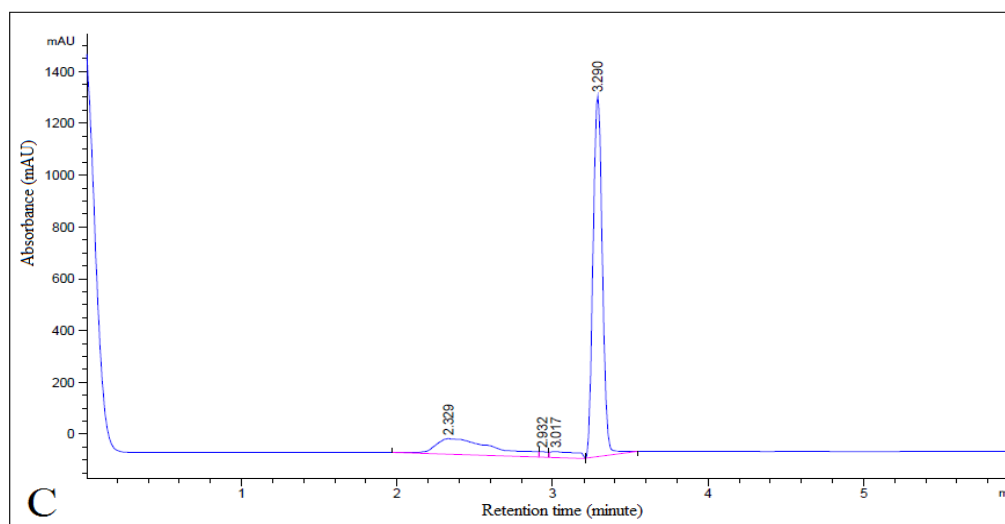
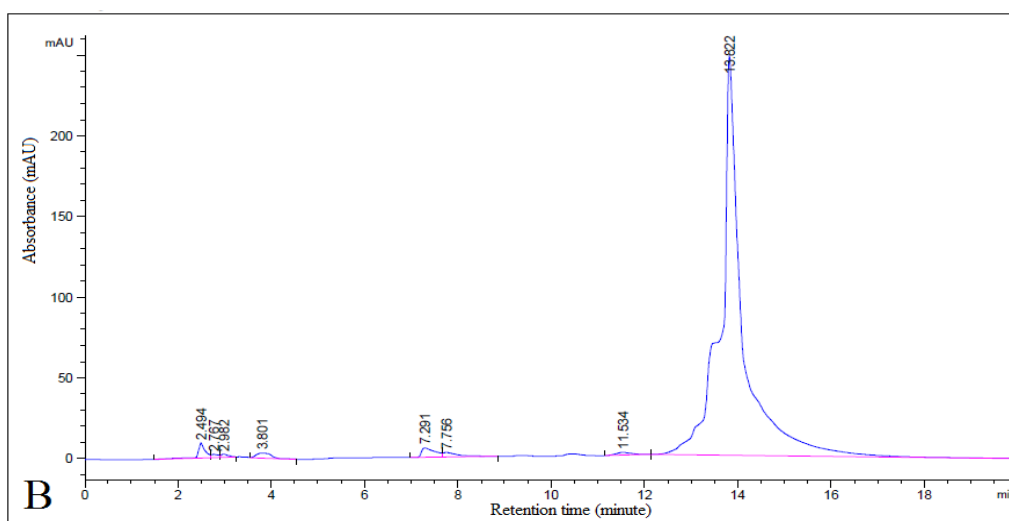
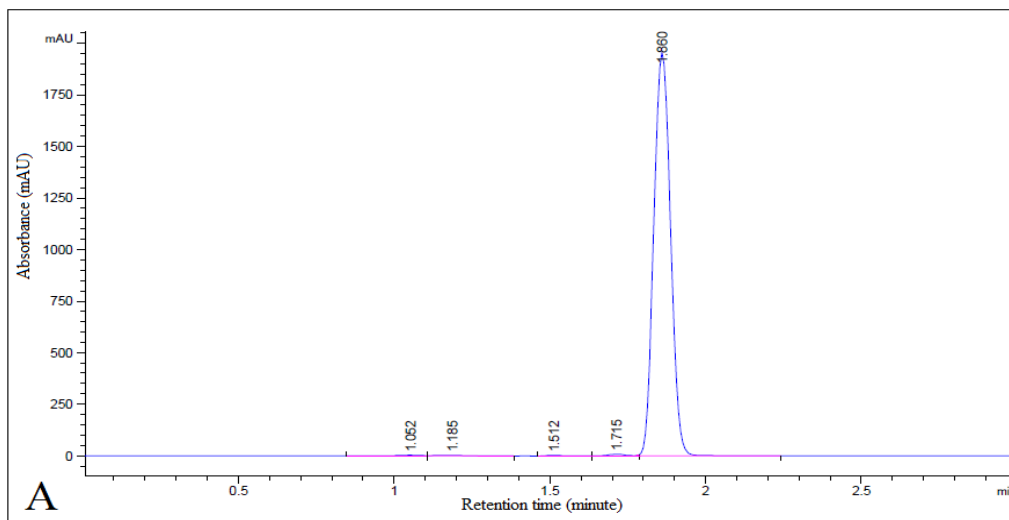


Figure 5.3 Chromatograms for CAF (A), PIR (B), and TP (C) under the same HPLC conditions

5.3.2 Mobile phase composition and elution method

One of the preliminary and essential parameters in HPLC method development is choosing the elution mode, isocratic or gradient elution. If the composition and flow rate of the MP remains constant throughout the sample run, then it is referred as isocratic elution. On the other hand, changing the ration of polar to non-polar compounds in the MP during the sample run is known as gradient elution (Schellinger & Carr, 2006).

Gradient elution is usually used in analysing multi-component samples of a wide range of polarities (Barkovich, 2017; Schellinger & Carr, 2006), by which separation can be achieved in shorter run times (Barkovich, 2017). However, isocratic elution is simpler, easier to transfer between columns, instruments and laboratories (Schellinger & Carr, 2006), maintain constant flow rate and provides better reproducibility (Barkovich, 2017).

Essentially, both elution methods can be used for any sample analysis and the choice is based on the number and polarity of the sample components (Schellinger & Carr, 2006). In this study, samples will contain one component only, thus, isocratic elution was chosen for both CUR and SP analytical methods.

5.3.2.1 HPLC method for CUR determination

Heath *et al.* (2003b) developed an HPLC method for determination of CUR in plasma and urine using MP containing acetonitrile: methanol: de-ionized water: acetic acid at ratio 41:23:36:1, respectively. 20µl of samples containing EST as the IS were injected onto the HPLC system. The MP was run at 1 ml/min and samples detected at 262 nm.

Based on the aforementioned conditions, a preliminary run of 20 $\mu\text{g/ml}$ CUR and 10 $\mu\text{g/ml}$ EST as IS solution in methanol was performed under the same conditions. Figure 5.4 shows the chromatogram obtained where both EST and CUR peaks appear sharp and fairly symmetric at 6.38 and 9.32 min., respectively.

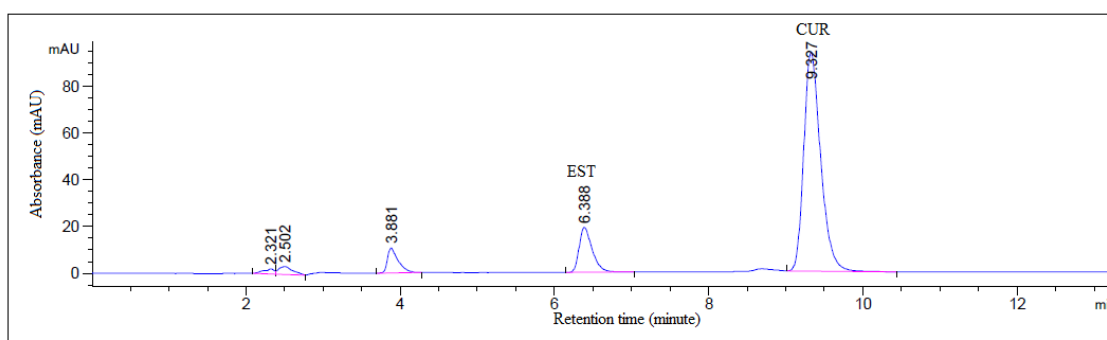


Figure 5.4 Chromatograms for EST and CUR using Heath *et al.* (2003b) method

Although the peaks obtained by Heath *et al.* (2003b) method were sharp, resolved, and fairly symmetric, the sensitivity of the detector to CUR was poor. It must be added that it is not very crucial if the sensitivity of the detector to the IS is not high because that can be compensated by using a higher concentration. From a prior UV scan, we are aware that CUR absorb at maximum at 435 nm. Therefore, sample run was detected simultaneously at two separate wavelengths of 262 nm and 425 nm. Chromatograms obtained (Figure 5.5) clearly shows a more intense detector response to CUR, however, EST peak was not detectable at 425 nm. Since the HPLC instrument is capable of simultaneously detecting samples at multi-wavelengths without the need to re-run the samples, both wavelengths 262 nm and 425 nm were subsequently used for detecting EST and CUR, respectively. Detecting the IS at different wavelength of the analyte was previously reported (Pak *et al.*, 2003), where the IS (EST) and CUR were detected at 280 nm and 430 nm, respectively.

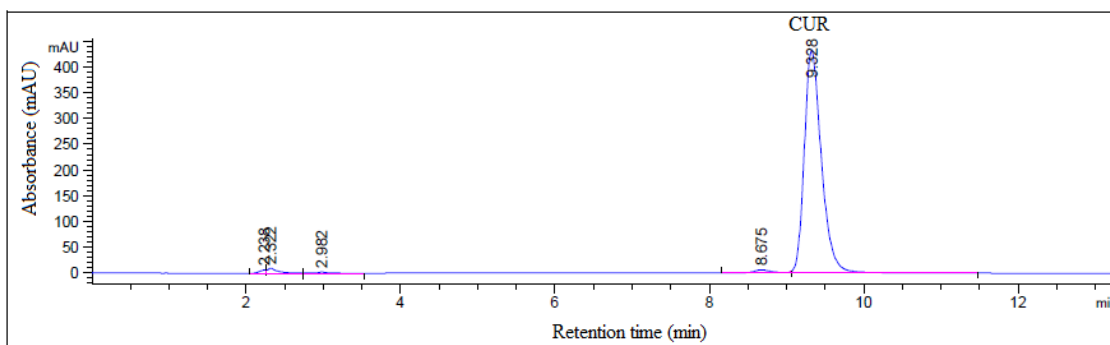


Figure 5.5 Chromatogram of CUR at 425 nm

5.3.2.2 HPLC method for SP determination

The HPLC method for SP determination was developed based on Amekyeh *et al.* (2015) method for the determination of SP along with amphotericin B and paracetamol. In Amekyeh *et al.* (2015) method, gradient elution of the MP comprised of Acetate buffer (pH 4) and acetonitrile, SP was detected at 254 nm.

Preliminary runs comprised of three samples of 40 $\mu\text{g/ml}$ SP dissolved in the following solvents: (i) DSMO: methanol, 1:1, (ii) methoanol, and (iii) acetate:methanol, 1:1. A 30 μl aliquot of the samples were injected into the HPLC system and the MP was run at 1 ml/min and SP detected at 254 nm. The MP comprised of [A] acetate buffer (pH 4), and [B] acetonitrile, with isocratic elution was used and the ratios of A to B was varied between 60-90:40-10 for each of the 3 samples. Optimum analyte peak in terms of shape and retention time was achieved at the MP ratio of 70:30 with methanol (ii) as solvent. Figure 5.6 shows the chromatogram obtained from 40 $\mu\text{g/ml}$ SP dissolved in methanol where, the peak was eluted at 3.83 min. Thus, these chromatographic conditions were selected for further optimization of the analytical method.

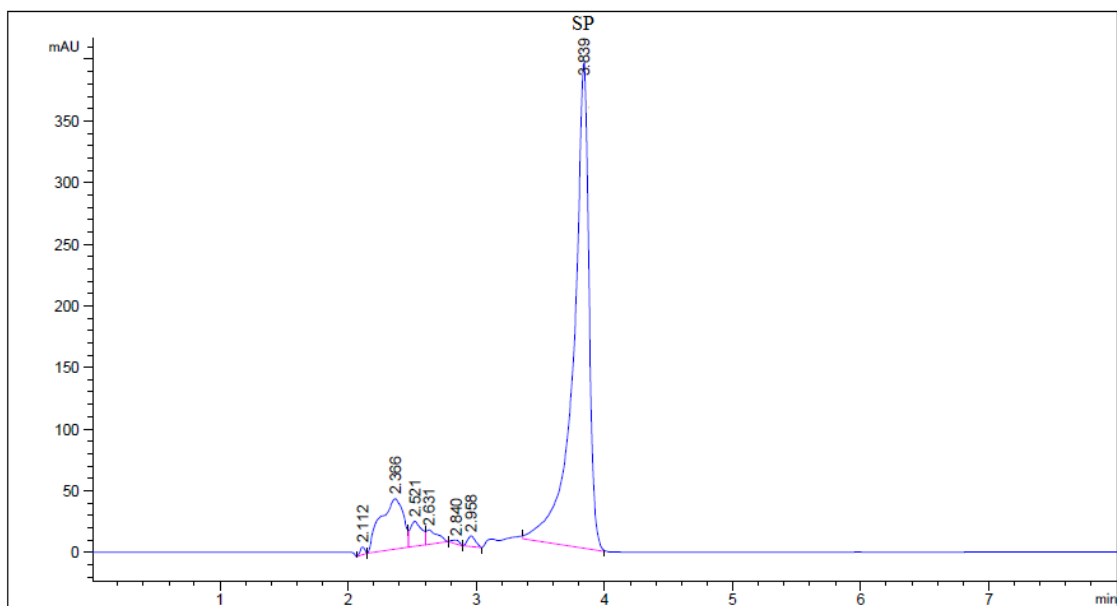


Figure 5.6 Chromatogram of SP dissolved in methanol using MP ratio 70:30 (acetate buffer (pH 4) : acetonitrile)

A mixture of 20 $\mu\text{g/ml}$ SP and 5 $\mu\text{g/ml}$ TP as IS was run using the aforementioned method, however, unresolved peaks with high noise was obtained (Figure 5.7A), hence, the analytical method was further optimized with MP ratio set at 80:20 (acetate buffer at pH4 :acetonitrile), flow rate 1.2 ml/min and detection wavelength 260 nm. Figure 5.7B illustrates the resulting chromatogram showing distinctive and fairly symmetric peaks of both SP and TP eluted at 3.00 and 5.07 min, respectively. The optimized chromatographic conditions were further selected for subsequent work.

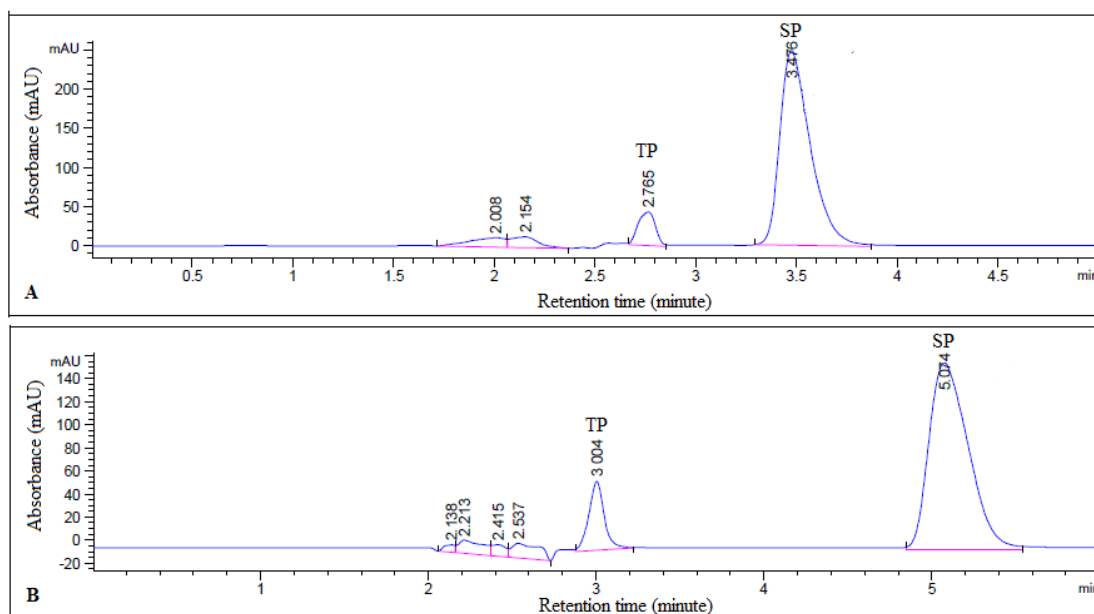


Figure 5.7 Chromatograms of TP and SP at MP ratio and detection wavelength of 70:30, 254 nm (A) and 80:20, 260 nm (B), respectively

5.3.3 Effects of the plasma and the deproteinising agent on peak resolution and symmetry

Precipitation of protein is essential in excluding artefacts and interferences from biological samples in analytical work (Daykin *et al.*, 2002). It is the most commonly used method due to its simplicity and ability to denature protein and destroy its drug binding ability (Polson *et al.*, 2003). Protein solubility in biological fluids is attributed to its hydrophilic surface and ionic interactions (Chang *et al.*, 2007) and to the repulsive electronic forces between similarly charged molecules. At the isoelectric point (pI) proteins become insoluble due to the lack of a net charge (Polson *et al.*, 2003).

The goal of protein precipitation is essentially to decrease its solubility by direct and indirect interactions between the deproteinizing agent and protein moieties (Chang *et al.*, 2007). A vast array of methods have been used for protein precipitation such as

pH adjustment, addition of salts, ultrafiltration (Daykin *et al.*, 2002), use of strong acids or bases (Chamberlain, 1995) and thermal precipitation (Burgess, 2009). However, the drawbacks of these methods are their potentially degradative effects on the analyte and the possibility of the analyte becoming trapped in protein aggregates (Chang *et al.*, 2007).

Organic solvents such as acetone, ethanol, and acetonitrile have been used for decades as deproteinizing agents (Burgess, 2009). They decrease the dielectric constant of the plasma protein solubility, displace the water molecules on the protein surface, thus decreasing its hydrophobic interaction and eventually leading to protein precipitation (Polson *et al.*, 2003).

Protein precipitation using organic solvents is an easy, simple, and fast method that can be used for a wide range of applications. In addition, these agents are volatile and can be used as MP (Sedgwick *et al.*, 1991). The type and amount of the organic solvent determine the protein precipitation efficiency (Chang *et al.*, 2007). Another concern with regard to the use of deproteinizing agents is that if they are markedly different from the MP, there could be a transient modification to the MP at the time of injection and this can perturb the elution dynamics of the analyte. The most preferable practice is using the MP as the deproteinizing agent and its addition to the IS solution as this would cause only a nuanced change in MP composition when injected.

In this study, the MP described in sections 5.3.2.1 and 5.3.2.2 were used both as deproteinizing agents and solvents for the IS in CUR and SP analytical methods, respectively. However, modifications to the peak such as broadening, baseline bias and tailing were observed (Figure 5.8). The MP were thus substituted with methanol (Figure 5.9) where peaks clearly appear well resolved, sharp, fairly symmetrical, on the

baseline, and without splitting. Thus, methanol was used subsequently both as the deproteinizing agent and solvent for the IS. Using different solvents as deproteinizing agents and solubilizing the IS would result in analytes dilution in the plasma samples, this effect was avoided in this study while effective protein precipitation was maintained.

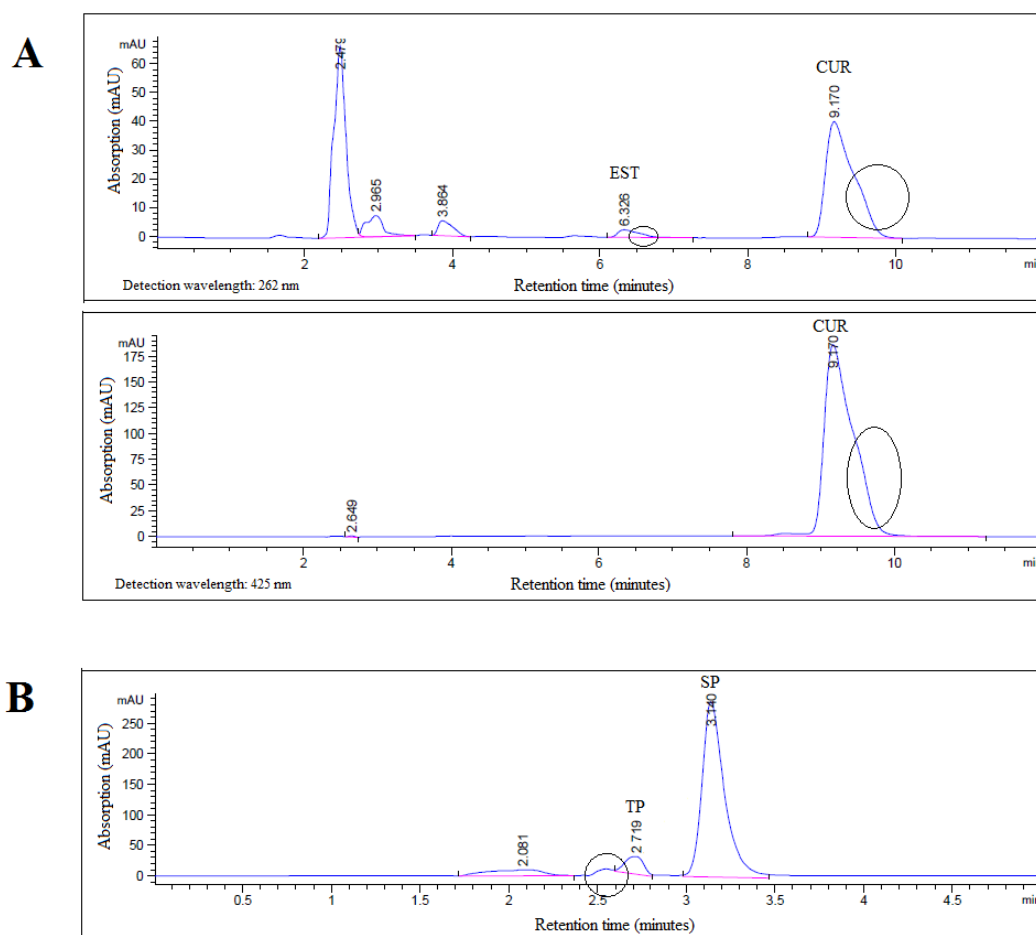


Figure 5.8 Chromatograms of CUR (A) and SP (B) and their respective IS using the MP as deproteinizing agent

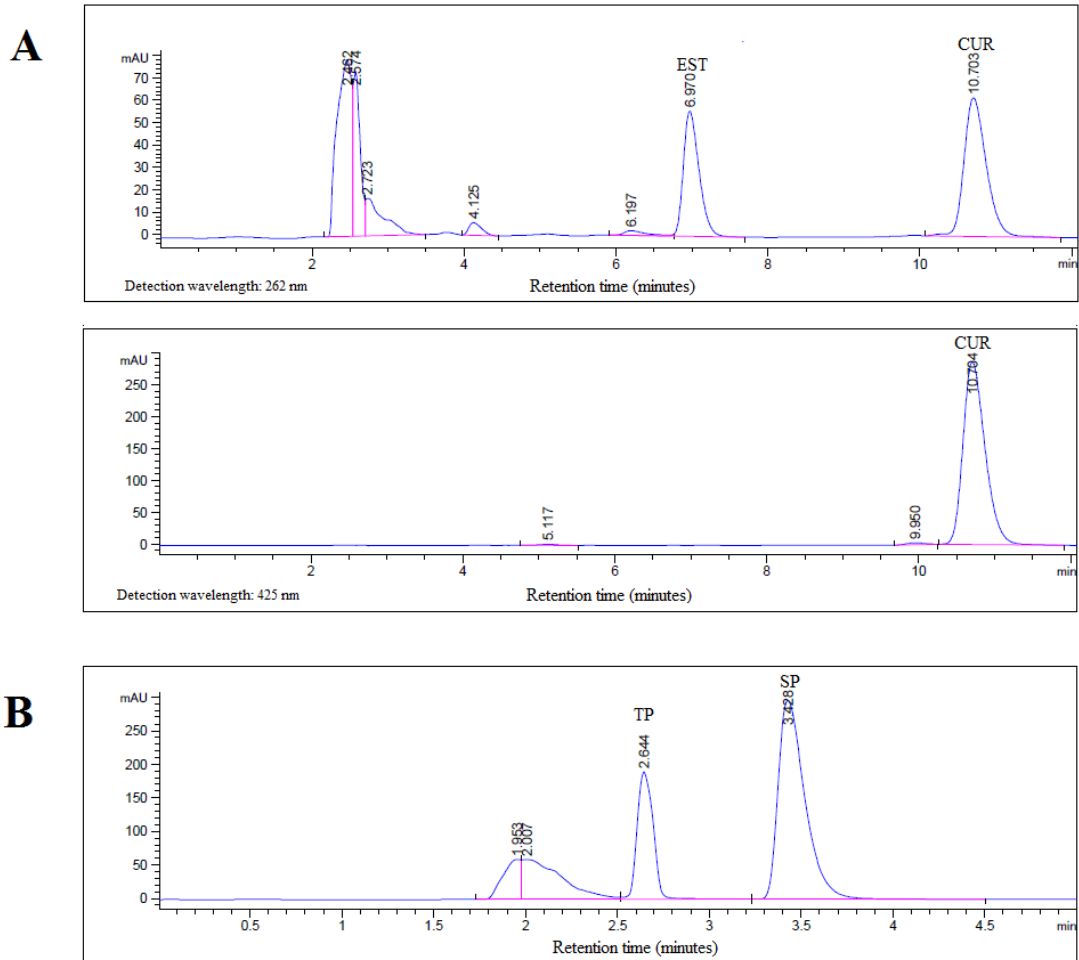


Figure 5.9 Chromatograms of CUR (A) and SP (B) and their respective IS using methanol as deproteinizing agent

5.3.4 HPLC method validation

A number of HPLC methods for the detection of CUR and suitable IS in biological fluids have been reported (Yang *et al.*, 2005; Gou *et al.*, 2011; Wan *et al.*, 2012; Khatik *et al.*, 2013; Anitha *et al.*, 2014). In general, SP is detected using complex methods simultaneously with other sulphonamides (Maudens *et al.*, 2004; Gu *et al.*, 2011; Tolika *et al.*, 2011). In the present study, two separate methods for analyses of CUR and SP, which would be suitable for the bioavailability studies of CUR using SP as a marker drug, were developed. EST and TP were used as the IS for the CUR and

SP analytical methods, respectively. The results of the method validation parameters for CUR and SP are summarized in Tables 5.1 and 5.2, respectively.

5.3.4.1 Specificity

The specificity is one of the firstly checked and most crucial validation parameter in analytical method development to ascertain that the analytical method is specific to the particular analytes. In this regard, individual drugs and their respective IS were injected onto the HPLC system separately to obtain the individual retention times to assign each peak. The MP compositions, simple isocratic elution method, and the RP- ZORBAX Eclipse Plus[®] column (C18, 250 mm x 4.6 mm, 5 μ m) were suitable for the determination methods of CUR and SP. Figure 5.10 illustrates the chromatograms obtained when pure drug solutions containing identical concentrations (22.0 μ g/ml each) of CUR and EST (IS) (A), and SP and TP (IS) (B) were injected on the system.

The retention times obtained were 7.21 and 10.98 min. for EST and CUR, respectively, and 3.58 and 7.26 min. for TP and SP, respectively. The chromatograms obtained show low baseline noise and no interfering peaks which reflects the specificity of the methods for the analytes.

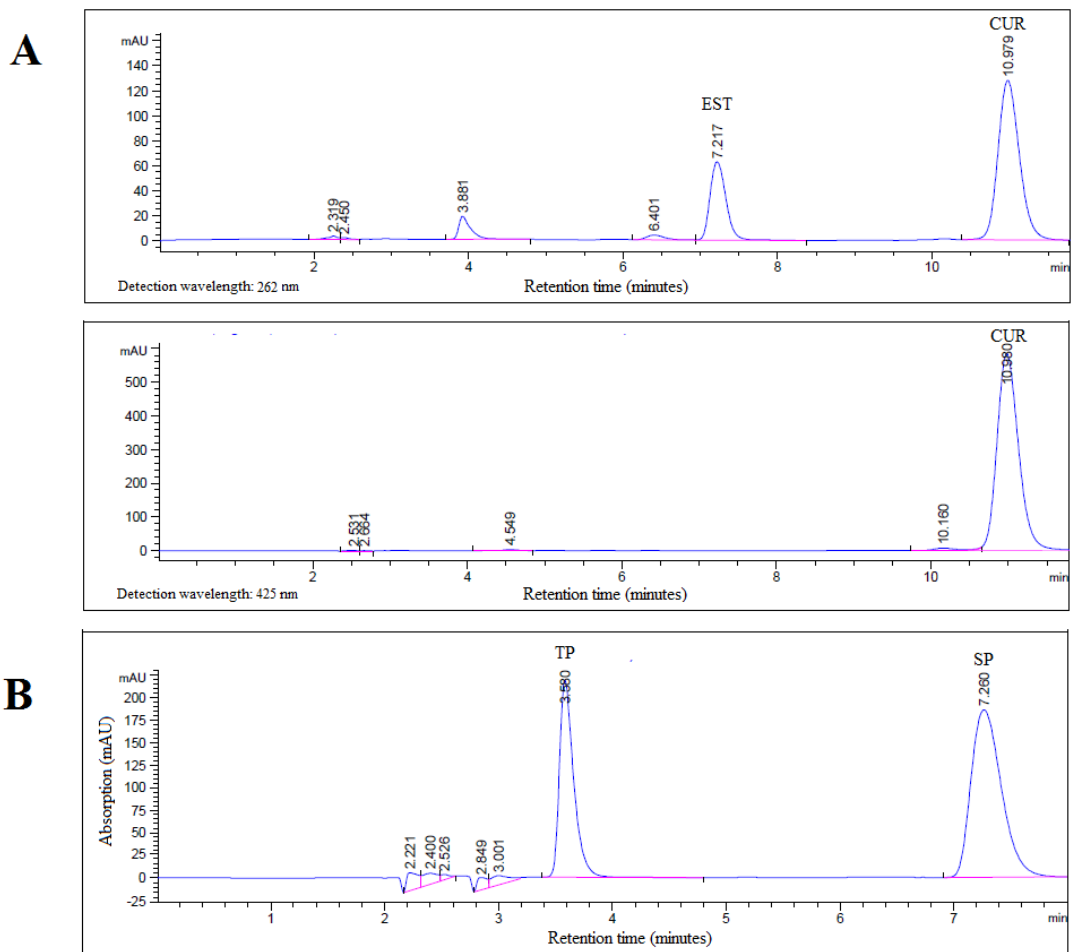


Figure 5.10 Chromatograms of pure solutions of CUR and EST (A) and SP and TP (B).

5.3.4.2 Effect of plasma (matrix effect)

Injecting blank plasma onto the HPLC system showed low baseline noise and no interfering peaks at the retention times for CUR (Figure 5.11A) at both studied wavelengths and for SP (Figure 5.11B) as well as their respective IS, further confirming the specificity of the HPLC analytical methods.

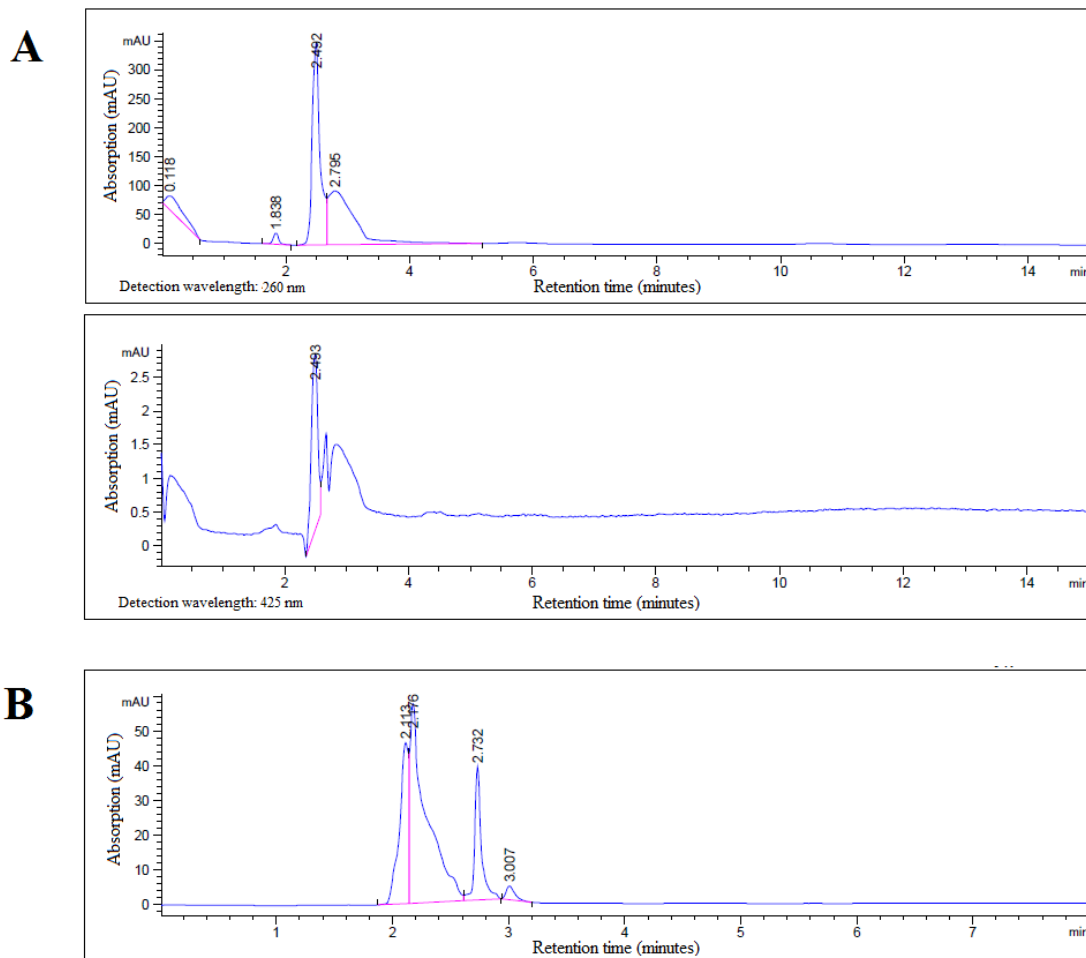


Figure 5.11 Chromatograms of the methanolic extract of blank human plasma using CUR (A) and SP (B) analytical methods

Plasma samples spiked with the analytes and IS, treated as described in section 5.3.3 and injected onto the HPLC system produced the chromatograms shown in Figures 5.12A for CUR and Figure 5.12B for SP and their respective IS. The figure clearly shows that the peaks for all drugs maintained their resolution and symmetry in plasma, with slight increases in the retention times of some of the analytes compared with the respective peaks obtained from the pure drug solutions in Figure 5.10. Particularly, the retention times of CUR, which increased from 10.98 to 11.19 at 262 and 425 nm, whereas EST retention time increased from 7.21 to 7.26 at 262 nm. However, no change in retention times was observed for TP and SP. The peaks in

Figure 5.12 were obtained by spiking solutions of the analytes into plasma to the same analyte concentrations in solution as in Figure 5.10. Differences in the peak response (absorption) was observed in CUR and SP peaks at 425 and 260 nm, respectively. Particularly, CUR and SP absorption increased from 600 to 700 mAU and from 175 to 250 mAU at 425 and 260 nm, respectively. This is attributable to the plasma matrix effect and it shows that it varies for different analytes. However, this difference was consistent for all of the subsequent plasma analyses and therefore inconsequential.

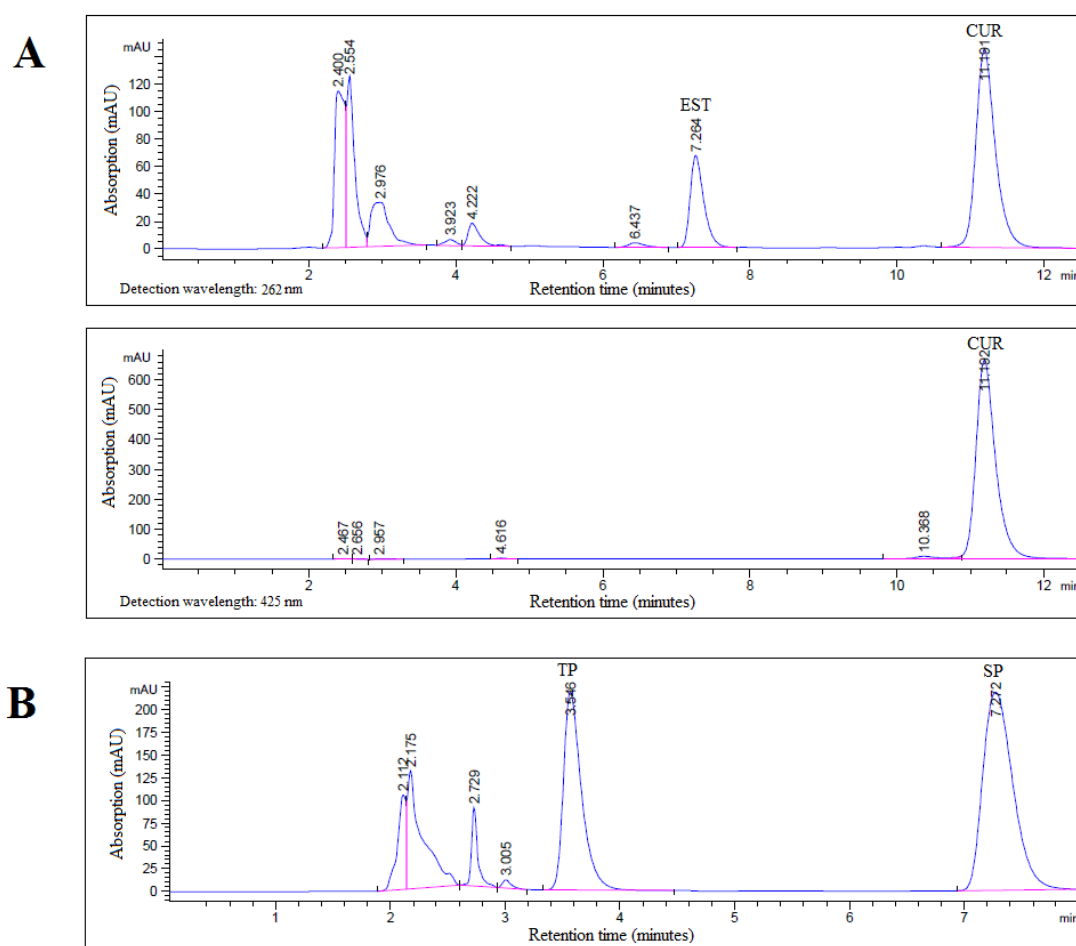


Figure 5.12 Chromatograms for spiked plasma showing CUR and EST (22.0 $\mu\text{g}/\text{ml}$, each) (A) and SP and TP (22.0 $\mu\text{g}/\text{ml}$, each)

HPLC is a powerful, sensitive and reproducible analytical technique used for the quantitative determination of drugs and their metabolites in biological fluids. However, one of the major challenges in bioanalytical method development is the “matrix effect” (Mei *et al.*, 2003). “Matrix” refers to all components in the sample other than the analytes of interest (Trufelli *et al.*, 2011). Body fluids are complex matrices that comprise of various compounds (Lagerwerf *et al.*, 2000). These fluids include blood, urine, bile, faeces, and tissue samples and the effects of these matrices may vary among individuals (Hall *et al.*, 2012).

The matrix effect may compromise the reproducibility, accuracy, and linearity of the bioanalytical methods (Trufelli *et al.*, 2011). The co-eluting molecules may cause suppression or enhancement of the analytes signals compared to the matrix-free samples (Stüber & Reemtsma, 2004; Taylor, 2005).

The exact mechanism by which the matrix effect manifests is not well understood, however, it is believed that the co-eluting matrix compete with the analytes of interest on the stationary phase, hence, influences the signal intensity (Taylor, 2005; Trufelli *et al.*, 2011). The majority of plasma components are water-soluble, thus, highly polar analytes are generally affected at greater extent compared to non-polar analytes (Taylor, 2005; Hall *et al.*, 2012). This was manifested in the present study where SP was the most effected analyte.

The matrix effect can arise from various matrix components including endogenous biological components such as carbohydrates, phospholipids, and residual formulation components (Hall *et al.*, 2012). Thus, the Sprague-Dawley rats used in the present study had not been used prior to this project and were not subjected to any drug substance prior to the study. Furthermore, they were fasted before the study.

The matrix components such as salts, amines, triglycerides, and fatty acids, among others, that contribute in the matrix effect can be reduced by diluting their amount in plasma, however, this further dilutes the analytes of interest (Stüber & Reemtsma, 2004). Other approaches to remove matrix components during the sample clean-up process are protein precipitation, liquid-liquid extraction, and solid phase extraction (Lagerwerf *et al.*, 2000). The usage of IS also helps in minimizing the matrix effect which was employed in this study (Mei *et al.*, 2003).

The results obtained so far clearly showed that the developed HPLC methods were suitable for the assay of CUR and SP along with their respective IS, in the presence or absence of the biological matrix, plasma.

5.3.4.3 Linearity and range

The linearity of the method was assessed based on the coefficient of correlation between peak response and analyte concentration over the working drug concentration ranges. Figure 5.13 illustrates the calibration curves for CUR and SP in plasma; both calibration curves are linear over the concentration ranges of 0.05-10 µg/ml and 0.1-20 µg/ml, respectively. The coefficients of determination were 1 and 0.9999, respectively, indicating good linearity in both analytical methods.

Shaikh *et al.* (2009); Wan *et al.* (2012); Khatik *et al.* (2013) studied the pharmacokinetics of CUR after oral administration of CUR formulations at doses 10-100 mg/kg which resulted in C_{max} values of 0.08-0.5 µg/ml. Whereas doses of 20 mg/kg of SSZ produced C_{max} values of SP ranging 0.15-4.76 µg/ml (Bates *et al.*, 1977; Sjödin *et al.*, 2011; Zamek-Gliszczyński *et al.*, 2012). In the present study, 10 mg/kg doses of CUR-CS-PEC-NPs and SSZ-CS-PEC-NPs were orally administered to the rats. Based

on the aforementioned data, the concentrations ranges were selected to be suitable for the plasma detection of the analytes in rat plasma.

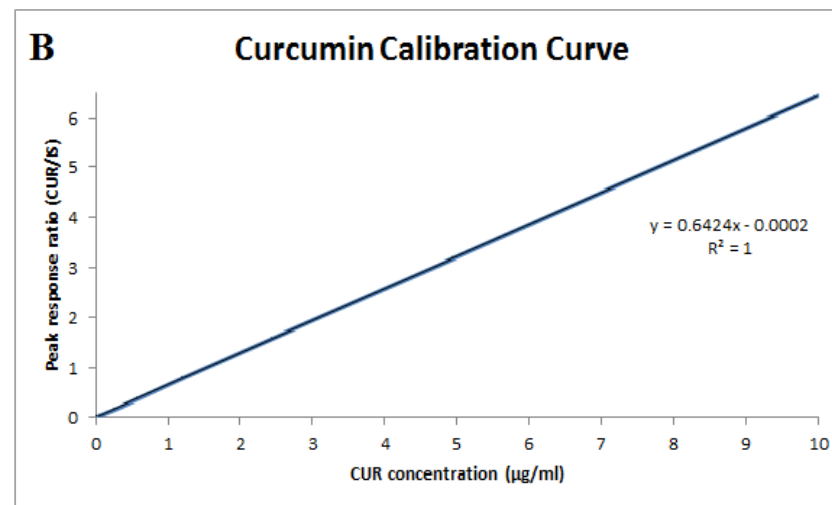
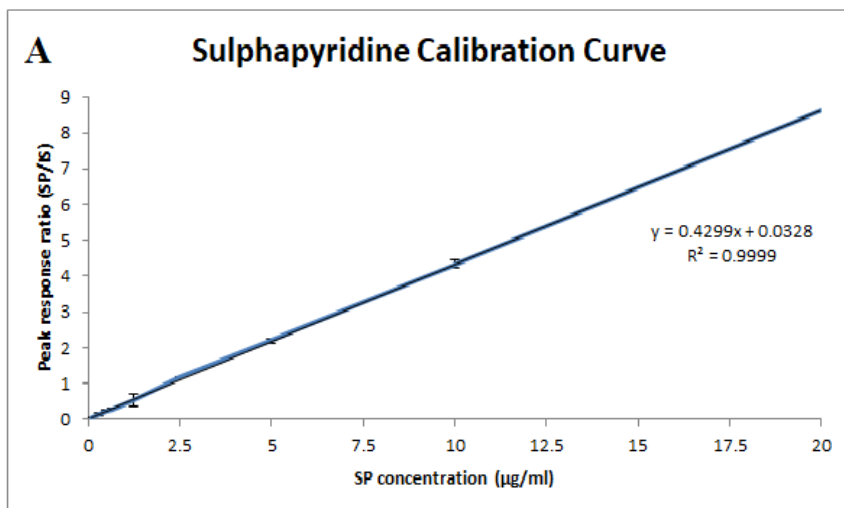


Figure 5.13 Standard calibration curves of the peak response ratios of analyte to IS versus the corresponding concentration of CUR (A) and SP (B) in human plasma

5.3.4.4 Precision

The precision reflects the closeness of individual measures of an analyte when the analytical method is applied repeatedly and is represented as %CV (WHO, 2017). The intra-day precision determines the precision during a single analytical run (under the same conditions), whereas the inter-day precision assesses precision with time and may involve different equipment, reagents, laboratories, and analysts. The intra-day precision assessment gave values of 1.29-1.90% for CUR and 1.58-10.51% for SP. On the other hand, the inter-day evaluation were 1.05-9.66% for CUR and 1.16-9.81 for SP. The precision (%CV) must ideally be less than 15% at all concentrations except for the LC where it should not exceed 20% (WHO, 2017). Based on the aforementioned data, the maximum value of precision was 10.51%, which indicates an acceptable degree of variation in both analytical methods.

The analytical methods for determination of CUR developed by Han *et al.* (2011); Heath *et al.* (2003b); Sun *et al.* (2013) produced maximum intra-day precision values of 12.0%, 6.2%, and 5.33%, respectively, and maximum inter-day precision values of 3.77%, 13.9%, and 5.33%, respectively. For SP, Intra-day and inter-day precision were in the ranges of 2.2-9.2% and 2.17-8.4%, respectively. The data from this study are either tantamount or even better than those obtained in the aforementioned studies.

5.3.4.5 Accuracy

The accuracy of an analytical procedure is a measure of the closeness between the actual and expected concentrations of an analyte and is represented as percentage relative error (Shabir, 2004). The relative error for this study were in the ranges 2.09-12.90% for CUR and 1.91-7.70% for SP, and 2.82-10.87% for CUR and 1.36-8.86%

for SP, in the intra-day and inter-day accuracy precision assessments, respectively. The relative error value should ideally be a maximum of 15% and 20% for HC and MC, and LC, respectively (Shabir, 2004). As all of the accuracy results in this study are below 15%, this indicates that both of the analytical methods are of acceptable accuracy. The accuracy values reported in the literature were in the range of 1.2-12.7% and 2.0-6.6% for CUR (Heath *et al.*, 2003b; Pak *et al.*, 2003; Han *et al.*, 2011) and SP (Maudens *et al.*, 2004; Gu *et al.*, 2011), respectively.

The data obtained from the precision and accuracy assessments show that both of the developed analytical methods for the determination of CUR and SP are repeatable and reproducible.

5.3.4.6 Recovery

The recovery of an analyte from a biological fluid against a biological matrix is crucial in choosing analytical procedure. The recovery is measured as the ratio of the peak response obtained of the analyte spiked in plasma, compared to that obtained of the same amount of analyte in pure solution (UNODC, 2009). For CUR, the recovery values obtained were 91.81, 96.53, 93.07% for LC, MC, and HC, respectively. For SP, the recovery values were 87.83, 103.74, and 89.91% for LC, MC, and HC, respectively. The data obtained shows maximum 12% matrix effect in the quantification of the analytes at all concentrations. Since the % recovery should ideally be in the range of 85-115%, the above data confirms good analyte recoveries in both analytical methods. The mean recoveries reported in the literature were in the range of 82.9-112.0% for CUR (Heath *et al.*, 2003b; Han *et al.*, 2011) and 87.0-96.0% for SP (Kasprzyk-Hordern *et al.*, 2007; Gu *et al.*, 2011). The recoveries values obtained in the present study are

comparable to those reported in the literature and this confirms the suitability of the developed methods for the determination of CUR and SP in plasma.

5.3.4.7 LOD and LOQ

LOD refers to the smallest concentration of an analyte that can be detected but not necessarily quantified. Whereas LOQ is the smallest concentration of analyte that can be quantified with acceptable accuracy and precision. LOD and LOQ are estimated to be three and ten times the noise level, respectively (Shrivastava & Gupta, 2011). LOD and LOQ were 0.5 ng/ml and 1.93 ng/ml for CUR and 73.10 ng/ml and 243.68 ng/ml for SP, respectively. Other LOD and LOQ values from the literature are 27.99-90.00 ng/ml and 2.50-84.84 ng/ml, respectively, for CUR (Heath *et al.*, 2003a; Jadhav *et al.*, 2007; Wichitnithad *et al.*, 2009) and 50 ng/ml and 10-20 ng/ml, respectively, for SP (Kasprzyk-Hordern *et al.*, 2007; Gu *et al.*, 2011). The LOD and LOQ values obtained in this study are either comparable or better than those reported in the literature. A low LOQ indicates that very low concentrations of the analyte can be detected and therefore give more credence to the procedure compared to methods with higher LOQ. The LOQ values should be lower than the expected analyte concentration at the first and last blood sampling in oral pharmacokinetics studies. A search through the literature revealed that CUR concentrations between 10-80 ng/ml occurs at the first blood sampling of a 10-100 mg/kg oral dosing (Yang *et al.*, 2007; Li *et al.*, 2009; Wan *et al.*, 2012; Khatik *et al.*, 2013). Likewise, SP concentrations of 80-100 ng/ml is produced at 20 mg/ml oral doses of sulfasalazine (Sjödin *et al.*, 2011; Zamek-Gliszczynski *et al.*, 2012). Based on the aforementioned studies, we may conclude that the LOQ values obtained in this study are suitable for the detection and quantification of CUR and SP following oral administration of 10 mg/kg for each.

Table 5.1 Summary of HPLC method validation parameters for CUR (MP: 41:36:23:1 acetonitrile: water: methanol: glacial acetic acid, detected at 425 nm and 262 nm for CUR and EST, respectively)

Parameter	Concentration ($\mu\text{g/ml}$)		Intra-day	Inter-day
	LC	0.03		
Precision (%CV)	LC	0.03	1.63	1.05
	MC	0.30	1.29	9.66
	HC	10.00	1.80	2.41
Accuracy (%)	LC	0.03	11.07	10.87
	MC	0.30	15.34	8.35
	HC	10.00	5.44	2.82
Recovery (%)	LC	0.03	92.04 \pm 5.20	
	MC	0.30	96.54 \pm 1.62	
	HC	10.00	93.07 \pm 1.44	
Sensitivity	LOD	0.50 ng/ml		
	LOQ	1.93 ng/ml		
Linearity Range	0.05-10.00 $\mu\text{g/ml}$			

Table 5.2 Summary of HPLC method validation parameters for SP (MP: 80:20 acetate buffer (pH 4): Acetonitrile, detected at 260 nm)

Parameter	Concentration ($\mu\text{g/ml}$)		Intra-day	Inter-day
	LC	MC		
Precision (%CV)	LC	0.10	10.51	9.81
	MC	0.50	2.29	2.95
	HC	20.00	1.58	1.16
Accuracy (%)	LC	0.10	2.65	3.76
	MC	0.50	7.70	8.86
	HC	20.00	1.91	1.36
Recovery (%)	LC	0.10	90.22 \pm 15.85	
	MC	0.50	105.48 \pm 15.12	
	HC	20.00	90.10 \pm 7.80	
Sensitivity	LOD	73 ng/ml		
	LOQ	243 ng/ml		
Linearity Range	0.05-10.0 $\mu\text{g/ml}$			

5.3.5 *In vivo* Pharmacokinetics studies

5.3.5.1 Selection of animal model

Small animals such as mice, rats, guinea pigs, and rabbits are more suitable for conducting drug absorption and bioavailability studies of powder or solution formulations, whereas larger animals such as dogs, pigs, and monkeys are more suitable to assess other types of formulations (Kararli, 1995). Rats share remarkable expression of anatomical and physiological features of the GIT to that of humans (Kararli, 1995).

Using rats in biological studies possess numerous advantages such as their suitable size which is important during handling and blood sampling, feasible cost (Lannaccone & Jacob, 2009), and a large volume of historical safety data in the use of rats for biological studies (Tomety, 2017). Thus, rats have been commonly used as animal model for determining drug absorption and bioavailability in various formulations, including nanoparticulate formulations (Girard *et al.*, 1987; Srinivasan & Iversen, 1995; Poulin & Theil, 2002; Kalaria *et al.*, 2009). A search through the literature has revealed that rats have been used in pharmacokinetics studies on CUR encapsulated in PLGA-NPs (Shaikh *et al.*, 2009; Khalil *et al.*, 2013), monomethoxy poly(ethyleneglycol)-poly(ϵ -caprolactone) micelles (Gou *et al.*, 2011), self-emulsifying liquid and pellet formulations (Setthacheewakul *et al.*, 2010), and CS-poly(butyl cyanoacrylate) NPs (Duan *et al.*, 2010). In the present study, male Sprague-Dawley rats were selected due to the fact that male rats are less prone to hormonal changes than female rats. Hormonal changes can affect physiological modalities that can affect pharmacokinetic profiles (Zhou *et al.*, 2002; Roehr, 2007).

5.3.5.2 *Pharmacokinetics studies*

Despite the potent anti-proliferative activity of CUR and its low toxicity, its use as an anticancer agent has been restricted due to its poor absorption and poor bioavailability. Therefore, we have formulated a nanoparticulate delivery system with a resoluteness to improve the oral bioavailability and efficiently deliver CUR to the colon. CUR-CS-PEC-NPs and free CUR were orally administered at 10 mg/ml to monitor the pharmacokinetics properties for 24 hr. CUR is water insoluble and easily hydrolysed in the physiological conditions, thus, SSZ-CS-PEC-NPs were administered orally at the same dose as marker in estimating the drug for the oro-caecal transit time of CUR-CS-PEC-NPs.

Prior to administration, the SSZ-CS-PEC-NPs were characterized in terms of particle size and zeta potential and EE% as described in sections 2.1.4 and 3.2.5, respectively to ensure the parity between the physical characteristics of CUR-CS-PEC-NPs and SSZ-CS-PEC-NPs. The particle size and zeta potential were 326.50 ± 5.6 and 21.7 ± 0.8 , respectively for SSZ-CS-PEC-NPs however, the EE% was $21.0 \% \pm 3.1\%$. A review of the literature revealed seldom encapsulation of SSZ in polymeric NPs due to its relatively good bioavailability following oral administration (Amekeyeh *et al.*, 2015) and is reported to manifest low EE% (Lamprecht *et al.*, 2000; Tavakol *et al.*, 2013) which could be attributed to its hydrophobic nature. In this study, no SP was detected at any time during the 24hr study period, which could be due to the low EE% of SSZ-CS-PEC-NPs. The SP detection and quantification in the plasma would have provided more information about the *in vivo* behaviour of the CS-PEC-NPs, but nonetheless, CUR was detected and statistically significant data were collected and discussed below for the proof of concept.

One rat from the free CUR group was excluded after 2 hr of the study due to insufficient blood samples volume and discomfort observed in this rat. The relevant pharmacokinetic parameters including C_{\max} , T_{\max} , $AUC_{0-\infty}$, and $t_{1/5}$ for CUR-CS-PEC-NPs and free CUR are summarized in Table 5.3.

Table 5.3 Pharmacokinetic studies of CUR-CS-PEC-NPs and free CUR

Pharmacokinetic parameters	CUR-CS-PEC-NPs	Free CUR
C_{\max} (ng/ml)	1000.57 \pm 15.23	704.67 \pm 73.17
T_{\max} (hr)	5.65 \pm 0.51	1.35 \pm 0.21
K_a (hr)	0.91 \pm 0.12	0.45 \pm 0.03
K_{el} (hr)	0.04 \pm 0.01	0.16 \pm 0.001
AUC_{0-t} (ng hr/ml)	4479.50 \pm 137.00	2181.91 \pm 195.04
$AUC_{0-\infty}$ (ng hr/ml)	10041.95 \pm 1859.78	2397.97 \pm 216.07
$t_{1/2}$ (hr)	17.65 \pm 1.40	4.88 \pm 0.19

The mean CUR concentration in the serum after oral administration of both CUR-CS-PEC-NPs and free CUR are illustrated in Figure 5.14. Maximum serum availability of CUR is 704.677 \pm 15.230 (ng/ml) and 1000.571 \pm 73.176 (ng/ml) were observed after 30 min. and 6 hr of free CUR and CUR-CS-PEC-NPs administration, respectively. This short C_{\max} observed from CUR suspension is attributable to the readily availability of free CUR for immediate absorption from the upper digestive tract, whilst CUR encapsulated in CUR-CS-PEC-NPs was at most available for absorption in the later part of the GIT. A higher $AUC_{0-\infty}$ value was observed in CUR-CS-PEC-NPs (10041.946 \pm 1859.783) compared to free CUR (2397.974 \pm 216.074) suggesting that the formulation aids in a better bioavailability of CUR than when administered alone. Unlike free CUR, higher concentration of CUR was detected at 24 hr.

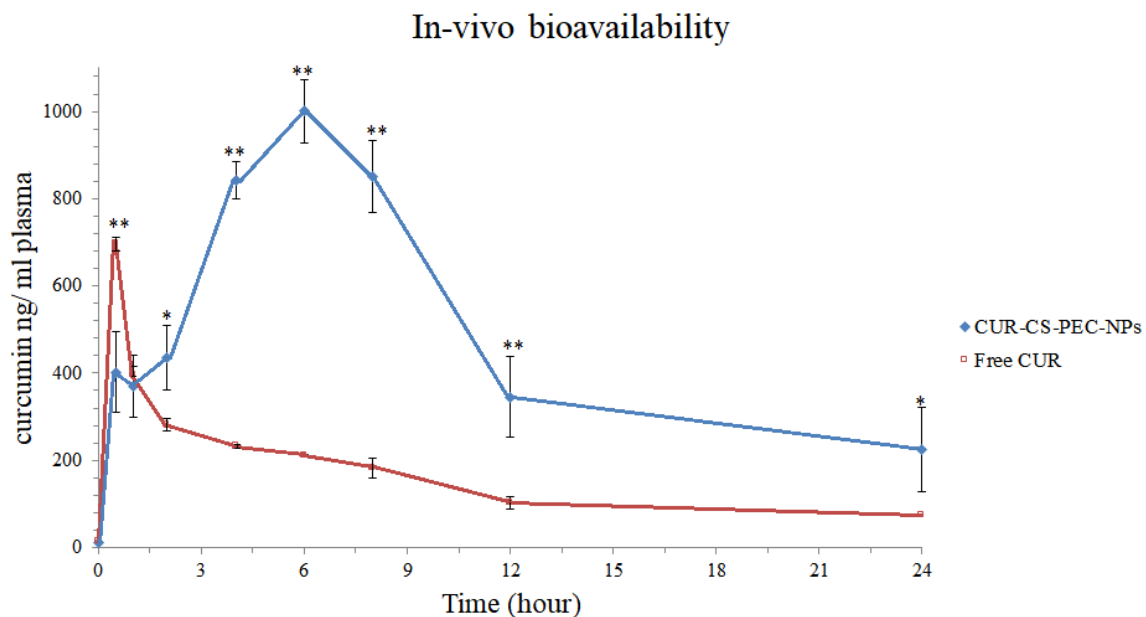


Figure 5.14 Plasma concentration profile of CUR in rats after the oral administration of equivalent doses of free CUR (n=3) and CUR-CS-PEC-NPs (n=4). (significant is identified with respect to free CUR *p<0.01, **p<0.001)

Shaikh *et al.*, (2009) encapsulated CUR in PLGA-NPs to enhance the oral bioavailability of CUR. After oral administration of 100mg/Kg of CUR-PLGA-NPs and 250 mg/Kg of CUR suspension, values of C_{max} (ng/ml), T_{max} (hr), and $AUC_{0-\infty}$ (ng/ml.hr) obtained from CUR-PLGA-NPs were 260.50 ± 26.40 ng/ml, 2.00 hr, and 3224.00 ng/ml.hr ± 329.00 and from CUR suspension were 90.3 ± 15.50 ng/ml, 0.50 hr, and 312.00 ng/ml.hr, respectively. Thus, as in the present study, improved oral bioavailability was observed when CUR was encapsulated in PLGA-NPs. In another study, Khalil *et al.*, (2013) fabricated CUR-PLGA-NPs to enhance its oral bioavailability. After oral administration of the nanoparticulate system at 50mg/kg, enhanced absorption of CUR from CUR-PLGA-NPs was observed as the reported C_{max} of the latter was 11.78 ± 0.454 ng/ml compared to 4.06 ± 0.564 ng/ml obtained from CUR suspension. In addition, T_{max} values were increased up to four folds in CUR-PLGA-NPs compared to CUR suspension. Khatik *et al.*,. (2013) studied the pharmacokinetics behaviour of CUR-Eudragit-CS-NPs compared to free CUR. In the

study, significant enhancement in CUR absorption and oral bioavailability after its encapsulation was observed. Reported C_{\max} and $AUC_{0-\infty}$ values were 904.74 ± 38.46 ng/ml and 16906.62 ± 103.87 ng/ml.hr of the NPs compared to 514.12 ± 14.09 ng/ml and 4722.55 ± 76.98 ng/ml.hr of free CUR, respectively. The pharmacokinetics data obtained from CUR-CS-PEC-NPs in this study were either comparable or even better than those reported in the literature which indicates enhanced oral bioavailability and successful delivery of CUR to the colon. In view of the fact that the CUR-CS-PEC-NP were designed to be delivered to the colon, we envisage that this is manifested *in vivo* and that absorption proper of CUR occurs at this site of the GIT. Therefore, in the event of a colorectal cancer therapy, we believe that this delivery system has a promising outlook for a favourable therapy.

5.4 Conclusion

In the first part of this chapter, simple, rapid, accurate, reproducible, and reliable HPLC methods for the determination and quantification of CUR and SP in plasma using EST and TP as IS, respectively, were developed and validated. The peaks for all of the analytes were well resolved in a relatively short run time (<10 min. for each). The volume of plasma used was appropriate for pharmacokinetic studies in rats. In the second part of this chapter, we discussed pharmacokinetics studies of CUR-CS-PEC-NPs and free CUR after oral administration in rats. Our findings reflect a successful delivery of CUR to the colon with increased oral absorption and bioavailability of CUR with time as observed for 24 hr. In contrast, lower bioavailability of free CUR was observed, possibly as a result of rapid metabolism of free CUR. The CUR-CS-PEC-NPs were developed to specifically deliver CUR to the colon without being degraded by the onslaught effects of the upper digestive tract and we believe that this is realised *in vivo* so that the high bioavailability observed from CUR-CS-PEC-NPs is due to

delivery to the colon followed by absorption. Thus, CUR-CS-PEC-NPs might serve as a suitable delivery system for CUR to the colon in which CUR will be available on site for its chemotherapeutic activity and induction of apoptosis in tumour cells.

Chapter 6

Conclusion and Future Work

6 Conclusion and future work

6.1 Conclusion

Despite the extensive research in trying to fully understand the manifestation of carcinogenesis as well as intensive research in the provision of a framework for the prevention and treatment of the disease, cancer remains one of the most challenging and complex causes of mortality around the world with ever increasing prevalence (Johnson & Mukhtar, 2007). The two major challenges in the management of cancer treatment are: (i) non-selectivity in the treatment whereby all tissues are a target for a viable formulation and (ii) the constraint of needing to overcome the biological barriers that hinders the effectiveness of the cancer therapeutic (Ferrari, 2005). In order to avoid the side effects that arise from (i) there is a move towards the use of natural chemotherapeutic agents derived from plant sources such as CUR, whose anticancer potential is unquestionable and has been extensively reviewed in Chapter 1 of this thesis. Despite this potential, the use of CUR as anticancer agent is somewhat curtailed due to its poor biopharmaceutical properties comprising of low water solubility, low oral bioavailability, extensive metabolism, and rapid elimination rates (Yallapu *et al.*, 2012; Naksuriya *et al.*, 2014). In the present study, we have successfully fabricated CUR-containing mucoadhesive nanoparticulate delivery system with demonstrable potential for the treatment of colorectal cancer. In a further project from the present work, we aim to use biodegradable excipients so that reported toxicity of the “courier” system can be minimised.

The use of a simple and non-toxic ionic gelation technique, CUR-CS-PEC-NPs were successfully prepared. The optimized formulation has mean particle size of 200.6 nm (± 6.6 nm) and zeta potential of +32.8 mV (± 0.5 mV). The size of CUR-CS-PEC-NPs was suitable for delivery to the colorectal tumour, whereas the zeta potential

reflected a considerably stable formulation. The SEM images showed spherical and well-separated NPs with sizes in agreement with those obtained from the photon correlation analysis. FT-IR, DSC, and XRD analyses confirmed the encapsulation of CUR onto the CS-PEC-NPs in its inactive, amorphous phase.

The mucoadhesive propensities of CUR-CS-PEC-NPs were confirmed and mainly attributed to the ionic interaction between the positively charged CUR-CS-PEC-NPs and negatively charged mucin. The EE% of the freshly prepared CUR-CS-PEC-NPs was found to be 64% (± 1.40 %) where cumulative release of 86% of CUR was observed after 7 hr of the study in gastrointestinal simulated fluids. Stability studies showed “fair” storage stability of CUR-CS-PEC-NPs as well as the protection of CUR against thermal- and photo-degradation.

In vitro cellular studies confirmed that CUR retained its antiproliferative properties against colorectal cancer cell line HT-29 after encapsulation in CUR-CS-PEC-NPs. The safety and selectivity of the formulation as well as free CUR were confirmed. CUR-CS-PEC-NPs showed less than 65% and 12% cell viability at lowest and highest treatment doses, respectively, after three days of cell viability study. The cellular apoptosis effects of CUR-CS-PEC-NPs were confirmed via fluorescent nuclear images whereas quantitative and qualitative cellular uptake studies demonstrated considerable uptake of CUR-CS-PEC-NPs by colorectal cancer cell line HT-29.

A simple, sensitive, accurate, and reproducible HPLC analytical procedure was developed for the quantitative determination of CUR and SP using suitable IS for each and validated in human plasma for subsequent *in vivo* analyses. The methods required a small volume of plasma, which makes them applicable for pharmacokinetics studies in rats. A proof of concept study was conducted to evaluate the pharmacokinetics of

CUR-CS-PEC-NPs. Enhanced oral absorption and bioavailability as well as decreased elimination rate of CUR-CS-PEC-NPs compared to free CUR. The concentration-time profile indicates successful delivery of CUR-CS-PEC-NPs to the colon.

In conclusion, successful fabrication of CUR-CS-PEC-NPs with mucoadhesive propensities resulted in enhancing the oral bioavailability of CUR as well as its targeted delivery to the colon whilst retaining its antiproliferative efficiency. The formulation tends to be selective against tumour cells. Therefore, CUR-CS-PEC-NPs is a promising potential nanoformulation for the treatment of colorectal cancer.

6.2 Suggestions for future work

The research on enhancing the oral bioavailability of CUR and its delivery to the target site using nanoparticulate delivery systems is winning growing interest. CUR-CS-PEC-NPs developed in this study shows promising data for future clinical translation. To reach that point, a few suggestions for future work are discussed below.

High EE% of a formulation provides higher payload of the drug using the same amount of the carrier. The EE% of the current formulation can be enhanced by increasing the initial concentration of the drug, this might require modification of the nanoparticulate system to attain higher drug loading while maintaining its physico-chemical properties. Other approaches for increasing the EE% include increasing working pH, using pH-responsive excipients such as lauric acid, caprylic acid, and poly(methyl methacrylate-co-methacrylic acid) (PMMA-MAA) (Hans & Lowman, 2002), and the addition of co-polymers such as pluronic F127 (Das *et al.*, 2010).

In general, the storage stability of the polymeric NPs is one of the major hurdles which might regressively effect its development, which is applicable to this formulation as well (Wu *et al.*, 2011). Strategies for improving nanoparticulate shelf-life including the use of stabilizers such as polyethylene glycol (PEG), poly(vinylalcohol) (PVA), and poly(L-lysine) (PLL), however, using them might cause toxicity issues (Wu *et al.*, 2011). Safer strategies include freeze drying of the NPs with the use of suitable cryoprotectant such as sucrose and trehalose and the formulation of the nanoparticles with higher zeta potential (Shaikh *et al.*, 2009).

The *in vivo* studies have undoubtedly proven the enhanced oral bioavailability and pharmacokinetics behavior of CUR upon its encapsulation in CS-PEC-NPs.

However, other *in vivo* evaluation would help to better understand the fate of CUR-CS-PEC-NPs such as Gamma Scintigraphy and histological analyses.

Certainly, cellular studies confirmed the anticancer efficiency of both free CUR and CUR-CS-PEC-NPs against colorectal cancer cells. However, their effects were evaluated against one cell line only, HT-29, evaluation using other colorectal cancer cell lines such as SW1417, SW480, DLD-1, and HCT-15 would represent more information about CUR-CS-PEC-NPs efficiency against various colorectal cancer types with different gene expressions. Moreover, *in vivo* anticancer evaluation of CUR-CS-PEC-NPs is necessary as the obtained *in vitro* data, although provides basic indication, does not necessarily represent the *in vivo* anticancer behavior of the formulation. In such evaluations, human cancer xenograft can be established in animal modules and the anticancer effects of the formulation can be subsequently assessed via *in vivo* imaging and measuring the change in the tumour volume.

LIST OF PUBLICATIONS FROM THE PRESENT WORK

1. E. Alkhader, N. Billa, & CJ. Roberts. Mucoadhesive Chitosan-Pectinate Nanoparticles for the Delivery of Curcumin to the Colon. *AAPS PharmSciTech*, 18(4), 1009-1018.
2. E. Alkhader & N. Billa. Chitosan-pectinate mucoadhesive nanoparticles for the treatment of colorectal cancer. BIT6th Annual World Congress of Nanoscience & Technology. 26th-28th October, 2016. Holiday Inn Singapore Atrium, Singapore, Oral presentation.
3. Enas Alkhader & Nashiru Billa. A spice for cancer treatment, 3MT 2016. Semenyih, Malaysia. Oral presentation.
4. Enas Alkhader & Nashiru Billa. Mucoadhesive Chitosan Pectinate Nanoparticles for the Delivery of Curcumin in Colon Cancer. Faculty of Biosciences Workshop, 2016. Semenyih, Malaysia. Poster Presentation.
5. Enas Alkhader & Nashiru Billa. Chitosan-pectinate mucoadhesive nanoparticles for the treatment of colorectal cancer. Faculty of Science research talk, 2015. Semenyih, Malaysia, Oral presentation.

References

- Adams, K., Ferstl, M., Davis, C., Herold, M., Kurtkaya, S., Camalier, F., & Shoji, M. (2004). Synthesis and biological evaluation of novel curcumin analogs as anti-cancer and anti-angiogenesis agents. *Bioorganic and Medicinal Chemistry*, *12*(14), 3871–3883. <https://doi.org/10.1016/j.bmc.2004.05.006>
- Adams, M., & Cory, S. (2007). Bcl-2-regulated apoptosis : mechanism and therapeutic potential. *Elsevier Science Inc*, *19*, 488–496. <https://doi.org/10.1016/j.coi.2007.05.004>
- Adelstein, A., Macaskill, P., Chan, F., Katelaris, H., & Irwig, L. (2011). Most bowel cancer symptoms do not indicate colorectal cancer and polyps: a systematic review. *BMC Gastroenterology*, *11*(65), 1–10. <https://doi.org/10.1186/1471-230X-11-65>
- Adrouny, R. (2002). Understanding Health & Sickness : Understanding Colon Cancer. *University Press of Mississippi*, *1*, 1-10
- Aggarwal, B., Bhatt, D., & Ichikawa, H. (2006). 10 Curcumin — Biological and Medicinal Properties, *10*, 297–368.
- Aggarwal, B., Kumar, A., Bharti, C., & Anderson, D. (2003). Anticancer Potential of Curcumin Preclinical and Clinical Studies. *Anticancer Research*, *398*, 363–398.
- Aggarwal, B., & Sung, B. (2008). Pharmacological basis for the role of curcumin in chronic diseases : an age-old spice with modern targets. *Elsevier Science Inc*, (December), 85–94. <https://doi.org/10.1016/j.tips.2008.11.002>
- Aggarwal, B., Surh, J., & Shishodia, S. (2007). The Molecular Targets and Therapeutic Uses of Curcumin in Health and Disease. *Health*, *595*, 1-18. Publishing.

<https://doi.org/10.1007/978-0-387-46401-5>

Agnihotri, A., Mallikarjuna, N., & Aminabhavi, M. (2004). Recent advances on chitosan-based micro- and nanoparticles in drug delivery. *Journal of Controlled Release*, *100*(1), 5–28. <https://doi.org/10.1016/j.jconrel.2004.08.010>

Akram, M., Shahab-uddin, Ahmed, A., Usmanghani, K., Hannan, A., Mohiuddin, E., & Asif, M. (2010). Curcuma longa and curcumin: a review article. *Romanian Journal of Biology*, *55*(2), 65–70.

Alkilany, M., & Murphy, J. (2010). Toxicity and cellular uptake of gold nanoparticles : what we have learned so far ? *Journal of Nanoparticle Research*, *12*, 2313–2333. <https://doi.org/10.1007/s11051-010-9911-8>

Allaire, A., Luong, X., & Smith, P. (2010). Basics of Cell Culture. *Human Stem Cell Technology and Biology: A Research Guide and Laboratory Manual*. <https://doi.org/10.1002/9780470889909.ch3>

Allémann, E., Gurny, R., & Doelker, E. (1992). Preparation of aqueous polymeric nanodispersions by a reversible salting-out process: influence of process parameters on particle size. *International Journal of Pharmaceutics*, *87*(1–3), 247–253. [https://doi.org/10.1016/0378-5173\(92\)90249-2](https://doi.org/10.1016/0378-5173(92)90249-2)

Allen, A. & Garner, A. (1980). Mucus and bicarbonate secretion in the stomach and their possible role in mucosal protection. *Gut*, *21*(3), 249–262. <https://doi.org/10.1136/gut.21.3.249>

Allen, A., & Snary, D. (1972). The structure and function of gastric mucus. *Gut*, *13*(Table I), 666–672. <https://doi.org/10.1136/gut.13.8.666>

- Allen, M., & Cullis, R. (2013). Liposomal drug delivery systems: From concept to clinical applications. *Advanced Drug Delivery Reviews*, 65(1), 36–48. <https://doi.org/10.1016/j.addr.2012.09.037>
- Amekeyeh, H. (2016). Formulation, gastrointestinal transit studies and absorption of amphotericin B-containing solid lipid nanoparticles in rats. PhD Thesis, 161-198.
- Amekeyeh, H., Billa, N., Yuen, H., & Chin, S. (2015). A Gastrointestinal Transit Study on Amphotericin B-Loaded Solid Lipid Nanoparticles in Rats. *AAPS PharmSciTech*, 16(4), 871–877. <https://doi.org/10.1208/s12249-014-0279-4>
- American Cancer Society. (2004). Colorectal Cancer Staging. *CA: A Cancer Journal for Clinicians*, 54(6), 362–365. <https://doi.org/10.3322/canjclin.54.6.362>
- Ammayappan, L., & Moses, J. (2009). Study of Antimicrobial Activity of Aloe vera , Chitosan , and Curcumin on Cotton , Wool , and Rabbit Hair, *10*(2), 161–166. <https://doi.org/10.1007/s12221-009-0161-2>
- Anand, P., Kunnumakkara, B., Newman, A., & Aggarwal, B. (2007). reviews Bioavailability of Curcumin: Problems and Promises, *4*(6), 807–818. <https://doi.org/10.1021/mp700113r>
- Anand, P., Kunnumakkara, B., Newman, A., Aggarwal, B., Anand, P., Kunnumakkara, B., & Newman, A. (2007). Bioavailability of Curcumin : Problems and Promises reviews Bioavailability of Curcumin : Problems and Promises, *4*(November), 807–818. <https://doi.org/10.1021/mp700113r>
- Anand, P., Thomas, G., Kunnumakkara, B., Sundaram, C., Harikumar, B., Sung, B., & Aggarwal, B. (2008). Biological activities of curcumin and its analogues (Congeners) made by man and Mother Nature. *Biochemical Pharmacology*, 76,

1590–1611. <https://doi.org/10.1016/j.bcp.2008.08.008>

Anderson, D. (2003). Anticancer Potential of Curcumin: Preclinical and Clinical Studies. *Anticancer Research*, 398, 363–398.

Andrews, P., Laverty, P., & Jones, S. (2009). Mucoadhesive polymeric platforms for controlled drug delivery. *European Journal of Pharmaceutics and Biopharmaceutics*, 71(3), 505–518. <https://doi.org/10.1016/j.ejpb.2008.09.028>

Anitha, A., Deepa, N., Chennazhi, P., Lakshmanan, K., & Jayakumar, R. (2014). Combinatorial anticancer effects of curcumin and 5-fluorouracil loaded thiolated chitosan nanoparticles towards colon cancer treatment. *Biochimica et Biophysica Acta - General Subjects*, 1840(9), 2730–2743. <https://doi.org/10.1016/j.bbagen.2014.06.004>

Anitha, A., Deepagan, G., Divya Rani, V., Menon, D., Nair, V., & Jayakumar, R. (2011). Preparation, characterization, in vitro drug release and biological studies of curcumin loaded dextran sulphate-chitosan nanoparticles. *Carbohydrate Polymers*, 84(3), 1158–1164. <https://doi.org/10.1016/j.carbpol.2011.01.005>

Anitha, A., Deepagan, G., Rani, D., Menon, D., Nair, V., & Jayakumar, R. (2011). Preparation , characterization , in vitro drug release and biological studies of curcumin loaded dextran sulphate – chitosan nanoparticles. *Carbohydrate Polymers*, 84(3), 1158–1164. <https://doi.org/10.1016/j.carbpol.2011.01.005>

Anitha, A., Maya, S., Deepa, N., Chennazhi, P., Nair, V., Tamura, H., & Jayakumar, R. (2011). Efficient water soluble O-carboxymethyl chitosan nanocarrier for the delivery of curcumin to cancer cells. *Carbohydrate Polymers*, 83(2), 452–461. <https://doi.org/10.1016/j.carbpol.2010.08.008>

- Anitha, A., Sreeranganathan, M., Chennazhi, K., Lakshmanan, K., & Jayakumar, R. (2014). In vitro combinatorial anticancer effects of 5-fluorouracil and curcumin loaded N,O-carboxymethyl chitosan nanoparticles toward colon cancer and in vivo pharmacokinetic studies. *European Journal of Pharmaceutics and Biopharmaceutics*, 88(1), 238–251. <https://doi.org/10.1016/j.ejpb.2014.04.017>
- Aoki, H., Takada, Y., Kondo, S., Sawaya, R., & Aggarwal, B. (2007). Evidence That Curcumin Suppresses the Growth of Malignant Gliomas in Vitro and in Vivo through Induction of Autophagy : Role of Akt and Extracellular Signal-Regulated Kinase Signaling Pathways □. *Molecular Pharmacology*, 72, 29–39. <https://doi.org/10.1124/mol.106.033167>.
- Arain, M., Campbell, J., Cooper, L., & Lancaster, A. (2010). What is a pilot or feasibility study? A review of current practice and editorial policy. *BMC Medical Research Methodology*, 10, 1–7. <https://doi.org/10.1186/1471-2288-10-67>
- Archana, D., Dutta, J., & Dutta, K. (2013). Evaluation of chitosan nano dressing for wound healing : Characterization , in vitro and in vivo studies. *International Journal of Biological Macromolecules*, 57, 193–203. <https://doi.org/10.1016/j.ijbiomac.2013.03.002>
- Aseh, A., & Ríos, N. (2009). Fabrication and characterization of silk fibroin-derived curcumin nanoparticles for cancer therapy. *International Journal of Nanomedicine*, 4, 115–122.
- Ashford, M., Fell, J., Attwood, D., Sharma, H., & Woodhead, P. (1993). An evaluation of pectin as a carrier for drug targeting to the colon. *Journal of Controlled Release*, 26(3), 213–220. [https://doi.org/10.1016/0168-3659\(93\)90188-B](https://doi.org/10.1016/0168-3659(93)90188-B)

- Astete, E., & Sabliov, M. (2006). Synthesis and characterization of PLGA nanoparticles. *Journal of Biomaterials Science. Polymer Edition*, 17(3), 247–289. <https://doi.org/10.1163/156856206775997322>
- Asua, M. (2004). Emulsion polymerization: From fundamental mechanisms to process developments. *Journal of Polymer Science Part A: Polymer Chemistry*, 42(5), 1025–1041. <https://doi.org/10.1002/pola.11096>
- Ataie, A., Sabetkasaei, M., & Haghparast, A. (2010). Pharmacology , Biochemistry and Behavior Neuroprotective effects of the polyphenolic antioxidant agent , Curcumin , against homocysteine-induced cognitive impairment and oxidative stress in the rat. *Pharmacology, Biochemistry and Behavior*, 96(4), 378–385. <https://doi.org/10.1016/j.pbb.2010.06.009>
- ATCC. (2003). ATCC primary cell culture guide. <https://doi.org/10.1002/ejoc.201200111>
- ATCC. (2017a). HT-29. Available at: <https://www.atcc.org/~ps/HTB-38.ashx>
- ATCC. (2017b). MRC-5. Available at: <https://www.atcc.org/~ps/CCL-171.ashx>
- ATCC. (2017c). MTT Cell Proliferation Assay. ATCC. <https://doi.org/ATCC 30-1010K>
- Atuma, C., Strugala, V., Allen, A., & Holm, L. (2001). The adherent gastrointestinal mucus gel layer: thickness and physical state in vivo. *American Journal of Physiology. Gastrointestinal and Liver Physiology*, 280(5), G922-9. Retrieved from <http://www.ncbi.nlm.nih.gov/pubmed/11292601>
- Avadi, R., Sadeghi, M., Mohammadpour, N., Abedin, S., Atyabi, F., Dinarvand, R., &

- Rafiee-Tehrani, M. (2010). Preparation and characterization of insulin nanoparticles using chitosan and Arabic gum with ionic gelation method. *Nanomedicine: Nanotechnology, Biology, and Medicine*, 6(1), 58–63. <https://doi.org/10.1016/j.nano.2009.04.007>
- Awasthi, R. (2011). Selection of pectin as pharmaceutical excipient on the basis of rheological behavior. *International Journal of Pharmacy and Pharmaceutical Sciences*, 3(1), 229–231.
- Bahari, M., Ross, N., & Turnberg, A. (1982). Demonstration of a pH gradient across the mucus layer on the surface of human gastric mucosa in vitro. *Gut*, 23, 513–516.
- Bahr, D., & Kuhnmuensch, N. (2003). *US 6,665,372 B2*. [https://doi.org/10.1016/j.\(73\)](https://doi.org/10.1016/j.(73))
- Bala, K., Tripathy, C., & Sharma, D. (2006). Neuroprotective and anti-ageing effects of curcumin in aged rat brain regions. *Biogerontology*, 7, 81–82. <https://doi.org/10.1007/s10522-006-6495-x>
- Bansil, R., & Turner, S. (2006). Mucin structure, aggregation, physiological functions and biomedical applications. *Current Opinion in Colloid & Interface Science*, 11(2–3), 164–170. <https://doi.org/10.1016/j.cocis.2005.11.001>
- Barkovich, M. (2017). High performance liquid chromatography. *Available at: chem.libretexts.org*.
- Barton, M. (1985). The application of differential scanning calorimetry (DSC) to the study of epoxy resin curing reactions. In *Advances in Polymer Science* (pp. 111–154). https://doi.org/10.1007/3-540-15546-5_5

- Barzegar, A. (2012). The role of electron-transfer and H-atom donation on the superb antioxidant activity and free radical reaction of curcumin. *Food Chemistry*, *135*(3), 1369–1376. <https://doi.org/10.1016/j.foodchem.2012.05.070>
- Basnet, P., & Skalko-basnet, N. (2011). Curcumin: An Anti-Inflammatory Molecule from a Curry Spice on the Path to Cancer Treatment. *Molecules*, *16*, 4567–4598. <https://doi.org/10.3390/molecules16064567>
- Bates, T., Blumenthal, P., & Pieniaszek, J. (1977). Salivary excretion and pharmacokinetics of sulfapyridine after sulfasalazine. *Clinical Pharmacology and Therapeutics*, *22*(6), 917–927.
- Baud, C., Couture, A., Baert, L., Couture, A., Avni, F., Ferran, L., & Veyrac, C. (2008). Gastrointestinal Tract Sonography in Fetuses and Children. Retrieved from <https://books.google.com/books?id=aMeJv8l-3WAC&pgis=1>
- Baun, A., & Hansen, F. (2008). Environmental challenges for nanomedicine. *Nanomedicine*, *3*(5), 605–608.
- Bayat, A., Dorkoosh, A., Dehpour, R., Moezi, L., Larijani, B., Junginger, E., & Rafiee-Tehrani, M. (2008). Nanoparticles of quaternized chitosan derivatives as a carrier for colon delivery of insulin: Ex vivo and in vivo studies. *International Journal of Pharmaceutics*, *356*(1–2), 259–266. <https://doi.org/10.1016/j.ijpharm.2007.12.037>
- Bayomi, M., Mahmoud, E., El-Ashmawy, B., Nasr, A., El-Sherbeny, A., Badria, A., & Abdel-Aziz, I. (2013). Synthesis and biological evaluation of new curcumin derivatives as antioxidant and antitumor agents. *Medicinal Chemistry Research*, *22*, 1147–1162. <https://doi.org/10.1007/s00044-012-0116-9>

- Beaulieu, L., Savoie, L., Paquin, P., & Subirade, M. (2002). Elaboration and characterization of whey protein beads by an emulsification/cold gelation process: Application for the protection of retinol. *Biomacromolecules*, 3(2), 239–248. <https://doi.org/10.1021/bm010082z>
- Bentzen, M. (2006). Preventing or reducing late side effects of radiation therapy: Radiobiology meets molecular pathology. *Nature Reviews Cancer*, 6(9), 702–713. <https://doi.org/10.1038/nrc1950>
- Berman, S., Ryan, P., & Wo, J. (2016). *PDQ® Adult Treatment Editorial Board. PDQ Colon Cancer Treatment*. National Cancer Institute. Retrieved from www.cancer.gov/types/colorectal/hp/colon-treatment-pdq
- Bernabé-pineda, M., Ram, T., Romero-romo, M., González-vergara, E., & Rojas-hernández, A. (2004). Determination of acidity constants of curcumin in aqueous solution and apparent rate constant of its decomposition. *Spectrochimica Acta Part A*, 60, 1091–1097. [https://doi.org/10.1016/S1386-1425\(03\)00342-1](https://doi.org/10.1016/S1386-1425(03)00342-1)
- Bernkop-Schnürch, A. (2005). Thiomers: The next generation of mucoadhesive polymers. *Advanced Drug Delivery Reviews*, 57, 1569–1582. <https://doi.org/10.2165/00137696-200503030-00001>
- Bhaskar, S., Tian, F., Stoeger, T., Kreyling, W., Fuente, J. M. De, Grazú, V., & Razansky, D. (2010). Multifunctional Nanocarriers for diagnostics , drug delivery and targeted treatment across blood-brain barrier : perspectives on tracking and neuroimaging. *Particle and Fibre Toxicology*, 7(3), 1–25.
- Bhatta, S., Chandasana, H., Chhonker, S., Rathi, C., Kumar, D., Mitra, K., & Shukla, K. (2012). Mucoadhesive nanoparticles for prolonged ocular delivery of

natamycin: In vitro and pharmacokinetics studies. *International Journal of Pharmaceutics*, 432(1–2), 105–112.
<https://doi.org/10.1016/j.ijpharm.2012.04.060>

Bhattacharyya, P., Skandalis, A., Ganesh, A., Groden, J., & Meuth, M. (1994). Mutator phenotypes in human colorectal carcinoma cell lines. *Proceedings of the National Academy of Sciences of the United States of America*, 91(July), 6319–6323.
<https://doi.org/10.1073/pnas.91.14.6319>

Bhullar, S., Jha, A., Youssef, D., & Rupasinghe, V. (2013). Curcumin and Its Carbocyclic Analogs: Structure-Activity in Relation to Antioxidant and Selected Biological Properties. *Molecules*, 18, 5389–5404.
<https://doi.org/10.3390/molecules18055389>

Bhutani, K., Bishnoi, M., & Kulkarni, K. (2009). Anti-depressant like effect of curcumin and its combination with piperine in unpredictable chronic stress-induced behavioral, biochemical and neurochemical changes. *Pharmacology Biochemistry and Behavior*, 92(1), 39–43.
<https://doi.org/10.1016/j.pbb.2008.10.007>

Bickel, M., & Kauffman, J. (1981). Gastric gel mucus thickness: effect of distention, 16,16 - dimethyl prostaglandin E 2 and carbenoxolone. *Gastroenterology*, 80(4), 770–775.

Bigucci, F., Luppi, B., Cerchiara, T., Sorrenti, M., Bettinetti, G., Rodriguez, L., & Zecchi, V. (2008). Chitosan/pectin polyelectrolyte complexes: Selection of suitable preparative conditions for colon-specific delivery of vancomycin. *European Journal of Pharmaceutical Sciences*, 35(5), 435–441.

<https://doi.org/10.1016/j.ejps.2008.09.004>

Bilati, U., Allémann, E., & Doelker, E. (2005). Development of a nanoprecipitation method intended for the entrapment of hydrophilic drugs into nanoparticles. *European Journal of Pharmaceutical Sciences*, 24(1), 67–75.
<https://doi.org/10.1016/j.ejps.2004.09.011>

Biology, C., Aggarwal, B., & Harikumar, B. (2009). Potential therapeutic effects of curcumin , the anti-inflammatory agent , against neurodegenerative , cardiovascular , pulmonary , metabolic , autoimmune and neoplastic diseases. *The International Journal of Biochemistry*, 41, 40–59.
<https://doi.org/10.1016/j.biocel.2008.06.010>

Birgisson, H., Pählman, L., Gunnarsson, U., & Glimelius, B. (2005). Adverse Effects of Preoperative Radiation Therapy for Rectal Cancer : Long-Term Follow-Up of the Swedish Rectal Cancer Trial. *Journal of Clinic*, 23(34), 8697–8705.
<https://doi.org/10.1200/JCO.2005.02.9017>

Bisht, S., Khan, A., Bekhit, M., Bai, H., Cornish, T., Mizuma, M., & Anders, A. (2011). A polymeric nanoparticle formulation of curcumin (NanoCurc) ameliorates CCl₄-induced hepatic injury and fibrosis through reduction of pro-inflammatory cytokines and stellate cell activation. *Laboratory Investigation*, 91(9), 1383–1395.
<https://doi.org/10.1038/labinvest.2011.86>

Björnsson, E., & Olsson, R. (2005). Outcome and prognostic markers in severe drug-induced liver disease. *Hepatology*, 42(2), 481–489.
<https://doi.org/10.1002/hep.20800>

Blasi, P., Giovagnoli, S., Schoubben, A., Ricci, M., & Rossi, C. (2007). Solid lipid

- nanoparticles for targeted brain drug delivery. *Advanced Drug Delivery Reviews*, 59(6), 454–477. <https://doi.org/10.1016/j.addr.2007.04.011>
- Boddupalli, M., Mohammed, ZK., Nath, A., & Banji, D. (2010). Mucoadhesive drug delivery system: An overview. *Journal of Advanced Pharmaceutical Technology and Research*, 1(4), 381–387.
- Boga, C., Delpivo, C., Ballarin, B., Morigi, M., Galli, S., Micheletti, G., & Tozzi, S. (2013). Investigation on the dyeing power of some organic natural compounds for a green approach to hair dyeing. *Dyes and Pigments*, 97(1), 9–18. <https://doi.org/10.1016/j.dyepig.2012.11.020>
- Bogner, A., Jouneau, H., Thollet, G., Basset, D., & Gauthier, C. (2007). A history of scanning electron microscopy developments: Towards “wet-STEM” imaging. *Micron*, 38(4), 390–401. <https://doi.org/10.1016/j.micron.2006.06.008>
- Boonsongrit, Y., Mitrevej, A., & Mueller, W. (2006). Chitosan drug binding by ionic interaction. *European Journal of Pharmaceutics and Biopharmaceutics*, 62(3), 267–274. <https://doi.org/10.1016/j.ejpb.2005.09.002>
- Bootz, A., Vogel, V., Schubert, D., & Kreuter, J. (2004). Comparison of scanning electron microscopy, dynamic light scattering and analytical ultracentrifugation for the sizing of poly(butyl cyanoacrylate) nanoparticles. *European Journal of Pharmaceutics and Biopharmaceutics*, 57(2), 369–375. [https://doi.org/10.1016/S0939-6411\(03\)00193-0](https://doi.org/10.1016/S0939-6411(03)00193-0)
- Borchard, G. (2001). Chitosans for gene delivery. *Advanced Drug Delivery Reviews*, 52(2), 145–150. [https://doi.org/10.1016/S0169-409X\(01\)00198-3](https://doi.org/10.1016/S0169-409X(01)00198-3)
- Bornstein, A., Recht, A., Connolly, L., Schnitt, J., Cady, B., Koufman, C., & Harris, J.

- R. (1991). Results of treating ductal carcinoma in situ of the breast with conservative surgery and radiation therapy. *Cancer*, 67(1), 7–13. [https://doi.org/10.1002/1097-0142\(19910101\)67:1<7::AID-CNCR2820670103>3.0.CO;2-B](https://doi.org/10.1002/1097-0142(19910101)67:1<7::AID-CNCR2820670103>3.0.CO;2-B)
- Bouchemal, K., Briançon, S., Fessi, H., Chevalier, Y., Bonnet, I., & Perrier, E. (2006). Simultaneous emulsification and interfacial polycondensation for the preparation of colloidal suspensions of nanocapsules. *Materials Science and Engineering C*, 26(2–3), 472–480. <https://doi.org/10.1016/j.msec.2005.10.022>
- Bouchemal, K., Briançon, S., Perrier, E., & Fessi, H. (2008). Nano-emulsion formulation using spontaneous emulsification: solvent, oil and surfactant optimisation. *Journal of Pharmacy and Pharmaceutical Sciences*, 11(1), 104–130. <https://doi.org/10.1016/j.ijpharm.2004.05.016>
- Bowman, K, Leong, K. (2006). Chitosan Nanoparticles for Oral Drug and Gene Delivery. *International Journal of Nanomedicine*, 1(2), 117–128.
- Braun, L., & Cohen, M. (2010). *Herbs and Natural Supplements Inking: An Evidence-Based Guide* (3rd ed.). Elsevier Australia.
- Bravo-Osuna, I., Vauthier, C., Farabollini, A., Palmieri, G. F., & Ponchel, G. (2007). Mucoadhesion mechanism of chitosan and thiolated chitosan-poly(isobutyl cyanoacrylate) core-shell nanoparticles. *Biomaterials*, 28(13), 2233–2243. <https://doi.org/10.1016/j.biomaterials.2007.01.005>
- Brown, G. (2007a). Colorectal Cancer. *Cambridge University Press*, 1, 15-33
- Brown, G. (2007b). Contemporary Issues in Cancer Imaging: Colorectal Cancer., (October), 5-10.

- Buhl, K., Frohmu, S., Herbay, A., Dueck, M., & Schlag, M. (1999). Original Paper Reduction of Chemotherapy-induced Side-effect by Parenteral Glutamine Supplementation in Patients with Metastatic Colorectal Cancer, *35*(2), 202–207.
- Burgess, R. (2009). Protein Precipitation Techniques. *Methods in Enzymology*, *463*, 331–342. Elsevier Inc. [https://doi.org/10.1016/S0076-6879\(09\)63020-2](https://doi.org/10.1016/S0076-6879(09)63020-2)
- Cabrera, H., & Kataoka, K. (2014). Progress of drug-loaded polymeric micelles into clinical studies. *Journal of Controlled Release*, *190*, 465–476.
- Calvo, P., & Remunan-Lopez, C. (1997). Novel hydrophilic chitosan-polyethylene oxide nanoparticles as protein carriers. *Journal of Applied sciences*, 125–132. [https://doi.org/10.1002/\(SICI\)1097-4628\(19970103\)63:1<125::AID-APP13>3.0.CO;2-4](https://doi.org/10.1002/(SICI)1097-4628(19970103)63:1<125::AID-APP13>3.0.CO;2-4)
- Canny, O., & McCormick, A. (2008). Bacteria in the intestine, helpful residents or enemies from within? *Infection and Immunity*, *76*(8), 3360–3373. <https://doi.org/10.1128/IAI.00187-08>
- Carbajal, D., Molina, V., Noa, M., Valdés, S., Arruzazabala, L., Aguilar, C., & Más, R. (2000). Effect of D-002 on gastric mucus composition in ethanol-induced ulcer. *Pharmacological Research : The Official Journal of the Italian Pharmacological Society*, *42*(4), 329–332. <https://doi.org/10.1006/phrs.2000.0693>
- Carroll, E., Benya, V, Turgeon, K., Vareed, S., Neuman, M., Rodriguez, L., & Brenner, E. (2011). Phase IIa Clinical Trial of Curcumin for the Prevention of Colorectal Neoplasia. *Cancer Prevention Research*, *4*(March), 1-20. <https://doi.org/10.1158/1940-6207.CAPR-10-0098>
- Carvalho, C., Bruschi, L., Evangelista, C., & Gremiao, D. (2010). Mucoadhesive Drug

Delivery Systems. *Brazilian Journal of Pharmaceutical Sciences*, 46(1), 1–17.

<https://doi.org/10.3109/03639049709148498>

WHO media center. (2014). Available at: www.who.org

Chamberlain, J. (1995). The analysis of drugs in biological fluids. *CRC Press*, 2, 139–163.

Chan, M., Valencia, M., Zhang, L., Langer, R., & Farokhzad, C. (2010). polymeric nanoparticles for drug delivery. *Cancer Nanotechnology: Methods and Protocols* 11, 163–164.

Chan, M., Huang, H., & Fenton, R. (1998). In Vivo Inhibition of Nitric Oxide Synthase Gene Expression by Curcumin , a Cancer Preventive Natural Product with Anti-Inflammatory Properties. *Biochemical Pharmacology*, 55(98), 1955–1962.

Chang, S., Ji, Q., Zhang, J., & El-Shourbagy, A. (2007). Historical Review of Sample Preparation for Chromatographic Bioanalysis: Pros and Cons. *Drug Development Research*, 68, 107–133. <https://doi.org/10.1002/ddr>

Chang, Y., Peng, F., Lee, Y., Lu, C., Tsai, C., Shieh, M., & Yang, S. (2013). Curcumin-loaded nanoparticles induce apoptotic cell death through regulation of the function of MDR1 and reactive oxygen species in cisplatin-resistant CAR human oral cancer cells. *International Journal of Oncology*, 43(4), 1141–1150. <https://doi.org/10.3892/ijo.2013.2050>

Charehsaz, M., Gürbay, A., Aydın, A., & Şahin, G. (2014). Simple , Fast and Reliable Liquid Chromatographic and Spectrophotometric Methods for the Determination of Theophylline in Urine , Saliva and Plasma Samples. *Iranian Journal of Pharmaceutical Sciences*, 13(May 2013), 431–439.

- Chattopadhyay, I., Biswas, K., Bandyopadhyay, U., & Banerjee, K. (2004). Turmeric and curcumin : Biological actions and medicinal applications. *Current Science*, 87(1), 44–53.
- Chauhan, A., & Chauhan, P. (2014). Powder XRD Technique and its Applications in Science and Technology. *Journal of Analytical & Bioanalytical Techniques*, 5(5), 1–5. <https://doi.org/10.4172/2155-9872.1000212>
- Chen, L., & Subirade, M. (2005). Chitosan/B-lactoglobulin core-shell nanoparticles as nutraceutical carriers. *Biomaterials*, 26(30), 6041–6053. <https://doi.org/10.1016/j.biomaterials.2005.03.011>
- Chen, W., Deng, S., Zhou, B., Yang, L., & Liu, Z. (2006). Curcumin and its analogues as potent inhibitors of low density lipoprotein oxidation : H-atom abstraction from the phenolic groups and possible involvement of the 4-hydroxy-3-methoxyphenyl groups. *Free Radical Biology & Medicine*, 40, 526–535. <https://doi.org/10.1016/j.freeradbiomed.2005.09.008>
- Cheng, L., Hsu, H., Lin, K., Hsu, M., Ho, F., & Shen, S. (2001). Phase I clinical trial of curcumin , a chemopreventive agent , in patients with high- risk or pre-malignant lesions. *Anticancer Research*, 21, 2895–2900.
- Cheng, K., Yeung, F., Ho, W., Chow, F., Chow, L., & Baum, L. (2013). Highly Stabilized Curcumin Nanoparticles Tested in an In Vitro Blood–Brain Barrier Model and in Alzheimer’s Disease Tg2576 Mice. *The AAPS Journal*, 15(2), 324–336. <https://doi.org/10.1208/s12248-012-9444-4>
- Cheng, Y., Xu, Z., Ma, M., & Xu, T. (2008). Dendrimers as Drug Carriers : Applications in Different Routes of Drug Administration. *Journal of*

Pharmaceutical Sciences, 97(1), 123–143. <https://doi.org/10.1002/jps>

Chickering, E., & Mathiowitz, E. (1999). Bioadhesive Drug Delivery Systems: Fundamentals, Novel Approaches, and development. *Marcel Dekker Inc.*, 98, 1-8.

Cho, K., Wang, X., Nie, S., Chen, G., & Shin, M. (2008). Therapeutic Nanoparticles for Drug Delivery in Cancer. *Clinical Cancer Research*, 14(5), 1310–1317. <https://doi.org/10.1158/1078-0432.CCR-07-1441>

Choudhary, A. Steps for HPLC Method Development: Pharmaceutical Guidelines. Available at: <https://www.pharmaguideline.com/2015/10/procedure-to-develop-hplc-method.html>

Chourasia, K., & Jain, K. (2003). Pharmaceutical approaches to colon targeted drug delivery systems. *Journal of Pharmacy and Pharmaceutical Sciences*, 6(1), 33–66.

Christie, W. (1992). Detectors for high-performance liquid chromatography of lipids with special reference to evaporate light-scattering detection. *Advances in Lipid Methodology—One*, 239–271.

Chuah, H., Billa, N., Roberts, J., Burley, C., & Manickam, S. (2011). Curcumin-containing chitosan nanoparticles as a potential mucoadhesive delivery system to the colon. *Pharmaceutical Development and Technology*, 18(November 2011), 1–9. <https://doi.org/10.3109/10837450.2011.640688>

Chungi, S., Rekhi, S., & Shargel, L. (1989). A simple and rapid chromatographic method for the determination of major metabolites of sulfasalazine in biological fluids. *Journal of Pharmaceutical Sciences*, 78(3), 235–238.

- Clogston, D., & Patri, K. (2011). Zeta potential measurement. *characterization of nanoparticles intended for drug delivery*, 697,63–67.
- Coates, A., Abraham, S., Kaye, B., Sowerbutts, T., Frewin, C., Fox, M., & Tattersall, N. (1983). On the receiving end-patient perception of the side-effects of cancer chemotherapy. *European Journal of Cancer & Clinical Oncology*, 19(2), 203–208.
- Cohen, L., Hack, F., Moor, C, Katz, J., & Goss, E. (2000). The Effects of Type of Surgery and Time on Psychological Adjustment in Women After Breast Cancer Treatment, 7(6), 427–434.
- Cole, M., Teter, B., & Frautschy, A. (2007). Neuroprotective effects of curcumin. *The Molecular Targets and Therapeutic uses of curcumin in Health and Diseases*, 6, 197–198.
- Complexes, M., Curcumin, F., For, E., Radical, E., Ability, S., & Activity, N. (2003). Manganese complexes of curcumin and its derivatives: evaluation for the radical scavenging ability and neuroprotective activity. *Free Radical Biology and Medicine*, 35(12), 1632–1644.
<https://doi.org/10.1016/j.freeradbiomed.2003.09.011>
- Conlan, S., Pisano, S., Oliveira, I., Ferrari, M., & Mendes I. (2017). Exosomes as Reconfigurable Therapeutic Systems. *Trends in Molecular Medicine*, 23(7), 636–650. <https://doi.org/10.1016/j.molmed.2017.05.003>
- Connell, O., Maggard, A., & Ko, Y. (2004). Colon Cancer Survival Rates With the New American, 96(19), 6–11. <https://doi.org/10.1093/jnci/djh275>
- Coradini, K., Lima, O., Oliveira, M., Chaves, S., Athayde, L., Carvalho, M., & Beck,

- R. (2014). Co-encapsulation of resveratrol and curcumin in lipid-core nanocapsules improves their in vitro antioxidant effects. *European Journal of Pharmaceutics and Biopharmaceutics*, 88(1), 178–185. <https://doi.org/10.1016/j.ejpb.2014.04.009>
- Crawford, C., Vasey, A., Paul, J., Hay, A., Davis, A., & Kaye, B. (2005). Does Aggressive Surgery Only Benefit Patients With Less Advanced Ovarian Cancer? Results From an International Comparison Within the SCOTROC-1 Trial. *Journal of Clinical Oncology*, 23(34), 8802–8811. <https://doi.org/10.1200/JCO.2005.02.1287>
- Cui, J., Yu, B., Zhao, Y., Zhu, W., Li, H., Lou, H., & Zhai, G. (2009). Enhancement of oral absorption of curcumin by self-microemulsifying drug delivery systems. *International Journal of Pharmaceutics*, 371, 148–155. <https://doi.org/10.1016/j.ijpharm.2008.12.009>
- Cui, L., Miao, J., & Cui, L. (2007). Cytotoxic Effect of Curcumin on Malaria Parasite *Plasmodium falciparum*: Inhibition of Histone Acetylation and Generation of Reactive Oxygen Species. *Antimicrobial Agents and Chemotherapy*, 51(2), 488–494. <https://doi.org/10.1128/AAC.01238-06>
- Cutsem, E., Lenz, H., Köhne, C., Heinemann, V., Tejpar, S., & Melezínek, I. (2015). Fluorouracil, Leucovorin, and Irinotecan Plus Cetuximab Treatment and RAS Mutations in Colorectal Cancer. *Journal of Clinical Oncology*, 33(7), 692–702. <https://doi.org/10.1200/JCO.2014.59.4812>
- Dallas, P., Niarchos, D., Vrbanic, D., Boukos, N., Pejovnik, S., Trapalis, C., & Petridis, D. (2007). Interfacial polymerization of pyrrole and in situ synthesis of

- polypyrrole/silver nanocomposites. *Polymer*, 48(7), 2007–2013.
<https://doi.org/10.1016/j.polymer.2007.01.058>
- Dandawate, R., Vyas, A., Ahmad, A., Banerjee, S., Deshpande, J., & Swamy, V. (2012). Inclusion Complex of Novel Curcumin Analogue CDF and β - Cyclodextrin (1 : 2) and Its Enhanced In Vivo Anticancer Activity Against Pancreatic Cancer. *Pharmaceutical Research*, 29, 1775–1786.
<https://doi.org/10.1007/s11095-012-0700-1>
- Dandekar, P., Jain, R., Patil, S., Dhumal, R., Tiwari, D., Sharma, S., & Patravle, V. (2010). Curcumin- loaded hydrogel nanoparticles: application in anti-malarial therapy and toxicological evaluation. *Pharmaceutical Nanotechnology*, 99(12), 4992–5010. <https://doi.org/10.1002/jps>
- Daniel, S., Limson, L., Dairam, A., Watkins, M., & Daya, S. (2004). Through metal binding , curcumin protects against lead- and cadmium-induced lipid peroxidation in rat brain homogenates and against lead-induced tissue damage in rat brain. *Journal of Inorganic Biochemistry*, 98, 266–275.
<https://doi.org/10.1016/j.jinorgbio.2003.10.014>
- Das, K., Kasoju, N., & Bora, U. (2010). Encapsulation of curcumin in alginate-chitosan-pluronic composite nanoparticles for delivery to cancer cells. *Nanomedicine: Nanotechnology, Biology, and Medicine*, 6(1), 153–160.
<https://doi.org/10.1016/j.nano.2009.05.009>
- Daykin, A., Foxall, D., Connor, C., Lindon, C., & Nicholson, K. (2002). The Comparison of Plasma Deproteinization Methods for the Detection of Low-Molecular-Weight Metabolites by ^1H Nuclear Magnetic Resonance Spectroscopy.

Analytical Biochemistry, 304(2), 220–230.
<https://doi.org/10.1006/abio.2002.5637>

de Pinho Neves, L., Milioli, C., Müller, L., Riella, G., Kuhnen, C., & Stulzer, K. (2014). Factorial design as tool in chitosan nanoparticles development by ionic gelation technique. *Colloids and Surfaces A: Physicochemical and Engineering Aspects*, 445, 34–39. <https://doi.org/10.1016/j.colsurfa.2013.12.058>

De, R., Kundu, P., Swarnakar, S., Ramamurthy, T., Chowdhury, A., Nair, B., & Mukhopadhyay, K. (2009). Antimicrobial Activity of Curcumin against *Helicobacter pylori* Isolates from India and during Infections in Mice. *American Society of Microbiology*, 53(4), 1592–1597. <https://doi.org/10.1128/AAC.01242-08>

Dearnaley, P., Khoo, S., Norman, R., Meyer, L., Nahum, A., Tait, D., & Horwich, A. (1999). Comparison of radiation side-effects of conformal and conventional radiotherapy in prostate cancer: A randomised trial. *Lancet*, 353(9149), 267–272. [https://doi.org/10.1016/S0140-6736\(98\)05180-0](https://doi.org/10.1016/S0140-6736(98)05180-0)

Deng, L., Gui, Z., Zhao, L., Wang, J., & Shen, L. (2012). Diabetes Mellitus and the Incidence of Colorectal Cancer: An Updated Systematic Review and Meta-Analysis. *Digestive Diseases and Sciences*, *Digestive Diseases and Sciences*, 57, 1576–1585

des Rieux, A., Fievez, V., Garinot, M., Schneider, J., & Pr eat, V. (2006). Nanoparticles as potential oral delivery systems of proteins and vaccines: A mechanistic approach. *Journal of Controlled Release*, 116(1), 1–27. <https://doi.org/10.1016/j.jconrel.2006.08.013>

- Dhar, S., Gu, X., Langer, R., Farokhzad, C., & Lippard, J. (2008). Targeted delivery of cisplatin to prostate cancer cells by aptamer functionalized Pt(IV) prodrug-PLGA-PEG nanoparticles. *Proceedings of the National Academy of Sciences of the United States of America*, *105*(45), 17356–17361. <https://doi.org/10.1073/pnas.0809154105>
- Dhillon, N., Aggarwal, B., Newman, A., Wolff, A., Kunnumakkara, B., Abbruzzese, J. L., & Kurzrock, R. (2008). Cancer Therapy : Clinical Phase II T rial of Curcumin in Patients with Advanced Pancreatic Cancer. *Cance Therapy: Clinical*, *14*(16), 4491–4500. <https://doi.org/10.1158/1078-0432.CCR-08-0024>
- Dodane, V., & Vilivalam, D. (1998). Pharmaceutical applications of Chitosan. *Reviews*, *1*(6), 246–253.
- Dodou, D., Breedveld, P., & Wieringa, A. (2005). Mucoadhesives in the gastrointestinal tract: Revisiting the literature for novel applications. *European Journal of Pharmaceutics and Biopharmaceutics*, *60*(1), 1–16. <https://doi.org/10.1016/j.ejpb.2005.01.007>
- Dolan, W. (2012). When should an internal standard be used? *LCGC*, *30*(5), 474–480. <https://doi.org/http://www.chromacademy.com/ajax/create-key-read-file.asp?keycode=778040&sFullpath=http://www.chromatographyonline.com/lcgc/Column: LC Troubleshooting/When-Should-an-Internal-Standard-be-Used/ArticleStandard/Article/detail/778040>
- Drexler, G., & Uphoff, C. (2002). Mycoplasma contamination of cell cultures: Incidence, sources, effects, detection, elimination, prevention. *Cytotechnology*, *39*(2), 75–90. <https://doi.org/10.1023/A:1022913015916>

- Duan, J., Zhang, Y., Han, S., Chen, Y., Li, B., Liao, M., & Huang, B. (2010). Synthesis and in vitro / in vivo anti-cancer evaluation of curcumin-loaded chitosan / poly (butyl cyanoacrylate) nanoparticles, *400*, 211–220. <https://doi.org/10.1016/j.ijpharm.2010.08.033>
- Dukes, E., Ahn, B., Cheruku, R., Cantor, D., Rennel, E., Fredriksson, S., & Gangura, G. (1932). The classification of cancer of the rectum. *The Journal of Pathology and Bacteriology*, *35*(3), 323–332. <https://doi.org/10.1002/path.1700350303>
- Dutta, K., & Sahu, S. (2012). Development of diclofenac sodium loaded magnetic nanocarriers of pectin interacted with chitosan for targeted and sustained drug delivery. *Colloids and Surfaces B: Biointerfaces*, *97*, 19–26. <https://doi.org/10.1016/j.colsurfb.2012.04.030>
- Eaden, A., Abrams, R., & Mayberry, F. (2001). The risk of colorectal cancer in ulcerative colitis: a meta-analysis. *Gut*, *48*(4), 526–35. <https://doi.org/10.1136/gut.48.4.526>
- El-Aasser, , Lack, D., Vanderhoff, W., & Fowkes, F. (1988). The Miniemulsification Process-Different Form of Spontaneous Emulsification. *Colloids and Surfaces*, *29*, 103–118.
- Elmore, S. (2007). Apoptosis : A Review of Programmed Cell Death. *Toxicologic Pathology*, *35*, 495–516. <https://doi.org/10.1080/01926230701320337>
- Emanuele, D., & Attwood, D. (2005). Dendrimer – drug interactions. *Advanced Drug Delivery Reviews*, *57*, 2147–2162. <https://doi.org/10.1016/j.addr.2005.09.012>
- Engelhardt, H. (1979). High Performance Liquid Chromatography. *Chromatographia*, *14*, 325-332.

- Engin, O. (2015). Colon polyps and the prevention of colorectal cancer. <https://doi.org/10.1007/978-3-319-17993-3>
- Epstein, J., Sanderson, R., & Macdonald, T. (2017). Curcumin as a therapeutic agent : the evidence from in vitro , animal and human studies. *British Journal of Nutrition*, (2010), 1545–1557. <https://doi.org/10.1017/S0007114509993667>
- Esfand, R., & Tomalia, A. (2001). Poly (amidoamine) (PAMAM) dendrimers : from biomimicry to drug delivery and biomedical applications. *Research Focus*, 6(8), 427–436.
- Evans, F., Pye, G., Bramley, R., Clark, G., Dyson, J., & Hardcastle, D. (1988). Measurement of gastrointestinal pH profiles in normal ambulant human subjects. *Gut*, 29(8), 1035–41. <https://doi.org/10.1136/gut.29.8.1035>
- Fan, W., Yan, W., Xu, Z., & Ni, H. (2012). Formation mechanism of monodisperse, low molecular weight chitosan nanoparticles by ionic gelation technique. *Colloids and Surfaces B: Biointerfaces*, 90, 21–27. <https://doi.org/10.1016/j.colsurfb.2011.09.042>
- Farokhzad, C., & Langer, R. (2006). Nanomedicine: Developing smarter therapeutic and diagnostic modalities. *Advanced Drug Delivery Reviews*, 58, 1456–1459. <https://doi.org/10.1016/j.addr.2006.09.011>
- Farrell, C., Brearley, G., Pilling, M., & Molassiotis, A. (2013). The impact of chemotherapy-related nausea on patients' nutritional status, psychological distress and quality of life. *Supportive Care in Cancer*, 21(1), 59–66. <https://doi.org/10.1007/s00520-012-1493-9>
- Fatima, H., & Robin, B. (2009). Colorectal Cancer Epidemiology: Incidence, Mortality,

Survival, and Risk Factors. *Clinics in Colon and Rectal Surgery*.

FDA (2018). FDA In Brief: FDA approves new use of Exparel for nerve block pain relief following shoulder surgeries. Retrieved from <http://search.ebscohost.com/login.aspx?direct=true&AuthType=ip,shib&db=jlh&AN=111511302&site=ehost-live&scope=site>

Fedirko, V., Tramacere, I., Bagnardi, V., Rota, M., Scotti, L., Islami, F., & Jenab, M. (2011). Alcohol drinking and colorectal cancer risk: An overall and dose-Response meta-analysis of published studies. *Annals of Oncology*, 22(9), 1958–1972. <https://doi.org/10.1093/annonc/mdq653>

Ferrari, M. (2005). Cancer nanotechnology: Opportunities and challenges. *Nature Reviews Cancer*, 5(3), 161–171. <https://doi.org/10.1038/nrc1566>

Fessi, H., Application, F., & Data, P. (1992). Process for the preparation of dispersible colloidal systems of amphiphilic lipids in the form of oligolamellar liposomes of submicron dimensions. Patent US 5174930 A

Fessi, H., Puisieux, F., Devissaguet, P., Ammoury, N., & Benita, S. (1989). Nanocapsule formation by interfacial polymer deposition following solvent displacement. *International Journal of Pharmaceutics*, 55(1), 1–4. [https://doi.org/10.1016/0378-5173\(89\)90281-0](https://doi.org/10.1016/0378-5173(89)90281-0)

Finegold, M., & Angeles, L. (1969). Intestinal bacteria. The role they play in normal physiology, pathologic physiology, and infection. *California Medicine*, 110(6), 455–9. Retrieved from <http://www.pubmedcentral.nih.gov/articlerender.fcgi?artid=1503548&tool=pmc.ncbi&rendertype=abstract>

- Fitzpatrick, J., & McClelland, M. (1983). A simple rapid method for determining theophylline in serum by HPLC. *Annals Clinical Biochemistry*, *20*, 123–126.
<https://doi.org/10.1177/000456328302000213>
- Flemstrom, G., & Kivilaakso, E. (1983). Demonstration of a pH gradient at the luminal surface of rat duodenum in vivo and its dependence on mucosal alkaline secretion. *Gastroenterology*, *84*(4), 787–794. Retrieved from <http://www.ncbi.nlm.nih.gov/pubmed/6572163>
- Frixen, H., Behrens, J., Sachs, M., Eberle, G., Voss, B., Warda, A., & Birchmeier, W. (1991). E-Cadherin-Mediated Cell Cell-Adhesion Prevents Invasiveness of Human Carcinoma-Cells. *Journal of Cell Biology*, *113*(1), 173–185.
<https://doi.org/10.1083/jcb.113.1.173>
- Froehlich, E. (2016). The role of surface charge in cellular uptake and cytotoxicity of medical nanoparticles. *International Journal of Nanomedicine*, (February), 5577–5591. <https://doi.org/10.2147/IJN.S36111>
- Galindo-rodriguez, S., Alle, E., Fessi, H., & Doelker, E. (2004). Physicochemical Parameters Associated with Nanoparticle Formation in the Salting-out , Nanoprecipitation Methods. *Pharmaceutical Research*, *21*(8), 1428–1439.
<https://doi.org/10.1023/B:PHAM.0000036917.75634.be>
- Gamba, A., Romano, M., Grosso, M., Tamburini, M., Cantu, G., Molinari, R., & Ventafridda, V. (1992). Psychosocial adjustment of patients surgically treated for head and neck cancer. *Head & Neck*, *14*(3), 218–223. Retrieved from <http://www.ncbi.nlm.nih.gov/pubmed/1587739>
- Gan, Q., Wang, T., Cochrane, C., & McCarron, P. (2005). Modulation of surface

- charge, particle size and morphological properties of chitosan-TPP nanoparticles intended for gene delivery. *Colloids and Surfaces B: Biointerfaces*, 44(2–3), 65–73. <https://doi.org/10.1016/j.colsurfb.2005.06.001>
- Gandin, V., Pellei, M., Tisato, F., Porchia, M., Santini, C., & Marzano, C. (2012). A novel copper complex induces paraptosis in colon cancer cells via the activation of ER stress signalling. *Journal of Cellular and Molecular Medicine*, 16(1), 142–151. <https://doi.org/10.1111/j.1582-4934.2011.01292.x>
- Gao, N., Neutel, I., & Wai, E. (2008). Gender differences in colorectal cancer incidence, mortality, hospitalizations and surgical procedures in Canada. *Journal of Public Health (Oxford, England)*, 30(2), 194–201. <https://doi.org/10.1093/pubmed/fdn019>
- Garcea, G., Jones, L., Singh, R., Dennison, R., Farmer, B., Sharma, A., & Berry, P. (2004). Detection of curcumin and its metabolites in hepatic tissue and portal blood of patients following oral administration. *British Journal of Cancer*, 90(5), 1011–1015. <https://doi.org/10.1038/sj.bjc.6601623>
- Gaucher, G., Dufresne, H., Sant, P., Kang, N., Maysinger, D., & Leroux, C. (2005). Block copolymer micelles: Preparation, characterization, and applications in drug delivery. *Journal of Controlled Release*, 109, 169–188.
- Gelperina, S., Kisich, K., Iseman, D., & Heifets, L. (2005). The potential advantages of nanoparticle drug delivery systems in chemotherapy of tuberculosis. *American Journal of Respiratory and Critical Care Medicine*, 172(12), 1487–1490. <https://doi.org/10.1164/rccm.200504-613PP>
- George, M., & Abraham, E. (2006). Polyionic hydrocolloids for the intestinal delivery

- of protein drugs: Alginate and chitosan - a review. *Journal of Controlled Release*, 114(1), 1–14. <https://doi.org/10.1016/j.jconrel.2006.04.017>
- Ghulam A. Shabir. (2004). HPLC Method Development and Validation for Pharmaceutical Analysis. *Journal of Chromatography A*, 987 (2003) 57–66. Retrieved from <http://www.pharmtech.com/hplc-method-development-and-validation-pharmaceutical-analysis>
- Gill, P., Moghadam, T., & Ranjbar, B. (2010). Differential scanning calorimetry techniques: applications in biology and nanoscience. *Journal of Biomolecular Techniques : JBT*, 21(4), 167–193. Retrieved from [/pmc/articles/PMC2977967/?report=abstract](http://pubmed.ncbi.nlm.nih.gov/2977967/)
- Gill, S., Sauerbrunn, R., & Reading, M. (1993). Modulated Differential scanning calorimetry. *Journal of Thermal Analysis*, 40, 931–932.
- Gillies, R., & Fréchet, J. (2005). Dendrimers and dendritic polymers in drug delivery. *Drug Discovery Today*, 10(1), 35–41.
- Girard, E., Girard, D., English, R., Gootz, D., Cimochoowski, R., Faiella, A., & Retsema, A. (1987). Pharmacokinetic and in vivo studies with azithromycin (CP-62,993), a new macrolide with an extended half-life and excellent tissue distribution. *Antimicrobial Agents and Chemotherapy*, 31(12), 1948–1954. <https://doi.org/10.1128/AAC.31.12.1948>
- Goebel, H. (1994). X-ray diffractometer. Germany. US Patent US5373544A
- Goel, A., Boland, R., & Chauhan, P. (2001). Specific inhibition of cyclooxygenase-2 (COX-2) expression by dietary curcumin in HT-29 human colon cancer cells. *Cancer Letters*, 172(2), 111–118. <https://doi.org/S0304383501006553> [pii]

- Gómez-Gaete, C., Tsapis, N., Besnard, M., Bochot, A., & Fattal, E. (2007). Encapsulation of dexamethasone into biodegradable polymeric nanoparticles. *International Journal of Pharmaceutics*, 331(2), 153–159. <https://doi.org/10.1016/j.ijpharm.2006.11.028>
- Gopi, D., Kanimozhi, K., Bhuvaneshwari, N., Indira, J., & Kavitha, L. (2014). Novel banana peel pectin mediated green route for the synthesis of hydroxyapatite nanoparticles and their spectral characterization. *Spectrochimica Acta - Part A: Molecular and Biomolecular Spectroscopy*, 118, 589–597. <https://doi.org/10.1016/j.saa.2013.09.034>
- Gou, M., Men, K., Shi, H., Xiang, M., Zhang, J., Song, J., & Qian, Z. (2011). Curcumin-loaded biodegradable polymeric micelles for colon cancer therapy in vitro and in vivo. *Nanoscale*, 3, 1558–1567.
- Govender, T., Stolnik, S., Garnett, C., Illum, L., & Davis, S. (2016). PLGA nanoparticles prepared by nanoprecipitation : Drug loading and release studies of a water soluble drug. *Journal of Controlled Release*, 57(November), 171–185. [https://doi.org/10.1016/S0168-3659\(98\)00116-3](https://doi.org/10.1016/S0168-3659(98)00116-3)
- Grabovac, V., Gugli, D., & Bernkop-Schnürch, A. (2005). Comparison of the mucoadhesive properties of various polymers. *Advanced Drug Delivery Reviews*, 57(11), 1713–1723. <https://doi.org/10.1016/j.addr.2005.07.006>
- Gref, R., Lück, M., Quellec, P., Marchand, M., Dellacherie, E., Harnisch, S., & Müller, R. H. (2000). “Stealth” corona-core nanoparticles surface modified by polyethylene glycol (PEG): Influences of the corona (PEG chain length and surface density) and of the core composition on phagocytic uptake and plasma

- protein adsorption. *Colloids and Surfaces B: Biointerfaces*, 18(3–4), 301–313.
[https://doi.org/10.1016/S0927-7765\(99\)00156-3](https://doi.org/10.1016/S0927-7765(99)00156-3)
- Gregoriadis, G., & Florence, T. (1993). Liposomes in Drug Delivery. *Drugs*, 45(1), 15–28. <https://doi.org/10.2165/00003495-199345010-00003>
- Groopman, E., & Itri, M. (1999). Chemotherapy-induced anemia in adults: incidence and treatment. *Journal of the National Cancer Institute*, 91(19), 1616–1634.
<https://doi.org/10.1093/jnci/91.19.1616>
- Gu, G., Xia, H., Pang, Z., Liu, Z., Jiang, X., & Chen, J. (2011). Determination of sulphasalazine and its main metabolite sulphapyridine and 5-aminosalicylic acid in human plasma by liquid chromatography / tandem mass spectrometry and its application to a pharmacokinetic study. *Journal of Chromatography B*, 879(5–6), 449–456. <https://doi.org/10.1016/j.jchromb.2010.12.034>
- Gupta, B., Harpaz, N., Itzkowitz, S., Hossain, S., Matula, S., Kornbluth, A., & Ullman, T. (2007). {A figure is presented} Histologic Inflammation Is a Risk Factor for Progression to Colorectal Neoplasia in Ulcerative Colitis: A Cohort Study. *Gastroenterology*, 133(4), 1099–1105.
<https://doi.org/10.1053/j.gastro.2007.08.001>
- Gupta, V., Aseh, A., Ríos, N., Aggarwal, B., & Mathur, B. (2009). Fabrication and characterization of silk fibroin - derived curcumin nanoparticles for cancer therapy. *International Journal of Nanomedicine*, 4, 115–122.
<https://doi.org/10.2147/IJN.S5581>
- Ha, T., Le, H., Hoang, N., Huong Le, T., Duong, Q., Ha Tran, H., & Nguyen, P. (2012). Preparation and anti-cancer activity of polymer-encapsulated curcumin

- nanoparticles. *Advances in Natural Sciences: Nanoscience and Nanotechnology*, 3(3), 1–7. <https://doi.org/10.1088/2043-6262/3/3/035002>
- Ha, T., Le, H., Hoang, N., Le, H., Duong, Q., Tran, H., & Nguyen, P. (2012). Preparation and anti-cancer activity of polymer-encapsulated curcumin nanoparticles. *Advances in Natural Sciences: Nanoscience and Nanotechnology*, 3(3), 1–8. <https://doi.org/10.1088/2043-6262/3/3/035002>
- Hall, G., Smukste, I., Bresciano, R., Wang, Y., McKearn, D., & Savage, E. (2012). Identifying and Overcoming Matrix Effects in Drug Discovery and Development. *Tandem Mass Spectrometry - Application and Principles, 2012*, 389–420
- Halliwell, B. (2012). Free radicals and antioxidants: updating a personal view. *Nutrition Reviews*, 70(5), 257–265. <https://doi.org/10.1111/j.1753-4887.2012.00476.x>
- Hamidi, M., Azadi, A., & Rafiei, P. (2008). Hydrogel nanoparticles in drug delivery. *Advanced Drug Delivery Reviews*, 60(15), 1638–1649. <https://doi.org/10.1016/j.addr.2008.08.002>
- Han, R., Zhu, J., Wang, R., Wang, S., & Liao, H. (2011). A simple RP-HPLC method for the simultaneous determination of curcumin and its prodrug, curcumin didecanoate, in rat plasma and the application to pharmacokinetic study. *Biomedical Chromatography*, 25(10), 1144–1149. <https://doi.org/10.1002/bmc.1584>
- Hans, L., & Lowman, M. (2002). Biodegradable nanoparticles for drug delivery and targeting. *Current Opinion in Solid State and Materials Science*, 6(September), 319–327.

- Hatcher, H., Planalp, R., Cho, J., Torti, M., & Torti, V. (2008). Review Curcumin : From ancient medicine to current clinical trials. *Cellular and Molecular Life Sciences*, *65*, 1631–1652. <https://doi.org/10.1007/s00018-008-7452-4>
- He, C., Hu, Y., Yin, L., Tang, C., & Yin, C. (2010). Effects of particle size and surface charge on cellular uptake and biodistribution of polymeric nanoparticles. *Biomaterials*, *31*(13), 3657–3666. <https://doi.org/10.1016/j.biomaterials.2010.01.065>
- He, Z., Santos, L., Tian, H., Huang, H., Hu, Y., Liu, L., & Mao, Q. (2017). Scalable fabrication of size-controlled chitosan nanoparticles for oral delivery of insulin. *Biomaterials*, *130*, 28–41. <https://doi.org/10.1016/j.biomaterials.2017.03.028>
- Heath, D., Pruitt, M., Brenner, E., & Rock, L. (2003). Curcumin in plasma and urine : quantitation by high-performance liquid chromatography. *Journal of Chromatography B*, *783*, 287–295.
- Hegde, K., Haniadka, R., Alva, A., Periera-Colaco, M., & Baliga, S. (2013). *Bioactive Food as Dietary Interventions for Liver and Gastrointestinal Disease*. Academic Press, *1*, 537-542. <https://doi.org/10.1016/B978-0-12-397154-8.00040-3>
- Herlyn, M., Steplewski, Z., Herlyn, D., & Koprowski, H. (1979). Colorectal carcinoma-specific antigen: detection by means of monoclonal antibodies. *Proceedings of the National Academy of Sciences of the United States of America*, *76*(3), 1438–42. <https://doi.org/10.1073/pnas.76.3.1438>
- Hjorth, H., Masson, M., & Loftsson, T. (2002). Studies of curcumin and curcuminoids . XXVII . Cyclodextrin complexation : solubility , chemical and photochemical stability. *Internation Journal of Pharmaceutics*, *244*, 127–135.

- Hockenbery, M., Milliman, L., & Korsmeyer, J. (1993). Bcl-2 Functions in an Antioxidant Pathway to Prevent Apoptosis. *Cell*, 75, 241–251.
- Höhne, G., Hemminger, F., & Flammersheim, J. (2003). Differential Scanning Calorimetry. *Springer*, 2, 9-30.
- Hoo, M., Starostin, N., West, P., & Mecartney, L. (2008). A comparison of atomic force microscopy (AFM) and dynamic light scattering (DLS) methods to characterize nanoparticle size distributions. *Journal of Nanoparticle Research*, 10, 89–96. <https://doi.org/10.1007/s11051-008-9435-7>
- Hour, T., Chen, J., Huang, C., Guan, J., & Lu, S. (2002). Curcumin Enhances Cytotoxicity of Chemotherapeutic Agents in Prostate Cancer Cells by Inducing p21 WAF1 / CIP1 and C / EBP b Expressions and Suppressing NF- k B Activation. *The Prostate*, 51, 211–218. <https://doi.org/10.1002/pros.10089>
- Howells, M., Sale, S., Sriramareddy, N., Irving, B., Jones, L., Ottley, J., & Brown, K. (2011). Curcumin ameliorates oxaliplatin-induced chemoresistance in HCT116 colorectal cancer cells in vitro and in vivo. *International Journal of Cancer*, 129(2), 476–486. <https://doi.org/10.1002/ijc.25670>
- Hsu, H., Hsu, M., Ho, F., & Lin, R. (2001). Phase I clinical trial of curcumin , a chemopreventive agent , in patients with high- risk or pre-malignant lesions. *Anticancer Research*, 21, 2895–2900.
- Hunter, J. (1981). Zeta Potential in Colloid Science: Principles and Applications. Principles and Applications, *Academic Press*, 4-6
- Huxley, R., Ansary-Moghaddam, A., Clifton, P., Czernichow, S., Parr, L., & Woodward, M. (2009). The impact of dietary and lifestyle risk factors on risk of

- colorectal cancer: A quantitative overview of the epidemiological evidence. *International Journal of Cancer*, *125*(1), 171–180. <https://doi.org/10.1002/ijc.24343>
- Ibrahim, H., Bindschaedler, C., Doelker, E., Buri, P., & Gurny, R. (1992). Aqueous nanodispersions prepared by a salting-out process. *International Journal of Pharmaceutics*, *87*(1–3), 239–246. [https://doi.org/10.1016/0378-5173\(92\)90248-Z](https://doi.org/10.1016/0378-5173(92)90248-Z)
- Ing, Y., Zin, M., Sarwar, A., & Katas, H. (2012). Antifungal activity of chitosan nanoparticles and correlation with their physical properties. *International Journal of Biomaterials*, *2012*, 1–9. <https://doi.org/10.1155/2012/632698>
- Invitrogen. (2010). Cell Culture Basics. *In Vitro Cellular and Developmental Biology - Animal*, *45*, 1-4. <https://doi.org/10.1007/s11626-009-9197-2>
- Ireson, C., Orr, S., Jones, L., Verschoyle, R., Lim, C., Luo, J., & Gescher, A. (2001). Characterization of Metabolites of the Chemopreventive Agent Curcumin in Human and Rat Hepatocytes and in the Rat in Vivo , and Evaluation of Their Ability to Inhibit Phorbol Ester-induced Prostaglandin E₂ Production. *Cancer Research*, *61*, 1058–1064.
- Ireson, R., Jones, J., Orr, S., Coughtrie, W., Boocock, J., Williams, L., & Gescher, J. (2002). Metabolism of the cancer chemopreventive agent curcumin in human and rat intestine. *Cancer Epidemiol, Biomarkers Prevention*, *11*(January), 105–111.
- Irving, T., Julio, A., & Robyn, W. (2010). Fast Facts: Colorectal Cancer, *Health Press*, *1*, 12-15
- Sarosiek, J., Marshall, B., Peura, D., Hoffman, S., Feng, T., McCallum, R. (1991).

- Gastroduodenal Mucus Gel Thickness in Patients with *Helicobacter pylori*: A method for assessment of biopsy specimens. *American Journal of Gastroenterology*, 86, 729–734.
- Jacob, A., Wu, R., Zhou, M., & Wang, P. (2007). Mechanism of the Anti-inflammatory Effect of Curcumin: PPAR- γ Activation. *PPAR Research*, 2007, 1–5. <https://doi.org/10.1155/2007/89369>
- Jadhav, K., Mahadik, R., & Paradkar, R. (2007). Development and validation of improved reversed phase-HPLC method for simultaneous determination of curcumin, demethoxycurcumin and bis-demethoxycurcumin. *Chromatographia*, 65(7–8), 483–488. <https://doi.org/10.1365/s10337-006-0164-8>
- Jaggi, N. (2006). *Handbook of Applied Solid State Spectroscopy*. <https://doi.org/10.1007/0-387-37590-2>
- Jain, A., Gupta, Y., & Jain, K. (2007). Perspectives of Biodegradable Natural Polysaccharides for Site-Specific Drug Delivery to the Colon. *Journal of Pharmaceutical Sciences*, 10(1), 86–128. Retrieved from https://sites.ualberta.ca/~csps/JPPS10_1/REVIEW_1167/review_1167.html
- Jain, S., Sharma, K., & Vyas, P. (2006). Chitosan nanoparticles encapsulated vesicular systems for oral immunization: preparation, in-vitro and in-vivo characterization. *Journal of Pharmacy and Pharmacology*, 58(3), 303–310. <https://doi.org/10.1211/jpp.58.3.0003>
- Jiang, J., Wang, W., Sun, J., Hu, M., Li, F., & Zhu, Y. (2007). Neuroprotective effect of curcumin on focal cerebral ischemic rats by preventing blood – brain barrier damage. *European Journal of Pharmacology*, 561, 54–62.

<https://doi.org/10.1016/j.ejphar.2006.12.028>

Jiang, N., Kim, S., Rutka, T., & Chan, W. (2008). Nanoparticle-mediated cellular response is size-dependent. *Nature Nanotechnology*, 3, 145–150.

<https://doi.org/10.1038/nnano.2008.30>

Johnson, J., & Mukhtar, H. (2007). Curcumin for chemoprevention of colon cancer.

Cancer Letters, 255(2), 170–181. <https://doi.org/10.1016/j.canlet.2007.03.005>

Johnson, M., Gulhati, T., & Arrieta, I. (2009). Curcumin Inhibits Proliferation of Colorectal Carcinoma by Modulating Akt / mTOR Signaling. *Anticancer Research*, 3190, 3185–3190.

Jung, J., Arnold, D., & Wicker, L. (2013). Pectin and charge modified pectin hydrogel beads as a colon-targeted drug delivery carrier. *Colloids and Surfaces B: Biointerfaces*, 104, 116–121. <https://doi.org/10.1016/j.colsurfb.2012.11.042>

Jung, T., Kamm, W., Breitenbach, A., Kaiserling, E., Xiao, X., & Kissel, T. (2000).

Biodegradable nanoparticles for oral delivery of peptides: Is there a role for polymers to affect mucosal uptake? *European Journal of Pharmaceutics and Biopharmaceutics*,

50(1), 147–160. [https://doi.org/10.1016/S0939-](https://doi.org/10.1016/S0939-6411(00)00084-9)

6411(00)00084-9

Jurenka, S., & Ascp, T. (2009). Anti-inflammatory Properties of Curcumin , a Major Constituent of Curcuma longa : A Review of Preclinical and Clinical Research.

Alternative Medicine Review, 14(2), 141–154.

Kalaria, R., Sharma, G., Beniwal, V., & Ravi Kumar, V. (2009). Design of biodegradable nanoparticles for oral delivery of doxorubicin: In vivo pharmacokinetics and toxicity studies in rats. *Pharmaceutical Research*, 26(3),

492–501. <https://doi.org/10.1007/s11095-008-9763-4>

Kalepu, S., & Nekkanti, V. (2015). Insoluble drug delivery strategies: Review of recent advances and business prospects. *Acta Pharmaceutica Sinica B*, 5(5), 442–453.

<https://doi.org/10.1016/j.apsb.2015.07.003>

Kamat, M., Sethi, G., & Aggarwal, B. (2007). Curcumin potentiates the apoptotic effects of chemotherapeutic agents and cytokines through down-regulation of nuclear factor- κ B and nuclear factor- κ B – regulated gene products in IFN- α – sensitive and IFN- α – resistant human bladder cancer cells. *Molecular Cancer Therapeutics*, 6, 1022–1031. <https://doi.org/10.1158/1535-7163.MCT-06-0545>

Kanai, M., Imaizumi, A., Otsuka, Y., Sasaki, H., Hashiguchi, M., Tsujiko, K., & Chiba, T. (2012). Dose-escalation and pharmacokinetic study of nanoparticle curcumin, a potential anticancer agent with improved bioavailability, in healthy human volunteers. *Cancer Chemotherapy and Pharmacology*, 69(1), 65–70. <https://doi.org/10.1007/s00280-011-1673-1>

Kanai, M., Yoshimura, K., Asada, M., & Imaizumi, A. (2011). A phase I / II study of gemcitabine-based chemotherapy plus curcumin for patients with gemcitabine-resistant pancreatic cancer. *Cancer Chemotherapy and Pharmacology*, 68, 157–164. <https://doi.org/10.1007/s00280-010-1470-2>

Kararli, T. (1995). Comparison of the gastrointestinal anatomy, physiology and biochemistry of humans and commonly used laboratory animals. *Biopharmaceutics & Drug Disposition*, 16, 351–380.

Kashyap, D. (2001). Applications of pectinases in teh commercial sector: a review. *Bioresource Technology. Amsterdam*, 77, 215–227.

- Kasprzyk-Hordern, B., Dinsdale, R. M., & Guwy, A. J. (2007). Multi-residue method for the determination of basic / neutral pharmaceuticals and illicit drugs in surface water by solid-phase extraction and ultra performance liquid chromatography – positive electrospray ionisation tandem mass spectrometry. *Journal of Chromatography A*, *1161*, 132–145. <https://doi.org/10.1016/j.chroma.2007.05.074>
- Kataoka, K., Harada, A., & Nagasaki, Y. (2012). Block copolymer micelles for drug delivery: Design, characterization and biological significance. *Advanced Drug Delivery Reviews*, *64*, 37–48. <https://doi.org/10.1016/j.addr.2012.09.013>
- Katas, H., & Alpar, O. (2006). Development and characterisation of chitosan nanoparticles for siRNA delivery. *Journal of Controlled Release*, *115*(2), 216–225. <https://doi.org/10.1016/j.jconrel.2006.07.021>
- Kaur, S., Modi, H., Panda, D., & Roy, N. (2010). Probing the binding site of curcumin in *Escherichia coli* and *Bacillus subtilis* FtsZ: A structural insight to unveil antibacterial activity of curcumin. *European Journal of Medicinal Chemistry*, *45*(9), 4209–4214. <https://doi.org/10.1016/j.ejmech.2010.06.015>
- Kawamori, T., Lubet, R., Steele, E., Kelloff, J., Kaskey, B., Rao, V., & Reddy, S. (1999). Chemopreventive Effect of Curcumin, a Naturally Occurring Anti-Inflammatory Agent, during the Promotion / Progression Stages of Colon Cancer. *Cancer Research*, 597–601.
- Kayser, O., Lemke, A., & Hernandez-Trejo, N. (2005). The impact of nanobiotechnology on the development of new drug delivery systems. *Curr.Pharm.Biotechnol.*, *6*(1389–2010), 3–5.

<https://doi.org/10.2174/1389201053167158>

Kazemi-Lomedasht, F., Rami, A., & Zarghami, N. (2013). Comparison of inhibitory effect of curcumin nanoparticles and free curcumin in human telomerase reverse transcriptase gene expression in breast cancer. *Advanced Pharmaceutical Bulletin*, 3(1), 127–30. <https://doi.org/10.5681/apb.2013.021>

Kedar, U., Phutane, P., Shidhaye, S., & Kadam, V. (2010). Advances in polymeric micelles for drug delivery and tumor targeting. *Nanomedicine: Nanotechnology, Biology, and Medicine*, 6(6), 714–729. <https://doi.org/10.1016/j.nano.2010.05.005>

Khalil, N. M., Castro, T., Casa, M., Dalmolin, F., Mattos, C. De, I., & Mainardes, R. (2013). Pharmacokinetics of curcumin-loaded PLGA and PLGA – PEG blend nanoparticles after oral administration in rats. *Colloids and Surfaces B: Biointerfaces*, 101, 353–360. <https://doi.org/10.1016/j.colsurfb.2012.06.024>

Khalil, N., Nascimento, T., Casa, D., Dalmolin, L., Mattos, A., Hoss, I., & Mainardes, R. (2013). Pharmacokinetics of curcumin-loaded PLGA and PLGA-PEG blend nanoparticles after oral administration in rats. *Colloids and Surfaces B: Biointerfaces*, 101, 353–360. <https://doi.org/10.1016/j.colsurfb.2012.06.024>

Khatik, R., Mishra, R., Verma, A., & Dwivedi, P. (2013). Colon-specific delivery of curcumin by exploiting Eudragit-decorated chitosan nanoparticles in vitro and in vivo. *Journal of Nanoparticle Research*, 15, 1–15. <https://doi.org/10.1007/s11051-013-1893-x>

Khatik, R., Mishra, R., Verma, A., Dwivedi, P., Kumar, V., Gupta, V., & Dwivedi, A. K. (2013). Colon-specific delivery of curcumin by exploiting Eudragit-decorated chitosan nanoparticles in vitro and in vivo. *Journal of Nanoparticle Research*,

15(9), 1–15. <https://doi.org/10.1007/s11051-013-1893-x>

Khot, A., Wenk Lang, K., & Murali,. (2002). Systematic review of the efficacy and safety of colorectal stents. *British Journal of Surgery*, (September), 1096–1102.

Khutoryanskiy, V. (2011). Advances in Mucoadhesion and Mucoadhesive Polymers. *Macromolecular Bioscience*, 11(6), 748–764. <https://doi.org/10.1002/mabi.201000388>

Kim, T, Jiang, H., Youn, Y., Park, C., Tak, K., Lee, S., & Lee, C. (2011). Preparation and characterization of water-soluble albumin-bound curcumin nanoparticles with improved antitumor activity. *International Journal of Pharmaceutics*, 403(1–2), 285–291. <https://doi.org/10.1016/j.ijpharm.2010.10.041>

Kirkegaard, H., Johnsen, F., Christensen, J., Frederiksen, K., Overvad, K., & Tjonneland, A. (2010). Association of adherence to lifestyle recommendations and risk of colorectal cancer: a prospective Danish cohort study. *Bmj*, 341, 5504-5509. <https://doi.org/10.1136/bmj.c5504>

Kocher, A., Schiborr, C., Behnam, D., & Frank, J. (2015). The oral bioavailability of curcuminoids in healthy humans is markedly enhanced by micellar solubilisation but not further improved by simultaneous ingestion of sesamin, ferulic acid, naringenin and xanthohumol. *Journal of Functional Foods*, 14, 183–191. <https://doi.org/10.1016/j.jff.2015.01.045>

Kolev, M., Velcheva, A., Stamboliyska, A., & Spiteller, M. (2005). DFT and experimental studies of the structure and vibrational spectra of curcumin. *International Journal of Quantum Chemistry*, 102(6), 1069–1079. <https://doi.org/10.1002/qua.20469>

- Kranz, C., Eaton, C., & Mizaikoff, B. (2011). Analytical challenges in nanomedicine. *Analytical and Bioanalytical Chemistry*, 399, 2309–2311. <https://doi.org/10.1007/s00216-010-4631-6>
- Kudo, M., Yamamoto, Y., Koga, Y., Hamaguchi, T., Akimoto, T., Yasunaga, M., & Matsumura, Y. (2016). Effect of combined treatment with micelle-incorporated cisplatin (NC-6004) and S-1 on human gastric cancer xenografts. *Molecular and Clinical Oncology*, 5(6), 817–822. <https://doi.org/10.3892/mco.2016.1070>
- Kumara, V., & Madhysyghan, B. (2015). Synthesis, characterization and hemocompatibility evaluation of curcumin encapsulated chitosan nanoparticles for oral delivery. *International Journal of Advanced Research*, 3(4), 604–611.
- Kumari, A., Yadav, K., & Yadav, C. (2010). Biodegradable polymeric nanoparticles based drug delivery systems. *Colloids and Surfaces B: Biointerfaces*, 75(1), 1–18. <https://doi.org/10.1016/j.colsurfb.2009.09.001>
- Kunnumakkara, B., Guha, S., Krishnan, S., Diagaradjane, P., Gelovani, J., & Aggarwal, B. (2007). Curcumin Potentiates Antitumor Activity of Gemcitabine in an Orthotopic Model of Pancreatic Cancer through Suppression of Proliferation , Angiogenesis , and Inhibition of Nuclear Factor- K B – Regulated Gene Products. *Cancer Research*, 8, 3853–3862. <https://doi.org/10.1158/0008-5472.CAN-06-4257>
- Kunwar, A., Barik, A., Mishra, B., Rathinasamy, K., Pandey, R., & Priyadarsini, I. (2008). Quantitative cellular uptake, localization and cytotoxicity of curcumin in normal and tumor cells. *Biochimica et Biophysica Acta - General Subjects*, 1780(4), 673–679. <https://doi.org/10.1016/j.bbagen.2007.11.016>

- Kunwar, A., & Priyadarsini, K. (2011). Free radicals, oxidative stress and importance of antioxidants in human health. *Journal of Medical & Allied Sciences*, *1*(2), 2231.
- Kuo, W., & Wen, C. (2008). Dispersible polyaniline nanoparticles in aqueous poly(styrenesulfonic acid) via the interfacial polymerization route. *European Polymer Journal*, *44*(11), 3393–3401.
<https://doi.org/10.1016/j.eurpolymj.2008.07.018>
- Kurtoglu, E., Navath, S., Wang, B., Kannan, S., Romero, R., & Kannan, M. (2009). Poly (amidoamine) dendrimer – drug conjugates with disulfide linkages for intracellular drug delivery. *Biomaterials*, *30*(11), 2112–2121.
<https://doi.org/10.1016/j.biomaterials.2008.12.054>
- Kwon, Y., Lee, Y., Jang, Y., & Kim, H. (2001). Preparation of PLGA nanoparticles containing estrogen by emulsification–diffusion method. *Colloids and Surfaces A: Physicochemical and Engineering Aspects*, *182*, 123–130.
- Lacourse, R. (2002). Column Liquid Chromatography: Equipment and Instrumentation. *Analytical Chemistry*, *74*(12), 2813–2832.
- Lagerwerf, M., Van Dongen, D., Steenvoorden, M., Honing, M., & Jonkman, G. (2000). Exploring the boundaries of bioanalytical quantitative LC-MS-MS. *Trends in Analytical Chemistry*, *19*(7), 418–427. [https://doi.org/10.1016/S0165-9936\(00\)00009-1](https://doi.org/10.1016/S0165-9936(00)00009-1)
- Lamontagne, J., Dumas, P., Mouillet, V., & Kister, J. (2001). Comparison by Fourier transform infrared (FTIR) spectroscopy of different ageing techniques: application to road bitumens. *Fuel*, *80*, 483–488.
- Lamprecht, A., Rodero Torres, H., Schäfer, U., & Lehr, M. (2000). Biodegradable

- microparticles as a two-drug controlled release formulation: a potential treatment of inflammatory bowel disease. *Journal of Controlled Release*, 69(3), 445–454. [https://doi.org/10.1016/S0168-3659\(00\)00331-X](https://doi.org/10.1016/S0168-3659(00)00331-X)
- Langdon, P. (2003). Cancer Cell Culture methods and protocols. *Methods in molecular medicine*, Humana Press, 1, 3–39. <https://doi.org/10.1385/1592594069>
- Lannaccone, P., & Jacob, H. (2009). Rats. *Disease Models and Mechanisms*, 2, 206–210.
- Larsson, C., Orsini, N., & Wolk, A. (2005). Diabetes Mellitus and Risk of Colorectal Cancer : A Meta-Analysis, 97(22), 1679–1687. <https://doi.org/10.1093/jnci/dji375>
- Lavasanifar, A., Samuel, J., & Kwon, S. (2002). Poly (ethylene oxide) - block -poly (L -amino acid) micelles for drug delivery. *Advanced Drug Delivery Reviews*, 54, 169–190.
- Lavrentovich, D. (2012). Confocal Fluorescence Microscopy. *Characterization of Materials*, 1–27. <https://doi.org/10.1002/0471266965.com127>
- Lee, M., Cho, W., Park, H., Chung, H., Jeong, Y., Choi, K., & Kwon, C. (2006). Size control of self-assembled nanoparticles by an emulsion/solvent evaporation method. *Colloid and Polymer Science*, 284(5), 506–512. <https://doi.org/10.1007/s00396-005-1413-3>
- Lee, C., Oh, T., Jang, H., & Chung, I. (1999). Quantitative analysis of polyvinyl alcohol on the surface of poly (D, L-lactide-co-glycolide) microparticles prepared by solvent evaporation method: effect of particle size and PVA concentration. *Journal of Controlled Release*, 59(2), 123–132.

- Lee, K., Park, Y., Kim, M., & Park, J. (2009). Regulatory effect of the AMPK-COX-2 signaling pathway in curcumin-induced apoptosis in HT-29 colon cancer cells. *Annals of the New York Academy of Sciences*, 1171, 489–494. <https://doi.org/10.1111/j.1749-6632.2009.04699.x>
- Legrand, P., Lesieur, S., Bochot, A., Gref, R., Raatjes, W., Barratt, G., & Vauthier, C. (2007). Influence of polymer behaviour in organic solution on the production of polylactide nanoparticles by nanoprecipitation. *International Journal of Pharmaceutics*, 344(1–2), 33–43. <https://doi.org/10.1016/j.ijpharm.2007.05.054>
- Lehr, M., Bowstra, A., Schacht, H., & Juginger, E. (1992). In vitro evaluation of mucohesive properties of chitosan and some others natural polymers. *International Journal of Pharmaceutics*, 78, 43–48.
- Leung, S., & Robinson, R. (1988). The contribution of anionic polymer structural features to mucoadhesion. *Journal of Controlled Release*, 5, 223–231.
- Li, J., Jiang, Y., Wen, J., Fan, G., Wu, Y., & Zhang, C. (2009). A rapid and simple HPLC method for the determination of curcumin in rat plasma: assay development, validation and application to a pharmacokinetic study of curcumin liposome. *Biomedical Chromatography*, 23(11), 1201–1207. <https://doi.org/10.1002/bmc.1244>
- Lian, T., & Ho, J. (2001). Trends and developments in liposome drug delivery systems. *Journal of Pharmaceutical Sciences*, 90(6), 667–680. <https://doi.org/10.1002/jps.1023>
- Lichtman, W., & Conchello, A. (2005). Fluorescence microscopy. *Nature Methods*, 2(12), 910–919. <https://doi.org/10.1038/nmeth817>

- Lim, P., Chu, T., Yang, F., Beech, W., Frautschy, A., & Cole, M. (2001). The Curry Spice Curcumin Reduces Oxidative Damage and Amyloid Pathology in an Alzheimer Transgenic Mouse. *The Journal of Neuroscience*, 21(21), 8370–8377.
- Lin, C., & Lin, J. (2008). Curcumin : a Potential Cancer Chemopreventive Agent through Suppressing NF- κ B Signaling. *Journal of Cancer Molecules*, 4(1), 11–16.
- Linkov, I., Satterstrom, K., & Corey, M. (2008). Nanotoxicology and nanomedicine : making hard decisions. *Nanomedicine*, 4, 167–171.
<https://doi.org/10.1016/j.nano.2008.01.001>
- Liu, J., Xu, L., Liu, C., Zhang, D., Wang, S., Deng, Z., & Ma, J. (2012). Preparation and characterization of cationic curcumin nanoparticles for improvement of cellular uptake. *Carbohydrate Polymers*, 90(1), 16–22.
<https://doi.org/10.1016/j.carbpol.2012.04.036>
- Liu, L., Fishman, L., & Hicks, B. (2006). Pectin in controlled drug delivery – a review. *Cellulose*, 14(1), 15–24. <https://doi.org/10.1007/s10570-006-9095-7>
- Liu, S., Fishman, L., Hicks, B., & Kende, M. (2005). Interaction of various pectin formulations with porcine colonic tissues. *Biomaterials*, 26(29), 5907–5916.
<https://doi.org/10.1016/j.biomaterials.2005.03.005>
- Liu, M., & Fréchet, J. (1999). Designing dendrimers for drug delivery. *Research Focus*, 2(10), 393–401.
- Liu, Y., Miyoshi, H., & Nakamura, M. (2007). Nanomedicine for drug delivery and imaging : A promising avenue for cancer therapy and diagnosis using targeted functional nanoparticles. *International Journal of Cancer*, 120, 2527–2537.

<https://doi.org/10.1002/ijc.22709>

- Liua, L., Fishmana, L., Kostb, J., & Hicksa, B. (2003). Pectin-based systems for colon-specific drugdelivery via oral route. *Biomaterials*, *24*, 3333–3343.
- Livraghi, T., Solbiati, L., Meloni, F., Gazelle, S., Halpern, F., & Goldberg, N. (2003). Treatment of Focal Liver Tumors with Percutaneous Radio-frequency Ablation : Complications Encountered in a Multicenter Study, *Radiology*, *1*, 441–451.
- Lobo, V., Patil, A., Phatak, A., & Chandra, N. (2010). Free radicals, antioxidants and functional foods: Impact on human health. *Pharmacognosy Review*, *4*(8), 118–125.
- López-León, T., Carvalho, S., Seijo, B., Ortega-Vinuesa, L., & Bastos-González, D. (2005). Physicochemical characterization of chitosan nanoparticles: Electrokinetic and stability behavior. *Journal of Colloid and Interface Science*, *283*(2), 344–351. <https://doi.org/10.1016/j.jcis.2004.08.186>
- Lorenzo-Lamosa, L., Remuñán-López, C., Vila-Jato, L., & Alonso, J. (1998). Design of microencapsulated chitosan microspheres for colonic drug delivery. *Journal of Controlled Release*, *52*(1–2), 109–118. [https://doi.org/10.1016/S0168-3659\(97\)00203-4](https://doi.org/10.1016/S0168-3659(97)00203-4)
- Lough, J., & Wainer, W. (1995). High Performance Liquid Chromatography: Fundamental Principles and Practice. *Blackie academic and professional*, *1*, 97–113
- Luo, L., Xu, J., Du, Y., & Chen, Y. (2004). A glucose biosensor based on chitosan-glucose oxidase-gold nanoparticles biocomposite formed by one-step electrodeposition. *Analytical Biochemistry*, *334*(2), 284–289.

<https://doi.org/10.1016/j.ab.2004.07.005>

Luo, Y., Teng, Z., & Wang, Q. (2012). Development of zein nanoparticles coated with carboxymethyl chitosan for encapsulation and controlled release of vitamin D3. *Journal of Agricultural and Food Chemistry*, 60(3), 836–843. <https://doi.org/10.1021/jf204194z>

Luo, Y., & Wang, Q. (2014). Recent development of chitosan-based polyelectrolyte complexes with natural polysaccharides for drug delivery. *International Journal of Biological Macromolecules*, 64, 353–367. <https://doi.org/10.1016/j.ijbiomac.2013.12.017>

Lushchak, I. (2014). Chemico-Biological Interactions Free radicals , reactive oxygen species , oxidative stress and its classification. *Chemico-Biological Interactions*, 224, 164–175. <https://doi.org/10.1016/j.cbi.2014.10.016>

Hans, M. & Lowman, A. M. (2002). Biodegradable nanoparticles for drug delivery and targeting. *Current Opinion in Solid State and Materials Science*, 6(4), 319–327.

Ma, Z., Shayeganpour, A., Brocks, R., Lavasanifar, A., & Samuel, J. (2007). High-performance liquid chromatography analysis of curcumin in rat plasma: application to pharmacokinetics of polymer micellar formulation of curcumin. *Biomedical Chromatography*, 21, 546–552. <https://doi.org/10.1002/bmc>

Maciel, V, Yoshida, P., Pereira, S., Goycoolea, M., & Franco, T. (2017). Electrostatic Self-Assembled Chitosan-Pectin Nano-and Microparticles for Insulin Delivery. *Molecules*, 22(10), 1707. <https://doi.org/10.3390/molecules22101707>

Maheshwari, K., Singh, K., Gaddipati, J., & Srimal, C. (2006). Multiple biological activities of curcumin: A short review. *Life Sciences*, 78(18), 2081–2087.

<https://doi.org/10.1016/j.lfs.2005.12.007>

Majumdar, R., Fletcher, H., & Evans, T. (1999). How does colorectal cancer present? Symptoms, duration, and clues to location. *American Journal of Gastroenterology*, 94(10), 3039–3045. <https://doi.org/10.1111/j.1572-0241.1999.01454.x>

Makhlof, A., Tozuka, Y., & Takeuchi, H. (2011). Design and evaluation of novel pH-sensitive chitosan nanoparticles for oral insulin delivery. *European Journal of Pharmaceutical Sciences*, 42(5), 445–451. <https://doi.org/10.1016/j.ejps.2010.12.007>

Malam, Y., Loizidou, M., & Seifalian, M. (2009). Liposomes and nanoparticles : nanoasized vehicles for drug delivery in cancer. *Trends in Pharmacological Sciences*, 30(11), 592–599. <https://doi.org/10.1016/j.tips.2009.08.004>

Malviya, R., & Kulkarni, T. (2012). Extraction and characterization of mango peel pectin as pharmaceutical excipient. *Original Papers*, 42, 185–190. <https://doi.org/10.17219/acem/58887>

Manguian, M., Save, M., & Charleux, B. (2006). Batch emulsion polymerization of styrene stabilized by a hydrophilic macro-RAFT agents. *Macromolecular Rapid Communications*, 27(6), 399–404. <https://doi.org/10.1002/marc.200500807>

Manju, S., & Sreenivasan, K. (2011). Conjugation of curcumin onto hyaluronic acid enhances its aqueous solubility and stability. *Journal of Colloid And Interface Science*, 359(1), 318–325. <https://doi.org/10.1016/j.jcis.2011.03.071>

Manolova, Y., Deneva, V., Antonov, L., Drakalska, E., Momekova, D., & Lambov, N. (2014). The effect of the water on the curcumin tautomerism: A quantitative

- approach. *Spectrochimica Acta - Part A: Molecular and Biomolecular Spectroscopy*, 132, 815–820. <https://doi.org/10.1016/j.saa.2014.05.096>
- Marshall,, Bayne, C., Baier, R., Tomsia, P., & Marshall, W. (2010). A review of adhesion science. *Dental Materials*, 26(2), 11–16. <https://doi.org/10.1016/j.dental.2009.11.157>
- Marten, S., Margraf, M., & Textor, C. (2017). Quantitative analysis of Caffeine using the KNAUER HPLC Educational system, *KNAUER*, 1-9
- Martins, F., de Oliveira, M., Pereira, B., Rubira, F., & Muniz, C. (2012). Chitosan/TPP microparticles obtained by microemulsion method applied in controlled release of heparin. *International Journal of Biological Macromolecules*, 51(5), 1127–1133. <https://doi.org/10.1016/j.ijbiomac.2012.08.032>
- Martling, A., Smedby, E., Birgisson, H., Olsson, H., Granath, F., Ekbom, A., & Glimelius, B. (2016). Risk of second primary cancer in patients treated with radiotherapy for rectal cancer. *Colorectal Dis*. <https://doi.org/10.1002/bjs.10327>
- Mathew, A., Fukuda, T., Nagaoka, Y., Hasumura, T., Morimoto, H., Yoshida, Y., & Kumar, S. (2012). Curcumin loaded-PLGA nanoparticles conjugated with Tet-1 peptide for potential use in Alzheimer's disease. *PLoS ONE*, 7(3), 1–10. <https://doi.org/10.1371/journal.pone.0032616>
- Matsumura, Y. (2008). Poly (amino acid) micelle nanocarriers in preclinical and clinical studies ☆. *Advanced Drug Delivery Reviews*, 60, 899–914. <https://doi.org/10.1016/j.addr.2007.11.010>
- Matsumura, Y., & Kataoka, K. (2009). Preclinical and clinical studies of anticancer agent-incorporating polymer micelles. *Cancer Science*, 100(4), 572–579.

<https://doi.org/10.1111/j.1349-7006.2009.01103.x>

Maudens, E., Zhang, G., & Lambert, E. (2004). Quantitative analysis of twelve sulfonamides in honey after acidic hydrolysis by high-performance liquid chromatography with post-column derivatization and fluorescence detection. *Journal of Chromatography A*, *1047*, 85–92. <https://doi.org/10.1016/j.chroma.2004.07.007>

McGarrity, J., Carson, A., & Calif, M. (1983). Detection of mycoplasma infection in cell cultures. US patent: US4387161A

McMullan, D. (1995). Scanning Electron Microscopy 1928 - 1965. *Scanning*, *17*, 175–185. <https://doi.org/10.1002/sca.4950170309>

Mehnert, W., & Mader, K. (2001). Solid lipid nanoparticles: Production, characterization and applications. *Advanced Drug Delivery Reviews*, *47*, 165–196. <https://doi.org/10.1016/j.addr.2012.09.021>

Mei, H., Hsieh, Y., Nardo, C., Xu, X., Wang, S., Ng, K., & Korfmacher, A. (2003). Investigation of matrix effects in bioanalytical high-performance liquid chromatography/tandem mass spectrometric assays: Application to drug discovery. *Rapid Communications in Mass Spectrometry*, *17*(1), 97–103. <https://doi.org/10.1002/rcm.876>

Mezei, M., & Gulasekharan, V. (1980). Liposomes - a selective drug delivery system for the topical route of administration. *Life Sciences*, *26*(14), 1473–1477.

Mi, L., Sung, W., Shyu, S., Su, C., & Peng, K. (2003). Synthesis and characterization of biodegradable TPP/genipin co-crosslinked chitosan gel beads. *Polymer*, *44*(21), 6521–6530. [https://doi.org/10.1016/S0032-3861\(03\)00620-7](https://doi.org/10.1016/S0032-3861(03)00620-7)

- Mignani, S., El, S., Bousmina, M., & Majoral, J. (2013). Expand classical drug administration ways by emerging routes using dendrimer drug delivery systems : A concise overview. *Advanced Drug Delivery Reviews*, 65(10), 1316–1330. <https://doi.org/10.1016/j.addr.2013.01.001>
- Miller, A. (1988). Spontaneous Emulsification Produced by Diffusion - A Review. *Colloids and Surfaces*, 29(1), 89–102. [https://doi.org/10.1016/0166-6622\(88\)80173-2](https://doi.org/10.1016/0166-6622(88)80173-2)
- Milsom, W., Bohm, B., Hammerhofer, A., Fazio, V., Steiger, E., & Elson, P. (1998). A Prospective , Randomized Trial Comparing Laparoscopic Versus Conventional Techniques in Colorectal Cancer Surgery : A Preliminary Report. *Elsevier Science Inc*, 7515(98), 46–54.
- Mimche, N., Taramelli, D., & Vivas, L. (2011). The plant-based immunomodulator curcumin as a potential candidate for the development of an adjunctive therapy for cerebral malaria. *Malaria Journal*, 10, 1–9.
- Mishra, K., Dash, P., & Dey, N. (2011). Andrographolide : A Novel Antimalarial Diterpene Lactone Compound from *Andrographis paniculata* and Its Interaction with Curcumin and Artesunate. *Journal of Tropical Medicine*, 2011(365645), 1–7. <https://doi.org/10.1155/2011/579518>
- Mishra, K., Dash, P., Swain, K., & Dey, N. (2009). Anti-malarial activities of *Andrographis paniculata* and *Hedyotis corymbosa* extracts and their combination with curcumin. *Malaria Journal*, 9, 1–9. <https://doi.org/10.1186/1475-2875-8-26>
- Mishra, K., Banthia, K., & Majeed, A. (2012). Pectin based formulations for biomedical applications: A review. *Asian Journal of Pharmaceutical and Clinical Research*,

5(4), 1–7.

Miskovitz, P. & Betancourt, M. (2010). *The Doctor's Guide to Gastrointestinal Health*. Wiley, 1, 237-258.

Mitra, S., Gaur, U., Ghosh, C., & Maitra, N. (2001). Tumour targeted delivery of encapsulated dextran-doxorubicin conjugate using chitosan nanoparticles as carrier. *Journal of Controlled Release*, 74(1–3), 317–323. [https://doi.org/10.1016/S0168-3659\(01\)00342-X](https://doi.org/10.1016/S0168-3659(01)00342-X)

Mohanraj, V., Chen, Y., & Chen, M. (2006). Nanoparticles – A Review. *Tropical Journal of Pharmaceutical Research*, 5(1), 561–573. <https://doi.org/10.4314/tjpr.v5i1.14634>

Mohanty, C., & Sahoo, K. (2010). The in vitro stability and in vivo pharmacokinetics of curcumin prepared as an aqueous nanoparticulate formulation. *Biomaterials*, 31(25), 6597–6611. <https://doi.org/10.1016/j.biomaterials.2010.04.062>

Molassiotis, A., Russell, W., Hughes, J., Breckons, M., Lloyd-Williams, M., Richardson, J., & Ryder, D. (2014). The Effectiveness of Acupressure for the Control and Management of Chemotherapy-Related Acute and Delayed Nausea: A Randomized Controlled Trial. *Journal of Pain and Symptom Management*, 47(1), 12–25. <https://doi.org/10.1016/j.jpainsymman.2013.03.007>

Moran, J., & Jackson, A. (1992). Function of the human colon. *British Journal of Surgery*, 79(11), 1132–1137. <https://doi.org/10.1002/bjs.1800791106>

Mudduluru, G., George-William, N., Muppala, S., Asangani, A., Kumarswamy, R., Nelson, D., & Allgayer, H. (2011). Curcumin regulates miR-21 expression and inhibits invasion and metastasis in colorectal cancer. *Bioscience Reports*, 31(3),

185–197. <https://doi.org/10.1042/BSR20100065>

- Mueller, M. (2005). Introduction to confocal fluorescence microscopy, *SPIE Press*, 2, 1-40
- Muhlen, A., Schwarz, C., & Mehnert, W. (1998). Solid lipid nanoparticles (SLN) for controlled drug delivery --- drug release and release mechanism. *European Journal of Pharmaceutics and Biopharmaceutics*, 45, 149–155. [https://doi.org/10.1016/S0939-6411\(97\)00150-1](https://doi.org/10.1016/S0939-6411(97)00150-1)
- Mukherjee, S., Ray, S., & Thakur, S. (2009). Solid Lipid Nanoparticles A Modern Formulation Approach in Drug Delivery System. *Indian Journal of Pharmaceutical Sciences*, 71(4), 349–358.
- Mulik, S., Mönkkönen, J., Juvonen, O., Mahadik, R., & Paradkar, R. (2010). Transferrin mediated solid lipid nanoparticles containing curcumin : Enhanced in vitro anticancer activity by induction of apoptosis. *International Journal of Pharmaceutics*, 398(1–2), 190–203. <https://doi.org/10.1016/j.ijpharm.2010.07.021>
- Muller, H., Mader, K., & Gohla, S. (2000). Solid lipid nanoparticles (SLN) for controlled drug delivery - a review of the state of the art. *European Journal of Pharmaceutics and Biopharmaceutics*, 50(1), 161–177. [https://doi.org/10.1016/S0939-6411\(00\)00087-4](https://doi.org/10.1016/S0939-6411(00)00087-4)
- Müller, H., Radtke, M., & Wissing, A. (2002). Solid lipid nanoparticles (SLN) and nanostructured lipid carriers (NLC) in cosmetic and dermatological preparations. *Advanced Drug Delivery Reviews*, 1, 131–155.
- Mun, S., Joung, D., Kim, Y., Kang, O., Kim, S., Seo, Y., & Kwon, D. (2013).

- Synergistic antibacterial effect of curcumin against methicillin-resistant *Staphylococcus aureus*. *Phytomedicine*, 20(8–9), 714–718.
<https://doi.org/10.1016/j.phymed.2013.02.006>
- Munjeri, O., Collett, H., & Fell, T. (1997). Hydrogel beads based on amidated pectins for colon-specific drug delivery: The role of chitosan in modifying drug release. *Journal of Controlled Release*, 46(3), 273–278. [https://doi.org/10.1016/S0168-3659\(96\)01607-0](https://doi.org/10.1016/S0168-3659(96)01607-0)
- Mura, S., Nicolas, J., & Couvreur, P. (2013). Stimuli-responsive nanocarriers for drug delivery. *Nature Materials*, 12(October), 991–1003
<https://doi.org/10.1038/NMAT3776>
- Murkerjee, A. & Vishwantha, J. (2009). Formulation characterization and evaluation of curcumin loaded PLGA nanospheres for cancer therapy. *Anticancer Research*, 29(10), 3867–3875. <https://doi.org/29/10/3867> [pii]
- Nanoscience Instruments (2017). Scanning Electron Microscope. Retrieved from <http://www.nanoscience.com/products/sem/>
- Nagavarma, N., Yadav, S., Ayaz, A., Vasudha, S., & Shivakumar, G. (2012). Different Techniques for preparation of polymeric nanoparticles. *Asian Journal of Pharmaceutical and Clinical Research*, 5, 16–23.
- Nair, L., Thulasidasan, T., Deepa, G., Anto, J., & Kumar, V. (2012). Purely aqueous PLGA nanoparticulate formulations of curcumin exhibit enhanced anticancer activity with dependence on the combination of the carrier. *International Journal of Pharmaceutics*, 425(1–2), 44–52.
<https://doi.org/10.1016/j.ijpharm.2012.01.003>

- Nair, P. (2013). The Agronomy and Economy of Turmeric and Ginger. *Elsevier, 1*, 47-59. <https://doi.org/10.1016/B978-0-12-394801-4.00004-1>
- Nakmareong, S., Kukongviriyapan, U., Pakdeechote, P., Donpunha, W., Kukongviriyapan, V., Kongyingyoes, B., & Philsalaphy, C. (2011). Antioxidant and vascular protective effects of curcumin and tetrahydrocurcumin in rats with L-NAME-induced hypertension. *Naunyn-Schmied Arch Pharmacol, 383*, 519–529. <https://doi.org/10.1007/s00210-011-0624-z>
- Naksuriya, O., Okonogi, S., Schiffelers, M., & Hennink, E. (2014). Biomaterials Curcumin nanoformulations: A review of pharmaceutical properties and preclinical studies and clinical data related to cancer treatment. *Biomaterials, 35*(10), 3365–3383. <https://doi.org/10.1016/j.biomaterials.2013.12.090>
- Nam, Y., Kwon, M., Chung, H., Lee, Y., Kwon, H., Jeon, H., & Jeong, Y. (2009). Cellular uptake mechanism and intracellular fate of hydrophobically modified glycol chitosan nanoparticles. *Journal of Controlled Release, 135*(3), 259–267. <https://doi.org/10.1016/j.jconrel.2009.01.018>
- Nandakumar, N., Nagaraj, A., Vathsala, G., Rangarajan, P., & Padmanaban, G. (2006). Curcumin-Artemisinin Combination Therapy for Malaria. *Antimicrobial Agents and Chemotherapy, 50*(5), 1859–1860. <https://doi.org/10.1128/AAC.50.5.1859>
- Nautiyal, J., Kanwar, S., Yu, Y., & Majumdar, N. (2011). Combination of dasatinib and curcumin eliminates chemo-resistant colon cancer cells. *Journal of Molecular Signaling, 6*, 1–11. <https://doi.org/10.1186/1750-2187-6-7>
- Naz, S., Jabeen, S., Ilyas, S., Manzoor, F., Aslam, F., & Ali, A. (2010). Antibacterial activity of *Curcuma longa* varieties against different strains of bacteria. *Pakistan*

Journal of Botany, 42(1), 455–462.

Nie, S. (2010). Understanding and overcoming major barriers in cancer nanomedicine Editorial. *Future Medicine*, 5, 523–528.

Niwa, T., Takeuchi, H., Hino, T., Kunou, N., & Kawashima, Y. (1993). Preparation of biodegradable nanospheres of water soluble and insoluble drugs with D, L-lactide I glycolide copolymer by a novel spontaneous emulsification solvent diffusion method, and the drug release behaviour. *Journal of Controlled Release*, 25(5), 89–98.

Ogino, S., & Stampfer, M. (2010). Lifestyle factors and microsatellite instability in colorectal cancer: The evolving field of molecular pathological epidemiology. *Journal of the National Cancer Institute*, 102(6), 365–367. <https://doi.org/10.1093/jnci/djq031>

Onik, G., Rubinsky, B., Zemel, R., Weaver, L., Diamond, D., Cobb, C., & Porterfield, B. (1991). Ultrasound-guided hepatic cryosurgery in the treatment of metastatic colon carcinoma. Preliminary results. *Cancer*, 67(March 1991), 901–907. [https://doi.org/10.1002/1097-0142\(19910215\)67](https://doi.org/10.1002/1097-0142(19910215)67)

Ornaf, M., & Dong, W. (2005). Key concepts of HPLC in pharmaceutical analysis In Handbook of pharmaceutical analysis, *Elsevier Inc*, 19–30

Pak, Y., Patek, R., & Mayersohn, M. (2003). Sensitive and rapid isocratic liquid chromatography method for the quantitation of curcumin in plasma. *Journal of Chromatography B: Analytical Technologies in the Biomedical and Life Sciences*, 796(2), 339–346. <https://doi.org/10.1016/j.jchromb.2003.08.018>

Panyam, J., & Labhasetwar, V. (2003). Biodegradable nanoparticles for drug and gene

- delivery to cells and tissue. *Advanced Drug Delivery Reviews*, 55, 329–347.
[https://doi.org/10.1016/S0169-409X\(02\)00228-4](https://doi.org/10.1016/S0169-409X(02)00228-4)
- Park, H., Lee, S., Kim, H., Park, K., Kim, K., & Kwon, C. (2008). Polymeric nanomedicine for cancer therapy. *Progress in Polymers*, 33, 113–137.
<https://doi.org/10.1016/j.progpolymsci.2007.09.003>
- Park, K., & Robinson, R. (1984). Bioadhesive polymers as platforms for oral controlled drug delivery: Method to study bioadhesion. *International Journal of Pharmaceutics*, 19, 107–127.
- Park, S., & Lee, S. (2015). Significant enhancement of curcumin photoluminescence by a photosensitizing organogel : An optical sensor for pyrrole detection. *Sensors & Actuators: B. Chemical*, 220, 318–325.
<https://doi.org/10.1016/j.snb.2015.05.078>
- Patel, B., Sengupta, R., Qazi, S., Vachhani, H., & Yu, Y. (2008). Curcumin enhances the effects of 5-fluorouracil and oxaliplatin in mediating growth inhibition of colon cancer cells by modulating EGFR and IGF-1R. *International Journal of Cancer*, 122(2), 267–273. <https://doi.org/10.1002/ijc.23097>
- Patel, T., Zhou, J., Piepmeier, M., & Saltzman, M. (2012). Polymeric nanoparticles for drug delivery to the central nervous system. *Advanced Drug Delivery Reviews*, 64(7), 701–705. <https://doi.org/10.1016/j.addr.2011.12.006>
- Patil, S., Kamalapur, V, Marapur, C., & Kadam, V. (2010). Ionotropic Gelation and Polyelectrolyte Complexation: the Novel Techniques To Design Hydrogel Particulate Sustained, Modulated Drug Delivery System: a Review. *Digest Journal of Nanomaterials and Biostructures*, 5(1), 241–248. Retrieved from

https://www.researchgate.net/profile/Jagadevappa_Patil/publication/265991547_Ionotropic_gelation_and_polyelectrolyte_complexation_The_novel_techniques_to_design_hydrogel_particulate_sustained_modulated_drug_delivery_system_A_review/links/552fb6c40cf20ea0a

Patri, K., Kukowska-latallo, F., & Jr, B. (2005). Targeted drug delivery with dendrimers : Comparison of the release kinetics of covalently conjugated drug and non-covalent drug inclusion complex B. *Advanced Drug Delivery Reviews*, 57, 2203–2214. <https://doi.org/10.1016/j.addr.2005.09.014>

Paulino, T., Simionato, I., Garcia, C., & Nozaki, J. (2006). Characterization of chitosan and chitin produced from silkworm crysalides. *Carbohydrate Polymers*, 64(1), 98–103. <https://doi.org/10.1016/j.carbpol.2005.10.032>

Peppas, A., & Sahlin, J. (1996). Hydrogels as mucoadhesive and bioadhesive materials: A review. *Biomaterials*, 17(16), 1553–1561. [https://doi.org/10.1016/0142-9612\(95\)00307-X](https://doi.org/10.1016/0142-9612(95)00307-X)

Perlman, D. (1962). Use of Antibiotics in Cell Culture Media. In Basic methods in cell culture, *Elsevier*, LVIII, 110–116

Philip, A., & Philip, B. (2010). Colon Targeted Drug Delivery Systems: A Review on Primary and Novel Approaches. *Oman Medical Journal*, 25(2), 70–78. <https://doi.org/10.5001/omj.2010.24>

Pinto Reis, C., Neufeld, J., Ribeiro, J., & Veiga, F. (2006). Nanoencapsulation I. Methods for preparation of drug-loaded polymeric nanoparticles. *Nanomedicine*, 2(1), 8–21. <https://doi.org/10.1016/j.nano.2005.12.003>

Polson, C., Sarkar, P., Incledon, B., Raguvaran, V., & Grant, R. (2003). Optimisation

of protein precipitation based upon effectiveness of protein removal and ionisation effect in liquid chromatography-tandem mass spectrometry. *Journal of Chromatography B*, 785, 263–275.
[https://doi.org/http://dx.doi.org/10.1016/S1570-0232\(02\)00914-5](https://doi.org/http://dx.doi.org/10.1016/S1570-0232(02)00914-5)

Poulin, P., & Theil, P. (2002). Prediction of Pharmacokinetics Prior to In Vivo Studies. II. Generic Physiologically Based Pharmacokinetic Models of Drug Disposition. *Journal of Pharmaceutical Sciences*, 91(5), 1358–1370.
<https://doi.org/10.1002/jps.10128>

Prabhakar, U., Maeda, H., Jain, K., Sevick-muraca, M., Zamboni, W., Farokhzad, O. C., & Blakey, C. (2013). Challenges and Key Considerations of the Enhanced Permeability and Retention Effect for Nanomedicine Drug Delivery in Oncology. *Cancer Research*, 73(8), 2412–2418. <https://doi.org/10.1158/0008-5472.CAN-12-4561>

Priyadarsini, I. (2009). Photophysics, photochemistry, and photobiology of curcumin: Studies from organic solutions, bio-mimetics and living cells. *Journal of Photochemistry and Photobiology C: Photochemistry Reviews*, 10, 81–95.
<https://doi.org/10.1016/j.jphotochemrev.2009.05.001>

Priyadarsini, I. (2014). The Chemistry of Curcumin: From Extraction to Therapeutic Agent. *Molecules*, 20091–20112. <https://doi.org/10.3390/molecules191220091>

Pullan, D., Thomas, G., Rhodes, M., Newcombe, G., Williams, T., Allen, A., & Rhodes, J. (1994). Thickness of adherent mucus gel on colonic mucosa in humans and its relevance to colitis. *Gut*, 35, 353–359.

Qi, L., Xu, Z., Jiang, X., Hu, C., & Zou, X. (2004). Preparation and antibacterial activity

- of chitosan nanoparticles. *Carbohydrate Research*, 339(16), 2693–2700.
<https://doi.org/10.1016/j.carres.2004.09.007>
- Qian, H., Yang, Y., & Wang, X. (2011). Curcumin enhanced adriamycin-induced human liver-derived Hepatoma G2 cell death through activation of mitochondria-mediated apoptosis and autophagy. *European Journal of Pharmaceutical Sciences*, 43(3), 125–131. <https://doi.org/10.1016/j.ejps.2011.04.002>
- Quintanar-Guerrero, D., Allemann, E., Doelker, E., & Fessi, H. (1998). Preparation and Characterization of Nanocapsules from Preformed Polymers by a new process based on emulsification-diffusion technique. *Pharmaceutical Research*, 15(7), 1056–1062.
- Rahman, H., Ramanathan, M., & Sankar, V. (2014). Preparation , characterization and in vitro cytotoxicity assay of curcumin loaded solid lipid nanoparticle in IMR32 neuroblastoma cell line. *Pakistan Journal of Pharmaceutical Sciences*, 27(5), 1281–1285.
- Rai, D., Singh, K., Roy, N., & Panda, D. (2008). Curcumin inhibits FtsZ assembly : an attractive mechanism for its antibacterial activity. *Biochemical Journal*, 155, 147–155. <https://doi.org/10.1042/BJ20070891>
- Rajakrishnan, V., Viswanathan, P., Rajasekharan, N., & Menon, P. (1999). Neuroprotective role of curcumin from *Curcuma longa* on ethanol-induced brain damage Neuroprotective Role of Curcumin from *Curcuma Longa* on Ethanol-induced Brain Damage. *Phytotherapy Research*, 13, 571-574.
[https://doi.org/10.1002/\(SICI\)1099-1573\(199911\)13](https://doi.org/10.1002/(SICI)1099-1573(199911)13)
- Ramaswamy, S., Tamayo, P., Rifkin, R., Mukherjee, S., Yeang, H., Angelo, M., &

- Golub, R. (2001). Multiclass cancer diagnosis using tumor gene expression signatures. *Proceedings of the National Academy of Sciences of the United States of America*, 98(26), 15149–15154. <https://doi.org/10.1073/pnas.211566398>
- Rampino, A., Borgogna, M., Blasi, P., Bellich, B., & Cesàro, A. (2013). Chitosan nanoparticles: Preparation, size evolution and stability. *International Journal of Pharmaceutics*, 455(1–2), 219–228. <https://doi.org/10.1016/j.ijpharm.2013.07.034>
- Rao, J., & Geckeler, K. (2011). Polymer nanoparticles: Preparation techniques and size-control parameters. *Progress in Polymer Science*, 36(7), 887–913. <https://doi.org/10.1016/j.progpolymsci.2011.01.001>
- Ravi Kumar, V, Bakowsky, U., & Lehr, M. (2004). Preparation and characterization of cationic PLGA nanospheres as DNA carriers. *Biomaterials*, 25(10), 1771–1777. <https://doi.org/10.1016/j.biomaterials.2003.08.069>
- Ravindran, N., Babu, N., & Sivaraman, K. (2007). Turmeric: The genus *Curcuma*. *CRC press*, 235
- Reddy, C., Vatsala, G., Keshamouni, G., Padmanaban, G., & Rangarajan, N. (2005). Curcumin for malaria therapy. *Biochemical and Biophysical Research Communication*, 326, 472–474. <https://doi.org/10.1016/j.bbrc.2004.11.051>
- Reichert, R. (2007). Scanning Electron Microscopy In Science of microscopy, *Springer I*, 133–134. <https://doi.org/10.1016/B0-12-227410-5/00674-8>
- Reuter, S., Eifes, S., Dicato, M., Aggarwal, B., & Diederich, M. (2008). Modulation of anti-apoptotic and survival pathways by curcumin as a strategy to induce apoptosis in cancer cells. *Biochemical Pharmacology*, 76, 1340–1351.

<https://doi.org/10.1016/j.bcp.2008.07.031>

Riss, L., Moravec, A., Niles, L., Duellman, S., Benink, A., Worzella, J., & Minor, L. (2013). Cell Viability Assays. *Assay Guidance Manual*, 114(8), 1–31.

<https://doi.org/10.1016/j.acthis.2012.01.006>

Rochow, G. (1978). Scanning Electron Microscopy In An Introduction to microscopy by means of light, electrons, X-rays, or ultrasound, *Plenum Press*, 1,273–274.

<https://doi.org/10.1016/B0-12-227410-5/00674-8>

Rodrigues, S., Costa, A., & Grenha, A. (2012). Chitosan/carrageenan nanoparticles: Effect of cross-linking with tripolyphosphate and charge ratios. *Carbohydrate Polymers*, 89(1), 282–289. <https://doi.org/10.1016/j.carbpol.2012.03.010>

Roehr, B. (2007). Why Sex Matters in Mouse Models. Available at: <https://www.the-scientist.com/?articles.view/articleNo/25186/title/Why-Sex-Matters-in-Mouse-Models/>

Rottem, S., Kosower, S., & Kornspan, D. (2012). Contamination of Tissue Cultures by Mycoplasmas. *Biomedical Tissue Culture*, 35–58. <https://doi.org/10.5772/51518>

Roy, P., & Shahiwala, A. (2009). Multiparticulate formulation approach to pulsatile drug delivery: Current perspectives. *Journal of Pharmaceutical Sciences*, 134(2), 74–80. <https://doi.org/10.1016/j.jconrel.2008.11.011>

Roy, S., Pal, K., Anis, A., Pramanik, K., & Prabhakar, B. (2009). Polymers in Mucoadhesive Drug-Delivery Systems: A Brief Note. *Designed Monomers & Polymers*, 12(6), 483–495. <https://doi.org/10.1163/138577209X12478283327236>

Rubbia-Brandt, L., Audard, V., Sartoretti, P., Roth, a. D., Brezault, C., Le Charpentier,

- M., & Terris, B. (2004). Severe hepatic sinusoidal obstruction associated with oxaliplatin-based chemotherapy in patients with metastatic colorectal cancer. *Annals of Oncology*, *15*, 460–466. <https://doi.org/10.1093/annonc/mdh095>
- Rubenstein, A. (1990). Microbially Controlled Drug Delivery To the Colon. *Biopharmaceutics & Drug Disposition*, *11*(January), 465–475.
- Rubinstein, A. (2005). Colonic drug delivery. *Drug Discovery Today: Technologies*, *2*(1), 33–37. <https://doi.org/10.1016/j.ddtec.2005.05.021>
- Rubya, J., Babub, D., Rajasekharanb, N., & Kuttan, R. (1995). Anti-tumor and antioxidant activity of natural curcuminoids. *Cancer Letters*, *94*, 79–83.
- Saboktakin, R., Tabatabaie, M., Maharramov, A., & Ramazanov, A. (2011). Synthesis and in vitro evaluation of carboxymethyl starch-chitosan nanoparticles as drug delivery system to the colon. *International Journal of Biological Macromolecules*, *48*(3), 381–385. <https://doi.org/10.1016/j.ijbiomac.2010.10.005>
- Sadeghi, M., Dorkoosh, A., Avadi, R., Saadat, P., Rafiee-Tehrani, M., & Junginger, H. E. (2008). Preparation, characterization and antibacterial activities of chitosan, N-trimethyl chitosan (TMC) and N-diethylmethyl chitosan (DEMC) nanoparticles loaded with insulin using both the ionotropic gelation and polyelectrolyte complexation methods. *International Journal of Pharmaceutics*, *355*(1–2), 299–306. <https://doi.org/10.1016/j.ijpharm.2007.11.052>
- Saif, W. (2014). MM-398 Achieves Primary Endpoint of Overall Survival in Phase III Study in Patients with Gemcitabine Refractory Metastatic Pancreatic Cancer. *Pancreas News*, *15*(3), 278–279.
- Sajeesh, S., & Sharma, P. (2006). Cyclodextrin-insulin complex encapsulated

- polymethacrylic acid based nanoparticles for oral insulin delivery. *International Journal of Pharmaceutics*, 325(1–2), 147–154.
<https://doi.org/10.1016/j.ijpharm.2006.06.019>
- Salamat-Miller, N., Chittchang, M., & Johnston, P. (2005). The use of mucoadhesive polymers in buccal drug delivery. *Advanced Drug Delivery Reviews*, 57(11), 1666–1691. <https://doi.org/10.1016/j.addr.2005.07.003>
- Sandie Lindsay. (1997). Retention and Peak dispersion. In *High Performance Liquid Chromatography* (pp. 17–43). Wiley.
- Sangalli, E., Maroni, A., Zema, L., Busetti, C., Giordano, F., & Gazzaniga, A. (2001). In vitro and in vivo evaluation of an oral system for time and / or site-specific drug delivery. *Journal of Controlled Release*, 73, 103–110.
- Sanjeeb K., Jayanth, P., Swayam, P., & Vinod, L. (2002). Residual polyvinyl alcohol associated with poly (D , L-lactide-co-glycolide) nanoparticles affects their physical properties and cellular uptake Residual polyvinyl alcohol associated with poly (D , L -lactide-co- glycolide) nanoparticles affects thei. *Journal of Controlled Release*, 82(August 2015), 105–114. [https://doi.org/10.1016/S0168-3659\(02\)00127-X](https://doi.org/10.1016/S0168-3659(02)00127-X)
- Sanna, V., Pala, N., & Sechi, M. (2014). Targeted therapy using nanotechnology : focus on cancer. *International Journal of Nanomedicine*, 9, 467–483.
- Sanoj Rejinold, N., Muthunarayanan, M., Chennazhi, P., Nair, V., & Jayakumar, R. (2011). Curcumin Loaded Fibrinogen Nanoparticles for Cancer Drug Delivery. *Journal of Biomedical Nanotechnology*, 7(4), 521–534.
<https://doi.org/10.1166/jbn.2011.1320>

- Sanoj Rejinold, N., Muthunarayanan, M., Divyarani, V., Sreerekha, R., Chennazhi, K. P., Nair, V., & Jayakumar, R. (2011). Curcumin-loaded biocompatible thermoresponsive polymeric nanoparticles for cancer drug delivery. *Journal of Colloid and Interface Science*, 360(1), 39–51. <https://doi.org/10.1016/j.jcis.2011.04.006>
- Sanoj Rejinold, N., Sreerekha, R., Chennazhi, P., Nair, V., & Jayakumar, R. (2011). Biocompatible, biodegradable and thermo-sensitive chitosan-g-poly (N-isopropylacrylamide) nanocarrier for curcumin drug delivery. *International Journal of Biological Macromolecules*, 49(2), 161–172. <https://doi.org/10.1016/j.ijbiomac.2011.04.008>
- Sarmiento, B., Ferreira, D., Veiga, F., & Ribeiro, A. (2006). Characterization of insulin-loaded alginate nanoparticles produced by ionotropic pre-gelation through DSC and FTIR studies. *Carbohydrate Polymers*, 66(1), 1–7. <https://doi.org/10.1016/j.carbpol.2006.02.008>
- Sasikumar, B. (2012). Handbook of herbs and spices. *Woodhead Publishing Limited*. 526-546. <https://doi.org/10.1533/9780857095671.526>
- Scappaticci, A., Fehrenbacher, L., Cartwright, T., Hainsworth, John D., Heim, W., Berlin, J., & Hurwitz, H. (2005). Surgical Wound Healing Complications in Metastatic Colorectal Cancer Patients Treated with Bevacizumab. *Journal of Surgical Oncology*, 91(March), 173–180. <https://doi.org/10.1002/jso.20301>
- Schellinger, P., & Carr, W. (2006). Isocratic and gradient elution chromatography : A comparison in terms of speed , retention reproducibility and quantitation. *Journal of Chromatography A*, 1109, 253–266.

<https://doi.org/10.1016/j.chroma.2006.01.047>

Schiborr, C., Kocher, A., Behnam, D., Jandasek, J., & Toelstede, S. (2014). The oral bioavailability of curcumin from micronized powder and liquid micelles is significantly increased. *Molecular Nutrition & Food Research*, *58*, 516–527. <https://doi.org/10.1002/mnfr.201300724>

Scholefield, J., & Eng, C. (2014). Colorectal cancer: diagnosis and clinical management. *Wiley*, *1*, 27-44

Schwarz, C., Mehnert, W., Lucks, S., & Müller, H. (1994). Solid lipid nanoparticles (SLN) for controlled drug delivery. I. Production, characterization and sterilization. *Journal of Controlled Release*, *30*(1), 83–96. [https://doi.org/10.1016/0168-3659\(94\)90047-7](https://doi.org/10.1016/0168-3659(94)90047-7)

Sedgwick, W., Fenton, W., & Thompson, R. (1991). Effect of protein precipitating agents on the recovery of plasma free amino acids. *Canadian Journal of Animal Science*, *71*(3), 953–957. <https://doi.org/10.4141/cjas91-116>

Seifert, K., & Morris, L. (1998). Prognostic Factors After Cryotherapy for Hepatic Metastases From Colorectal Cancer, *228*(2), 201–208.

Seifert, K. & Morris, L. (1999). World Survey on the Complications of Hepatic and Prostate Cryotherapy, *Springer*, 109–114.

Selvam, C., Jachak, M., Thilagavathi, R., & Chakraborti, K. (2005). Design , synthesis , biological evaluation and molecular docking of curcumin analogues as antioxidant , cyclooxygenase inhibitory and anti-inflammatory agents. *Bioorganic & Medicinal Chemistry Letters*, *15*, 1793–1797. <https://doi.org/10.1016/j.bmcl.2005.02.039>

- Semdé, R., Amighi, K., Devleeschouwer, J., & Moës, J. (2000). Studies of pectin HM/Eudragit® RL/Eudragit® NE film-coating formulations intended for colonic drug delivery. *International Journal of Pharmaceutics*, 197(1–2), 181–192. [https://doi.org/10.1016/S0378-5173\(99\)00467-6](https://doi.org/10.1016/S0378-5173(99)00467-6)
- Sen, S., Chakraborty, R., Sridhar, C., Reddy, R., & De, B. (2010). Free radicals, antioxidants, diseases and phytomedicines: current status and future prospect. *International Journal of Pharmaceutical Sciences Review and Research*, 3(1), 91–100.
- Sethacheewakul, S., Mahattanadol, S., Phadoongsombut, N., Pichayakorn, W., & Wiwattanapatapee, R. (2010). Development and evaluation of self-microemulsifying liquid and pellet formulations of curcumin, and absorption studies in rats. *European Journal of Pharmaceutics and Biopharmaceutics*, 76(3), 475–485. <https://doi.org/10.1016/j.ejpb.2010.07.011>
- Shaikh, J., Ankola, D., Beniwal, V., Singh, D., & Kumar, R. (2009). Nanoparticle encapsulation improves oral bioavailability of curcumin by at least 9-fold when compared to curcumin administered with piperine as absorption enhancer. *European Journal of Pharmaceutical Sciences*, 37(3–4), 223–230. <https://doi.org/10.1016/j.ejps.2009.02.019>
- Shaikh, R., Singh, R., Garland, J., Woolfson, D., & Donnelly, F. (2011). Mucoadhesive drug delivery systems. *Journal of Pharmacy and Bioallied Sciences*, 3(1), 89–100.
- Shapira, A., Livney, D., Broxterman, J., & Assaraf, G. (2011). Nanomedicine for targeted cancer therapy: Towards the overcoming of drug resistance. *Drug Resistance Updates*, 14(3), 150–163. <https://doi.org/10.1016/j.drug.2011.01.003>

- Sharma, A., & Sharma, S. (1997). Liposomes in drug delivery: progress and limitations. *International Journal of Pharmaceutics*, *154*, 123–140.
- Sharma, A., Euden, A., Platton, L., Cooke, N., Shafayat, A., Hewitt, R., & Steward, P. (2004). Phase I Clinical Trial of Oral Curcumin : Biomarkers of Systemic Activity and Compliance. *Clinical Cancer Research*, *10*, 6847–6854.
- Sharma, A., Gescher, J., & Steward, P. (2005). Curcumin : The story so far. *European Journal of Cancer*, *41*, 1955–1968. <https://doi.org/10.1016/j.ejca.2005.05.009>
- Sharma, A., Mcllelland, R., Hill, A., Ireson, R., Euden, A., Manson, M., & Steward, W. P. (2001). Pharmacodynamic and Pharmacokinetic Study of Oral Curcuma Extract in Patients with Colorectal Cancer 1. *Clinical Cancer Research*, *7*(July), 1894–1900.
- Shekunov, Y., Chattopadhyay, P., Tong, Y., & Chow, L. (2007). Particle size analysis in pharmaceuticals: Principles, methods and applications. *Pharmaceutical Research*, *24*(2), 203–227. <https://doi.org/10.1007/s11095-006-9146-7>
- Shen, H., Hong, S., Prud'Homme, K., & Liu, Y. (2011). Self-assembling process of flash nanoprecipitation in a multi-inlet vortex mixer to produce drug-loaded polymeric nanoparticles. *Journal of Nanoparticle Research*, *13*(9), 4109–4120. <https://doi.org/10.1007/s11051-011-0354-7>
- Shen, L., & Ji, H. (2012). The pharmacology of curcumin: is it the degradation products? *Trends in Molecular Medicine*, *18*(3), 138–144. <https://doi.org/10.1016/j.molmed.2012.01.004>
- Shi, J., Kantoff, W., Wooster, R., & Farokhzad, C. (2016). Cancer nanomedicine : progress , challenges and opportunities. *Nature Publishing Group*, *17*(1), 20–37.

<https://doi.org/10.1038/nrc.2016.108>

Shi, L., & Gunasekaran, S. (2008). Preparation of pectin-ZnO nanocomposite. *Nanoscale Research Letters*, 3(12), 491–495. <https://doi.org/10.1007/s11671-008-9185-6>

Shikata, K., Ninomiya, T., & Kiyohara, Y. (2013). Diabetes mellitus and cancer risk : Review of the epidemiological evidence, 104(1), 9–14. <https://doi.org/10.1111/cas.12043>

Shinde, A., Ganu, J., & Naik, P. (2012). Effect of Free Radicals & Antioxidants on Oxidative Stress : A Review. *Journal of Dental & Allied Sciences*, 1(2), 63–66.

Shrivastava, A., & Gupta, V. (2011). Methods for the determination of limit of detection and limit of quantitation of the analytical methods. *Chronicles of Young Scientists*, 2(1), 21. <https://doi.org/10.4103/2229-5186.79345>

Shu, Z., & Zhu, J. (2002). The influence of multivalent phosphate structure on the properties of ionically cross-linked chitosan films for controlled drug release. *European Journal of Pharmaceutics and Biopharmaceutics*, 54, 235–243.

Singla, K., & Chawla, M. (2001). Chitosan: some pharmaceutical and biological aspects - an update. *Journal of Pharmacy and Pharmacology*, 53(8), 1047–1067. <https://doi.org/10.1211/0022357011776441>

Sinha, R., & Kumria, R. (2003). Microbially triggered drug delivery to the colon. *European Journal of Pharmaceutical Sciences*, 18, 3–18.

Sjödén, L., Visser, S., & Al-Saffar, A. (2011). Using pharmacokinetic modeling to determine the effect of drug and food on gastrointestinal transit in dogs. *Journal*

of Pharmacological and Toxicological Methods, 64(1), 42–52.

<https://doi.org/10.1016/j.vascn.2011.04.008>

Skaugrud, Ø., Hagen, A., Borgersen, B., & Dornish, M. (1999). Biomedical and Pharmaceutical Applications of Alginate and Chitosan. *Biotechnology and Genetic Engineering Reviews*, 16(1), 23–40.

<https://doi.org/10.1080/02648725.1999.10647970>

Smart, D. (2005). The basics and underlying mechanisms of mucoadhesion. *Advanced Drug Delivery Reviews*, 57(11), 1556–1568.

<https://doi.org/10.1016/j.addr.2005.07.001>

Smith, C. (2011). Fundamentals of Fourier Transform Infrared Spectroscopy. *Taylor & Francis Group*, 2, 1-53. <https://doi.org/10.1007/s10726-013-9375-1.6>.

Snell, R. S. (2008). Clinical Anatomy By Regions. *Lippincott Williams & Wilkins*, 9, 193

Solbiati, L., Livraghi, T., Goldberg, S., Ierace, T., Meloni, F., Dellanoce, M., & Gazelle, G.(2001). Percutaneous Radio-frequency Ablation of Hepatic Metastases from Colorectal Cancer: Long-term Results in 117 Patients. *Radiology*, 221, 159–166.

Song, G., Mao, B., Cai, F., Yao, M., Ouyang, L., & Bao, D. (2005). Curcumin induces human HT-29 colon adenocarcinoma cell apoptosis by activating p53 and regulating apoptosis-related protein expression. *Brazilian Journal of Medical and Biological Research*, 38(12), 1791–1798. <https://doi.org/S0100-879X2005001200007>

Soppimath, S., Aminabhavi, M., Kulkarni, R., & Rudzinski, E. (2001). Biodegradable polymeric nanoparticles as drug delivery devices. *Journal of Controlled Release*,

70, 1–20.

Sosnik, A., & Sarmento, B. (2014). Mucoadhesive polymers in the design of nano-drug delivery systems for administration by non-parenteral routes : A review. *Progress in Polymer Science*, 39(12), 2030–2075. <https://doi.org/10.1016/j.progpolymsci.2014.07.010>

Sreekanth, N., Bava, V, Sreekumar, E., & Anto, J. (2011). Molecular evidences for the chemosensitizing efficacy of liposomal curcumin in paclitaxel chemotherapy in mouse models of cervical cancer. *Oncogene*, 30, 9139–3152. <https://doi.org/10.1038/onc.2011.23>

Sriamornsak, P. (2003). Chemistry of pectin and its pharmaceutical uses: a review. *Silpakorn University International Journal*, 3(1–2), 207–228. <https://doi.org/10.5458/jag.54.211>

Sriamornsak, P., Wattanakorn, N., & Takeuchi, H. (2010). Study on the mucoadhesion mechanism of pectin by atomic force microscopy and mucin-particle method. *Carbohydrate Polymers*, 79(1), 54–59. <https://doi.org/10.1016/j.carbpol.2009.07.018>

Srinivasan, K., & Iversen, P. (1995). Review of in vivo pharmacokinetics and toxicology of phosphorothioate oligonucleotides. *Journal of Clinical Laboratory Analysis*, 9(2), 129–137. <https://doi.org/10.1002/jcla.1860090210>

Steele, J., & McDonald, P. (2014). Colorectal cancer: Diagnosis and clinical management. *John Wiley & Sons*. 44

Steinhauser, V. (2015). Turmeric Curcumin: Discover the Amazing Health Benefits and Healing Power of turmeric curcumin. *Gamma mouse*. 1-15

- Stockert, C., Blázquez-Castro, A., Cañete, M., Horobin, W., & Villanueva, Á. (2012). MTT assay for cell viability: Intracellular localization of the formazan product is in lipid droplets. *Acta Histochemica*, *114*(8), 785–796. <https://doi.org/10.1016/j.acthis.2012.01.006>
- Storka, A., Vcelar, B., Klickovic, U., Gouya, G., Weisshaar, S., Aschauer, S., & Wolzt, M. (2015). Safety, tolerability and pharmacokinetics of liposomal curcumin in healthy humans. *International Journal of Clinical Pharmacology and Therapeutics*, *53*(1), 54–65. <https://doi.org/10.5414/CP202076>
- Strugala, V., Allen, A., Dettmar, W., & Pearson, P. (2003). colonic mucin: methods of measuring mucus thickness. *Proceedings of the Nutrition Society*, *62*, 237–243.
- Stüber, M., & Reemtsma, T. (2004). Evaluation of three calibration methods to compensate matrix effects in environmental analysis with LC-ESI-MS. *Analytical and Bioanalytical Chemistry*, *378*(4), 910–916. <https://doi.org/10.1007/s00216-003-2442-8>
- Subudhi, B., Jain, A., Jain, A., Hurkat, P., Shilpi, S., Gulbake, A., & Jain, K. (2015). Eudragit S100 coated citrus pectin nanoparticles for colon targeting of 5-fluorouracil. *Materials*, *8*(3), 832–849. <https://doi.org/10.3390/ma8030832>
- Subudhi, M., Jain, A., Jain, A., Hurkat, P., Shilpi, S., Gulbake, A., & Jain, S. (2015). Eudragit S100 Coated Citrus Pectin Nanoparticles for Colon Targeting of 5-Fluorouracil. *Materials*, *8*(3), 832–849. <https://doi.org/10.3390/ma8030832>
- Sudhakar, Y., Kuotsu, K., & Bandyopadhyay, A. K. (2006). Buccal bioadhesive drug delivery - A promising option for orally less efficient drugs. *Journal of Controlled Release*, *114*(1), 15–40. <https://doi.org/10.1016/j.jconrel.2006.04.012>

- Sun, J., Bi, C., Chan, M., Sun, S., Zhang, Q., & Zheng, Y. (2013). Curcumin-loaded solid lipid nanoparticles have prolonged in vitro antitumour activity, cellular uptake and improved in vivo bioavailability. *Colloids and Surfaces B: Biointerfaces*, *111*, 367–375. <https://doi.org/10.1016/j.colsurfb.2013.06.032>
- Sunesen, H., Vedelsdal, R., Kristensen, G., Christrup, L., & Müllertz, A. (2005). Effect of liquid volume and food intake on the absolute bioavailability of danazol, a poorly soluble drug. *European Journal of Pharmaceutical Sciences*, *24*(4), 297–303. <https://doi.org/10.1016/j.ejps.2004.11.005>
- Suwannateep, N., Wanichwecharungruang, S., Haag, F., Devahastin, S., Groth, N., Fluhr, J. W. & Meinke, C. (2012). Encapsulated curcumin results in prolonged curcumin activity in vitro and radical scavenging activity ex vivo on skin after UVB-irradiation. *European Journal of Pharmaceutics and Biopharmaceutics*, *82*(3), 485–490. <https://doi.org/10.1016/j.ejpb.2012.08.010>
- SW846. (2003). Determinative chromatographic separations, method 8000c.
- Syed, K., Liew, K. Bin, G., & Peh, K. (2015). Stability indicating HPLC-UV method for detection of curcumin in *Curcuma longa* extract and emulsion formulation. *Food Chemistry*, *170*, 321–326. <https://doi.org/10.1016/j.foodchem.2014.08.066>
- TAInstruments. (2017). Differential Scanning Calorimetry. Retrieved from <http://www.tainstruments.com/products/>
- Tak, Y., Lin, M., Wang, Y., Zheng, J., Vecchione, A., Park, Y., & Lencioni, R. (2018). Phase III HEAT study adding lyso-thermosensitive liposomal doxorubicin to radiofrequency ablation in patients with unresectable hepatocellular carcinoma lesions. *Clinical Cancer Research*, *24*(1), 73–83. <https://doi.org/10.1158/1078->

- Takeuchi, H., Thongborisute, J., Matsui, Y., Sugihara, H., Yamamoto, H., & Kawashima, Y. (2005). Novel mucoadhesion tests for polymers and polymer-coated particles to design optimal mucoadhesive drug delivery systems. *Advanced Drug Delivery Reviews*, 57(11), 1583–1594. <https://doi.org/10.1016/j.addr.2005.07.008>
- Tamburic, S., & Craig, M. (1997). A comparison of different in vitro methods for measuring mucoadhesive performance. *European Journal of Pharmaceutics and Biopharmaceutics*, 44(2), 159–167. [https://doi.org/10.1016/S0939-6411\(97\)00073-8](https://doi.org/10.1016/S0939-6411(97)00073-8)
- Tamvakopoulos, C., Dimas, K., Sofianos, D., Hatziantoniou, S., Han, Z., Liu, Z., & Pantazis, P. (2007). Metabolism and Anticancer Activity of the Curcumin Analogue , Dimethoxycurcumin. *Cancer Therapy: Preclinical*, 13(24), 1269–1278. <https://doi.org/10.1158/1078-0432.CCR-06-1839>
- Tan, S., Tiong, H., Muruhadas, A., Randhawa, N., Choo, L., Bradshaw, D., & Leong, O. (2011). CYP2S1 and CYP2W1 Mediate 2-(3,4-Dimethoxyphenyl)-5-Fluorobenzothiazole (GW-610, NSC 721648) Sensitivity in Breast and Colorectal Cancer Cells. *Molecular Cancer Therapeutics*, 10(10), 1982–1992. <https://doi.org/10.1158/1535-7163.MCT-11-0391>
- Tang, H., Murphy, J., Zhang, B., Shen, Y., Van Kirk, A., Murdoch, J., & Radosz, M. (2010). Curcumin polymers as anticancer conjugates. *Biomaterials*, 31(27), 7139–7149. <https://doi.org/10.1016/j.biomaterials.2010.06.007>
- Tavakol, M., Vasheghani-farahani, E., & Hashemi-najafabadi, S. (2013). The effect of

polymer and CaCl₂ concentrations on the sulfasalazine release from alginate- N , O - carboxymethyl chitosan beads. *Progress in Biomaterials*, 2, 1–8.

Taylor, J. (2005). Matrix effects: The Achilles heel of quantitative high-performance liquid chromatography-electrospray-tandem mass spectrometry. *Clinical Biochemistry*, 38(4), 328–334. <https://doi.org/10.1016/j.clinbiochem.2004.11.007>

Thabane, L., Ma, J., Goldsmith, C., Hu, R., Cheng, J., Ismaila, A., & Robson, R. (2010). A tutorial on pilot studies : The what , why and A tutorial on pilot studies : the what , why and how. *BMC*, 10, 1–10. <https://doi.org/10.1186/1471-2288-10-1>

Thickett, C., & Gilbert, G. (2007). Emulsion polymerization: State of the art in kinetics and mechanisms. *Polymer*, 48(24), 6965–6991. <https://doi.org/10.1016/j.polymer.2007.09.031>

Thioune, O., Fessi, H., Devissagueta, P., & Puisieux, F. (1997). Preparation of pseudolatex by nanoprecipitation: Influence of the solvent nature on intrinsic viscosity and interaction constant. *International Journal of Pharmaceutics*, 146(2), 233–238. [https://doi.org/10.1016/S0378-5173\(96\)04830-2](https://doi.org/10.1016/S0378-5173(96)04830-2)

Thiyagarajan, M., & Sharma, S. (2004). Neuroprotective effect of curcumin in middle cerebral artery occlusion induced focal cerebral ischemia in rats. *Life Sciences*, 74, 969–985. <https://doi.org/10.1016/j.lfs.2003.06.042>

Timenestsky, J. (1997). Mycoplasma infection in cell cultures. *Journal of Brazilian Society for Virology*, 34–49.

Tokunaga, E., Oda, S., Fukushima, M., Maehara, Y., & Sugimachi, K. (2000). Differential growth inhibition by 5-fluorouracil in human colorectal carcinoma cell lines. *European Journal of Cancer*, 36(15), 1998–2006.

[https://doi.org/10.1016/S0959-8049\(00\)00200-8](https://doi.org/10.1016/S0959-8049(00)00200-8)

Tolika, E., Samanidou, F., & Papadoyannis, N. (2011). Development and validation of an HPLC method for the determination of ten sulfonamide residues in milk according to 2002 / 657 / EC. *Journal of Separation Sciences*, *34*, 1627–1635. <https://doi.org/10.1002/jssc.201100171>

Tomety, T. M. (2017). The power of rat models. *Available at: <https://www.horizondiscovery.com/in-vivo-models/the-power-of-rat-models>*

Torchilin, P. (2012). Multifunctional nanocarriers. *Advanced Drug Delivery Reviews*, *64*, 302–315. <https://doi.org/10.1016/j.addr.2012.09.031>

Trufelli, H., Palma, P., Famiglini, G., & Cappiello, A. (2011). An overview of matrix effects in liquid chromatography-mass spectrometry. *Mass Spectrometry Reviews*, *30*, 491–509. <https://doi.org/10.1002/mas>

Trujillo, J., Irasema, Y., Molina-jijón, E., Andérica-romero, C., Tapia, E., & Pedraza-chaverri, J. (2013). Renoprotective effect of the antioxidant curcumin: Recent findings. *Redox Biology*, *1*, 448–456. <https://doi.org/10.1016/j.redox.2013.09.003>

UNODC. (2009). Guidance for the validation of analytical methodology and calibration of equipment used for testing of illicit drugs in seized materials and biological specimens. *United Nations Publications*, 1-76

Vaghani, S., Patel, M., & Satish, S. (2012). Synthesis and characterization of pH-sensitive hydrogel composed of carboxymethyl chitosan for colon targeted delivery of ornidazole. *Carbohydrate Research*, *347*(1), 76–82. <https://doi.org/10.1016/j.carres.2011.04.048>

- Vaidya, A., Jain, A., Khare, P., Agraawal, R., & Jain, S. (2009). Metronidazole loaded pectin microspheres for colon targeting. *Journal of Pharmaceutical Sciences*, *98*, 4229–4236. <https://doi.org/10.1002/jps>
- Vauthier, C., & Bouchemal, K. (2009). Expert Review Methods for the Preparation and Manufacture of Polymeric Nanoparticles. *Pharmaceutical Research*, *26*(5), 1025–1026. <https://doi.org/10.1007/s11095-008-9800-3>
- Veetil, K., Ghee, K., Chaiyakunapruk, N., & Mooi, S. (2017). Colorectal cancer in Malaysia : Its burden and implications for a multiethnic country. *Asian Journal of Surgery*, *40*(6), 481–489. <https://doi.org/10.1016/j.asjsur.2016.07.005>
- Vimala, K., Mohan, M., Varaprasad, K., & Narayana, N. (2011). Fabrication of Curcumin Encapsulated Chitosan-PVA Silver Nanocomposite Films for Improved Antimicrobial Activity. *Journal of Biomaterials and Nanobiotechnology*, *2011*(January), 55–64. <https://doi.org/10.4236/jbnb.2011.21008>
- Vlachos, N., Skopelitis, Y., Psaroudaki, M., Konstantinidou, V., Chatzilazarou, A., & Tegou, E. (2006). Applications of Fourier transform-infrared spectroscopy to edible oils. *Analytica Chimica Acta*, *573–574*, 459–465. <https://doi.org/10.1016/j.aca.2006.05.034>
- Vlerken, E., Vyas, K., & Amiji, M. (2007). Poly (ethylene glycol) -modified Nanocarriers for Tumor-targeted and Intracellular Delivery. *Pharmaceutical Research*, *24*(8), 1405. <https://doi.org/10.1007/s11095-007-9284-6>
- Von Hoff, D., Mita, M., Ramanathan, K., Weiss, J., Mita, C., Lorusso, M., & Sachdev, C. (2016). Phase I study of PSMA-targeted docetaxel-containing nanoparticle BIND-014 in patients with advanced solid tumors. *Clinical Cancer Research*,

22(13), 3157–3163. <https://doi.org/10.1158/1078-0432.CCR-15-2548>

- Wagner, V., Dullaart, A., Bock, K., & Zweck, A. (2006). The emerging nanomedicine landscape. *Nature Biotechnology*, 24(10), 1211–1217. <https://doi.org/10.1038/nbt1006-1211>
- Wan, S., Sun, Y., Qi, X., & Tan, F. (2012). Improved Bioavailability of Poorly Water-Soluble Drug Curcumin in Cellulose Acetate Solid Dispersion. *AAPS PharmSciTech*, 13(1), 159–166. <https://doi.org/10.1208/s12249-011-9732-9>
- Wang, R., Billone, S., & Mullett, M. (2012). Nanomedicine in action: an overview of cancer nanomedicine on the market and in clinical trials. *Journal of Nanomaterials*, 2013, 1–12. <https://doi.org/10.12980/JCLM.3.2015JCLM-2015-0018>
- Wang, J., Pan, H., Cheng, L., Lin, I., Ho, S., Hsieh, Y., & Lin, K. (1997). Stability of curcumin in buffer solutions and characterization of its degradation products. *Journal of Pharmaceutical and Biomedical Analysis*, 15(12), 1867–1876. [https://doi.org/10.1016/S0731-7085\(96\)02024-9](https://doi.org/10.1016/S0731-7085(96)02024-9)
- Wattenberg, L., Lipkin, M., Boone, W., & Kelloff, J. (1992). Cancer Chemoprevention. *CRC Press*, 1, 19-41
- Webster, J. (2006). Nanomedicine: what's in a definition. *International Journal of Nanomedicine*, 1(2), 115–116.
- Wei, Q., Chen, W., Zhou, B., Yang, L., & Liu, Z. (2006). Inhibition of lipid peroxidation and protein oxidation in rat liver mitochondria by curcumin and its analogues. *Biochimica et Biophysica Acta*, 1760, 70–77. <https://doi.org/10.1016/j.bbagen.2005.09.008>

- White, L. (1981). HPLC in clinical microbiology laboratories. *Journal of Antimicrobial Chemotherapy*, 8, 1–4.
- WHO. (2017). Analytical considerations. Available at: www.who.org
- Wichitnithad, W., Jongaroonngamsang, N., Pummangura, S., & Rojsitthisak, P. (2009). A simple isocratic HPLC method for the simultaneous determination of curcuminoids in commercial turmeric extracts. *Phytochemical Analysis*, 20(4), 314–319. <https://doi.org/10.1002/pca.1129>
- Wicki, A., Witzigmann, D., Balasubramanian, V., & Huwyler, J. (2015). Nanomedicine in cancer therapy : Challenges , opportunities , and clinical applications. *Journal of Controlled Release*, 200, 138–157. <https://doi.org/10.1016/j.jconrel.2014.12.030>
- Willats, T., Knox, P., & Mikkelsen, D. (2006). Pectin: New insights into an old polymer are starting to gel. *Trends in Food Science and Technology*, 17(3), 97–104. <https://doi.org/10.1016/j.tifs.2005.10.008>
- Wilson, B., Samanta, K., Santhi, K., Kumar, S., Ramasamy, M., & Suresh, B. (2010). Chitosan nanoparticles as a new delivery system for the anti-Alzheimer drug tacrine. *Nanomedicine*, 6(1), 144–152. <https://doi.org/10.1016/j.nano.2009.04.001>
- Wissing, A., Kayser, O., & Müller, H. (2004). Solid lipid nanoparticles for parenteral drug delivery. *Advanced Drug Delivery Reviews*, 56(9), 1257–1272. <https://doi.org/10.1016/j.addr.2003.12.002>
- Woertz, C., Preis, M., Breikreutz, J., & Kleinebudde, P. (2013). Assessment of test methods evaluating mucoadhesive polymers and dosage forms: An overview. *European Journal of Pharmaceutics and Biopharmaceutics*, 85(3 PART B), 843–

853. <https://doi.org/10.1016/j.ejpb.2013.06.023>

- Wong, W., & Yuen, H. (2001). Improved oral bioavailability of artemisinin through inclusion complexation with beta- and gamma-cyclodextrins. *International Journal of Pharmaceutics*, 227, 177–185. [https://doi.org/10.1016/S0378-5173\(01\)00796-7](https://doi.org/10.1016/S0378-5173(01)00796-7)
- Wood, F., Rose, M., Chung, M., Allegra, P., Foshag, J., & Bilchik, J. (2000). Radiofrequency Ablation of 231 Unresectable Hepatic Tumors: Indications, Limitations, and Complications, 7(8), 593–600.
- Wu, L., Zhang, J., & Watanabe, W. (2011). Physical and chemical stability of drug nanoparticles. *Advanced Drug Delivery Reviews*, 63(6), 456–469. <https://doi.org/10.1016/j.addr.2011.02.001>
- Wu, T., Munra, J., Guanjian, L., & Liu, G. (2005). Chinese medical herbs for chemotherapy side effects in colorectal cancer patients. *Cochrane Database of Systematic Reviews*, 1. 1-23
- Xiao, J., Nian, S., & Huang, Q. (2015). Assembly of kafirin/carboxymethyl chitosan nanoparticles to enhance the cellular uptake of curcumin. *Food Hydrocolloids*, 51, 166–175. <https://doi.org/10.1016/j.foodhyd.2015.05.012>
- Xie, X., Tao, Q., Zou, Y., Zhang, F., Guo, M., Wang, Y., & Yu, S. (2011). PLGA nanoparticles improve the oral bioavailability of curcumin in rats: Characterizations and mechanisms. *Journal of Agricultural and Food Chemistry*, 59(17), 9280–9289. <https://doi.org/10.1021/jf202135j>
- Xu, R. (2008). Progress in nanoparticles characterization: Sizing and zeta potential measurement. *Particuology*, 6(2), 112–115.

<https://doi.org/10.1016/j.partic.2007.12.002>

Yallapu, M., Gupta, K., Jaggi, M., & Chauhan, C. (2010). Fabrication of curcumin encapsulated PLGA nanoparticles for improved therapeutic effects in metastatic cancer cells. *Journal of Colloid and Interface Science*, *351*(1), 19–29. <https://doi.org/10.1016/j.jcis.2010.05.022>

Yallapu, M., Jaggi, M., & Chauhan, C. (2012). Curcumin nanoformulations: a future nanomedicine for cancer. *Drug Discovery Today*, *17*(1/2), 71–80. <https://doi.org/10.1016/j.drudis.2011.09.009>

Yallapu, M., Maher, M., Sundram, V., Bell, M. C., Jaggi, M., & Chauhan, C. (2010). Curcumin induces chemo/radio-sensitization in ovarian cancer cells and curcumin nanoparticles inhibit ovarian cancer cell growth. *Journal of Ovarian Research*, *3*, 1–11. <https://doi.org/10.1186/1757-2215-3-11>

Yallapu, M., Nagesh, B., Jaggi, M., & Chauhan, C. (2015). Therapeutic Applications of Curcumin Nanoformulations. *The AAPS Journal*, *17*(6), 1341–1356. <https://doi.org/10.1208/s12248-015-9811-z>

Yang, L., Chu, S., Fix, A. (2002). Colon-specific drug delivery: new approaches and in vitro/in vivo evaluation. *International Journal of Pharmaceutics*, *235*, 1–15.

Yang, C., Zhang, X., Fan, H., & Liu, Y. (2009). Curcumin upregulates transcription factor Nrf2, HO-1 expression and protects rat brains against focal ischemia. *Brain Research*, *1282*, 133–141. <https://doi.org/10.1016/j.brainres.2009.05.009>

Yang, F., Lim, P., Begum, N., Ubeda, J., Simmons, R., Ambegaokar, S., & Cole, M. (2005). Curcumin inhibits formation of amyloid β oligomers and fibrils, binds plaques, and reduces amyloid in vivo. *Journal of Biological Chemistry*, *280*(7),

5892–5901. <https://doi.org/10.1074/jbc.M404751200>

Yang, Y., Lin, C., Tseng, Y., Wang, C., & Tsai, H. (2007). Oral bioavailability of curcumin in rat and the herbal analysis from *Curcuma longa* by LC-MS/MS. *Journal of Chromatography B*, 853(1–2), 183–189. <https://doi.org/10.1016/j.jchromb.2007.03.010>

Yang, L., Chu, S., & Fix, A. (2002). Colon-specific drug delivery : new approaches and in vitro / in vivo evaluation. *International Journal of Pharmaceutics*, 235, 1–15.

Yen, L., Wu, H., Tzeng, W., Lin, T., & Lin, C. (2010). Curcumin nanoparticles improve the physicochemical properties of curcumin and effectively enhance its antioxidant and antihepatoma activities. *Journal of Agricultural and Food Chemistry*, 58(12), 7376–7382. <https://doi.org/10.1021/jf100135h>

Yih, C., & Al-Fandi, M. (2006). Engineered nanoparticles as precise drug delivery systems. *Journal of Cellular Biochemistry*, 97(6), 1184–1190. <https://doi.org/10.1002/jcb.20796>

Yin Win, K., & Feng, S. (2005). Effects of particle size and surface coating on cellular uptake of polymeric nanoparticles for oral delivery of anticancer drugs. *Biomaterials*, 26(15), 2713–2722. <https://doi.org/10.1016/j.biomaterials.2004.07.050>

Yordanov, G., & Dushkin, D. (2010). Preparation of poly(butylcyanoacrylate) drug carriers by nanoprecipitation using a pre-synthesized polymer and different colloidal stabilizers. *Colloid and Polymer Science*, 288(9), 1019–1026. <https://doi.org/10.1007/s00396-010-2226-6>

Yu, Y., Yin, C., Zhang, W., Cheng, X., Zhang, Z., & Zhuo, X. (2009). Composite

- microparticle drug delivery systems based on chitosan, alginate and pectin with improved pH-sensitive drug release property. *Colloids and Surfaces B: Biointerfaces*, 68(2), 245–249. <https://doi.org/10.1016/j.colsurfb.2008.10.013>
- Yu, H., & Huang, Q. (2012). Improving the oral bioavailability of curcumin using novel organogel-based nanoemulsions. *Journal of Agricultural and Food Chemistry*, 60(21), 5373–5379. <https://doi.org/10.1021/jf300609p>
- Yu, Y., Kanwar, S., Patel, B., Nautiyal, J., Sarkar, H., & Majumdar, N. (2009). Elimination of Colon Cancer Stem – Like Cells by the Combination of Curcumin. *Translational Oncology*, 2(4), 321–328. <https://doi.org/10.1593/tlo.09193>
- Yun, H., Min, S., Chung, H., Lee, S., Kwon, S., Jeon, H., & Young, S. (2009). Cellular uptake mechanism and intracellular fate of hydrophobically modified glycol chitosan nanoparticles. *Journal of Controlled Release*, 135(3), 259–267. <https://doi.org/10.1016/j.jconrel.2009.01.018>
- Zamek-Gliszczyński, J., Bedwell, W., Bao, Q., & Higgins, W. (2012). Characterization of SAGE Mdr1a (P-gp), Bcrp, and Mrp2 knockout rats using loperamide, paclitaxel, sulfasalazine, and carboxydichlorofluorescein pharmacokinetics. *Drug Metabolism and Disposition*, 40(9), 1825–1833. <https://doi.org/10.1124/dmd.112.046508>
- Zhang, B., Yan, B., Zhang, B., Li, X., & Yan, B. (2008). Advances in HPLC detection — towards universal detection. *Analytical and Bioanalytical Chemistry*, (February), 7–10. <https://doi.org/10.1007/s00216-007-1633-0>
- Zhang, K., Na, T., Wang, L., Gao, Q., Yin, W., Wang, J., & Yuan, Z. (2014). Human diploid MRC-5 cells exhibit several critical properties of human umbilical cord-

- derived mesenchymal stem cells. *Vaccine*, 32(50), 6820–6827.
<https://doi.org/10.1016/j.vaccine.2014.07.071>
- Zhang, L., Gu, X., Chan, M., Wang, Z., Langer, S., & Farokhzad, C. (2008). Nanoparticles in Medicine: Therapeutic Applications and Developments. *Translational Medicine*, 83(5), 761–769. <https://doi.org/10.1038/sj.clp>
- Zhang, Y., Chen, T., Yuan, P., Tian, R., Hu, W., Tang, Y., & Zhang, L. (2015). Encapsulation of honokiol into self-assembled pectin nanoparticles for drug delivery to HepG2 cells. *Carbohydrate Polymers*, 133, 31–38.
<https://doi.org/10.1016/j.carbpol.2015.06.102>
- Zhao, J., Li, L., Shi, J., Li, Y., Xu, X., Li, K., & Lu, H. (2017). Safety and efficacy of paliperidone palmitate 1-month formulation in Chinese patients with schizophrenia: a 25-week, open-label, multicenter, Phase IV study. *Neuropsychiatric Disease and Treatment*, 13, 2045–2056.
<https://doi.org/10.2147/NDT.S131224>
- Zhao, J., & Wu, J. (2006). Preparation and Characterization of the Fluorescent Chitosan Nanoparticle Probe. *Chinese Journal of Analytical Chemistry*, 34(11), 1555–1559.
[https://doi.org/10.1016/S1872-2040\(07\)60015-2](https://doi.org/10.1016/S1872-2040(07)60015-2)
- Zhou, S., Kestell, P., Tingle, D., & Paxton, W. (2002). Gender differences in the metabolism and pharmacokinetics of the experimental anticancer agent 5,6-dimethylxanthenone-4-acetic acid (DMXAA). *Cancer Chemotherapy and Pharmacology*, 49(2), 126–132. <https://doi.org/10.1007/s00280-001-0383-5>
- Zhu, J., Liu, M., Yang, H., & Shen, D. (2014). Effect of the stirring rate on physical and electrochemical properties of LiMnPO₄ nanoplates prepared in a polyol

process. *Ceramics International*, 40(5), 6699–6704.

<https://doi.org/10.1016/j.ceramint.2013.11.131>

Zweers, T., Engbers, M., Grijpma, W., & Feijen, J. (2004). In vitro degradation of nanoparticles prepared from polymers based on DL-lactide, glycolide and poly(ethylene oxide). *Journal of Controlled Release*, 100(3), 347–356.

<https://doi.org/10.1016/j.jconrel.2004.09.008>